UNIVERSITY OF CAMBRIDGE

Novel intracellular signalling regulators of cartilage progenitor cell populations

Anna Albiero

Division of Trauma and Orthopaedic Surgery, Department of Surgery

University of Cambridge

This dissertation is submitted for the degree of

Doctor of Philosophy

Jesus College **September 2019**

Declaration

This dissertation is the result of my work and includes nothing which is the outcome of work done in collaboration except as declared in the Preface and specified in the text.

This thesis is not substantially the same as any that I have submitted, or, is being concurrently submitted for a degree or diploma or other qualification at the University of Cambridge or any other University or similar institution except as declared in the Preface and specified in the text. I further state that no substantial part of my dissertation has already been submitted, or, is being concurrently submitted for any such degree, diploma or other qualification at the University of Cambridge or any other University or similar institution except as declared in the Preface and specified in the text.

It does not exceed the prescribed word limit for the relevant Degree Committee.

Abstract

Novel intracellular signalling regulators of cartilage progenitor cell populations.

Cartilage is a viscoelastic tissue that absorbs shocks and facilitates low friction of the joint. Adult articular cartilage is limited in its ability to self-repair. Lesions or gradual wear-and-tear affect cartilage integrity and lead to damage that, when untreated, can ultimately develop to osteoarthritis. Osteoarthritis is a considerable health burden and is a leading cause of disability worldwide. In order to address this burdensome condition, several treatments have been developed. In particular, therapies that allow delivery of bone marrow and its constituent cell populations to the site of cartilage damage to form a regenerative clot have proved promising in repairing joint cartilage defects. In order to improve such regenerative technique, further research is required to provide a deeper understanding of the mechanisms underlying cartilage regeneration. One of the critical players are the cells that originally reside in the cartilage surrounding the damage. How these resident cells contribute to the activity of cells within the repair tissue at the site of cartilage damage is largely undescribed.

In this thesis chondrocytes from three different cartilage areas were compared: chondrocytes from 1) the superficial (SZ) and 2) the middle-deep (MDZ) zone of non-weight bearing femoral condyles, and from 3) the osteoarthritic zone (OAZ) of patients undergoing knee replacement. More inflammatory factors and cytokines are present in MSCs co-culture with OA cartilage chips, and with MDZ cartilage chips. To assess how chondrocyte-MSC crosstalk would affect MSCs chondrogenesis, cartilage chips from the three different zones were co-cultured with BMSC pellets. Results indicated that the SZ induce chondrogenic differentiation of BMSCs, whereas MDZ and OAZ have a negative effect, compared to control conditions. The findings suggest that the presence of SZ, which has been reported to reduce with age, is important to direct BMSCs differentiation towards the chondrogenic fate.

In order to better understand the molecular mechanism that differentiate SZ from MDZ and OA chondrocytes, DACTs (Dapper antagonist of catenin) were studied. DACT1 and DACT2 are known to be Wnt and TGFβ pathways regulators, but their role in chondrocytes and MSCs has not been described before. Both proteins are present in chondrocytes throughout the osteoarthritic human tissue, including in chondrocytes

forming cell clusters. On the non-weight bearing and visually undamaged cartilage, DACT1 and DACT2 expression is localised to the articular surface. In mouse embryos (E.15.5), DACT2 is expressed at the interzone, site of developing synovial joint, indicating that DACT2 is expressed in cells that give rise to the articular joint. Subsequently the expression of DACT1 and DACT2 was analysed in MSCs: both are expressed in synovial and bone marrow-derived MSCs. Following this observation an RNAi knockdown experiment showed that DACT1 knockdown in both chondrocyte and MSCs causes the cells to undergo apoptosis within 24 hours. To understand the pathway regulated by DACT1, next generation sequencing gene expression analysis was performed on BMSCs where DACT1 had been reduced by RNAi. The study showed that loss of DACT1 influences the expression ($p<0.05$) of genes involved in both TGFβ and Wnt pathways and putative link to relevant cell regulatory pathways (Ingenuity® Pathway Analysis). SMURF2 and other genes involved in protein phosphorylation and degradation are downregulated following DACT1 knockdown. This suggests that DACT1 is an upstream regulator of SMAD protein phosphorylation affecting proliferation and survival of MSCs.

The data presented in this thesis has indicated that different types of chondrocytes are present within human articular cartilage and that they cross talk with MSCs differently according to their regional origin. This information offers a new level of complexity to consider to improve regenerative techniques. In addition, this work describes for the first time, the presence and biological relevance of DACT1 and DACT2 in chondrocytes and MSCs. DACT1 is involved in MSCs survival and is downregulated in OA which suggest that this is an important regulatory protein. Further studies of DACT1 could help elucidate mechanisms involved in OA, but also uncover the relevance of cartilage progenitors loss in the development of cartilage degeneration.

Preface

Chapter 4

All work carried out was supervised and guided by Prof. Andrew W. McCaskie and Dr Mark A. Birch. The extracellular vesicles study was performed under the supervision and technical support of Dr Xiao Wang and Dr Rachel Crossland. The bioinformatic analysis of the NanoString data was performed by Dr Rachel Crossland. The Transmission electron microscopy data were obtained with the help of the Electron Microscopy Research Services at Newcastle University. The author carried out all the experiments listed.

Chapter 5

All work carried out was supervised and guided by Prof. Andrew W. McCaskie and Dr Mark A. Birch. Dr Virginia Piombo helped with the timed mating of the mice. She trained the author to perform the harvesting of both embryos and adult mice limbs. The author carried out all the experiments listed.

Chapter 6

All work carried out was supervised and guided by Prof. Andrew W. McCaskie and Dr Mark A. Birch. The RNA quality control for the RNA sequencing, the libraries for the sequencing was performed by Maike Paramor. The sequencing was performed at the CRUK Institute. Dr Lila Diamanti performed the bioinformatics analysis on the sequencing data, providing the list with the significantly differentially expressed genes. The author carried out all the experiments listed.

Part of this work has been presented as follows:

- 2019 Oral Presentation at ICORS/CORS, Canada. Cartilage and Synovium Session. Title: “Wnt and TGFβ Pathway Protein, DACT1, is Important in Chondrocyte and Mesenchymal Stem/Stromal Cell Survival”

- 2019 Oral Presentation at the Gordon Research Conference in Cartilage Biology and Pathology, Texas. GRS Session. Title: “DACT1 can play a significant role in balancing chondrocyte and mesenchymal stromal cell survival through the TGFß family and Wnt signalling pathways”.

- 2018 Oral Presentation at the Tissue Engineering and Regenerative Medicine, TERMIS World Summit, Japan. Students and Young Investigators Session. Title: “DACT1 and DACT2: novel regulators of mesenchymal stromal cells.”

- 2017 Oral Presentation at the European Orthopaedic Research Society Meeting EORS, Germany. Bone and Cartilage Biology Session. Title: “Chondrocytes influence chondrogenic differentiation of bone marrow-derived mesenchymal stromal cells differently depending on the zonal origin within human articular cartilage”.

Acknowledgements

Firstly, I would like to express my gratitude to my supervisors Prof. Andrew McCaskie and Dr. Mark Birch for giving me the opportunity to carry out my PhD in the DTOS lab. I would like to thank them for their guidance and support, and for giving me the freedom to pursue my research interests.

I gratefully acknowledge Arthritis Research UK, which provided the funding which made this PhD possible.

I am very thankful to Dr Xiao Wang and Dr Rachel Crossland for welcoming to their Lab in Newcastle and their generosity in sharing their time and knowledge on extracellular vesicles.

I would like to thank Dr Maike Paramore and Dr Lila Diamanti for their help in performing RNA sequencing and data analysis.

I also would like to thank the many excellent scientists, from PhD students to internationally renowned professors, I had the pleasure to meet during the years at various meeting and conference for their interest in my work, valuable comments and kind words of encouragement.

This work was made possible by tissue donations from the patients of the Addenbrooke's Hospital Orthopaedic Unit and the medical staff, including Mr Wasim Khan and Mr Stephen McDonnel.

I thank my fellow lab mates, past and present, and in particular to Sarah, Fran, Karim, and Andy, and all the others for always making coming to the lab something to look forward to, and for their constant help and encouragement.

I am overwhelmed in realising how many loving friends have been supporting me through the past 4 years of this PhD.

First, my oldest and dearest: Eva and Federica. I would like to thank them for the constant support and encouragement and for never making me miss a good party when I come back home. I cannot wait to see what beautiful and loving mothers to my future niece and nephew they will become.

I would like to express my gratitude to Giuliana and Elena for their precious friendship. We all embarked on a PhD journey together and it was great to share this adventure with them.

Thanks to all the kind, interesting, talented people I had the chance to meet during these 4 year at Jesus College: Paul, Yani, Rohan, Ellie, Dennis, Thea, Sohaib, Jazz, Chunwen, and all the others with whom I share so many fun memories with.

A special and heartfelt thanks to my family in Cambridge: grazie Neapolitans for the best times, the best dinners and all the laughter. I want to singularly thank Alessandra, Anjali, Gianni, Stefano, Iacopo, Veronica, Karla, Chicco, Francesco, Shivani, Julie, Matteo and Ingrid for their precious friendship. Special thanks to Edoardo Gianni for the sleepy company while exploring Cambridge libraries to write this thesis.

I am very thankful to Miriam Belmonte for choosing me as her new housemate last year and gifting me with a wonderful new friend. I would like to thank her for all the gym session at 7am, her kindness and spontaneity, the delicious Indian recipes and camomile-accompanied chats at 2 am. I am looking forward to seeing which ventures we will get into in the future.

Many thanks to May Hen for constantly providing giggles, though workouts, delicious food, and travel adventures. Her kindness, intelligence and beauty are only matched by her incredible strength.

I would like to thank Dr. Francesca De Domenico for coming up to me on our first days in College for never leaving my side since. She has been the most amazing friend and my rock through this PhD.

I would like to thank my parents Emanuela and Roberto, for inspiring me to do my best and work hard, and for never expecting me to be anyone else than who I am. A warm thanks to my brother Francesco for his support, for occasionally picking me up from the airport, and for always making a proud big sister.

Last but definitely not least, a special thanks goes to my partner Bart. He was the first I shared the news that I would do a PhD at the University of Cambridge and the first the person that came to mind when I thought of writing these acknowledgments. Without his love and support there would probably still be a thesis, but its author would not the happy and confident person she is today.

Table of Contents

List of Figures

List of tables

List of abbreviations

3D	three-dimensional
°C	Celsius
µg	microgram
µL	microlitre
µM	micromolar
µm	micrometre
AC	articular chondrocyte
ACI	autologous cartilage implantation
ADAM	a disintegrin and metalloprotease
AIF4A1	ATP-dependent RNA helicase
ALK	activin report-like kinase
ANOVA	analysis of variance.
ARUK	arthritis research United Kingdom
B2M	β-2-microglobulin
BD	BD Biosciences
BM	bone marrow
BMSCs	bone marrow-derived mesenchymal stem/stromal cells
BSA	bovine serum albumin
BCA	bicinchoninic acid assay
BMP	bone morphogenetic protein
CD	cluster of differentiation
CDK	cyclin dependent kinase
CLK2	CDC (cell division cycle) Like Kinase 2
CFU	colony forming unit
CK	casein kinase
COL1	collagen Type I
COL2	collagen Type II
COL11	collagen Type XI
COL10	collagen Type X
COMP	Cartilage Oligomeric Matrix Protein
CTGF	connective tissue growth factor
CCL2	C-C Motif Chemokine Ligand 2
cDNA	complementary Deoxyribonucleic Acid
Ct	cycle threshold
CXCL10	C-X-C motif chemokine Ligand 10

CXCL12	C-X-C motif chemokine Ligand 12
DAPI	4′,6-diamidino-2-phenylindole
DEL1	Developmental endothelial locus-1
DKK1	Dickkopf-related protein 1
DMMB	1,9-dimethylmethylene blue
DMSO	dimethyl sulfoxide
DNA	deoxyribonucleic Acid.
DNAse	deoxyribonuclease
DVL	dishevelled
DYRK1A	dual specificity tyrosine phosphorylation regulated kinase
DZ	deep zone
E	embryonic day
ECM	extracellular matrix
EDTA	ethylenediaminetetraacetic acid
ERK	extracellular signal–regulated kinase
EVs	extracellular vesicles
FCS	foetal calf serum
FDR	false discovery rate
FGF2	fibroblast growth factor 2
FGF8	fibroblast growth factor 8
FGF14	fibroblast growth factor 14
FGF18	fibroblast growth factor 18
Fig	figure
FRZB	secreted frizzled-related protein 1
FZD	frizzled
GADD45	Growth arrest and DNA-damage-inducible, alpha
GAG	glycosaminoglycan
GAPDH	Glyceraldehyde-3-Phosphate Dehydrogenase
GSK3	glycogen synthase kinase 3
GWAS	genome-wide association study
gDNA	genomic deoxyribonucleic acid
GOI	gene of interest
HK	house keeping
HPRT	Hypoxanthine-guanine phosphoribosyl transferase
IFN	Interferon
IgG	immunoglobulin G
IHH	Indian Hedgehog

IL-6	Interleukin 6
IL-8	Interleukin 8
IGF-1	insulin-like growth factor
IPA	Ingenuity Pathway Analysis
ITS-X	Insulin-Transferrin-Selenium-Ethanolamine
JNK	c-Jun N-terminal kinase
kDa	kilodaltons
KO	knockout
LDL	low density lipoprotein
lncRNA	long non-coding RNA
LONRF1	LON Peptidase N-Terminal Domain And Ring Finger 1
mAb	monoclonal antibody
mg	milligram
MAPK	mitogen-activated protein kinase
miRNA	micro-RNA
MIP	macrophage Inflammatory Protein 3
MRI	magnetic resonance imaging
MDZ	middle-deep zone
MMP13	matrix metalloproteinase 13
mRNA	messenger RNA
MSCs	mesenchymal stem/stromal cells
mL	millilitre
mM	millimolar
MZ	middle zone
NHS	national Health Service
NICE	National Institute of Clinical Excellence
NIH	national Institute for Health Research
ng	Nanogram
nm	Nanometer
NPA	nanoparticle tracking analysis
OA	osteoarthritis
p	p-value
pAb	polyclonal antibody
pg	picogram
PBS	phosphate-buffered saline
PCA	principle component analysis
PCP	planar cell polarity

pH	potential of hydrogen
PRG4	proteoglycan 4 or lubricin
RASSF3	Ras Association Domain Family Member 3
RCF	relative centrifugal force
RIN	RNA integrity number
RNA	ribonucleic acid
RNAi	RNA interference
RNASeq	RNA sequencing
RNAse	ribonuclease
RT	room temperature
RNF130	Ring Finger Protein 130
RT-qPCR	reverse transcription quantitative polymerase chain reaction
RUNX1	Runt-related Transcription Factor 1
RUNX2	Runt-related Transcription Factor 2
RUNX1T1	RUNX1 Partner Transcriptional Co-Repressor 1
SD	standard deviation
SDF1	stromal cell-derived factor 1
siRNA	short interfering ribonucleic acid
SIRT1	Sirtuin 1
sFRP1	secreted frizzled-related protein 1
SMAD	S from "small" C. *Elegans* phenotype and Drosophila MAD "Mothers Against Decapentaplegic" family of genes
SMURF1	SMAD Specific E3 Ubiquitin Protein Ligase 1
SMURF2	SMAD Specific E3 Ubiquitin Protein Ligase 2
SynMSCs	synovium-derived mesenchymal stem/stromal cells
SZ	superficial zone
TCF/LEF	T-cell factor/lymphoid enhancer-binding factor
TGFβ	transforming growth factor beta
TIMP	tissue inhibitor of metalloproteinases
TEM	transmission electron microscopy
TNFa	tumour necrosis factor alpha
USP46	Ubiquitin Specific Peptidase 46
WIF	Wnt inhibitory factor 1
Wnt	Wingless-related integration site
WT	wild type

1 Introduction

Adult joints are anatomical parts of the human body where different types of tissues come together to allow movement. Diseases that affect these articulations and consequently mobility are a major cause of pain and disability. Cartilage is a connective tissue present at the articulating end of each bone that makes up a synovial joint. Cartilage is composed of specialised cells called chondrocytes that are surrounded by matrix, and it act to absorbs mechanical shocks and to facilitates smooth, low friction movement of the joint. Adult articular cartilage is limited in its ability to self-repair. Lesions sustained after sports or the result of a chronic disease and age-related breakdown affect cartilage integrity and lead to damage that, when untreated, can ultimately develop to osteoarthritis. Osteoarthritis (OA) is a joint disease that affects millions of people and is a leading cause of disability worldwide. End stage OA can be effectively treated by surgical operation to replace the joint, but other surgical and non-surgical treatments have been developed to address early stage OA. Therapies that recruit bone marrow to the site of cartilage damage to form a regenerative clot have proved promising in repairing small joint cartilage defects. One approach called microfracture consists of drilling holes into the underlying subchondral bone to recruit a number of resident cell type including mesenchymal stromal cells (MSC). However, fibrotic features of the regenerated cartilage may affect its mechanical properties and therefore the longevity of such treatments. In order to improve this regenerative technique, as well as other similar treatments, further research is required to provide a deeper understanding of the mechanisms underlying cartilage regeneration. One of the critical players are the cells that originally reside in the cartilage surrounding the damage. How these resident cells contribute to the activity of cells within the repair tissue at the site of cartilage damage is largely undescribed. Despite recent progress in determining the origin and process of cartilage development by chondrocytes progenitors in mouse, which cells and mechanism are involved in cartilage repair in human are still elusive. In this chapter, a literature review will illustrate the current understanding of the synovial joint and specifically cartilage development and repair from a cell and molecular point of view. Tissue engineering and cell-based strategies that have recently been developed for the repair of early cartilage damage will be presented and their potential and limitation will be discussed. Finally, the review will

focus on proteins that might be important chondrocytes and cartilage progenitor regulators.

1.1 The social impact of musculoskeletal disorders

Among the newest challenges faced by our society, the UK government policy makers have identified ageing as one of the main 5 to address in 2019. Elderly population is set to become a large part of the UK population in the coming years and a large amount of resources have been allocated to improve their lives. 98£ millions in investments have been destined to Healthy Ageing Industrial Strategy Fund to stimulate innovative solutions to ensure that older people can lead an active and independent life for longer (UK government, 2019b). An extra £130 million of investment is specifically being allocated towards the development of healthcare innovation and new treatment to enable people to live longer and healthier lives (UK government, 2019b). Specific focus on the quality of life of older people seems a strong and leading target for these national investments.

Another main concern to improve national health is to promote adult engagement in physical activity, because of the many associated health benefits including reduction of the incidence of life-threatening diseases such as cardiovascular disease, diabetes, cancer, and general mortality (fig. 1). Engaging is regular physical activity is also critically increasing quality of live by improving mental health, ensuring that we can enjoy living longer.

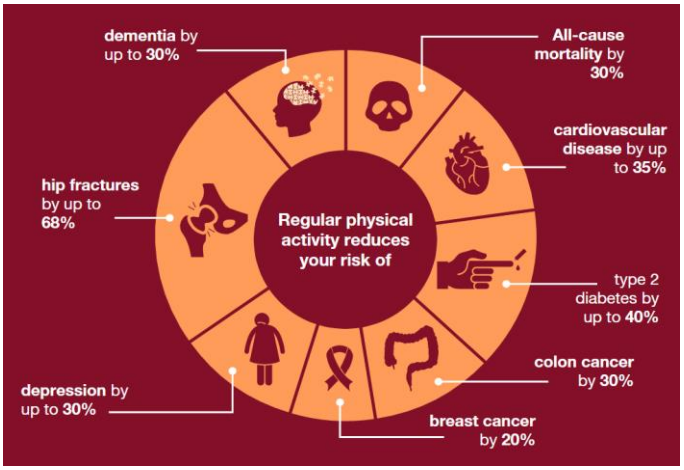

Figure 1 **Health benefits of physical activity.**
Exercising every day has been associated with overall increase of life span by reducing the incidence of many diseases. Being physically active also increase quality of life by improving mental health and improve conditions such as depression (UK government report, 2019b).

Both challenges of providing the elderly with better healthcare solutions and making the general population more active and consequently healthier, can be addressed by treating musculoskeletal disorders. In the past three decades, health concerns involving joints, bones and muscle have been the main cause of disability in the UK, affecting about 30% of the adult population (fig.2). Disability can severely affect mental health, ability to perform physical activity and being independent, which have a large impact not only on the self but also on society. Several risk factors can increase the incidence of musculoskeletal conditions, including physical inactivity, being overweight or obesity, older age and genetic predisposition (Palazzo, Ravaud, Papelard, Ravaud, & Poiraudeau, 2014). About 1 in 5 people seek doctor help about musculoskeletal problems, which spans from inflammatory conditions, for example, rheumatoid arthritis, to conditions that result in chronic pain such as OA and back pain (UK government, 2019a). Developing therapies that target musculoskeletal disorder, such as OA, is imperative to tackle the societal challenges outlined above. In addition, this disorder category affects today about 18 million people in the UK only and accounts for one of the largest expenditure areas for the National Health Service (fig. 2).

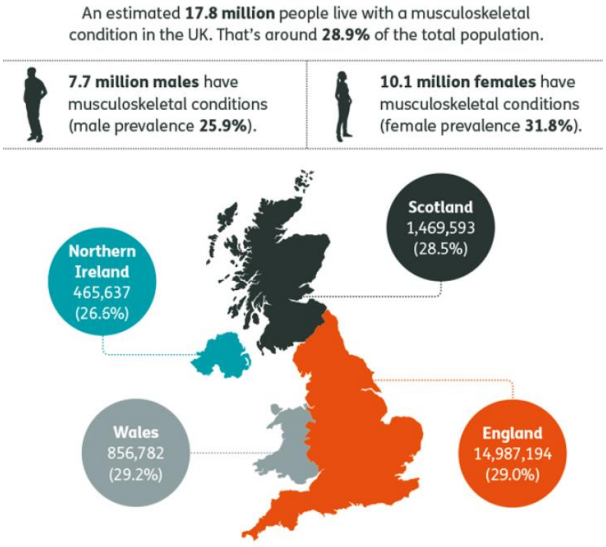

Figure 2 **Musculoskeletal disease in the UK.**
"Global Burden of Disease Study 2016 (GBD 2016) Results". Institute for Health Metrics and Evaluation (IHME). Seattle, 2017.

1.2 The knee joint

Articulations can be described by a number of different classifications, depending on anatomy and biomechanics (depending on how many articular surfaces they connect), the movements they perform, and the type of connective tissue which binds the articular bones. This work will focus on the knee joint, an articular synovial joint that allows a hinge type of movement.

The knee is the largest joint system in the body and connects the femur, the thigh bone, with the tibia, the shin bone, and with the patella, or “knee cap” (Flandry & Hommel, 2011). This structure is made of articular cartilage at the end of the long bones, the synovial fluid produced by the synovium, ligaments and tendons to hold the structure together and connected to muscles and bones (fig. 3). Together, they permit and transmit biomechanical loads during skeletal movement.

Cartilage is a connective tissue that provides support and flexibility to the other joint tissues. It is found in the knee in two main forms:

- Articular cartilage, that covers the ends of the bones and allows for the bones to slide and glide on each other with limited friction (Flandry & Hommel, 2011).
- Menisci, two C-shaped pieces of cartilage that are placed medially and laterally between the femur and tibia. The role of the meniscus is thought to be for shock absorption and to stabilize joint (Flandry & Hommel, 2011).

The layer of bone underlying articular cartilage is called subchondral bone. The role of this structure is to help distribute the mechanical loads across the joint. Alteration in the subchondral bone, therefore, has an effect on cartilage and could cause cartilage degeneration (Imhof et al., 2000). Cartilage and subchondral bone can communicate thanks to the presence of channels between the two structures (Imhof et al., 2000). The biochemical communication between the two and their exact relationship affecting the physiological and diseased state of the knee is still largely undefined.

The synovium, a smooth and thin membranous tissue produces a fluid that helps the lubrication of the healthy knee, reduces friction, and provides a mean of contact between the knee tissues. Synovium is also proposed to be the stem cell niche that maintains and can potentially repair adult joint tissues (Roelofs et al., 2017). The

synovium is made up of predominantly synovial fibroblasts, but also immune cells, and is highly vascularised. The synovium is responsible for the maintenance of synovial fluid volume and composition. Synovial fluid is secreted by the synovium into the synovial cavity and contains products derived from blood plasma and proteins produced by the cells from both cartilage and synovium. The synovial fluid contains hyaluronan, lubricin, and waste products produced by the chondrocytes, like CO_2 and metabolic waste. Because of its highly vascularised nature, the synovium, via synovial fluid, supports articular chondrocytes by supplying oxygen and nutrients and removing waste products.

Other components of the knee joints are ligaments and tendons (Flandry & Hommel, 2011). Ligaments are made of strong connective tissue that is responsible for giving the knee stability from front to back by directly connecting the different bones. Ligaments support the joint by holding the bones together and resisting excess or abnormal joint motions. Tendons are also responsible for stabilizing the different joint parts by connecting bones to the muscles that move the knee.

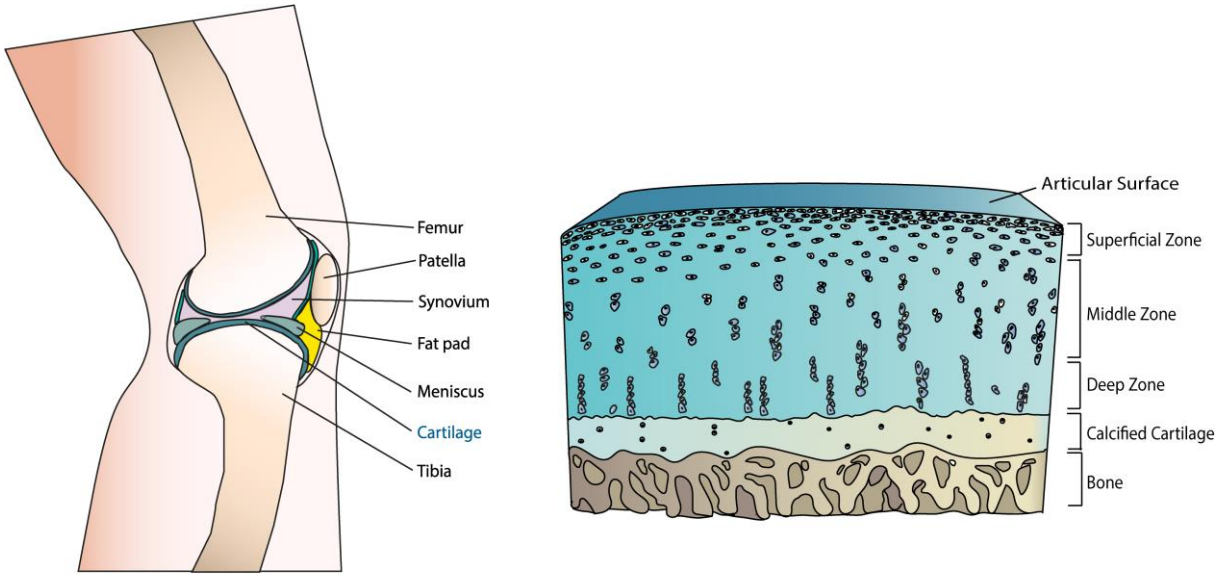

Figure 3 **Anatomy of the human knee and articular cartilage.**
The human knee is a synovial joint that connects the femoral and tibial bones and is contained by the synovial membrane. The synovial fluid that nourishes and lubricate the cartilage at the end of the tibial and femoral bones. The synovium is closely connected to the fat pad. Anteriorly, the patellar a bone which protects the knee joint from trauma. The cartilage lays between the synovial space and the bone. The structure of articular cartilage changes in the various zones in terms of chondrocytes phenotype, water content, ECM components. Original work.

1.3 Cartilage biology

Cartilage is an avascular, aneural and alymphatic tissue. Articular cartilage is about 3 mm thick and is composed of chondrocytes, highly specialised cells of mesenchymal origin, which make up only 5% of the whole cartilaginous tissue with the extracellular matrix (ECM), that surrounds the cells, constituting the remaining 95%.

ECM has a fundamental role in giving cartilage-specific characteristics. The main components of articular cartilage ECM are:

- Collagens, that constitute 60% of the total dry weight of the ECM, often interact with proteoglycans or are assembled with other collagens proteins. Collagen type II is the most abundant type of collagen in cartilage, which typically binds to collagen type XI.
- Proteoglycans, large molecules made of polysaccharides and a small protein part, which provides hydration and swelling pressure to the tissue enabling it to withstand compressional forces. Proteoglycans possess a protein core which is bound to glycosaminoglycans (GAG), like hyaluronic acid, chondroitin sulphate, keratan sulphate binds. GAGs are negatively charged and therefore attract and help retaining water enabling cartilage to withstand load and compression. Aggrecan is one of the major proteoglycan present in articular cartilage (Becerra *et al.*, 2010).
- Other proteins include fibronectin that anchor chondrocytes to the surrounding matrix (Becerra *et al.,* 2010).
- The fluid component, including water, gas, metabolites and cations that balance the negative charge of GAG, help the tissue to resist compression. The metabolic exchange with synovial tissue that surrounds the articulation provides chondrocytes with nutrients (Fukui *et al.*, 2008).

Despite composing only a minimal part of the adult tissue, chondrocytes have an important role in remodelling the ECM to maintain cartilage mechanical properties. Cartilage cells are arranged in four different layers: superficial, middle, deep, and calcified zones (fig.3).

These zones are easily distinguishable in terms of different cell morphologies and spatial arrangement (Zhu *et al.,* 2009). Transcriptional heterogeneity within cartilage and matrix composition has further confirmed the difference between chondrocytes

from different regions (Darling, Hu, & Athanasiou, 2004; Quinn, Häuselmann, Shintani, & Hunziker, 2013). The superficial zone (SZ) is 10-20% of total cartilage volume and displays high numbers of flattened cells that lay parallel to the articular surface. This zone is believed to secrete biomolecules that provide lubrication and resistance to shear stresses, and its integrity is fundamental to protect and maintain the deeper cartilage layers. Notably, proteoglycan 4 (PRG4), or lubricin, is produced mostly by SZ cells. This large glycoprotein is responsible for lubrication and is also called superficial zone protein (SZP) (G. D. Jay, Tantravahi, Britt, Barrach, & Cha, 2001; Koyama et al., 2008). PRG4 is also expressed by cells lining the synovial membrane (Rhee et al., 2005). Cartilage Oligomeric Matrix Protein (COMP) is also more highly expressed in the SZ where it is believed to mediate matrix molecules interactions in cartilage and is involved with load-bearing regulation (Chen et al., 2007). The protein developmental endothelial locus-1 (DEL1) is also a marker for SZ cartilage (Pfister, Aydelotte, Burkhart, Kuettner, & Schmid, 2001). The matrix surrounding SZ chondrocytes is mainly composed of tightly arranged collagen fibres, mainly type II and IX collagen that are aligned parallel to the articular surface. The combination of these proteins provides the water-retaining property and the ability to resist tensile stress. Several studies have reported that the superficial layer includes cells with stem-like properties both in human, mouse and bovine articular cartilage (Coates & Fisher, 2014; Dowthwaite et al., 2004; Hattori, Oxford, & Reddi, 2007; Kozhemyakina et al., 2015; Li et al., 2017; Williams et al., 2010). These cells exhibit stem cell characteristics such as migratory activity, ability to form colonies, and trilineage differentiation and were shown to give rise to adult chondrocytes in mouse (Li et al., 2017). This suggests that the superficial layer could host a subpopulation of progenitor cells, whose role in adult tissue repair has not been exhaustively investigated.

The middle zone (MZ) represents 40-60% of the total cartilage volume. The chondrocytes in this zone are rounder and their disposition is oblique and scattered, occasionally forming clusters of 2-3 cells that tend to have a vertical orientation. The matrix in the MZ is characterised by collagen fibre orientated both vertically and horizontally. Collagens concentration diminishes in the MZ in favour of proteoglycans. In the deeper zone (DZ), which takes up to 30-40% of total volume, cells are clearly organised in vertical columns and have a round morphology (Coates & Fisher, 2014; Hunziker et al., 2002). Vertical fibrils of collagen, including collagen type X, are present

in the DZ. The DZ has the highest proteoglycans concentration and the lowest water concentration compared to the rest of the tissue.

Finally, the tide mark delineates the deep zone from the calcified cartilage which sits on the subchondral bone. The calcified zone is a transitional space between cartilage and subchondral bone.

1.4 Joint and cartilage development

Skeletogenesis is the process by which the vertebrate skeleton is formed. In early embryonic life, in the process called gastrulation, the initial cluster of cells that will become the embryo organizes into layers that will give rise to all of the organs and structures of the body. The endoderm (inner layer), the ectoderm (outer layer) and the mesoderm (middle layer) are called the primary germ layers. The embryonic tissue that gives rise to bones, cartilage and connective tissue is the mesenchyme (S. F. Gilbert, 2000). The mesoderm produces most of the mesenchyme, however also the neural crest, a specialised structure of the ectoderm, give rise to a small amount of mesenchyme (S. F. Gilbert, 2000). The mesenchyme in the neural crest can become specialised into craniofacial cartilage and bones. In higher vertebrates, the mesoderm is subdivided into different parts. The skeleton originates from three regions: the neural crest forms the skull, the vertebrae are formed by the somites, and the limb buds that will go on to form the limbs arise from the lateral plate mesoderm. The limb buds form at 4 weeks of gestation in the flank and are made up of a core of loose mesenchyme surrounded by the epidermis. Embryonic limb formation requires the interplay of two main signalling pathways: Wnt and TGFβ pathways (Decker, Koyama, & Pacifici, 2014; Khan et al., 2007). The limb bud formation is initiated by Wnt/β-catenin through Wnt2b/Wnt8c activity resulting in the stable expression of FGF10. Wnt3a then induces the expression of FGF4 and FGF8 at the top of the limb bud- the apical ectodermal ridge (AER), that produces a feedback loop with FGF10 in the mesenchyme that drives growth and proximodistal patterning. From the coordination of the AER and the zone of polarising activity (ZPA) located at the posterior limb mesenchyme, the limb starts forming. A common pattern for the limbs is set up with a long bone in the proximal region (stylopod) and two long bones in the intermediate part (zeugopod) to culminate in the distal part (autopod) with several small bones and typically 5 digits (S. F. Gilbert, 2000).

Each limb bud starts to grow and elongate during the sixth week: the mesenchyme gradually differentiates into models of the future bones composed of hyaline cartilage (S. F. Gilbert, 2000). In the continuous anlages of developing limbs, a region of condensed cells, called the interzone, forms at putative joint sites. Holder showed in 1977 that upon removal of interzone cells, joints do not develop in chick and bones remained fused (Holder, 1977). Wnt signalling is involved in the specification of the interzone: Wnt4, Wnt16 and Wnt9a (also known as Wnt14) are markers of synovial joint formation and joint fusion results from β-catenin removal from the interzone (Xizhi Guo et al., 2004; Hartmann & Tabin, 2001).

Cells at the centre of the interzone region undergo cell death to form the joint cavity while surrounding mesenchyme cells will form the articular capsule and supporting ligaments.

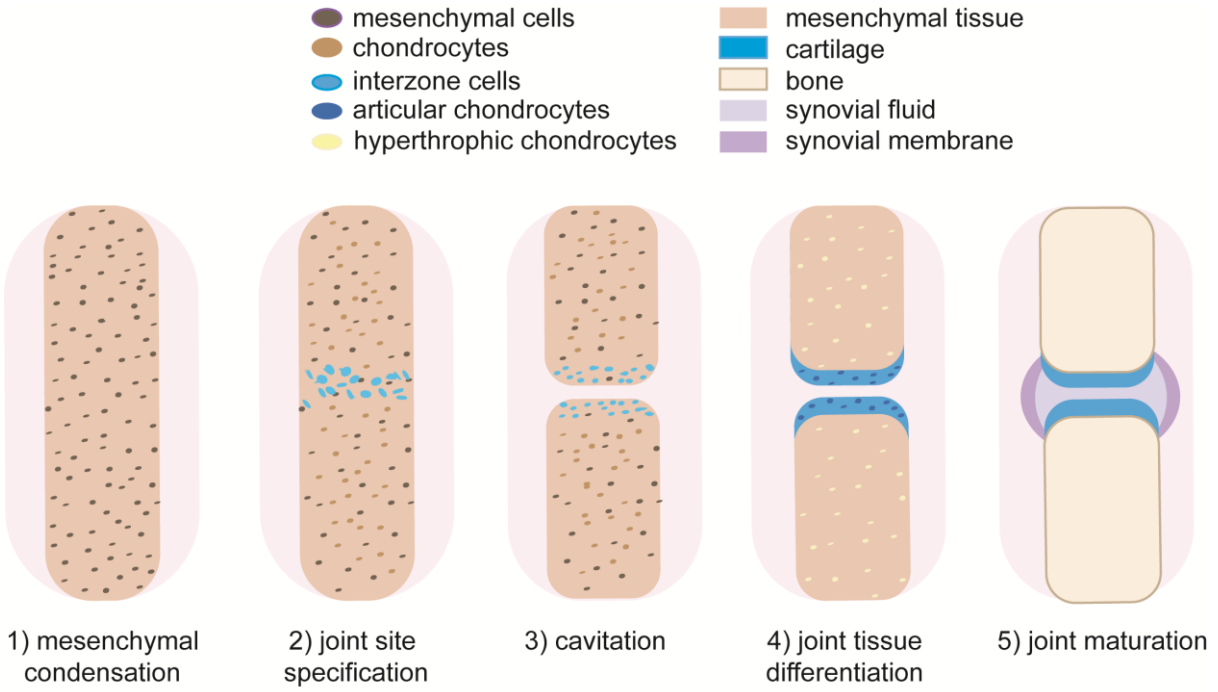

Figure 4 **Synovial joint development**.
The morphogenesis of synovial joint starts with 1) the condensation of mesenchymal cells which are present during endochondral ossification. 2) Highly condensate cells are present at the joint specification site, the interzone. Cells around the interzone start expressing Col2. 3) Cavitation occurs as the opposite ends of the interzone begin to differentiate into articular cartilage surfaces. 4) Cells start differentiating to give rise to different tissues including synovial membrane and articular cartilage and progressively 5) joint maturation is achieved. Adapted from (Decker, Koyama, & Pacifici, 2014).

The embryonic connective tissue is replaced by the skeleton in two main mechanisms: intramembranous and endochondral ossification (Shapiro, 2008). Intramembranous ossification occurs in the flat bones of the skulls and the clavicles. The mesenchymal cells differentiate into mature bone cells, osteoblasts. The osteoblasts secrete uncalcified bone matrix and then deposit calcium and other mineral salts, hardening the matrix. The osteoblasts then become resting cells on the surface of the bone with a smaller number becoming entombed in the bone matrix and termed osteocytes. In time, a layer of dense connective tissue (periosteum) is formed around the bone, while the centre gets infiltrated with blood vessels to form red bone marrow.

The process of endochondral ossification converts the early cartilaginous structures into long bones through a longer process: most bones of the vertebrate body are formed by this process. After birth, the ossification process of long bones is mostly complete and hyaline cartilage is only present at the end of bones of synovial joints. According to the current model, the precursor mesenchymal cells differentiate into "early chondrocytes" that form the embryonic hyaline cartilage structures. Starting from the primary ossification centre, at the centre of the prospective bone, early proliferative chondrocytes undergo differentiation to hypertrophic chondrocytes. The terminally differentiated hypertrophic chondrocytes undergo apoptosis and the calcified matrix is invaded by blood vessels along with osteoprogenitors and osteoclasts and is replaced by bone and marrow.

1.4.1 Current understanding of cartilage development

Cartilage development starts at the embryonic stage, however, the molecular mechanisms and their organisation are not fully understood. How cartilage develops has been discussed for many decades, but only recently *in vivo* genetic tracing studies in mice have shed light on the origin of chondrocytes precursors and how they originate embryonic and adult cartilage.

The main question about cartilage development revolved around a few major points:

- Which are the cells from the interzone that give rise specifically to the joint articular cartilage?
- How and when do cartilage cells differentiate from the progenitors to form an organised structure?

In 1996 Storm and Kingsley showed that the condensating cells in the interzone overexpress growth differentiation factor 5 (Gdf5) (Storm & Kingsley, 1996), more recently genetic tracing studies in mice showed in Gdf5-Cre reporter mice that cells of all mature joint components originate from Gdf5-expressing lineages (Koyama et al., 2007, 2008; Shwartz et al., 2016).

From Gdf5 expressing cells derive chondrocyte cells with different lineages. Depending on receiving Wnt signalling, and not BMP, Gdf5 cells are competent to differentiate into articular cartilage (Ray, Singh, Sohaskey, Harland, & Bandyopadhyay, 2015).

In the past three years, three new lineage tracing studies in mouse have advanced our understanding of cartilage development from embryonic progenitors to mature chondrocytes. Although the presence of cartilage stem cell has for a long time been postulated, a marker to genetically study these cells has been elusive for a long time. Many studies have suggested the presence of a stem cell population in the superficial zone of cartilage, which expresses among others PRG4 as previously described in paragraph 2 of this chapter. Three independent studies have described how PRG4+ cells not only self-renew and are positive for stem cell markers, but they also differentiate into chondrocytes in postnatal knee joints (Decker et al., 2017; Kozhemyakina et al., 2015; Li et al., 2017). Despite showing that this stem cell population is present in juvenile-adult mice cartilage, Decker et al. (Decker et al., 2017) reported that in response to cartilage injury the PRG4+ cells nor their progeny proliferate, whereas the PRG4+ cells in the synovial lining significantly grow in number and are found at the site of repair. Because of this observation, both Decker et al. and Chagin et al. (Chagin & Medvedeva, 2017) argue that PRG4+ cells present in cartilage do not take part in cartilage regeneration. However, proliferation is not necessarily a positive response to injury. As shown by Zhang et al. (Minjie Zhang et al., 2016), cell death induced by diphtheria toxin in the superficial cells before inducing cartilage degeneration, provides protection from degeneration. It is not impossible that the role of chondroprogenitors in cartilage repair is not just to proliferate and replace damaged chondrocytes, but perhaps maintaining homeostatic signalling to prevent matrix catabolism and inflammation. The study suggests that tissue degeneration is caused by cells catabolism and not by chondrocytes proliferation.

1.5 Cartilage defects and degeneration

Adult articular cartilage is limited in its ability to self-repair. Lesions in articular cartilage are thought to be caused by trauma (generally focal lesion) or could be due to degeneration ('wear and tear' or degenerative lesion). Particularly common in the knee, lesions like a tear or a fracture tend to be undiagnosed. With cartilage being an aneural tissue, a lesion can be asymptomatic and therefore left untreated for long periods. Cartilage defects of both kinds may cause pain, loss of function and could lead to long term complications, like OA (Palazzo, Ravaud, Papelard, Ravaud, & Poiraudeau, 2014).

OA is a disease that affects the whole joint, not only affecting articular cartilage but also subchondral bone and synovium. It causes patients serious limitation of daily activities and as a result, affects significantly the quality of life. By 2020 OA is estimated to become the fourth-largest cause of disability worldwide and is already representing a major cost for developed countries, amounting to 1-2% of GDP (Wittenauer, Smith, & Aden, 2013). To date, approximately 10% of men and 18% of women above the age of 60 worldwide presents to their clinician with stiffness, pain, and limitation of movement as a result of OA (Wittenauer et al., 2013). Because older age and obesity are two of the main risk factors for OA, this social burden is destined to rise as a consequence of longer life expectancy and the obesity epidemic (Arthritis By The Numbers, n.d.; Wittenauer et al., 2013).

Many hypotheses to explain the aetiology of OA have been proposed. Historically, cartilage degradation resulting in OA was considered an inevitable consequence of old age, partly because of the age-related reduced production of collagens which is also observed in other tissues. OA risk factors include, in addition to age, obesity, sports injuries, and lack of exercise (Wittenauer et al., 2013). All these risk factors have such an effect on cartilage because regular movement and joint loading is required for optimal metabolic activity and regulates homeostatic pathways in articular cartilage (S. J. Gilbert & Blain, 2018; Vincent & Wann, 2019). At the latest OARSI meeting in Toronto (2019), Tonia Vincent and Frank Beier argued in a plenary session that OA is, in fact, one single disease with different underlying causes. Professor Vincent used the term "mechanoflamation" to indicate the combination of altered mechanical loading and inflammation that would lead to an inability to repair cartilage due to underlying factors, like age, genes, obesity, etc. However, clear mechanisms underlying OA

aetiology and development remain elusive and consequently, a clear strategy to prevent or heal this disease is currently lacking.

When articular cartilage is damaged its zonal architecture is compromised, cell clusters appear around the site of injury and are considered a hallmark of osteoarthritis. Cell clusters are defined as five or more cartilage cells residing in one large lacuna and their significance is still not fully understood (Lotz et al., 2010). This type of cell organization is well described in OA cartilage and it is thought to result through cells migrating from degrading matrix and then proliferating. The phenotype of the cells residing in cartilage clusters has not been thoroughly delineated, so it is not known if clusters are composed of clonal cell populations or heterogeneous chondrocytes and whether they include cartilage progenitors. As a consequence, it is not fully understood if cell clusters are simply the result of cell migration in response to damage or if they have a role in cartilage repair (Lotz et al., 2010). A recent study has suggested that cell clusters present in late OA stages in humans include cells with stem-like progenitors properties (Hoshiyama et al., 2015). OA cell clusters could be the result of chondroprogenitor proliferation or de-differentiation of chondrocytes to address cartilage damage and repair the lesion. In a recent study, Matthew Warman's group showed that the death of superficial chondrocytes protects from cartilage degeneration in a mouse model of OA (Zhang et al., 2016). This would indicate that the high cellularity found in OA cartilage is contributing to exacerbating matrix catabolism and OA development. When performing bone marrow recruiting techniques (one of the therapeutic techniques discussed in the next paragraph), surgeons remove defibrillated cartilage around the site of damage to provide a neat interface for the clot to interact with cartilage. Microscopically, OA cell clusters are probably removed with this operation and could contribute to creating a less catabolic environment and therefore aid tissue regeneration.

1.6 Therapeutic approaches for cartilage repair

Surgical replacement of the joint (arthroplasty) is the gold standard method for end-stage OA, first introduced in the UK in 1960s (Knight, Aujla, & Biswas, 2011). This surgical approach has been described as one of the most successful for its safety and efficacy. Despite its effectiveness in re-establishing patients' motility and reducing or removing associated pain, this solution presented some disadvantages. Joint

replacement lasts between 10 and 20 years, but when performed on patients aged 50 or younger, the likelihood of a revision surgery to substitute the artificial implant is high. This comes at a greater financial cost and further risks of complications for the patient. Revision total joint replacement surgeries are becoming more common as patients may undergo joint replacement surgery as young at 30 years old. Secondly, patients suffering from cartilage defects and/or OA are faced with many years of an increasingly painful and debilitating condition until a total knee replacement is prescribed. Symptom management and palliative cures are only partially able to reduce pain and return full mobility (fig. 5).

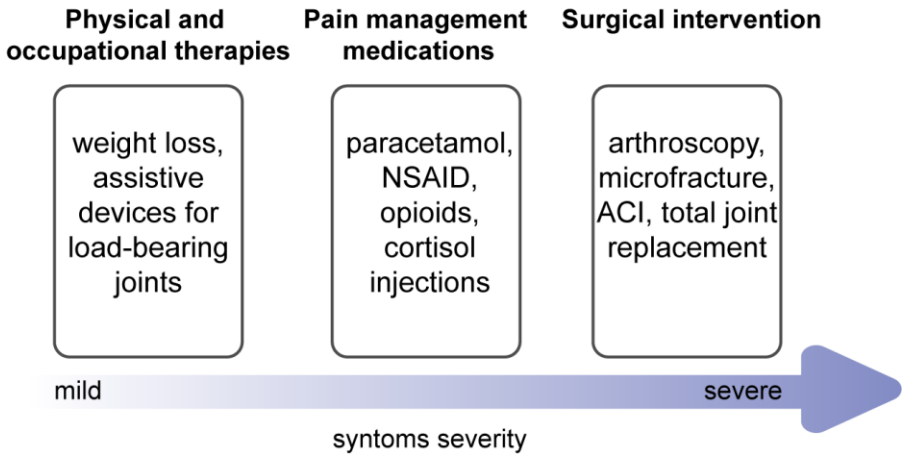

Figure 5 **Symptoms management and current treatments for patients with Osteoarthritis**
(Adapted from McAlindon et al., 2014).

To address this unmet clinical problem, alternative approaches have been developed to tackle the early stages of OA to repair cartilage damage (Mastbergen, Saris, & Lafeber, 2013). Several surgical methods and approaches such as subchondral drilling, microfracture, autologous chondrocyte implantation (ACI), MSC injections exploit relevant cell types to promote repair.

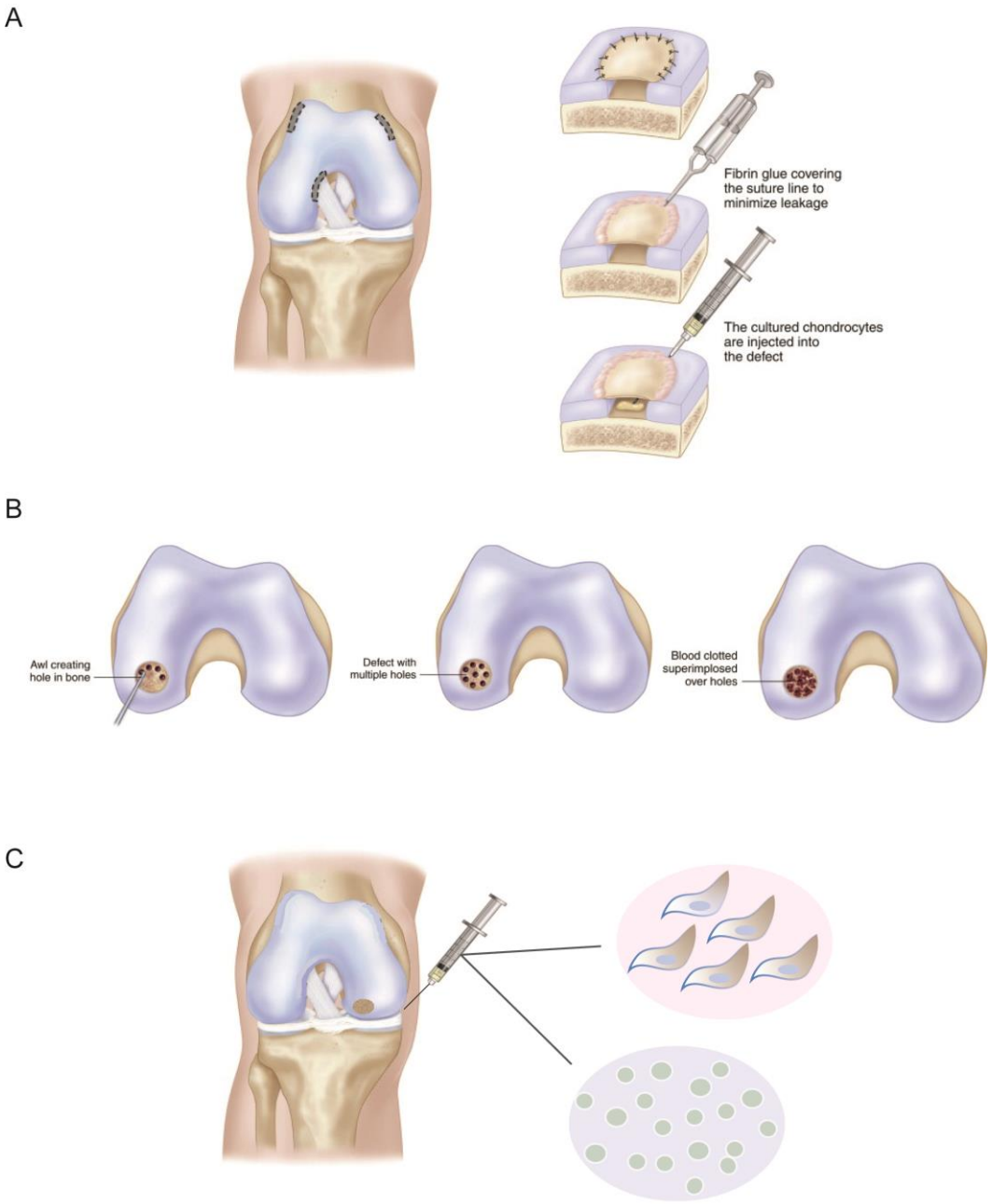

Figure 6 **Surgical and cellular therapies for cartilage repair**.
Novel approaches that are targeted to treat cartilage defects: a) ACI, B) Marrow stimulating technique and C) MSCs/EVs injections. Adapted from *Cartilage Surgery* by M. Brittberg and W. Gersoff.

1.6.1 Autologous chondrocytes implantation (ACI)

In 1994, Brittberg and colleagues described a two-stage method to heal moderate size cartilage defects (Brittberg et al., 1994). After inspecting the cartilage lesions, chondrocytes are harvested from non-weight bearing areas of the long bones and expanded ex-vivo. In a second stage, expanded chondrocytes from non-weight bearing areas of the long bones are transplanted into the defect (fig. 6A). Currently,

ACI is a standard procedure for the treatment of moderately sized cartilage defects of the knee and is recommended by the National Institute for Health and Care Excellence (NICE) and other international medical associations (*NICE*, 2017).

Follow up studies showed that although the repair is achieved, the resulting cartilage is fibrotic and has reduced mechanical properties. One of the reasons for the development of fibrotic rather than hyaline cartilage is the expansion phase of chondrocytes *ex vivo*. Chondrocytes tend to de-differentiated when expanded, resulting in an unstable phenotype (Benya, Padilla, & Nimni, 1978).

To overcome this issue, a couple of interesting approaches have recently been proposed. First, Saris and colleagues performed a one-stage procedure to repair chondral lesion by using a 10-90 or 20-80 mix of autologous chondrocytes and allogeneic MSCs in fibrin glue. The autologous chondrocytes were obtained from the debrided tissue to create stable borders at the site of the defect. Debrided cartilage was enzymatically digested and mixed with allogenic BMSCs. This proof-of-concept study showed that the procedure is safe and on follow up MRI the regenerated tissues looked well integrated. Hyaline cartilage was observed, indicating that the repaired tissues were similar or superior to the classic ACI technique (de Windt et al., 2017). Genetic analysis also showed that the regenerated tissue contained patient-DNA only, indicating that the allogeneic MSCs were not differentiating into cartilage but instead stimulated host tissue regeneration.

Another recent approach that tries to overcome the unstable phenotype observed when culturing chondrocytes *ex vivo*, is the use of nasal chondrocytes. A recent study published by Mumme et al., derived chondrocytes from nasal septum for ACI (Mumme et al., 2016). A study conducted in 10 patients with knee full-thickness cartilage lesions (2-6 cm^2) show that nasal chondrocytes have more stable chondrogenic phenotype during expansion *ex vivo*, less inter-donor variability and equal responsiveness to mechanical loading to chondrocytes from articular cartilage. After 2 years from surgery, the cartilage damages treated with nasal chondrocytes resulted in well-integrated regenerated cartilage from histological analysis in 3 of the 10 patients (Mumme et al., 2016). However, low patient number, no mechanical tests, and the absence of a control group are substantial limits to the conclusions that can be drawn from the study. A large multicentre clinical trial (including patients with late-stage OA) is underway (NCT02673905) to confirm the initial results. The authors of this work suggest that the different epigenetic signature of nasal compared to articular chondrocytes, probably

due to a different embryonic derivation, could explain the difference between the two cell populations.

1.6.2 Bone Marrow stimulating techniques

Subchondral drilling is a surgical technique first proposed for the treatment of OA by Pridie in 1959 (Pridie and Gordon, 1959). It is now a widely used marrow stimulation technique for articular cartilage repair in the clinical setting. Bone marrow stimulation techniques produce controlled bone damage and allow bone marrow and blood cells to accumulate at the joint surface, at the site of cartilage damage (Erggelet & Vavken, 2016) (fig. 6B). The underlying rationale is that by allowing MSCs contained in the bone marrow and other blood inflammatory cells to the damage site, a reparative environment can create and trigger repair. The outcomes of these techniques are similar to what is achieved with ACI, 5 and 15 years after surgery (Knutsen et al., 2007, 2016). Smaller size defect tends to heal quite well but fibrocartilage containing collagen type I is often formed, especially in larger defects, and the resulting cartilage is biochemically and structurally unstable. In addition, observed subchondral bone overgrowth (25%–49%) is often observed following subchondral drilling, which might hinder the long-term effect of this therapy.

1.6.3 MSCs as cell therapy

Friedenstein and colleagues suggested in the late 1960s that a subpopulation of cells present in the bone marrow were an adult reservoir of cells able to restore skeletal tissues (Friedenstein, Chailakhjan, & Lalykina, 1970; Friedenstein, Chailakhyan, Latsinik, Panasyuk, & Keiliss-Borok, 1974). MSCs were first described as a fibroblast-like stem cell subpopulation in the bone marrow, distinct from haematopoietic stem cells, able to give rise to skeletal tissues upon heterotopic transplantation. Caplan et al. in 1991 proposed the term “Mesenchymal Stem Cell” after showing *in vitro* differentiation of MSCs to cells of cartilage, bone, fat and muscle fate (Caplan, 1991). Since then, MSCs have been isolated from several other tissues: synovium, fat, placenta, Wharton jelly, heart, liver, etc. In an effort to create a consensus in the field about how to define MSCs isolated from different tissues, in 2006 the International Society for Cellular Therapy (ISCT) established that MSCs are plastic adherent cells that express the surface markers CD73, CD90 and CD105 and stain negative for CD14

or CD11b, CD34, CD45, CD79α or CD19, and HLADR. MSCs should show multipotency through their ability to differentiate into adipocytes, osteoblasts, myocytes and chondrocytes *in vivo* and *in vitro*, and be able to self-renew (Dominici et al., 2006). Currently, the idea that such defined MSCs are true progenitors of skeletal cell types of the mesodermal lineage is no longer considered accurate. Different studies have shown differentiation of MSCs into not only cells of mesodermal lineage other than skeletal, but also cells of ectodermal origin, such as neurons and epithelial cells. It is difficult to reconcile the exact implications of these studies. Mostly, they make the point that *in vitro* experimental conditions can lead to a variety of outcomes and artefacts.

Nevertheless, the ability to obtain cartilage tissues *in vitro* has made MSCs an interesting tool for cartilage regeneration As MSCs offer a less invasive approach to treat both cartilage lesions and OA. The use of MSCs to treat cartilage damage has been largely explored in recent years and is well summarised in a review article by Iijima and colleagues (Iijima, Isho, Kuroki, Takahashi, & Aoyama, 2018). The field has generally moved away from the assumption that MSCs would differentiate into chondrocytes and form *de novo* cartilage at the site of damage. In the clinical studies that explored the therapeutic effect of bone marrow-derived- or adipose-derived-MSCs, the isolated cells were administered as an intra-articular injection in the OA joint. After homing to the site of injury, MSCs are described to be present for only a limited amount of time and then no longer trackable. The disease-modifying effect detected in the damaged joints upon MSCs injection is thought to be due to the release of bioactive factors (growth factors, cytokines, miRNAs and mRNAs) that are immunomodulatory and trophic (Iso et al., 2007).

For this reason, Caplan himself has proposed to change the name from Mesenchymal Stem Cells to Medicinal Stromal Cells, arguing that using the term “stem” is not just inaccurate but misleading (Caplan, 2017). Recent reports have highlighted that MSCs are beneficial and result in cartilage repair not by undergoing chondrogenic differentiation. Hence the term “medicinal” and these cells are acting more like drugs in situ that stem cells.

1.6.4 Novel MSCs mechanism of action: extracellular vesicles (EVs)

Despite MSCs being described more than 60 years ago, the exact mechanism of action is yet to be fully understood. As MSCs are thought to mediate tissue repair via

paracrine signals, EVs have been suggested to be one of the mechanisms by which MSCs signal to other cells, other than through releasing growth factors and cytokines (Cosenza, Ruiz, Maumus, Jorgensen, & Noël, 2017).

EVs are membranous vesicles secreted by a number of different cell types, in both normal and pathological conditions, including MSCs, chondrocytes and bone cells. The term “EVs” is used as a general term to describe several types of vesicles that includes exosomes, microvesicles, and apoptotic bodies (van der Pol, Böing, Harrison, Sturk, & Nieuwland, 2012). These subtypes can be discriminated by their function and biogenesis. Because of their different origin, they display different membrane specific receptors that can be taken up specifically by other cells by ligand-receptor interaction to release intracellularly their cargo (van der Pol et al., 2012).

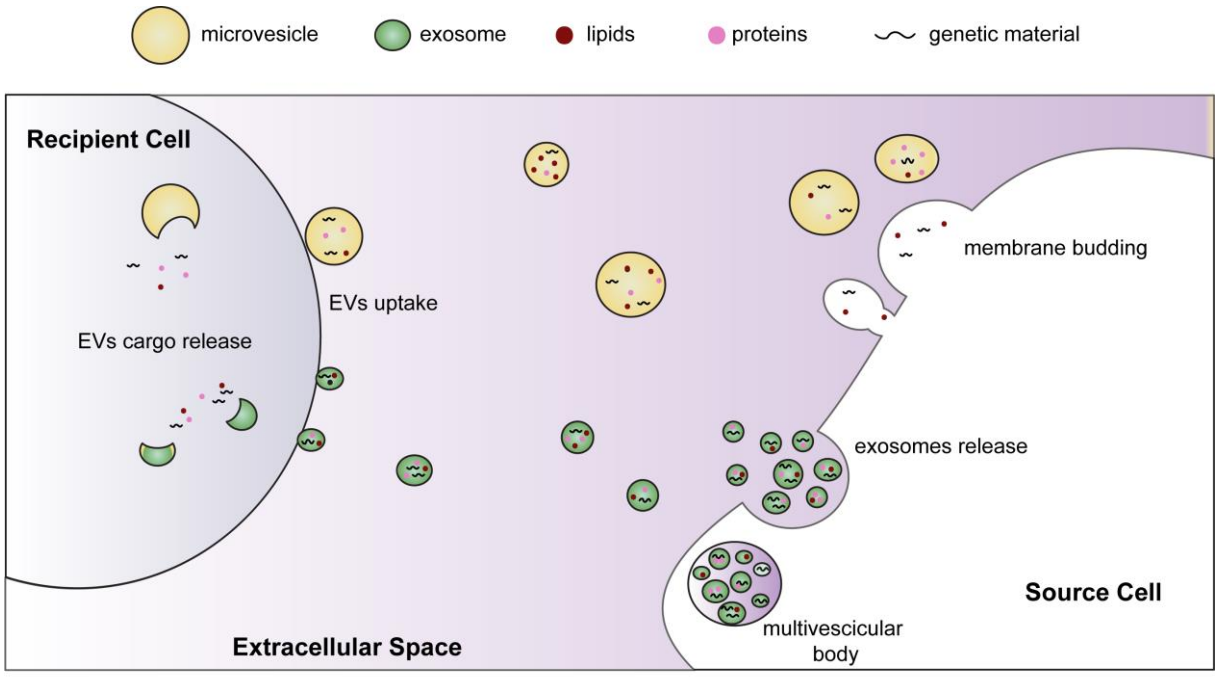

Figure 7 **Cell communication through EVs.**
EV cargo is sorted into two distinct EV populations: Exosomes or Microvesicles. Microvesicles are excreted in the intracellular space by membrane budding while exosomes are generated via inward budding of the multivesicular body. Cell communication through direct membrane fusion and release of EV contents into the target cell cytoplasm, or through endocytosis (original work).

Microvesicles and exosomes are specifically an interesting subtype of EVs as their role is primarily cell-cell communication (fig. 7). Exosomes are generally sized 30-150 nm in diameter and their function is to shuttle bioactive molecules to exchange information

between cells. The cargo is mostly composed of coding and non-coding RNAs, lipids, and proteins (van der Pol et al., 2012).

Currently, the use of exosomes derived from MSCs is being explored as an alternative therapy to MSCs transplantation for tissue regeneration (fig. 6C). The advantages are numerous: they have low immunogenicity, can be stored without losing function and have a long half-life, and being non-cellular are safer as a biological therapy (Lener et al., 2015). Already two studies using MSCs-derived EVs in human patients have been published. In one study EVs were administered to a patient suffering from steroid-refractory graft-versus-host disease (Bader et al., 2018), the other study evaluated their effect on forty patients with chronic kidney disease. In both cases, the treated groups showed no side effect but also a significant improvement of clinical symptoms. The MSCs derived EVs showed both immunomodulatory (anti-inflammatory) and regenerative (increased presence of progenitor cells) effects.

EVs are also studied in the context of cartilage damage and degeneration. In the last three years, the first studies showed that MSC-derived EVs indeed were able to induce osteochondral regeneration *in vivo* (Cosenza, Ruiz, Toupet, Jorgensen, & Noël, 2017; S. Zhang et al., 2018) and cartilage regeneration *in vitro* (Vonk et al., 2018).

1.7 Limits and challenges - what is missing to achieve the optimal repair.

Despite good outcomes of the listed therapies, a few shortcomings are linked to the techniques just described. First, the use of autologous cells in clinical therapy requires costly preparation and secondly, there is a lack of reproducibility between patients. In addition, the degree of repair is generally suboptimal (Knutsen et al., 2004). The quality of repair observed in various clinical trials using ACI, microfracture/subchondral drilling or MSCs cell therapy is highly heterogeneous and varies depending on age, sex, and most importantly size of the defect. It often displays fibrotic features and fails to reproduce the highly organised structure typical of hyaline cartilage which is instrumental to its ability to withstand loads and maintain the homeostasis of the tissue. This thesis argues that one important limitation preventing the development of a successful repair strategy is the lack of understanding of the cell and molecular biology of resident cartilage and their contribution to this repair. As discussed above, recent studies have highlighted how the superficial zone hosts chondroprogenitor cells. Superficial chondrocyte populations might, therefore, have very different behaviour

and therefore role in cartilage repair and in maintaining homeostasis than the chondrocytes from MDZ. Histogenesis, the process through which precursor cells form a tissue, and tissue repair share similar cell regulatory pathways. These signalling pathways drive stem cell specification to produce the target tissue. Extracellular signals are sensed and transmitted by signalling molecules, the effector proteins of molecular pathways, resulting in specific gene transcription. The regulation of such pathways in cartilage development and histogenesis is still incomplete and limiting our understanding of cartilage regeneration.

1.7.1 Developmental engineering

The idea of regenerative medicine and tissue engineering as a novel approach to repair tissues using stem cells in combination with intelligent materials and bioactive molecules has greatly revolutionized modern medicine. Only a few decades after the introduction of this concept, relevant solutions for tissue repair have been developed. The translation of cartilage engineered tissues into clinical settings has had however several issues. Again, effective production of therapeutic engineered tissues or regenerative cell therapies has been hindered by the limited molecular and cellular understanding underlying regeneration of this tissue. The term developmental engineering has been proposed as a novel approach. The idea is to harness our knowledge of developmental pathways and use this information to imitate the natural mechanisms that control cell differentiation to achieve tissue repair. Important molecular mediators of cartilage development, maintenance and repair are growth factors such as connective tissue growth factors (CTGF, or Cellular Communication Network Factor 2, CCN2), insulin-like growth factor (IGF)-1, fibroblast growth factor (FGF), transforming growth factor (TGF)-β, bone morphogenic proteins (BMPs), and other signalling proteins including indian headghog (IHH) and parathyroid hormone-related peptide (PTHrP).

1.7.1.1 CTGF

CTGF is a member of the CCN family of secreted proteins, which is an important inducer of ECM deposition and is expressed by chondrocytes in homeostatic and diseased cartilage (X. Tang et al., 2018). CTGF is known to drive the production of collagen type II and aggrecan (Aoyama et al., 2009). CTGF is also involved in cartilage

development as it stimulates chondrocyte proliferation and maturation of developing limbs (Ivkovic et al., 2003). CTGF KO mice do not survive after birth due to skeletal malformations (Ivkovic et al., 2003; Nuglozeh, 2017). CTGF was suggested to bind to TGFβ binding protein, and thus sequestering latent TGFβ in the matrix of cartilage in a heparan sulphate-dependent manner and controlling its release on cartilage injury (X. Tang et al., 2018).

1.7.1.2 IGF1

IGF-1 is a growth factor that shares 45% homology with insulin and is primarily produced in the liver, although is produced by many cells of the body, where it plays a role in embryonic development and postnatal growth. Immune cells, particularly lymphocytes and natural killer (NK) cells, are also responsive to IGF-1. IGF-1 has an important effect on cartilage as it regulates differentiation and apoptosis of ACs. In MSCs, administration of IGF-1 drives chondrogenic differentiation independently of TGFβ, and increased proliferation was also observed (Lara Longobardi et al., 2006). In support of the role of IGF-1 in proliferation, when antibodies against IGF-1 are added to chondrocytes, apoptosis is initiated in the cells (Loeser & Shanker, 2000). Different studies have reported increased production of proteoglycans *in vitro* upon administration of IGF-1 (Z. Zhang et al., 2017). In OA, the IGF-1 and IGF-1 receptor (IGFBP-3) are expressed in ACs and upregulated (J. A. Martin & Buckwalter, 2000; Olney et al., 1996). IGF-1 was incorporated in a scaffold for cartilage repair. *In vivo* animal model showed that the addition to IGF-1 to the scaffold was beneficial in a full-thickness cartilage defect for cartilage formation and integration (Z. Zhang et al., 2017).

1.7.1.3 FGF

FGF proteins are growth regulatory factors, and FGF2 is relevant to cells of mesenchymal origin, including MSCs and chondrocytes. FGF2 regulates MSCs growth and differentiation. For example, FGF2 is used in MSC culture expansion *in vitro* as it stimulates growth and the preservation of differentiation potential (Mastrogiacomo, Cancedda, & Quarto, 2001; Tsutsumi et al., 2001).

FGF2 has a different and contrasting role in murine and human cartilage OA, probably due to different FGF receptors present in different species (Xin Li et al., 2012). In

mouse, *Fgf2* has a chondroprotective effect. In OA mice models, both surgically induced and spontaneous, deletion of *Fgf2* exacerbate cartilage degradation (Chia et al., 2009; Vincent, Hermansson, Bolton, Wait, & Saklatvala, 2002). After cartilage injury, cartilage ECM releases FGF2 which shows chondroprotective effects in murine joints (Chia et al., 2009). In human, FGF2 induces catabolic changes in cartilage.

FGF2 activates signalling pathways through MAP kinases phosphorylation, that eventually results in transcription of target genes such as MMP13 (H.-J. Im et al., 2007; Muddasani, Norman, Ellman, van Wijnen, & Im, 2007). Through this mechanism, FGF2 was also found to was found to inhibit the synergistic anabolic effects of IGF-1 and BMP7 in human ACs (Loeser, Chubinskaya, Pacione, & Im, 2005).

FGF18 and FGF8 have been also been linked to cartilage homeostasis. FGF18 is an anabolic growth factor, affecting both chondrogenesis and osteogenesis depending on cell types (Moore et al., 2005; Ohbayashi et al., 2002). FGF18 in articular cartilage was found to reduce cartilage degradation and to have an anabolic effect on ECM deposition in rat post-traumatic osteoarthritis (Yao et al., 2019). FGF8 is growth regulatory factor that has a catabolic role in cartilage. When an anti-FGF8 antibody is injected into rat knee joints, ECM degradation is reduced, suggesting that FGF8 might play a role in cartilage degeneration in OA (Uchii et al., 2008).

1.7.1.4 TGFβ and BMPs

Another extensively studied growth factor in cartilage tissue-engineering is transforming growth factor-beta1 (TGFβ1), which is central in the development and differentiation of chondrocytes. TGFβ signalling has an important in the maintenance articular cartilage homeostasis alterations in the pathway leads to OA (Serra et al., 1997; Shen et al., 2013). The TGFβ superfamily, including TGFβ1, TGFβ2, TGFβ3 and bone morphogenic proteins (BMPs), have a major role in all stages of chondrogenesis. TGFβ is the key factor that drives MSCs differentiation to chondrogenic fate (Johnstone, Hering, Caplan, Goldberg, & Yoo, 1998). The SMAD- (the abbreviation refers to the homologies to the *Caenorhabditis elegans* SMA, "small" worm phenotype, and Drosophila MAD, "Mothers Against Decapentaplegic“ family of genes) dependent TGFβ signalling pathway is well understood. Type I and II receptors, also known as activin receptor-like kinases (ALKs) can start the signalling cascade. Signal transduction is initiated upon BMP ligand binding to ALK1, 2, 3 and 6, resulting in

SMAD 1/5/8 phosphorylation. Alternatively, TGFβ binds ALK 4, 5, and 7 which induce pathway activation SMAD 2/3 phosphorylation. The former is considered the TGFβ superfamily canonical signalling pathway (Tuli et al., 2003; Zhang, 2009). BMPs are regulated by different inhibitors that by competitively interacting with BMPs ligands block their binding to the receptor. These inhibitors include Noggin, inhibitory SMADs (SMAD6 and SMAD7), and SMAD Specific E3 Ubiquitin Protein Ligases (SMURFs), which can ubiquitinate BMP receptors as well as ligands (Itoh et al., 2001; Neul & Ferguson, 1998; Zhu, Kavsak, Abdollah, Wrana, & Thomsen, 1999). BMP2 enhances mesenchymal differentiation to the cartilage lineage through upregulation of the master regulator of chondrogenesis SOX9 (Jin et al., 2006). TGFβ signalling through the activation of the mitogen-activated protein kinase (MAPK) pathways results in stimulating chondrogenesis (Mu et al., 2012; Tuli et al., 2003; Zhang, 2009). SMAD turnover is critically regulated by the E3 ubiquitin ligases SMURF1 and SMURF2, which are recruited by SMAD6 and SMAD7. SMAD7 inhibits SMAD signalling, while SMAD6 acts selectively to inhibit the SMAD1/5/8 pathway.

BMPs are investigated to find an efficient dosage and mix of molecular cues to achieve proper MSCs differentiation into stable cartilage for cartilage tissue engineering purpose or used to induce repair of cartilage damage *in vivo*. BMP2 is expressed during mesenchymal condensation in limb development expression (Ducy & Karsenty, 2000) and is also expressed in adult MSCs (Kovermann et al., 2019). For cartilage reparative reasons, BMP2 use was explored in tissue engineering strategies with good reparative outcomes (Vayas, Reyes, Arnau, Évora, & Delgado, 2019). BMP6 has been shown to upregulate expression of cartilage ECM proteins such as namely type II collagen and aggrecan while inhibiting the expression of the hypertrophic chondrocyte marker, type X collagen (Estes, Wu, & Guilak, 2006). BMP7 also can induce matrix synthesis and promote repair in cartilage (X. Huang, Zhong, Post, & Karperien, 2018; Kuo et al., 2006).

Tissue engineering approaches to use TGFβ signalling to repair cartilage *in vivo* has shown promising results and is ongoing (Madry, Rey-Rico, Venkatesan, Johnstone, & Cucchiarini, 2014).

1.7.1.5 IHH and PTHrP

IHH is a member of the Hedghog family which is involved in cartilage development. IHH interacts with other major signalling pathways in joint and cartilage development, and its expression is regulated by a variety of peptides. The most well-studied peptide interaction is the IHH/PTHrP negative feedback loop. In the growth plate, IHH has a key role in regulating chondrogenic differentiation in concert with PTHrP. Pre-hypertrophic chondrocytes express IHH, and when its expression is altered, chondrocytes stop proliferating and undergo hypertrophic differentiation (Lanske et al., 1996). IHH induces the expression of PTHrP, establishing a negative feedback loop that affects the rate of chondrocyte differentiation (Lanske et al., 1996). PTHrP induces the expression of cartilage master regulator SOX9 and by increasing cell proliferation through induction of cyclin D1 (CCND1) (M. Zhang et al., 2009). In adult MSCs, PTHrP has been shown to induce chondrogenic differentiation and in chondrocytes (Fischer, Ortel, Hagmann, Hoeflich, & Richter, 2016; Kafienah et al., 2007), it prevented their hypertrophic differentiation (Bach et al., 2014). When injecting intra-articularly in osteochondral defects in animal models, PTH stimulated tissue regeneration *in vivo* (Kudo, Mizuta, Takagi, & Hiraki, 2011). PTHrP is key to maintain chondral phenotype in native cartilage, and its effect has been exploited to attempt to maintain the chondrogenic profile of in vitro expanded ACs for ACI (Rutgers et al., 2019).

1.8 DACTs: Wnt and TGFβ pathways regulators

1.8.1 Wnt signalling pathway

Wnt signalling pathways are initiated by Wnt proteins (a family of glycoproteins that includes 19 members in mammals) to regulate aspects of embryonic development, including chondrogenesis, and tissue homeostasis of all joint tissues (Lories, Corr, & Lane, 2013). Mutations in Wnt genes have been shown to be associated with skeletal malformations, osteoporosis, and dwarfism and more generally with joint disorders.

The canonical Wnt pathway transmits signals within cells by regulating the levels of cytoplasmic β-catenin. When Wnt proteins are not present, the β-catenin levels are kept in a steady state. When Wnt proteins are present and bind to their membrane receptors Frizzled (FZD) and low-density lipoprotein (LDL) receptor-related protein 5

and 6 (LRP5/6), a signalling cascade starts. In the canonical pathway, this cascade leads to β-catenin stabilisation, allowing β-catenin to translocate to the nucleus and upon binding to T-cell factor/lymphoid enhancer-binding factor TCF/LEF transcription factors result in the transcription of target genes. FZD binds to Dishevelled (DVL), which allows the recruitment of axin-GSK3 (glycogen synthase kinase 3) complex. This complex promotes the phosphorylation of LRP6 that inhibits the destruction complex (composed of AXIN, GSK3, DVL, and Casein Kinase 1), allowing β-catenin accumulation.

The non-canonical pathway is β-catenin independent and can be subdivided into the Planar Cell Polarity (PCP) pathway and the Wnt/Ca2+ pathway.

The Wnt pathways are shown in figure 8.

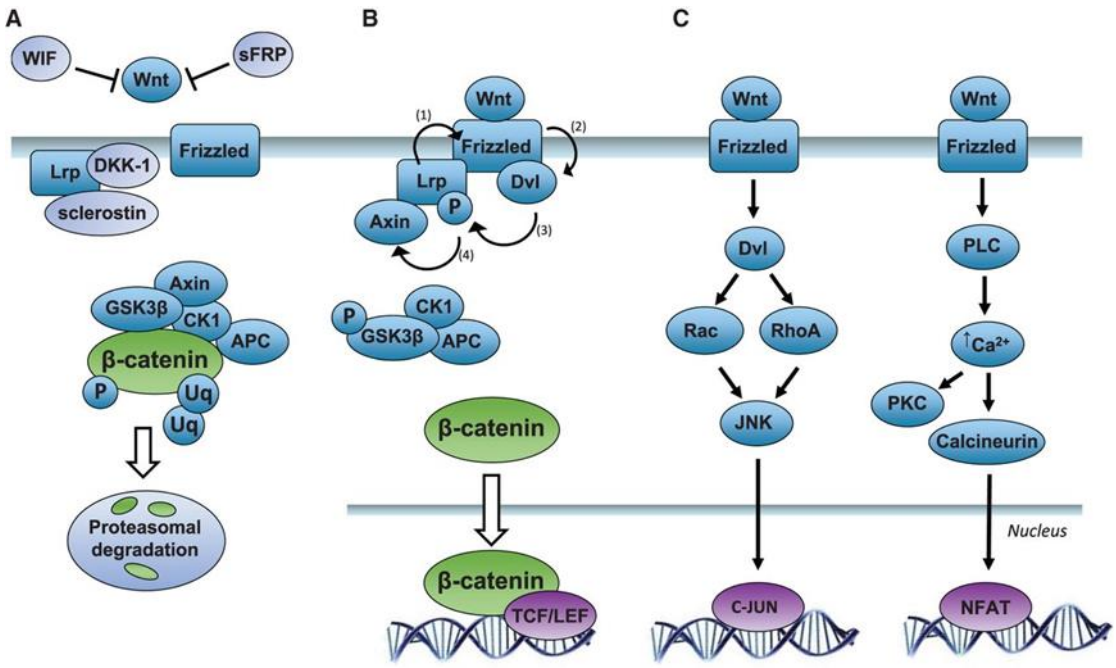

Figure 8 **Canonical and non-canonical WNT signalling pathways**.
When Wnt signal is not present (A), β-catenin is phosphorylated by a destruction complex consisting of APC, CK1, axin and GSK3β. This complex targets β-catenin for ubiquitination and then gets degraded by the proteasome. Depending on the ligand, FZD receptors activate the WNT canonical (B) or non-canonical pathways (C). Inhibitors of Wnt pathway can be Wnt inhibitory factor 1 (WIF), Secreted frizzled-related protein 1 (sFRPs), Dickkopf-related protein 1 (DKK1) and sclerostin. Binding of a Wnt ligand initiates a cascade of signals, starting with the recruitments of DVL which phosphorylates and activates LRP that then binds to Axin. The destruction complex is then dismantled so that dephosphorylated (active) β-catenin can accumulate and then translocate to the nucleus. In the nucleus, β-catenin binds to TCF/LEF to regulate the expression of Wnt target genes. Non-canonical pathways also rely on the Frizzled receptor. In the PCP pathway, DVL activate RAC and RHOA to regulate JNK activation (c, left). The Wnt/Ca2+ pathway does not rely on DVL and activates phospholipase C

to raise intracellular Ca2+ levels, which led to specific gene expression regulation. Image from C. Warboys (Warboys, 2018).

Wnt signalling is required during the development of all the tissues of the knee and involved in maintaining in an undifferentiated state, precursor cells (ten Berge, Brugmann, Helms, & Nusse, 2008). WNT3a is a key regulator of self-renewal, it maintains the potency of MSCs as well as improves their chondrogenic capacity (Boland, Perkins, Hall, & Tuan, 2004; Narcisi et al., 2015). It is possible that this is also true *in vivo*, as Wnt signalling is required to sustain the function and regulate chondroprogenitor rich cartilage SZ. Yasuhara et al. showed that by upon Wnt3a stimulus, SZ chondrocytes proliferate while maintaining PRG4 expression. If the β-catenin expression is blocked, proliferation and phenotypic expression are stopped (Yasuhara et al., 2011).

1.8.2 Wnt signalling and osteoarthritis

Alteration of molecules that belong to the Wnt pathway is involved in cartilage pathologies. Human genetic studies have identified genes for these molecules which are potentially linked to OA development. The gene sFrp3 codes for sFRP3 which a negative regulator of Wnt signalling. When a single-nucleotide polymorphism (SNP) is present in sFrp3, an increased risk for OA in weight-bearing regions of the joint is present (Loughlin et al., 2004; Min et al., 2005).

Despite signalling role for Wnt in maintaining the cartilage progenitor subpopulation, Wnt pathway activation results in the catabolic breakdown of cartilage matrix. Activation of β-catenin in articular chondrocytes in adult mice leads to the development of an OA-like phenotype (Zhu et al., 2009) and β-catenin levels are increased in human OA samples (Yuasa, Otani, Koike, Iwamoto, & Enomoto-Iwamoto, 2008).

Both negative and positive regulators of Wnt signalling are altered in OA.

Wnt1-inducible-signalling pathway protein 1 (WISP-1) is upregulated both in human and murine OA cartilage and synovium, regulating chondrocyte and macrophage MMP and aggrecanase expression (Blom et al., 2009).

Dickkopf-1 (Dkk-1) is a protein secreted by cells and inhibits Wnt/β-catenin signalling by binding competitively to the LRP5/6 co-receptors of FZD (fig. 8). DKK1 is present in plasma and synovial fluid at a lower concentration in OA patients (Honsawek et al., 2010).

Sclerostin is another inhibitor of Wnt which is deregulated in OA (fig.8) (Chan et al., 2011). Studies in OA mouse models suggested that Sclerostin plays a role in preserving articular cartilage integrity. In a Sclerostin knockout mouse, upon OA induction cartilage degradation is increased (Bouaziz et al., 2015). When Sclerostin treatment was applied to chondrocytes, Wnt canonical and non-canonical pathways were inhibited, preventing cartilage matrix catabolism (Bouaziz et al., 2015).
As previously discussed, mechanical loading is a central factor in OA development and progression (S. J. Gilbert & Blain, 2018). It is well established that Wnt pathways are modulated by mechanical loading but how exactly they contribute to cartilage degeneration is still unclear. Novel studies are unravelling the mechanism by which proteoglycans are sequestering Wnt ligands and suggest that blocking or reducing Wnt signalling could protect cartilage from degradation (Praxenthaler et al., 2018).

The regulation of the Wnt pathway in OA has been one of the main topics of research in the quest to find a therapy. Several inhibitors and modulators of Wnt signalling have been developed and are entering clinical trials, including OA treatment (Yazici et al., 2017). Further insight into the regulation of the Wnt pathway could greatly advance not only our current understanding of cartilage degeneration and repair but also offer novel targets for therapy.

1.8.3 DACT protein family

Dishevelled antagonist of β-catenin (DACT, or Dapper, or Frodo) are vertebrate proteins that were first described in Xenopus laevis and then in other organisms as binding protein of DVL, a cytoplasmic protein central to Wnt signalling (Cheyette et al., 2002; Gillhouse, Wagner Nyholm, Hikasa, Sokol, & Grinblat, 2004; Gloy, Hikasa, & Sokol, 2002; Hunter, Hikasa, Dymecki, & Sokol, 2006; Long Zhang, Gao, Wen, Ning, & Chen, 2006).
Three homologous proteins exist in humans: DACT1, DACT2 and DACT3 and each has been shown to have a different role in different tissue types. In zebrafish, DACT1 has an effect on the Wnt canonical pathway, whereas DACT2 has a greater impact on the Wnt/PCP pathway (Waxman, Hocking, Stoick, & Moon, 2004). In both zebrafish and mammalian cells, DACT2 can inhibit Nodal signalling by targeting for degradation TGFβ receptor, ALK4 (L. Zhang et al., 2004). Despite the documented role of DACT proteins in modulating both Wnt and TGFβ pathways, both fundamental regulators of

cartilage at different stages of development, adult homeostasis and degeneration, DACTs have not been studied extensively in joint tissues.

1.8.4 DACT1

DACT1 is highly conserved in vertebrate animals, suggesting its important physiological role. Dact proteins were first discovered in Xenopus laevis as a ligand of Dvl, which indicated its role as a Wnt pathway inhibitor (Cheyette et al., 2002).

The role of Dact in developmental biology was investigated in a classic mouse genetic knockout study by Wen et al. (Wen et al., 2010). Because Wnt plays a major role in embryogenesis, the study showed that Dact1 knockout has indeed a fundamental role: loss of Dact1 leads to embryological malformation in mice including neural tube defects, a shortened and/or curly tail, no genital tubercle, anorectal malformation, hydronephrotic kidneys, and loss of bladder. The severe posterior malformation observed in Dact1−/− mouse is explained by alteration of the Wnt/PCP pathway following high Dvl levels (Wen et al., 2010).

DACT1 is well studied in malignancies, as it has been found to be differentially expressed in many cancer types. In hepatic, gastrointestinal and non-small-cell lung cancer, Dact1 expression is reduced (Astolfi et al., 2010; Yang et al., 2010; Yau et al., 2005). In these malignancies, DACT1 seems to regulate the Wnt pathway by targeting for degradation DVL resulting in β-catenin cytoplasmic accumulation. On the other hand, in colon and squamous carcinomas, DACT1 is overexpressed and is suggested to regulate autophagy (Jian Hou et al., 2011; Yuan et al., 2012).

Several other studies on Dact1 have been carried out on cells from different tissues. DACT1 is also expressed in the brain. In mouse, Dact1 is expressed in the forebrain, and hippocampus of mouse embryos (Okerlund et al., 2010). It is thought to participate in neuronal maturation in a β-catenin-independent biochemical pathway. Dact1 also participates in the maturation of these neurons postnatally (Okerlund et al., 2010).

In cardiomyocytes, DACT1 regulates the non-canonical PCP pathway. DACT1 inhibition resulted in hypertrophy of cardiomyocytes and acts downstream of WNT5a.

In kidney cells, DACT1 was shown to be upregulated by TGFβ1 resulting in cell apoptosis (Jardim, Poço, & Campos, 2017).

In human and murine fat-derived-MSCs during *in vitro* adipogenesis, DACT1 expression is decreased. When DACT1 expression is knocked down, adipogenic

differentiation is blocked in a mouse cell line of pre-adipocytes. This suggests that Dact1 has a role in maintaining an undifferentiated phenotype (Lagathu et al., 2009)
Sirtuin 1 (Sirt1) acts as an inhibitor of MSC adipogenic differentiation by epigenetic regulation of different genes, including Dact1. Both studies were performed in mouse cell lines, and it remains to be shown if the same is true for human pre-adipocytes/fat-derived-MSCs (Zhou et al., 2016).
These studies illustrate how the role that DACT1 plays in modulating the Wnt pathway is highly dependent on cell and tissue contexts.

1.8.4.1 DACT1 in cartilage

Only a few published studies discuss DACT1 in cartilage tissues. The first published in 2014, links Dact1 and Dact2 to chick limb development (Sensiate et al., 2014). Dact1 expression is described in the undifferentiated limb mesenchyme at the region forming joints.
In a study by Chou et al., DACT1 was described to be downregulated in chondrocytes found in severely damaged human cartilage. This study compared the expression DACT1 in osteoarthritic cartilage from the weight bearing condyle to the non weight-bearing condyle of patients undergoing total knee replacement. DACT1 was downregulated in severe OA specimens (Chou et al., 2015).
Most recently, a small-molecule inhibitor of the Wnt pathway (SM04690) was developed by the company Samumed (San Diego, USA) and is being explored for the treatment of articular OA. On May 2nd 2019 it was announced that a Phase 3 clinical trial was underway ("Samumed Launches Phase 3 Lorecivivint (SM04690) Clinical Program in Knee Osteoarthritis"). In the work published by Samumed researcher Deshmukh and his colleagues, SM04690 was able to drive chondrogenic differentiation of BMSCs and when injected into a rat OA model showed cartilage regeneration (Deshmukh, Seo, Swearingen, & Yazici, 2018). The Wnt pathway inhibitor SM04690 acts by targeting two kinases, CDC Like Kinase 2 (CLK2) and Dual Specificity Tyrosine Phosphorylation Regulated Kinase 1A (DYRK1A), which result in the upregulation of DACT1 (Deshmukh, Seo, Swearingen, & Yazici, 2018). This pathway was however only tested in a colon cancer cell line.
Despite these interesting reports and involvement of DACT1 in cartilage, no work has yet shed light on the role and mechanism of DACT1 in chondrocytes or MSCs.

1.8.5 DACT2

As it can bind and facilitate Alk5 degradation, DACT2 has been described as a suppressor of TGFβ-dependent wound healing and Nodal-dependent mesoderm induction (Zhang et al., 2004). Dact2, mainly by binding to the Alk4/5 receptors, promotes their degradation (Zhang et al., 2004).

Dact2 expression is most prominent during organogenesis of the thymus, kidneys, and salivary glands, with much lower levels found in the somites and the developing CNS (Fisher et al., 2006). Compelling evidence of the different roles and activities of Dact family members was provided by the mouse mutant Dact2-/-. These mutant mice, not only are not affected during embryogenesis but also show no major abnormalities at birth (Meng et al., 2008). However, an effect on wound healing, probably resulting from TGF-β signalling was observed in Dact2-/- mice (Meng et al., 2008).

Similarly to DACT1, DACT2 is largely studied in cancer as its altered expression is associated with several different carcinomas. DACT2 mechanism of action differs in cancers that can be found in different tissues. DACT2 was showed to act as a cancer suppressor in breast cancer and it is often epigenetically silenced in affected patients (Guo et al., 2018). It acts by blocking the Wnt canonical pathway resulting in suppression of epithelial-to-mesenchymal transition. DACT2 is also a tumour suppressor gene in colon cancer through inhibiting Wnt/β-catenin signalling and the DACT2 gene shows hypermethylation in patients (Wang et al., 2015). DACT2 expression was shown to be reduced in gliomas. In glioma cells, DACT2 acts as a negative regulator of the Wnt canonical pathways by preventing Yes-associated protein translocation to the nucleus (Tan et al., 2017). DACT2 interferes with the TGFβ pathway in oesophageal cancer. Hou et al. showed that an increase in DACT2 correlates with poor survival of patients with oesophageal cancer (J. Hou et al., 2013).

1.8.5.1 DACT2 in cartilage

In limb development, Dact2 expression localised with Dact1, Sox9 and Gdf5 (Sensiate et al., 2014). Sensiate et al., suggest that Dact2 could act as an inhibitor of TGFβ signalling in the interzone, to suppress chondrogenesis and promote joint formation (Sensiate et al., 2014). Their work does not provide any mechanisms through which this might occur.

Recently, Dact2 was shown to be significantly more expressed in the superficial zone of articular cartilage (Mori, Chung, Tanaka, & Saito, 2014). Using laser microdissection of rat articular cartilage, Mori and colleagues were able to isolate SZ chondrocytes and compare their expression to deeper chondrocytes. Dact2 was among the 20 most upregulated genes in the SZ (Mori et al., 2014).

1.8.6 DACT3

The third Dact paralog is the most recently identified. When the Dact3 amino acid sequence is aligned to its paralogs, mouse Dact3 is more similar to Dact1 (27% alignment) then to Dact2 (24%) (Fisher et al., 2006). Dact3 is expressed in the limb bud and somites, as well as the central nervous system during development. A mouse mutant Dact3−/− was developed by Xue et al. showing that Dact3 is not as fundamentally important in embryogenesis as Dact1 (Xue et al., 2013). Mutant mice have a reduced body weight compared to wild type controls but mostly show a phenotype in kidneys where the loss of Dact3 results in renal fibrosis through regulation of the canonical Wnt/β-catenin pathway (Xue et al., 2013). Like its paralog *DACT1*, *DACT3* acts a regulator of canonical Wnt pathway and is transcriptionally downregulated in colorectal cancer (Jiang et al., 2008; H. Zhao et al., 2017). Currently, no study has studied Dact3 in cartilage.

2 Thesis Aims

The development of effective regenerative therapies to treat cartilage defects should derive from an in-depth understanding of the cell populations that participate in repair. In the context of bone marrow stimulation techniques to heal cartilage defects, understanding the contribution of resident chondrocytes to the repair is of great importance to implement the treatment, as it would allow stratification of patients that would determine best candidates for these regenerative approaches. Further progress must be made in understanding the mechanisms that regulate chondrocyte-progenitor (MSCs) interaction and communication. A better understanding of the differences between cartilage subpopulations and how these different chondrocytes regulate cartilage homeostasis and contribute (if they do) to repair. The specifics of such crosstalk are still largely undescribed, in particular, at cartilage subpopulation level. A better understanding of the differences between superficial and deeper chondrocytes is missing. In addition, because of the known importance of Wnt and TGFβ signalling in ensuring development and homeostasis of joint tissues, regulators of these pathways are optimal candidates for studying the regulations of progenitor cartilage cell populations.

Dact2 was identified in rodent cartilage to be significantly more expressed in the superficial zone. Given the presence chondroprogenitors in the superficial zone and the role of Wnt in maintaining MSCs in an undifferentiated state, the hypothesis is that DACTs might have an important role in pre-chondrocytes. To date, there is no thorough study of DACT proteins in cartilage homoeostasis and disease. DACT proteins could be interesting mediators of the cartilage reparative process as they are present in the superficial, stem cells/progenitors enriched zone of articular cartilage. A better understanding of how Dact proteins regulate early chondrogenesis and development would also help to unravel the molecular mechanisms that are also relevant in adult repair.

The aims of this thesis are therefore:

1. To resolve at a subpopulation level the cell communication in a model of subchondral drilling (Chapter 4).

Objectives:

- Develop an approach to reproducibly isolate chondrocyte subtypes based on distinct cartilage zones.
- Determine the cytokine profile secreted by cartilage from different zones.
- Study the miRNA cargo of EVs produced by chondrocytes from different zones.
- Analyse the influence of chondrocytes from different cartilage regions on MSC chondrogenesis.

2. To determine the presence of DACT1 and DACT2 in articular development and adult knees (Chapter 5).

Objectives:

- Study DACT proteins expression in different joint tissues at different point of development:
    - In adult human healthy and osteoarthritic articular cartilage and synovium.
    - in mouse developing joints and juvenile joints.
    - In bone marrow-derived- and synovium-derived-MSCs.

3. To investigate the role of DACT1 in MSCs (Chapter 6).

Objectives:

- Determine DACT1 and DACT2 expression in MSCs chondrogenic differentiation
- Elucidate the role of DACT1 and DACT2 by RNAi.
- Individuate Dact1 targets by RNA sequencing.
- Uncover the molecular mechanism that regulates DACT1 in MSCs.

3 Methods

3.1 Cell isolation and culture

Cells and tissue work were carried out in standard aseptic technique in a Category 2 certified biological safety cabinet. Cells were incubated at physiological 5 % CO_2 and 21 % O_2, and 37 ℃ humidified temperature. Cell culture media was changed twice per week during cell expansion. For long term storage, cells were cryopreserved in liquid nitrogen. For cryopreservation cells were re-suspended in a specific cryopreservation medium (FCS, 10% dimethyl sulfoxide, DMSO (Sigma) and transferred in cryovials. When required, cells were thawed in 37 °C water, transferred to complete media and media was refreshed the following day.

Passaging of cells was performed at 70-80% confluence by adding pre-warmed TrypLE Express (Thermo Fisher Scientific) to detach cells from plastic. Cells were recovered from suspension by pelleting at 300 x g for 5 minutes and then resuspended for counting or seeding. Cells were then counted manually using Glass Slide 10 with Grids (Kova International). Cells were seeded at a concentration that would ensure 40% confluence (for MSCs, 4,000 cells/cm^2).

When cells were obtained from patient tissues, that was done in accordance with Addenbrookes hospital ethics directives. All tissue samples were collected after obtaining written informed patient consent under the Cambridge Local Research Ethics Committee approval (No. 06/Q0108/213)

3.1.1 Isolation and Culture of human MSCs from Bone Marrow

Human bone marrow-derived MSCs (BMSCs) used in the thesis were either purchased from Lonza or isolated from patients' tissues.

Adult human MSCs were obtained from bone marrow femoral biopsies of donors undergoing total knee replacement. Upon given informed consent from donors, about 5 mL of bone marrow wash-out from the femoral bone was filtered in 70 µm filters (MACS) and then seeded on plastic flask in alpha-MEM (GIBCO) supplemented with 10% FCS, 25 µg/mL ascorbic acid-2-phosphate, 1 ng/mL FGFb (AbD Serotec), penicillin-streptomycin (Thermo Fisher Scientific) (From now referred to as MSC Expansion Medium). 48 hours after seeding unattached cells and debris were removed. MSCs between second and third passage were used in the experiments and

passaged After 4-5 days colonies were observed and enzymatically detached and expanded. BMSCs obtained from patients used in this thesis were not characterised by antigen marker profile, other cells isolated with the same method in the laboratory were phenotypically characterised and resulted positive for CD105, CD166, CD29, CD44 and negative for CD14, CD34, CD45, confirming they are MSCs. Pre-characterised human mesenchymal stem cells (Lonza) were also used. The supplier ensures multipotency at least till passage 5, and the cells express the essential markers according to the international standards for MSCs. Lonza BMSCs were used at passage 4-6 in the experiments.

3.1.2 Isolation and culture of human Synovial Membrane-MSCs

MSCs from synovial membrane tissue (SynMSCs) were obtained from the synovium lining the fat pad of patients undergoing total knee replacement at Addenbrooke's hospital. The synovial membrane was washed in Phosphate-Buffered Saline (PBS) and cut in small pieces before being incubated overnight in 2 mg/ml Collagenase A (Roche, Germany) at 37 ℃ on a shaker. The following day, the cell suspension was filtered through a 70 um filter and single cells were plated at 10,000 cells/cm^2 in MSC Expansion Medium. After 48h, cell debris and cell in suspension were removed and new medium was added to the attached cells. Once colonies formed, cells were passaged and expanded or directly used for experiments. Medium renewal was done twice weekly and cells were passaged up to passage 3 for the experiments when they reached 80% confluence.

3.1.3 Chondrogenic Differentiation

One of the key characteristics of MSCs is their ability to undergo tri-lineage differentiation *in vitro* when specific morphogenic stimuli are present. To determine the ability of MSCs to undergo chondrogenic differentiation, the following protocol was followed.

Before reaching confluence, MSCs were harvested and 250,000 cells were pelleted in a 15 mL plastic tube at 300 x g for 8 min. Pellets were cultured in chondrogenic medium containing DMEM-high-glucose GlutaMAX+ (GIBCO), 1:100 insulin, transferrin, and selenium (ITS+: BDBiosciences), 40 µg/mL L-proline (Sigma-Aldrich), 1 mM sodium pyruvate (GIBCO), 100 nM dexamethasone (Sigma-Aldrich), 10 ng/mL transforming growth factor β1 (TGFβ1, R&D Systems), penicillin-streptomycin. The medium was

refreshed twice a week. For the co-culture experiments, MSCs between passage 4-5 were used; these still possessed tri-lineage differentiation potential (as certified by the producer). Pellets were transferred to a trans-well for starting co-culture 24 hours after preparation or kept in culture for 24 days in DMEM with additional 10% FCS.

3.1.4 Isolation and Culture of Human Chondrocytes from Superficial, Middle/Deep and Osteoarthritic Articular Cartilage

Articular cartilage was obtained from different patients undergoing total knee replacement, following full consent from the donor to participate in the study. Within 2 hours of the operations, superficial and middle-deep cartilage chips of 150-200 µm were obtained with a dermatome (Swann-Norton, UK) from the “control” cartilage condyle, lateral condyle, hereafter referred to as superficial zone (SZ) and middle-deep zone (MDZ) chips. The use of lateral condyle when macroscopically non affected by OA is a generally used and valid approximation as showed by genome studies (Tachmazidou et al., 2019). From cartilage presenting fibrillated osteoarthritic parts, chips were removed around the fibrillations. Chips from fibrillated osteoarthritic regions of the cartilage are indicated osteoarthritic zone (OAZ) chips. Full-thickness cartilage samples were also obtained for evaluating tissue histological features.

Part of the chips was digested overnight in 6mg/mL Collagenase A (Roche) on a shaker at 55 rpm at 37 °C 5% CO_2. The following day, the digested cartilage was strained with a cell strainer (70 µm pores) to ensure a single cell suspension and consequently seeded in Dulbecco's Modified Eagle Medium (DMEM, ThermoFisher) supplemented with 10% Fetal Calf Serum (FCS) and 100 U/mL Penicillin/Streptomycin (Invitrogen) at 8000 cells/cm^2 density. Chondrocytes from SZ, MDZ, and OAZ were cultured either in normoxic (21 % O_2) or in hypoxic (5% O_2) condition.

The remaining cartilage chips were transferred to a 24 well plate well containing 500 µl of DMEM supplemented with 25 µg/mL ascorbic acid-2-phosphate (Sigma-Aldrich), 1:100 insulin, transferrin, and selenium acid (ITS+, BDBiosciences), 100 U/mL Penicillin/Streptomycin (Invitrogen) and 50 µg/mL L-Proline.

3.2 Colony Forming Unit Assay

In vitro self-renewal capacity of progenitors present in the different zones was demonstrated by colony-forming unit fibroblast (CFU-F) assay. The CFU-F assay was

performed by seeding 100, 200 or 300 chondrocytes from each zone (SZ, MDZ, or OAZ) in DMEM in 6-well plates. The plates were incubated in the hypoxic incubator and refreshed twice a week. On the 10th day from plating, each well was washed twice with 1x PBS (Gibco) and then fixed for staining with 4% formalin for 20 minutes. After fixation, the wells were washed twice with PBS and a 1% Crystal Violet solution was added and left for 40 minutes incubation. Finally, wells were washed with distilled water to remove staining solution excess and plates left to dry. The number and size of the colonies were determined by using ImageJ (NIH). Chondrocytes at passage 1 were used for this experiment to prevent the loss of chondrogenic phenotype during passaging.

3.3 Co-culture of chondrocytes and MSCs

For co-culture conditions, a 0.8 µm pore transwell (Corning®*)* containing MSCs pellets (day 1) was inserted into the well containing different zonal chips. DMEM with 1% FCS and 100 U/mL Penicillin/Streptomycin (Invitrogen), referred as “basal medium”,was refreshed twice weekly and the harvested media from each condition (total of 1 mL) was conserved for downstream analyses or stored at – 70 °C. 21 days after pellet formation, the different components were harvested for gene expression analysis or for histology.

3.4 Proliferation and Viability Assays

3.4.1 XCELLingence

To measure cell proliferation, cells were seeded on E-Plates (ACEA Bioscience) and cell adherence was measured by an XCELLigence System RTCA DP. This device can provide a real-time measure of electrical impedance allowing to determine changes on the plate surface covered by cells rendered with a parameter termed “cell-index”. The cell-index can, therefore, be used as a measure of cell proliferation over time.

A blank reading (cell culture medium only) is first measured to blank the XCELLigence System, and then the cells are seeded onto the E-Plate well and left to settle for 30-40 minutes. Different cell concentrations were tested and final 4,000 cells/well were finally

used, with each condition performed in technical duplicate. The plate device was then inserted in the xCELLigence cradle and the measurements were carried out every 15 minutes for up to 96 hours, and medium refresh was performed once. Cell-index values were normalised at the time at which treatment was added, and exported using the XCELLigence RTCA software (v2.0).

3.4.2 CyQUANT Assay

Cell proliferation was measured with a second technique using the CyQUANTDirect Cell Proliferation Assay Kit (Thermo Fisher Scientific). The kit allows determining the number of living cells present in a well, both adherent and non-adherent, by linking a cell-permeant fluorescent dye to DNA. Because of the presence of a masking die in the solution, only alive cells are stained, and the assay can determine both proliferation and cytotoxicity.

To test for cell proliferation and cytotoxicity, MSCs were plated in a 96 well plate at cell density of 4,000 c/cm^2. On the day after plating, the cells were treated and the CyQUANT assay was performed after 24 h or 48 h. 100 µl of 2X detection agent, which contains CyQuant® Direct nucleic acid stain, CyQuant® Direct background suppressor I and PBS in 0.004:0.021:1 proportion, was added to each well containing cells and incubated at 37 °C for 1 hour. After the incubation, the fluorescence was measured at an excitation wavelength of 480 nm and emission of 520 nm using a FluoStar Optima plate reader (BMG Labtech).

3.5 Cell Imaging Techniques and Analysis

3.5.1 Standard Light Microscopy

Cell morphology was assessed and imaged using a phase-contrast Leica DM IRB Inverted Brightfield microscope. Images were acquired with a microPublisher 3.3 RTV camera.

3.5.2 Immunocytochemistry

Immunocytochemistry allows the visualisation of proteins using antibodies for specific target antigens. The unconjugated primary antibody, when added to fixed cells, is able to bind to a target antigen. A fluorophore-conjugated secondary antibody is then added and binds to the primary antibody for detection. In this research, secondary antibodies

were conjugated with AlexaFluor488 or AlexaFluor555 (Invitrogen). These are subjected to short-wavelength, high energy light which is absorbed and emitted to a lower energy as light of a longer wavelength. The light emitted from the antibodies that are binding with high specificity to a cellular protein is detected using a fluorescence microscope. This technique enables multiple secondary antibodies to bind to one primary antibody, to amplify the detection signal. However, there is a higher chance of background signals, due to antibody cross-reactivity or non-specificity. 4',6-diamidino-2-phenylindole (DAPI) (Sigma Aldrich) was used as a counterstain, as it binds to AT-rich regions of DNA within the nucleus.

MSCs and ACs were seeded in an 8-well Millicell® EZ Slide (Millipore) at a density of 1 x 1,000 cells/well. At the end of the experiment, the medium was removed and the cells were washed twice with PBS and fixed with 4% paraformaldehyde for 15 minutes. After washing twice with PBS, the cells were permeabilised for five minutes with 0.2% Triton-X-100. Blocking was performed for twenty minutes with 10% PBS-Goat serum (blocking buffer), before incubating with the primary antibody solution overnight at 4°C. Cells were then washed three times for 5 minutes with blocking buffer before incubating with secondary antibodies diluted in blocking buffer. To visualise actin in the cytoskeleton, a 20-minute incubation of Alexa Fluor® 555 Phalloidin (Thermo Fisher). Primary and secondary antibodies and concentrations used for immunofluorescence are listed in Table 1. A coverslip was adhered to the slide using ProLong® Diamond Antifade Reagent with DAPI (Invitrogen) and visualised using the SP5 confocal microscope (Leica) with a Retiga EXi fast 1394 camera (QImaging). Images were analysed using Q-Capture Pro 6 software, ICY and FIJI (De Chaumont et al., 2012, Schindelin et al., 2012).

Table 1 Antibodies used for immunocytochemistry

Antigen	ID	Species	Company	Dilution
Primary antibodies				
DACT1	ab51260	Rabbit pAb	Abcam	1:500
DACT2	ab79042	Rabbit pAb	Abcam	1:500
Type II Collagen	ab34712	Rabbit pAb	Abcam	1:500
β-catenin	C2206	Rabbit pAb	Sigma	1:500
Active β-catenin	05-665	Mouse mAb	Millipore	1:500
Secondary antibodies				
Anti-Rb Alexa Fluor® 488	ab150077	Goat	Abcam	1:1000
Anti-Ms Alexa Fluor® 488	ab150117	Goat	Abcam	1:1000
Anti-Ms Alexa Fluor® 555	ab150118	Goat	Abcam	1:1000

3.6 EVs study

3.6.1 EVs isolation

EVs were isolated from the supernatants of co-cultured BMSCs and cartilage chips. They are released in the medium by cell types in culture. The Total Exosome Isolation (from cell culture media) reagent (Invitrogen) provides a simple and reliable method of isolating and concentrating EVs. The EVs are forced out of solution so that can be extracted and then collected after short and low-speed centrifugation. The term “EVs” is used in place of “exosomes” when referring to the samples collected from this kit. Although the kit claims to be isolating exosomes, that cannot be considered through in light of recent evidence that to be defined as exosomes, a stricter analysis must be performed.

First, medium depleted of FCS was used that ensures that isolated EVs originate from the cells in the co-culture, and do not derive from the FCS that contains high levels of EVS. Collected media after 48 hours of co-culture was centrifuged at 2000 × g for 30 minutes to remove cells and debris. About 1 mL of supernatant was transferred to a new tube without disturbing the pellet, to which 0.5 mL of kit reagent was added. The solution was then mixed by vortexing for a few seconds to produce a homogenous solution. The samples were then stored at 4°C overnight. Centrifugation at 10,000 × g for 1 hour at 4°C was performed the following day. A clear pellet containing the EVs was visible in all samples, the supernatant was aspirated and discarded. The pelleted EVs were resuspended in 0.1 mL of PBS and kept at 4°C before used in downstream analysis.

3.6.2 EVs characterisation

3.6.2.1 Electron Microscopy (TEM)

TEM is a widely used technique in EVs studies and is indicated as a standard method for EVs morphological evaluation, as it provides images at nanometre resolution (Coumans et al., 2017). TEM allows to image samples to distinguish single EVs from non-EV particles. TEM uses a high energy beam of electrons instead of light to image a sample. The interactions between the electrons and the atoms of the sample can be used to observe nanometre sized features and molecules.

Negative staining using uranyl-acetate was used to visualise the EVs contained in the sample. A 10µl droplet of isolated EVs in PBS was pipetted directly to the support film on 300 mesh grids (Gilder Grids, UK). The grids are filmed with pioloform, carbon coated, and plasma etched before use. After a few seconds to allow adsorption of the EVs, the excess PBS was removed by touching the edge of the droplet with filter paper. A 10 µ droplet of 2% aqueous uranyl acetate (Agar Scientific, UK) was added to the grid and after a few seconds was removed with filter paper. The grid containing the EVs was allowed to dry completely before acquiring the images. The grids were examined on a Hitachi HT7800 transmission electron microscope (TEM) using an Emsis Xarosa camera with Radius software (Electron Microscopy Research Services, Newcastle University). Images were collected using an AMT CCD camera (Deben). To ensure the selection of representative images, an unbiased selection of zones of 3 different samples was imaged.

3.6.2.2 Nanoparticle Tracking Analysis (NTA)

NTA is another standard method to characterize EVs, as it allows to measure nanoparticles in suspension in the range from 10 – 1000 nm. NTA calculates the size of particles from their Brownian motion. Particles in the sample are visualized by the illumination with a laser beam and the scattered light of the particles is recorded by a camera. Using a dedicated algorithm, particles paths are registered. NTA can, therefore, inform about the size distribution and concentration of the particles present in the sample.

NTA was performed using a NanoSight LM10-HS microscope equipped with NTA software v2.3 (NanoSight Ltd., UK). Background extraction was applied and the automatic setting for the minimum expected particle size and minimum track length. 60 s recordings at 30 frames per second were taken for each sample, which was diluted at 1:10,000 in sterile filtered PBS (Sigma). 4 different set of measurements were performed on the same samples and only measurements with > 1000 completed tracks were analysed.

3.6.3 RNA isolation from EVs and concentration

Amicon Ultra-0.5 centrifugal filter units with Ultracel-3 membrane (Merck Millipore) were used to concentrate the RNA. The eluted RNA was top up to 0.4 mL with RNase-free water and the volume was added to the filter column. The tube was centrifuged at 4° C 14,000 x g for 88 minutes (JA refrigerated centrifuge). The filter column was then inverted into a new collection tube and centrifuged 8,000 x g for 2 minutes to collect the concentrated sample.

3.6.4 miRNA Nanostring Analysis of EVs-isolated RNA

NanoString is a method that provides a digital count of a mRNA or miRNA of interest in a given sample. That is achieved using colour-coded molecular barcodes that hybridizes to specific nucleic acid sequence. The total RNA isolated from EVs was profiled using the nCounter® Human v3.0 miRNA Expression Assay Kit (NanoString Technologies), based on miRBase v21. The code set incorporated 799 mature microRNAs and included 6 positive controls, 8 negative controls, 6 ligation controls, and 5 mRNA housekeeping controls (ACTB, B2M, GAPDH, RPL19 and RPLP0). Starting material comprised of 3 µl of concentrated RNA. Data normalization was performed using nSolver Analysis Software v2.5 (NanoString Technologies), with code

set content normalization to the top 100 microRNAs established using geometric means.

3.7 Gene expression Analysis

Quantitative real time PCR (RT-qPCR) and RNA sequencing methods were utilised to study the mRNA transcribed by cells of interest in different experiments.

3.7.1 RNA Extraction

To assess gene expression profile of BMSCs and chondrocytes in the different experiments, RNA was isolated from the cells in monolayer, retro transcribed to cDNA and analyzed by qPCR. The RNeasy Kit (QIAGEN, Germany) was used initially for experiments with BMSCs in monolayer.

RLT plus lysis buffer (QIAGEN, Germany) additioned with 1% β-mercaptoethanol was added at 4 °C to monolayer cells at confluence previously washed with PBS (phosphate buffered saline, GIBCO®). Cells were detached with a cell scraper and collected. Chondrogenic induced pellets were harvested at different time points. Pellets were washed with PBS, then transfer in RLT plus lysis buffer where they were manually homogenized. Cell lysates were stored at - 70 °C before proceeding to RNA isolation.

Following low RNA yield, especially from cartilage tissue and MSCs pellets, TRIzol (scientific name: guanidinium isothiocyanate-phenol-chloroform) reagent was used as extracting agent and isolation performed with the Direct-zol method. The Direct-zol method for RNA extraction is based on using the TRIzol: the phenol and guanidinium isothiocyanate act to denature proteins and cell lysis, while solubilising organic material. The chloroform allowed isolation of proteins, DNA and RNA by causing phase separation. Protein partitioned to the organic phase, DNA to the interface and RNA to the aqueous phase (Rio et al. 2010). The kit allows an on-column method to specifically isolate the RNA phase by binding to a membrane, improving yields. Kit reagents were prepared as per the manufacturer's instructions. Between 350 to 500 µl Trizol was used, depending on the cell number and as specified by the manufacturer. Cell lysates were thawed on ice and an equal volume of 100% molecular-grade ethanol was added and thoroughly mixed by pipetting. The mix obtained was applied onto a spin-column containing the RNA binding membrane. The spin-column was centrifuged at 14000

RCF for 30 seconds at room temperature and the supernatant discarded. The spin-column was washed twice with RNA PreWash in the same way. The spin-column was then washed at 14000 RCF for 2 minutes with RNA Wash Buffer. The spin-column was transferred to a Ribonuclease (RNase) free tube and eluted with 30 µl of RNAse free water.

3.7.2 RNA quality assessment

To obtain an accurate measurement of RNA quality and concentration for NanoString and RNAseq experiments, the isolated RNA was run using the Agilent RNA 6000 Pico Assay kit (Agilent) and the Agilent 2100 bioanalyzer. The kit allows a fast analysis of the RNA by using a specific chip. The chip used was prepared following manufacturer's instructions. Briefly, 550 µl of the RNA 6000 Pico gel matrix were placed on a spin filter, centrifuged at 1500 g and divided into 65 µl aliquots. After the addition of 1 µl of the RNA 6000 Pico dye concentrate, the gel-dye mix was vortexed and centrifuged at 13000 g for 10 minutes prior to analysis. The gel-dye mix was injected into the channel system of the RNA 6000 Pico chip by using the chip priming station followed by the addition of conditioning solution. After the addition of 5 µl marker to the ladder and sample wells, 1 µl of each RNA sample was added in the 11 designated sample wells, followed by the addition of 1 µl of diluted RNA 6000 ladder (Ambion) in the ladder well. The RNA samples and ladder were prepared by heating the samples at 70º C for two minutes. All the procedures were performed maintaining an RNAse free environment. The 2100Expert Software (Agilent) was used to analyse data (Assay selected: Total RNA Pico assay).

For Real-Time qPCR analysis, the RNA concentration of samples was determined using a NanodropND-2000 Spectrophotometer (Thermo Fisher Scientific). Purity was analysed from the 260/280 nm wavelength ratio.

3.7.3 Complementary DNA (cDNA) retrotranscription

Polymerase Chain Reaction (PCR) uses double-stranded cDNA for its reaction and cannot be performed using RNA molecules. cDNA was synthesized using the QuantiTect Reverse Transcription kit (QUIAGEN). A reverse transcriptase enzyme synthesised the first strand DNA from the single-stranded mRNA using an RNA template and three-prime (3') complementary primer. The required amount of RNA (500 or 1000 ng). Genomic DNA was removed by adding 2 µl of "gDNase Wipeout

Buffer2" and the mix was incubated for 2 minutes at 42 °C and placed on ice. Reverse transcription was performed by adding to each sample a mix containing dNTPs, the reverse transcriptase enzyme, and reverse transcription buffer (as per manufacturer instructions). The samples were then incubated for 30 minutes at 42 °C, and a final 3 minutes incubation at 95 °C was performed to inactivate the reverse transcriptase. The resulting cDNA was diluted in dH_2O as required, or stored at – 20 °C.

3.7.4 RT-qPCR

PCR can be utilised to determine the relative expression of a gene of interest between samples using the amplification products synthesized by reverse transcription (Wittwer et al., 1997, Schneeberger et al., 1995). RT-qPCR uses Sybr Green to provide a real-time measure of the amplification products. Sybr Green is a dye which binds to double-stranded DNA produced during the amplification of a target sequence by DNA polymerase during PCR. The advantage of RT-qPCR is that it has lower running costs, as it only requires primers for PCR. However, a drawback is that false positive signals can occur as Sybr Green could bind to dsDNA for example primer dimers or any genomic DNA/contaminants. It is of importance to ensure genomic elimination when synthesising cDNA, as well as designing optimal primer pairs and checking their melting curve post-experimentally.

The cycle threshold (Ct) refers to the number of cycles required for the signal to surpass the background fluorescence level. The Ct value is used to quantify relative gene expression, using the comparative Ct method. To bypass variables such are the amount of starting material and quality of RNA, a stable housekeeping gene is used and the Ct value of the gene of interest (GoI) is subtracted from that of the housekeeping gene (HK). Quantification of mRNA expression was performed on a BioRad C1000 Thermal Cycler instrument. Primers utilised in for RT-qPCR were obtained published papers or purchased from Sigma (see section 3.7.5.).

GAPDH, *HPRT*, *B2M* were used as housekeeping genes for MSCs and ACs to determine the abundance of a variety of genes (Ragni, Viganò, Rebulla, Giordano, & Lazzari, 2013). The most stable housekeeping gene in control and experimental conditions was chosen to calculate the relative expression of the gene of interest. Relative expression was calculated following the formula $2^{-\Delta Ct}$ formula (Schmittgen & Livak, 2008).

The following equations were used for the comparative Ct method:

$$\Delta Ct = CtGOI - CtHK$$

$$\Delta\Delta Ct = \Delta Ctsample - Ctcalibrator$$

$$\text{Relative quantification} = 2^{-\Delta\Delta Ct}$$

The calibrator sample was set to show level 1 of expression when PCR data are reported in the charts.

3.7.5 RT-qPCR primer design

The primers utilised in this thesis were either purchased or designed in house. Some primers sequences were obtained by published articles and checked using NCBI PrimerBlast (NIH). Custom primers and primers obtained from Sigma were validated by testing the primer pair on a serial dilution of cDNA isolated from a cell (HEK293 for DACT1) or tissue (cartilage) expressing the gene of interest. cDNA was serially diluted to a range from 0.4 to 100 ng per reaction. The cycling profile was performed as described below. Primers validation was considered satisfactory if the primer pairs produced a slope of −3.3±0.3, an R^2 of > 0.90, an efficiency of (100±15)%. The melt curve produced had also to show a single, well-defined peak at the same temperature for all points on the serial dilution. A table with the primers used in this thesis is reported below (table 2).

Table **2 Primers used for RT-qPCR**

Gene	Sense (5'-3')	Antisense (3'-5')
HPRT1	TGACACTGGCAAAACAATGCA	GGTCCTTTTCACCAGCAAGCT
B2M	Quantitec ID: QT00088935	
GAPDH	AATCCCATCACCATCTTCCA	TGGACTCCACGACGTACTCA
COL2	GGCAATAGCAGGTTCACGTACA	CGATAACAGTCTTGCCCCACTT
COL10	CAAGGCACCATCTCCAGGAA	AAAGGGTATTTGTGGCAGCATATT
PRG4	CTGGCCTGAATCTGTGTATTTTT	TTCTTCCAGGGCACTTCTGT
COMP	AACAGTGCCCAGGAGGAC	TTGTCTACCACCTTGTCTGC
SOX9	GCAGGCGGAGGCAGAGGAG	GGAGGAGGAGTGTGGCGAGTC
MMP13	AAGGAGCATGGCGACTTCT	TGGCCCAGGAGGAAAAGC
CCL2	Sigma ID: 6347 Ref.Seq. NM_002982	

CXCL12	Sigma ID: 6387 Ref. Seq. NM_001033886	
CXCL10	Sigma ID: 3627 Ref. Seq.NM_001565	
SEPRIN1	Sigma ID: 5054 Ref. Seq. NM_000602	
MIF1	Sigma ID: 4282 Ref. Seq. NM_002415	
IL6	TTCAATGAGGAGACTTGCCTG	ACAACAACAATCTGAGGTGCC
DACT1	GAAGAGCACCTGGAGACAGACA	GCCCCATCACTCAGCTCATAA
TAPT1	Sigma ID 202018 Ref.Seq. NM_153365	
USP46	Sigma ID: 64854 Ref.Seq. NM_001134223	
CDK6	Sigma ID: Ref. Seq. NM_001145306	
SMURF2b	Sigma ID: 64750 Ref.Seq. NM_022739	
CCND1	TATTGCGCTGCTACCGTTGA	CCAATAGCAGCAAACAATGTGAAA
JAG1	N/A	N/A
ID1	CCAGAACCGCAAGGTGAG	GGTCCCTGATGTAGTCGATGA
FZD	CGCTCATCGTGGGCATCACGT	GCCGGCTGTTGGTGAGACGAG

3.7.6 RNA sequencing (RNAseq)

RNAseq is a method to study the transcriptome of cells of interest at a given point in time. First, a library is prepared with a dedicated kit starting from the RNA isolated from the cells. The library is then sequenced, and the data obtained are analysed with dedicated bioinformatics tools.

BMSCs (Lonza) from 4 healthy patients (average age 27±5 years) were transfected with either siDACT1 or siCTRL (see section 3.8 for details). RNA was isolated from the cells 16 hours after treatment and RNA concentration and quality was assessed as described in Section 3.7.2. The isolated RNA was then handed to Dr Maike Paramor for analysing RNA quality, preparing the libraries and finally, the bulk sequencing was performed at the CRUK at the Cambridge Institute Genomics Core. Libraries were prepared using the Illumina Nextera XT DNA preparation kit. Libraries were pooled and run on the Illumina Hi-Seq4000 at the CRUK. RNA sequencing data were analysed by Dr Lila Diamanti, Stem Cell Institute Bioinformatics department.

3.7.7 Ingenuity pathway analysis

The biological targets of identified mRNAs from the RNAseq analysis were investigated using QIAGEN's Ingenuity® Pathway Analysis (IPA®). IPA® is a web-based

application for integrating data obtained from hi-throughput experiments as RNAseq. Top 300 up- and down-regulated genes (for a total of 300) as determined by a bioinformatical analysis performed by Dr Lila Diamanti, were uploaded in the IPA software. Interactions and networks between the uploaded significant genes were mapped to pathways, regulators, diseases, and functions based on direct/indirect and experimentally validated targets.

3.8 RNA interference (RNAi)

RNA interference (RNAi) is a technique that allows to transiently and efficiently knockdown the transcription of a target protein by introducing in the cells the antisense sequence of the target mRNA. The siRNA (the antisense RNA) is a 21 to 25 nucleotides long molecule that binds to the target mRNA. The double RNA molecule is then recognised by the RNase complex, RNA-induced silencing complex (RISC), which acts on the targeted mRNA to degrade it. This results in the reduction or loss in the expression of the protein of interest, as its mRNA is not transcribed. The siRNA is delivered to the cell by transfection using lipid-based delivery methods (Agrawal et al., 2003).

MSCs or ACs were seeded in at a density of 5,000 cells/cm^2 in the appropriate media. DACT1 or DACT2 siRNA, GAPDH siRNA and negative control siRNA were obtained commercially (Life Technologies) and diluted to a final concentration of 1 pmol/µL in Opti-MEM™. This was mixed with 1.5 µL Lipofectamine™ RNAiMAX Reagent (Life Technologies), also diluted in Opti-MEM™, and incubated for 15 minutes at room temperature. The siRNA-Lipofectamine™ complexes were added on the day after seeding to the cells and incubated for up to 6 days before protein or RNA was harvested for downstream analysis.

3.9 Protein analysis

3.9.1 DMMB assay

The 1,9-dimethyl methylene blue (DMMB) dye is a thiazine chromotrope agent that presents a change in the absorption spectrum resulting from the induction of

metachromasia when bound to sulfated GAGs. By adding this dye to the supernatant of chondrocytes of chondrogenic differentiated MSCs, rapid detection of GAGs in solution is made possible (Whitley et al., 1989; Chandrasekhar et al., 1987; Farndale et al., 1982).

A ratio of 40 µL of sample supernatant with 250 µL of dye made of 16 mg/litre DMMB (Sigma), 3 g/L Glycine (Sigma), 40 mM NaCl (Sigma) finally adjusted to pH 3 was used. The samples were placed first in triplicate in clear 96 well plates (Costar, Corning, NY) and later DMMB dye was added to the wells. Samples were analysed for absorbance at room temperature immediately after adding DMMB dye at 545 nm wavelength with the FluoStar Optima plate reader (BMG Labtech).

3.9.2 Proteome profiler cytokine array

The proteome profiler cytokine array (R&D systems) is a membrane-based antibody array that is used for determining relative levels of human cytokines, chemokines, growth factors present in a certain solution.

After 48h of co-culture between BMSCs (Lonza) and cartilage chips from either SZ, MDZ, OAZ, supernatant from the three different conditions was probed with the proteome profiler cytokine array kit. Particles and debris were removed from the lysate by centrifugation of the samples for 10 min at 300 x g. The membranes were blocked on a rocker for 1 h with a blocking buffer provided in the kit. 15 µL of Human Cytokine Array Detection Antibody Cocktail was added to each sample supernatant, mixed and left at room temperature for one hour. The supernatant and Human Cytokine Array Detection Antibody Cocktail mix solution were then added to the membrane and left overnight on a rocker at 4 °C. After one wash with the kit Wash Buffer and 4 washes with dH2O (each was for 10 minutes), Streptavidin-HRP was added to the membranes and left to incubate for 30 minutes at room temperature. Membranes were then washed as just described. 1 mL of the prepared Chemi Reagent Mix was added evenly onto each membrane and incubated for 1 minute. An X-ray film was used to detect cytokines, which was exposed to the membrane for 3 minutes.

ImageJ was used to measure the pixel intensities of each spot of the array. The average pixel intensity of each pair of duplicate spots was calculated and the averaged background was subtracted to determine the intensity of each cytokine. Determine the average signal (pixel density) of the pair of duplicate spots representing each cytokine.

3.9.3 Protein isolation and quantification

To isolate proteins from BMSCs, a lysis reagent was added to cell culture plates after washing twice with PBS. The lysis reagent was prepared with RIPA buffer (Millipore) with the addition of cOmplete Protease Inhibitor Ccocktail (Sigma) and PhosSTOP phosphatase inhibitor reagent (Sigma). 100 µL/10cm^2 of lysis reagent was added to culture cells, incubated for less than a minute and finally, a cell scraper was used to help detaching and cell lysis. The lysate was then transferred to an Eppendorf tube and stored at – 70 °C. The cell lysate was centrifuged at 14,000 x g for 15 minutes before analysis to pellet cell debris and supernatant transfer to clean tubes. Samples were aliquoted in smaller volumes to avoid excessive freeze-thaw cycles that might result in protein degradation.

The BCA assay was used to quantify protein to standardise the amounts loaded in Western blotting using a Pierce™ BCA Protein Assay Kit (Life Technologies). The BCA assay allows determining the concentration of the samples by running a standard curve of known concentration alongside. A working reagent comprising of BCA added to CuSO4 pentahydride solution (4 % w/v) in a ratio of 1:50. The standard curve was generated by diluting bovine serum albumin (BSA) in cell extraction buffer at a range of 25 to 2000 ng/mL. The samples were diluted 1:8 by mixing 25 µL cell lysate or protein standards with 200 µL of working reagent and incubated for at least 30 minutes at 37°C. The absorbance for samples and the protein standards were measured in triplicate at a wavelength of 562 nm using a FluoStar Optima plate reader (BMG Labtech).

3.9.4 Western Blotting

Western Blotting is a method used to detect and analyse proteins (Towbin et al., 1992, Burnette, 1981). After isolation and quantification of the proteins from cell lysates (section 3.9.3), the cell lysates containing the proteins are diluted in a loading buffer containing glycerol which increases the density of the sample, along with a dye to aid visualisation. The mixture is heated at high temperature to denature the proteins. That helps the separation by the size of the proteins through gel electrophoresis. A marker is also run alongside the samples to allow the molecular weight determination of the protein of interest. After electrophoresis, the resolute proteins are transferred from the gel to a polyvinylidene difluoride (PVDF) membrane. The membrane is blocked to

avoid nonspecific binding of the primary antibody. The protein of interest is specifically bonded by the primary-antibody, which is then visualised by adding the secondary antibody. The secondary antibody is labelled with a fluorescent protein that is detected by a dedicated imaging system.

3.9.4.1 Electrophoreis and membrane transfer

After determining the lysate protein concentration, an equal amount of total protein per samples was mixed with 4XNuPAGE sample LDS loading buffer (Thermo Fisher Scientific) and 10X NuPAGE reducing agent (Thermo Fisher Scientific) and denaturated at 80 °C for 10 minutes. The denaturated mix was then loaded onto a mini-PROTEAN TGX pre-cast gel 10-well 4-20% stain free gel (BioRad) alongside a ladder (Chameleon Duo Pre-stained, Licor). Gels were run at 250 V for 30 minutes in Tris/Glycine/SDS running buffer (BioRad). The proteins were transferred to a 0.45 µm PVDF membrane (BioRad) using the Trans-Blot Turbo semi-dry System for 7 minutes at 25 V.

3.9.4.2 Immuno-probing and detection

The membranes were blocked for unspecific bindings in Odyssey blocking solution diluted 1:1 in TBS (Thermo Fisher Scientific) for 2 hours. Primary antibody anti-ubiquitin (Abcam, ab7780) was diluted (1:500) in TBS buffer containing 0.05% Tween20 (Sigma) (TBS-Tween) and added to the membrane. The incubation was carried out overnight at 4 °C. After washing with TBS-Tween for 3 times, the blotted membranes were incubated with donkey-anti-rabbit IRDye800CW (ID:925-32213, Licor) diluted 1:15,000 in TBS-Tween. The secondary antibody was incubated for 1.5 hours before washing the membrane with TBS and imaging with ChemiDoc system (BioRad) in automated settings.

3.10 Mouse ex-vivo work

3.10.1 Animal husbandry

Animal husbandry was performed in accordance with the regulations described in the Animals (Scientific Procedures) Act 1986. Mice used were housed in the Phenomics animal facility, University of Cambridge, under the projet licence 70/8635, according to

Home Office requirements. Mice were housed in groups in individually ventilated cages under a 12 h dark/12 h light cycle and fed a standard diet. All animals used in this thesis are wild type C57BL/6 strain, supplied by Charles River. Legs of adult animals were obtained from Dr. Virginia Piombo.

3.10.2 Mouse chondrocytes isolation

Mouse articular chondrocytes were isolated from the cartilage of femoral heads obtained from the legs of adult mice (3-6 weeks old). The cartilage at the top of the femur bone was dislocated with forceps, applying a small pressure. The hip cartilage from 4-5 mouse femoral heads was then collagenase digested as described in section 3.1.4.

3.10.3 Collection and storage of mouse embryos

Mice at different embryological (E) stage were used in this study: E13.5, E14.5, E15.5, E16.5, E17.5. Mice were mated and the morning of vaginal plug formation counted as E0.5. Pregnant mothers were killed by cervical dislocation and embryos fixed overnight in 4% formalin (Sigma) in phosphate buffered saline (PBS).

3.10.4 Collection and storage of mouse limbs

Mouse limbs were donated as unutilised samples from Dr Virginia Piombo. The knees were resected with a scalpel, skin and muscle tissues were removed and washed with PBS. To preserve the tissues, fixation with 4 % formalin was performed overnight.

3.11 Histological tissue processing

Tissue processing is the collection of the steps required to perform a histological or immunochemical analysis of the tissue of interest. Human or animal tissues are first harvested, then a fixation step is performed to preserve the tissue. Subsequently, the sample is treated so that is infiltrated by a suitable histological wax and then embedded so that it can be cut in µm thick section that can be stained.

3.11.1 Sample preparation

Osteochondral samples were harvested from the condyles of both lateral and medial condyles of osteoarthritic knees. The samples were obtained by using a surgical tool that retrieves a cylindrical osteochondral plug. The samples were then washing in PBS, fixed in 4% formalin overnight before decalcification.

Synovial tissue was also harvested by the surgeons during total knee replacement. The synovial samples were resected with a scalpel from the fat-pad, recognisable by different texture and colour and washed in PBS. The tissue was fixed in 4 % formalin overnight before embedding.

3.11.2 De-calcification

In order to stain human and mouse knee samples a decalcification step is necessary to allow sectioning, which is hindered by the mineralised calcium present in bones. Ethylenediaminetetraacetic acid (EDTA) was used to achieve gentle de-calcification that preserved tissue morphology and protein epitopes for immunohistochemistry. 14 % EDTA (Sigma) at pH 8 was added to the samples, after washing them in PBS to remove formalin residues. Samples were incubated for 2-3 weeks until the bone tissue appeared soft when poked with a needle. Samples were washed for 20 minutes in water before proceeding to further preparation.

3.11.3 Embedding and sectioning

To analyse histologically or by immunohistochemistry, the tissues were embedded in paraffin (Sigma). Paraffin embedding was achieved by using a Leica TP1020 Tissue Processor. Samples were de-hydrated through sequential steps of 1 hour each 50%, 70%, 80%, 90%, 95% ethanol solutions and three final 100% ethanol steps for 1 hour. Two additional steps of 2 hours each in xylene (Sigma) were performed before the samples were immersed in paraffin wax at 60 °C, for 2 hours. All the steps were performed under vacuum to improve penetration in the samples. A Leica HistoCore Arcadia H Embedding Station was utilised to embed and orientate samples for sectioning.

5 µM sections of the samples were obtained using a microtome Leica BM2255 and dried onto Superfrost Plus Slides (Thermo Fisher Scientific).

3.11.4 Histological Stains and counterstains

Before staining, paraffin sections mounted on slide were re-hydrated. Slides were located on a hot plate at 60 °C for a few minutes until the paraffin wax surrounding the sample melted. The slides were then transferred in xylene for 10 minutes, and the same step was repeated a second time to ensure removal of the paraffin. Slides were then transferred to a 100% ethanol bath for 5 minutes, and then in solution in

decreasing ethanol concentration (95%, 90%, 80%, 70%, 60%, 50%, 30%) for 5 minutes each. Finally, slides were incubated in two 5 minutes step in dH_2O before starting the staining protocol.

3.11.5 Immunohistochemistry (IHC)

IHC allows to identify a protein on a tissue sample by using antibodies to detect the location of proteins and other antigens in tissue sections. The antibody-antigen interaction is visualised by adding a secondary antibody conjugated to an enzyme that catalyses a reaction to form detectable compounds. That allows to visualize and localize specific antigens in a tissue sample. Diaminobenzidine (DAB) was used as a substrate because in presence of peroxidase and hydrogen peroxidase it produces a brown alcohol-insoluble precipitate at the site of the reaction (where the protein was detected by the antibody). By applying a secondary antibody conjugated with horseradish peroxidase (HRP), DAB precipitation can indicate the location of the protein of interest.

After the re-hydration procedure, an antigen retrieval procedure was applied to unmask the epitopes of proteins, as the fixation and embedding producer can alter the structure of the epitope. A specific protocol was optimised to avoid detachment of the samples. Slides were submerged in a solution pre-warmed 10 mM of sodium citrate (Sigma) buffer adjusted to pH 6 containing 0.05% Tween. The solution was maintained between 70-80 °C by submersion in a heated water bath. Slides were then rinsed for 10 min in running tap water.

To block unspecific binding, a blocking buffer 10% goat serum (Vector Laboratories) in PBS containing 0.05% Tween20 (PBS-Tween) was added to the slide and left for 1,5 hours. DACT1 and DACT2 primary antibodies (Table 1) were diluted in TBS-Tween 1:500 added to the slides and incubated overnight at 4 °C in a humidified chamber. After overnight incubation, slides were washed three times 5 minutes with PBS before incubation with 3% hydrogen peroxide (Sigma) for 15 minutes. This step ensured that endogenous peroxidase activity is blocked so that non-specific or high background staining will not occur upon DAB incubation.

The Rabbit Specific HRP/DAB Detection Kit (Abcam) was used to detect the primary antibody (raised in rabbit) using HRP-labelled-streptavidin and a biotinylated anti-rabbit secondary antibody. The biotinylated secondary antibody was added to the slides and

left for 10 minutes before it was removed, and the slide washed 3 times with PBS. Then the HRP-labelled streptavidin was added and incubated for 10 minutes to allow the binding to the secondary antibody. 4 washes with TBS, of 5 minutes each were performed on the slides before incubating the slides with DAB. DAB was removed after 15 seconds by washing the slides with PBS. The incubation time was determined by blocking the incubation when the brown coloured deposition at the site of primary antibody binding was visible under the microscope. Samples were then counterstained with Methylgreen.

3.11.6 Methylgreen counterstain

Methylgreen is used as a counterstain for the non-matrix structures and cell nuclei (Miyaki *et al.,*1994). Following IHC, slides were washed in dH_2O for 5 minutes before they were submerged for 5 minutes in methyl green (Sigma) solution pre-heated at 60 °C. Three washes in tap water were then done before dipping for a few seconds the slides in acetone containing 0.05% acetic acid. Sections were de-hydrated through 95% and 100% Ethanol solutions for 2 minutes each. Two changes in xylene for 5 minutes were then performed before mounting a glass cover slide with DPX Mountant for histology (Sigma) on each slide.

3.11.7 Safranin O/ Fast Green

Safranin O is a basic dye that stains cartilage matrix in red, at intensity proportional to the proteoglycan content in the cartilage tissue (Miyaki et al., 1994). Fast Green is used as counterstain for the non-matrix structures and cell nuclei.

Following rehydration, sections were stained for 10 minutes with Weigert's iron haematoxylin working solution (sigma) and then washed for 10 minutes with running tap water. The slides were then stained with 0.1% Fast Green FCF (Sigma) solution for 5 minutes and moved to a 1% acetic acid solution for 10 seconds. Finally, samples were stained with 0.1% SafraninO (Sigma) solution for 5 minutes, before being de-hydrated for 5 minutes in 100% EtOH for two times, and then cleared in two steps of xylene for 10 minutes in total. The slides were mounted with a glass cover slide with DPX.

3.11.8 Thionin

Thionin is a metachromatic dye that stains in purple/blue glycosaminoglycans to visualise the amount of matrix produced by cells. It is particularly used to determine the chondrogenic differentiation of MSCs in 3D pellet culture.

Deparaffinized and rehydrated slides were stained with a 0.5% thionin acetate salt (Sigma) solution for 5 minutes before dehydration in a 95% EtOH and two 100% EtOH (30 seconds each) changes. Two changes in xylene for 5 minutes were then performed before mounting a glass cover slide with DPX.

3.11.9 Toluidine Blue

Toluidine Blue is a cationic dye that stains cartilage matrix proteoglycans and nucleic acids. The staining properties of Toluidine blue may vary according to the solution pH. Like thionin stain, Toluidine Blue is used to determine the chondrogenic differentiation of MSCs in 3D pellet culture.

After submerging the slides in water after deparaffination and re-hydration, slides were incubated for 10 minutes in 0.04% Toluidine Blue (Sigma) in 0.1% sodium acetate at pH 4. Three 5 seconds washes in dH_2O. Slides were then dehydrated in consecutive changes in 90%, 95%, and two 100% of EtOH. Two changes in xylene were finally performed before a glass coverslip was mounted with DPX.

3.11.10 Histological Section Imaging

Stained histological sections were imaged with bright field microscopy using M8 microscope and scanner (Precipoint) using viewPoint software.

3.12 Data Analysis

Data analysis was performed with PSAW statistics 20 (SPSS Inc., Chicago, IL, USA) and GraphPad Prism8. The normal distribution of the data was determined by the Shapiro-Wilk test. Where data followed normal distribution, t-student test or ANOVA test was performed, otherwise non-parametric test were applied. Differences were considered statistically significant for $p < 0.05$.

For NanoString analysis, (performed by Dr. Rachel Crossland) fold change (FC) expression differences between two groups were calculated using nSolver v2.5 (NanoString Technologies) ratio data, based on normalized count data. Further analysis was performed using a pipeline designed by researchers at Newcastle University. This integrated a number of “R” (R project) statistical packages in the “R” programming language. *P*-values between the two groups were generated using a two-tailed *t*-test. Dendrograms were generated using functions within the “hclust” package, and heatmaps were constructed using “gplots” and “RColorBrewer”, based on an unsupervised clustering approach of the normalized expression counts, with a Euclidean distance measure.

For RNAseq data analysis (performed by Dr Lila Diamanti), a principal component analysis was performed on the data that indicated that the siDACT1 and control conditions cluster separately. A 10% false discovery rate threshold set for all the differentially (< 0.05% p-value) expressed genes.

4 Results: Chondrocytes from cartilage zones provide different signalling to bone marrow-derived MSCs.

4.1 Background and rationale

In the context of surgical therapies that deliver exogenous cells (e.g. culture expanded mesenchymal stem/stromal cells (MSCs) implantation) or recruit (bone marrow stimulation techniques) endogenous cells to the site of chondral damage, resident articular chondrocytes (ACs) become spatially adjacent to the MSCs.

Several studies have investigated the influence of full thickness (non zonally separated) ACs on MSCs. ACs are reported to produce factors that can induce chondrogenic differentiation of MSCs, as well as reducing markers associated with chondrocyte hypertrophy. However, there is only one published study that examines this effect using ACs specifically residing in the superficial zone and middle-deep zone. Coates and Fisher showed that in adult bovine articular cartilage, cells from the superficial zone induced bone marrow-derived MSCs to express hyaline cartilage genes in a highly efficient manner compared to those isolated from the middle and deeper zones cells (Coates & Fisher, 2014). This was also the case when compared to normal chondrogenic induction with TGFβ. Conditioned medium from superficial zone explants was not able to induce chondrogenesis. This indicates that MSCs and cartilage resident cells establish a positive feedback loop to produce differentiation signals. The authors also suggested that progenitor cells residing in the superficial zone may be responsible for the effective chondrogenic differentiation of BMSCs (Coates & Fisher, 2014). To explore this observation further, the hypothesis that SZ cartilage can induce BMSCs to differentiate more efficiently towards the chondrogenic lineage, in terms of proteoglycans deposition, than MDZ cartilage, was tested. In Coates and Fisher's work, the mechanism responsible for inducing chondrogenic differentiation was attributed to soluble signalling factors. The question as to which soluble factors are specifically responsible for the observed effect was not described. Cross-talk between cells is generally mediated by cytokines, growth factors, RNA (including mRNA, microRNA and lncRNAs), and other molecules. Recent studies have shown that EVs derived from MSCs have regenerative functions in several tissues, including kidney, heart, nervous tissues, liver, and lung (S. C. Abreu, Weiss, & Rocco, 2016; Cantaluppi et al., 2012; Lv et al., 2017; Nooshabadi et al., 2018). The driving

hypothesis in this chapter is that cytokines and EVs produced by both BMSCs and ACs would differ when cartilage is sampled from different regions of the knee condyle. To evaluate these differences, cytokines that mediate the communication between MSCs and ACs were investigated. EVs present in the supernatant of the co-cultures were isolated and analysed for their microRNA (miRNA) content. miRNAs importance in cartilage has become the centre of many studies and several miRNAs have been discovered and proposed as therapeutic targets for OA. miRNAs are on average 21-25 nt long RNAs that modulate the translation of targeted mRNAs by modifying their stability or translation through interaction with the RNA-induced silencing complex (Carthew & Sontheimer, 2009). miRNAs are a fundamental part of the mechanisms regulating cell fate determination, cell differentiation, organ development and physiology. miRNAs loci are mainly found in non-coding regions in gene transcripts, of which 40% are contained in the introns and 10% in the exons and the remaining in the introns of coding mRNA transcripts (Y.-K. Kim et al., 2009). Most miRNAs are present in clusters within the genome, at a distance of less than 10kb from another miRNA (Griffiths-Jones, Saini, van Dongen, & Enright, 2007). A single miRNA can also appear at several loci throughout the genome, as reflected by their nomenclature. When miRNAs present the same name but a different lettered suffix (e.g. miR-23a and miR 23b), this indicates that the two miRNAs have a similar sequence and precursors but can be found at different loci. Whereas, when miRNAs have identical mature sequences at different loci they are identified by a numbered suffix (e.g. hsa-miR-129-1 and hsa-miR-129-2) (Desvignes et al., 2015).

miRNAs were found to be selectively sorted into EVs. For example, in prostate cancer, specific miRNAs were underrepresented in EVs and sequencing analysis showed that some miRNAs were enriched in dendritic cells-derived EVs when compared with the cellular miRNAs (Nolte-'t Hoen et al., 2012). However, the mechanisms behind miRNA sorting are not well understood. Mechanistically, the loading of miRNAs into EVs may rely on factors including the binding motifs of the miRNAs and the miRNA-associated proteins. Such specific sorting argues for a specific and important role for miRNA found in EVs modulating target cells. A list of miRNAs specifically found in EVs is present on the EVs miRNA database (T. Liu et al., 2019). At the time of writing, cartilage derived EVs have not been studied. EVsmiRNA content from co-cultured BMSCs and cartilage and the comparison of such miRNA from either SZ or MDZ-derived EVs is described here for the first time.

4.2 Results

4.2.1 Method validation for the separation of ACs from human articular cartilage SZ, MDZ, and OAZ.

It has been suggested that different regions of human articular cartilage contain diverse cellular subtypes with different critical properties. The hypothesis is that such properties can modulate the phenotype of BMSCs that find themselves close to the chondrocytes after surgical approaches including bone marrow stimulation techniques. To study AC subpopulations a method was optimized to separate three cartilage zones. First, cartilage chips of between 200-300 µm from human femoral condyles (fig. 9A) were separated with a dermatome (fig. 9C). The SZ and MDZ cartilage chips were obtained from the non weight-bearing (lateral condyle) condyles that showed intact macroscopic and glossy features (fig. 9B). The OAZ cartilage chips were harvested from the medial condyle, from the side of visible cartilage damage (fig. 9B).

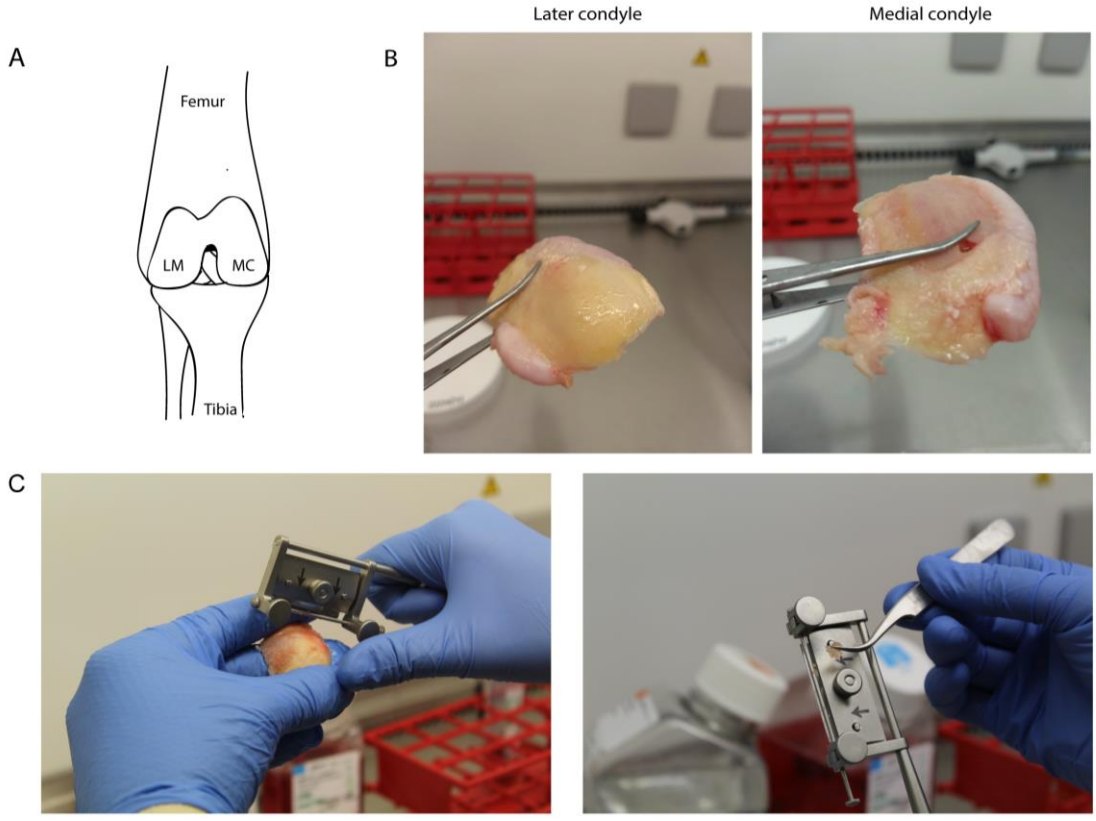

Figure 9 **Isolation of chondrocytes from different zones of articular cartilage with a dermatome.**
Schematic representation of the knee (A). Samples from lateral and medial condyle (B) were obtained following total knee replacement. About 0.200 mm of healthy

superficial or middle/deep cartilage are removed with a dermatome from the non-osteoarthritic part of the later femoral condyle (B, left). Osteoarthritic chips are removed from the eburnated medial condyle (B, right). The dermatome is visible in figure C, and a 0.200 mm thick cartilage chip removed from the knee condyle is held by forceps in figure C.

The average age of patients undergoing total knee replacement who donated the samples of cartilage used in the experiments presented in this thesis was 72±5 years. Age-related changes in articular cartilage generally include thinning (loss of cartilage height) and it has been suggested that the superficial zone may get progressively lost (Lotz 2012). To assess the zonal architecture of subjects, cartilage biopsies were taken from lateral and medial condyles and histological analysis was performed. Histological staining showed (representative sample in fig.10) cartilage thinning in the medial condyle and the presence of cell clusters, an OA hallmark. The lateral condyle presented in most cases a clear superficial population of cells positioned parallel to the surface. In the zone closer to the subchondral bone, ACs were rounder and occasionally organised in columns.

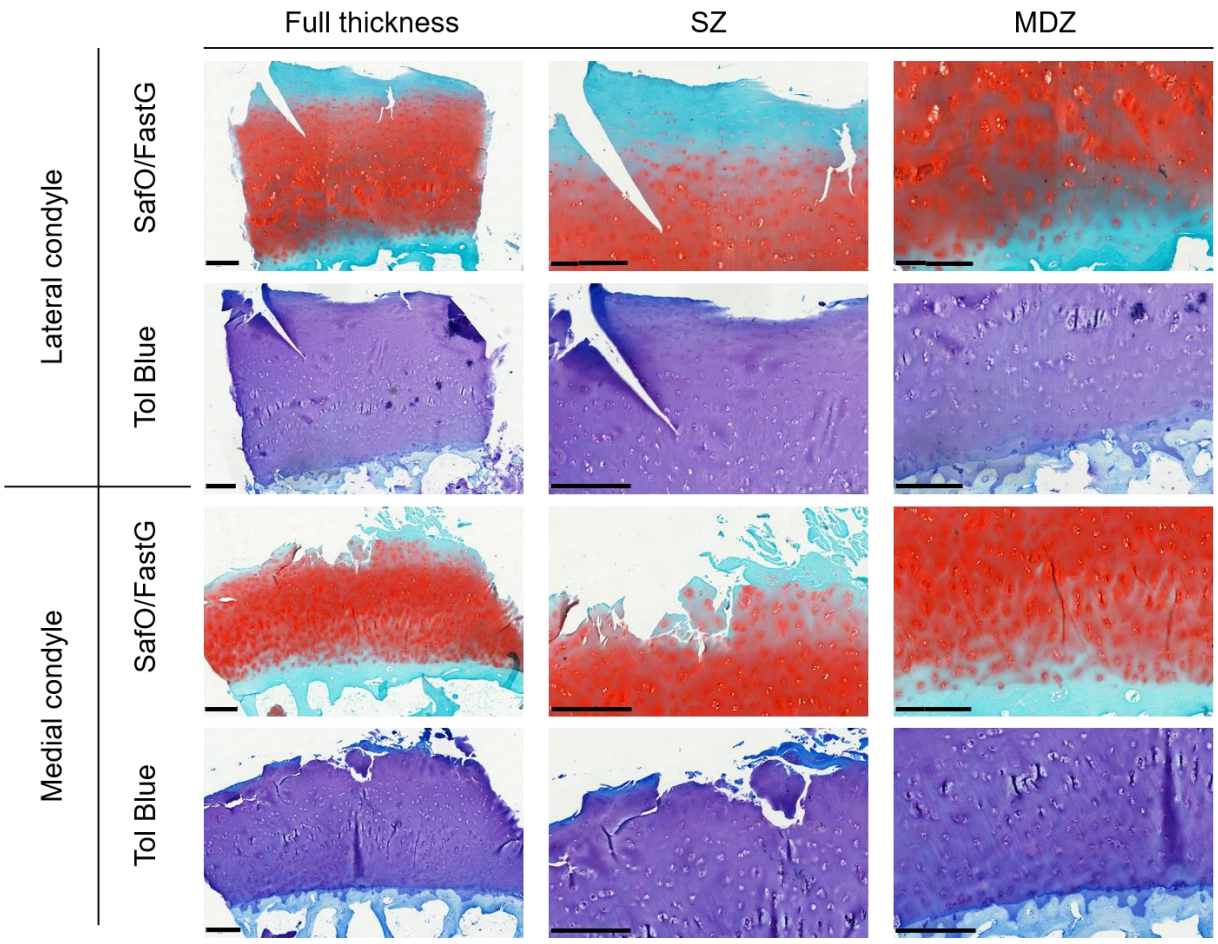

Figure 10 **Histology of lateral and medial knee condyle cartilage**.
SafraninO-FastGreen (SafO/FastG) and Toluidine Blue (Tol Blue) stainings on 5 µm section of paraffin-embedded human articular cartilage. The different regions are indicated as superficial zone (SZ), middle-deep zone (MDZ) and full-thickness. Scale bar = 0.5 mm, representative images (N=5).

Following overnight treatment with Collagenase A to obtain single cell suspensions from each cartilage zone, the cells were cultured for 4-5 days in normoxic conditions and images were taken with a phase-contrast microscope. ACs from the superficial zone (fig. 11, left) are elongated, in contrast to the ACs from the middle/deep zone, which have a more rounded shape. ACs from the edge of the osteoarthritic damage also showed an elongated shape, although a few rounded ACs are also present (fig. 11, right).

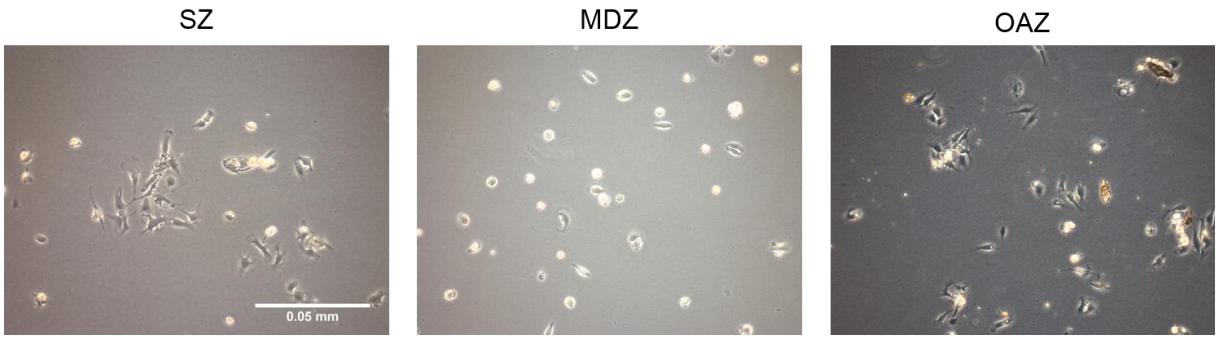

Figure 11 **Light Microscopy images of articular chondrocytes from different layers.**
Representative images from superficial (SZ), middle/deep (MDZ) and osteoarthritic (OAZ) chondrocytes after 3 days of culture in normoxic conditions. N=5, Scale bar: 0.05 mm.

To verify that the separation achieved with the dermatome resulted in effectively obtaining ACs from different zones, expression of zonal gene expression markers was investigated. *PRG4* and *COMP* were expressed in ACs isolated by enzymatic digestion from cartilage chips from the SZ, MDZ and OAZ with no statistically significant differences (fig.12). COL10 and COL2 are markers of mature cartilage and are expressed in the MDZ, but no difference could be detected at gene expression level in the analysed samples (fig. 12).

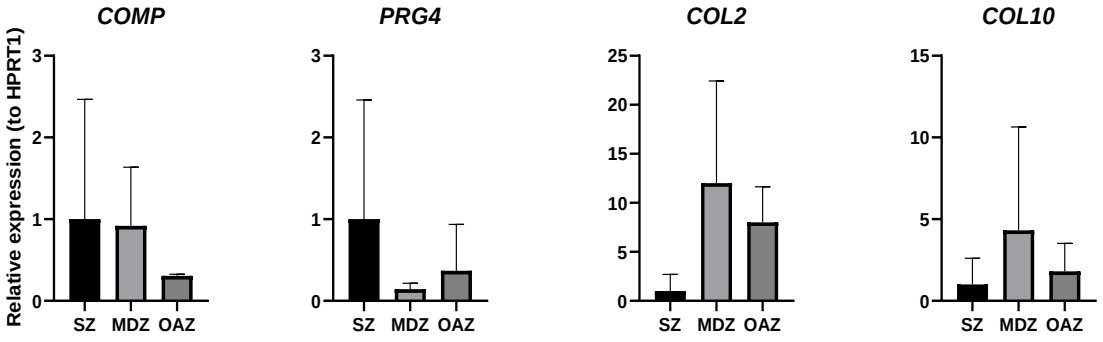

Figure 12 **Gene expression analysis of ACs from SZ, MDZ, or OAZ.**
qPCR was performed on cDNA obtained from the cartilage of patients undergoing total knee replacement. ACs were isolated through collagenase digestion and RNA harvested without further expansion. Error bars indicate samples standard deviation (N=3). (Kruskal-Wallis non-parametric test was run on the data, and there are no statistically significant differences).

The superficial origin of cartilage precursors has recently been described in mouse (Kozhemyakina et al., 2015; L. Li et al., 2017). The presence and role of these cartilage

precursors in human adult cartilage are still elusive. To evaluate the enrichment of proliferative chondrocytes in the SZ of mature human knee cartilage, a CFU assay was performed on cells from the femoral condyles from four different patients. Compared to the number of colonies/plates originating from MDZ ACs, SZ and OAZ ACs resulted in a significant increase in cell colonies (fig. 13).

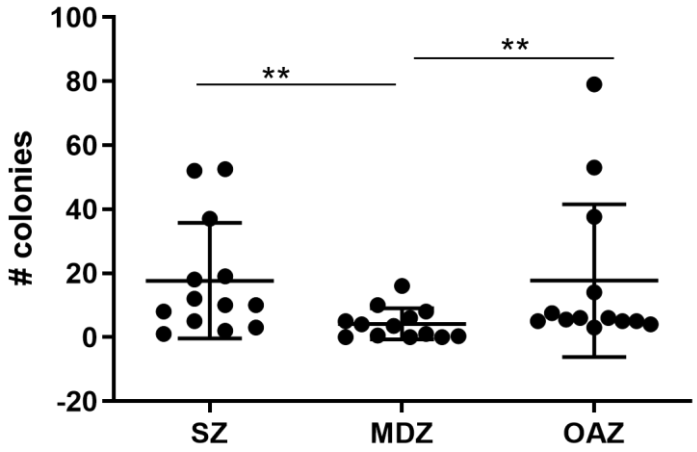

Figure 13 **Colony Forming Unit Assay on chondrocytes from the different cartilage zones.**
Relative CFU compared to MDZ CFU in a representative experiment from one donor. 3 to 4 replicates of the CFU assay per donor (N=4) are grouped per zonal derivation (Kruskal-Wallis non-parametric test was run on the data (∗∗ = p ≤ .01)).

4.2.2 BMSCs chondrogenic differentiation is differentially affected by the zonal regions of cartilage

ACs are known to drive chondrogenic differentiation of BMSCs when co-cultured. In recent work by Coates and Fisher, bovine SZ cartilage seemed to drive chondrogenesis and differentiation of BMSCs significantly better than MDZ ACs. We hypothesized that a similar result could be observed by co-culturing human BMSCs with human ACs from the femoral condyle. To evaluate the effect of secreted factors from ACs from different zones on BMSCs chondrogenic differentiation, BMSCs pellets were transferred to the co-culture system. A schematic summary of the final co-culture experiment is reported in figure 14.

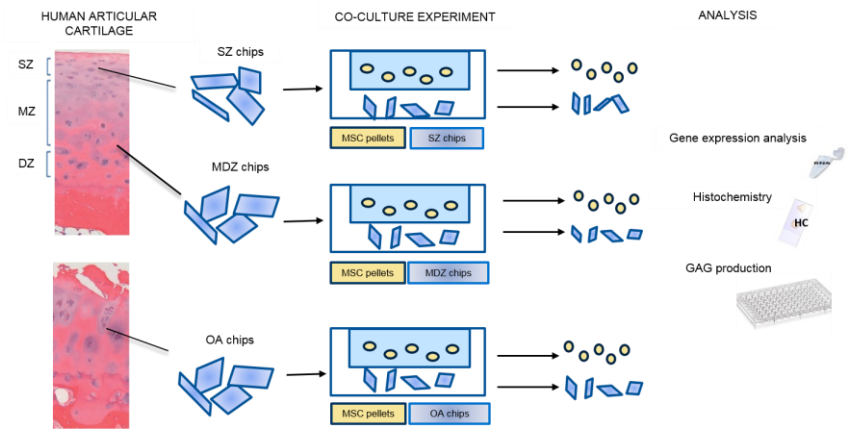

Figure 14 **Schematic representation of the co-culture experiment of BMSCs and cartilage chips from different regions.**
Cartilage chips from different cartilage areas are harvested (samples from 3 different donors) and co-cultured in a transwell with BMSCs pellets (from 1 patient) for 21 days. Through the experiment, basal medium was used. BMSCs pellets were prepared in tube containing basal medium and transferred to co-culture wells after 1 day. Control pellets were cultured in basal medium without cartilage chips for 21 days. At day 21, pellets were harvested and processed for mRNA analysis or histological assessment. The medium in the transwell was changed and stored at – 20 °C twice a week for GAGs production analysis by DMMB assay and cytokine proteome array.

A co-culture of cartilage chips and pellets of BMSCs was set up and maintained for 21 days at the end of which a gene expression analysis of pellets was performed. A third condition was included to analyse the effect of ACs from OAZ on BMSC differentiation. After 21 days of co-culture, pellets were harvested and processed for histological and gene expression analysis. It was noticed that pellets cultured with cartilage chips from MDZ and OAZ failed to assume the characteristic pearly white colour of BMSCs differentiated into cartilage (data not shown).

The relative fold change in mRNA levels was calculated using the RNA isolated from pellets maintained in basal medium for 21 days (fig. 15). The gene expression analysis from the three experiments showed large variability and resulted in no significantly different expression between the co-cultures, at the gene expression level. It was rare to observe gene expression of chondrogenic markers from these conditions higher than the positive control (not shown), indicating that the presence of the ACs might negatively affect MSC differentiation. The expression of chondrogenic marker SOX9 is higher in pellets co-cultured with MDZ chips for all three conditions. Sox9 directly regulates transcriptional activation of COL2, which is a marker of chondrogenic differentiation as it encodes for one of the major cartilage matrix proteins, collagen type

II. In only one experiment, COL2 was more expressed in the SZ than MDZ condition, and in the other conditions, it was less expressed than in the control. Generally, COL1 expression precedes COL2 expression during chondrogenic differentiation, and should decrease progressively during chondrogenesis. In the study presented here, COL1 expression still appeared in MDZ and OAZ conditions. ACAN is another marker of chondrogenic differentiation, encoding for another important matrix protein, aggrecan. Overall, chondrogenic markers do not present statically significant differences between conditions . PRG4 expression was not induced in pellets from SZ condition, but was expressed by pellets exposed to MDZ cartilage. MMP13 expression appears higher in the SZ compared to the other conditions, but was no statistically different.

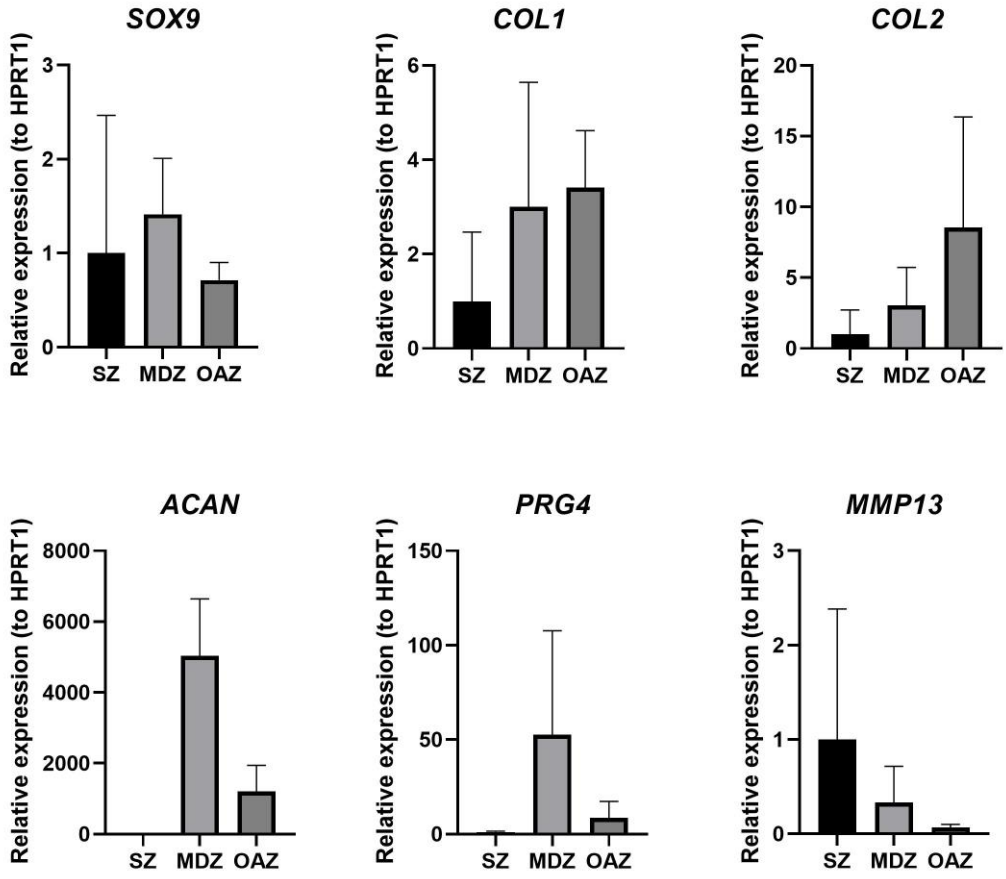

Figure 15 **Gene expression analysis of BMSCs pelleted after 21 days of co-culture with cartilage from different regions.**
Control samples are pellets in culture in basal medium only, the same medium added to the co-cultures. In SZ, MDZ, and OAZ are pellets co-cultured with cartilage chips from SZ, MDZ, or OAZ. The pellets were obtained from passage 5 BMSCs and 3-4 pellets were pooled per each condition. All expression are relative to the house keeping gene *HRPT1* expression and SZ condition is set as calibrator, N=3. (Kruskal-Wallis non-parametric test was run on the data, and there are no statistically significant differences between the conditions per each gene).

To evaluate the matrix protein production within the pellets co-cultured with cartilage from different zones, thionin staining on paraffin embedded pellets was performed. This method allowed the intensity of staining to be observed, which correlates with the amount of GAG present in the ECM produced by the cells.

The histology in figure 16 shows pellets from each condition, or 2 attached pellets in the case of SZ, OAZ and probably MDZ. The pellets were cultured in the same transwell and very often they merged. The pellet in co-culture with MDZ chips showed the reduced thionine staining indicating limited chondrogenic differentiation and GAGs deposition. Similarly, the pellet in co-culture with OAZ cartilage chips also showed limited purple colouration indicating little GAG deposition. Both conditions resulted in inferior differentiation compared to the control pellet. On the other hand, when co-cultured with SZ chips, the pellets were bigger (the micrograph in figure 16 probably represents a cluster of 2 pellets) and deeper purple stained. The histology seems to support more clearly than the gene expression analysis that a co-culture with SZ cartilage enhance chondrogenic differentiation of BMSCs.

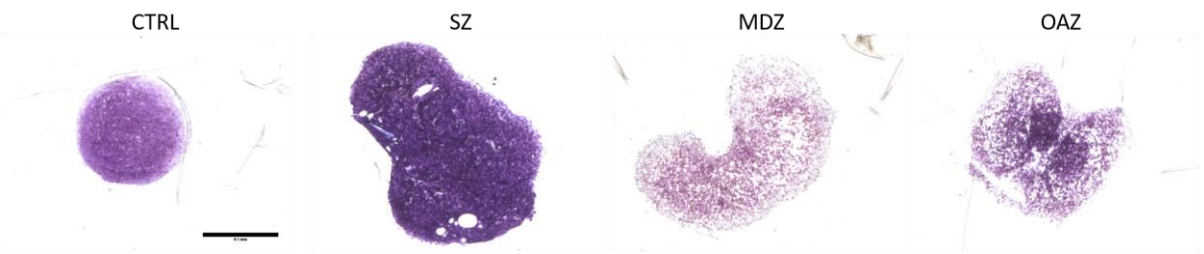

Figure 16 **Histology of paraffin embedded pellets at day 21 of co-culture with cartilage chips from different zones.**
CTRL are pellets in culture in basal medium, the same medium added to the co-cultures. In SZ, MDZ, and OAZ are pellets co-cultured with cartilage from SZ, MDZ, or OAZ. The pellets were obtained from passage 5 BMSCs. Thionin staining was performed on 5 µm thick sections from paraffin embedded samples and all the slides were stained at the same time, to allow a fair comparison. The scale bar indicates 1 mm (N=3).

To assess if there was any difference in GAG production between the different cartilage chips and MSCs pellet co-cultures and chips alone, we also performed a DMMB assay on the supernatant throughout the 21 days of the experiment. The absorbance measured at 545 nm in the DMB assay correlated with the amount of GAG present in the supernatant, although it cannot discriminate between the GAG that is newly produced and those resulting from the breakdown of the matrix. In all three graphs

presented in figure 17, the difference at each time point between co-culture and controls was not statistically significant, indicating that the presence of MSCs was not affecting GAG production or matrix catabolism. As free GAG in the culture supernatants did not significantly diminish over 21 days in SZ and MDZ experiments, it was concluded that matrix degradation is not a significant factor in this system. For both conditions, a gradual reduction in GAGs presence in the supernatant was registered in OAZ. The absorbance at day 0 measured at 700-800 nm whereas at day 21 it reduced to 500-600nm, a much greater reduction compared to SZ and MDZ conditions. This observation could be explained by a reduced production of GAGs over time, perhaps due to altered physiology of OAZ ACs.

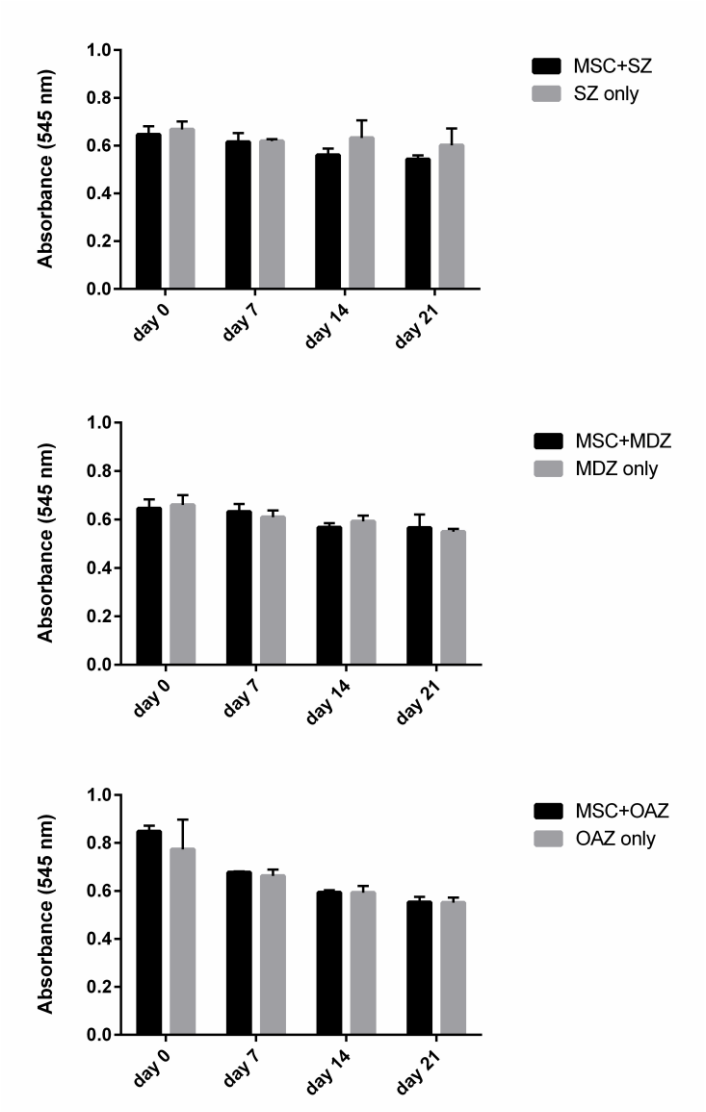

Figure 17 **DMMB assay on co-culture supernatant throughout 21 days.**
The absorbance is measured at 545 nm. Black columns indicate the co-culture condition, white column the control (only cartilage chips). The error bar indicates the standard deviation of the 3 independent measurements (N=3).

4.2.3 Co-culture of BMSCs with SZ cartilage results in less cytokine production compared to BMSCs-MDZ or BMSCs-OAZ co-cultures.

Cytokines and chemokines can have synergistic or antagonistic effects on cartilage catabolism and anabolism, fundamentally influencing tissue phenotype. Both ACs and MSCs produce cytokines and other molecules to communicate with neighbouring cells. Whether MSCs and ACs produce different cytokines depending on the zonal origin of cartilage, is not known. To explore this, supernatants after 48h of co-culture between either SZ-BMSC, MDZ-BMSCs and OAZ-BMSCs were probed for the presence of a number of cytokines (fig. 18).

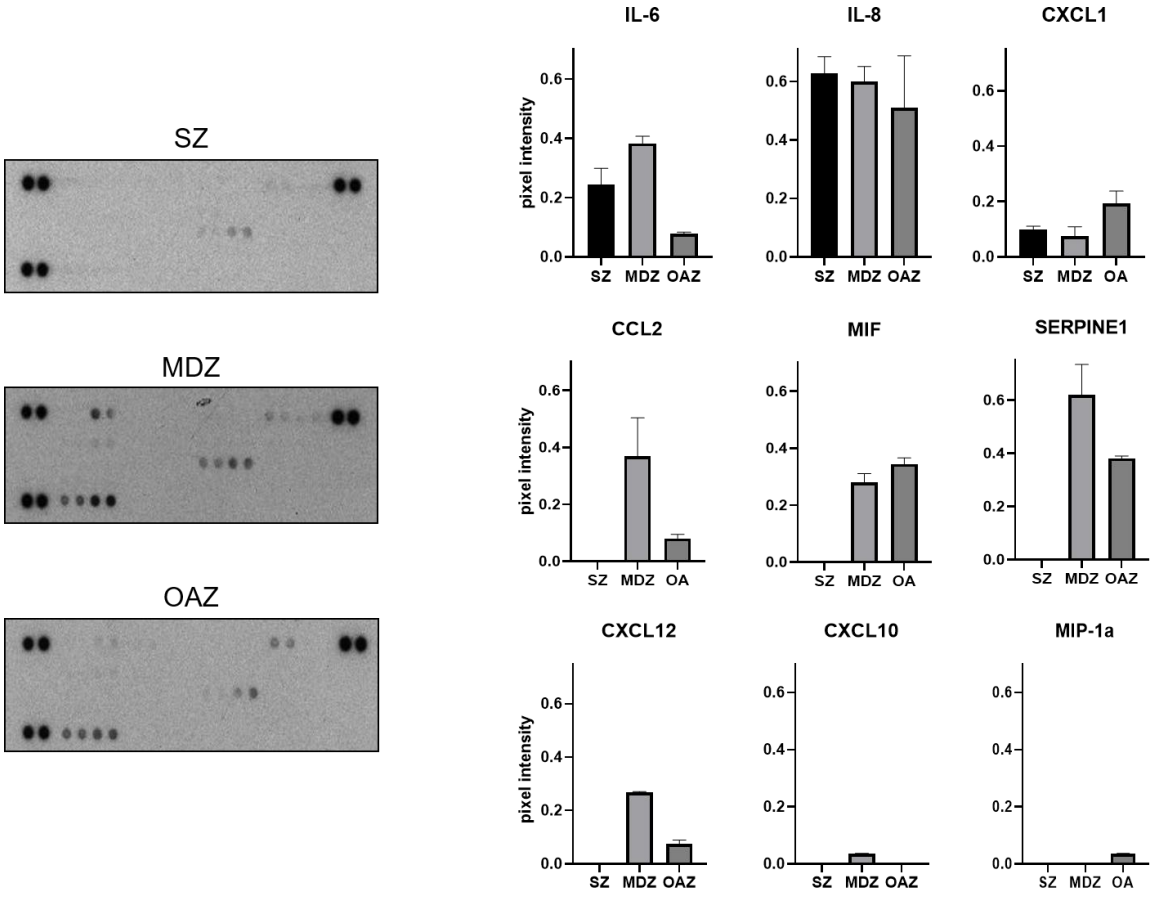

Figure 18 **Co-cultures of BMSCs and cartilage from different regions release different cytokines in the supernatant.**
The supernatant was harvested after 48h of co-culture and assayed to the array membrane. Membranes exposed for 5 min to an X-ray film (left) were quantified with ImageJ from the three co-culture conditions (right). Dots at the upper left and right corners and bottom left corner represent the internal controls (N=1).

The proteome array profile of BMSCs co-cultured with MDZ and OAZ cartilage appear similar and show higher amounts of cytokines compared to the SZ conditions. After

signal quantification with image software ImageJ, IL-6, IL-8 and CXCL1 were found in the supernatant of the SZ condition and were all also present in the other two conditions (fig. 18). The latter two conditions showed the presence of other cytokines: *CCL2, MIF, SERPINE1, CXCL12. CXCL10* was found only in the MDZ condition and *MIP-1a* in OAZ. The supernatant analysed was shared between the two cell types and therefore did not allow the identification of which cells were expressing a specific cytokine. The proteome array analysis was performed with samples from a single patient. To assess more patients, co-cultured BMSCs were analysed at gene expression level for the genes of the cytokines differentially detected by the array (fig. 19). A supernatant control containing only cartilage chips from the three zones would have offered additional information on the cytokines produced by the cartilage chips alone but was not performed due to the scarcity of material and the high cost of the assay. RNA was also isolated from the co-cultured cartilage. Because of the low amount of material and the difficulty of isolating RNA from the ECM bound cells, gene expression analysis from cartilage chips was not possible.

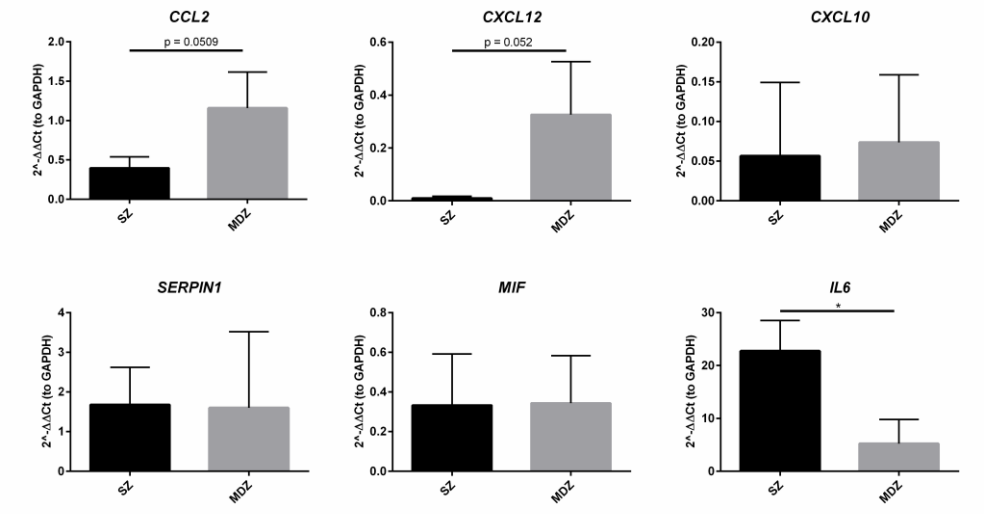

Figure 19 **Gene expression analysis of BMSCs in co-culture with cartilage from different regions.**
Samples were harvested for RNA analysis after 48h of co-culture (n=3). Expression fold changes are reported relative to BMSCs only control (culture in the same basal medium as the SZ and MDZ conditions). Figure A, B, and C display qPCR data from three biological replicates (Mann-Whitney non-parametric test was performed on the data, $* = p \leq 0.05$).

CXCL10, SERPINE1, MIF were expressed by BMSCs, but no difference was detected in the two conditions (fig. 19). IL6 was significantly more expressed by BMSCs co-

culture with SZ cartilage. CXCL12 and CCL2 were more expressed by BMSCs co-cultured with MDZ (fig. 19).

4.2.4 Extracellular vesicles may be involved in the cross-talk between ACs and BMSCs and their miRNA cargo is dependent upon the zonal origin of chondrocyte.

EVs are a well-known cell communication mechanism through which BMSCs and ACs signal to other cell types. To describe the communication between BMSCs and chondrocytes in the experimental conditions presented here, EVs were isolated from the supernatant. The BMSCs used for this co-culture experiment were obtained by pooling cells from three different healthy donors and remained constant across all the experiments in terms of passage number. The cartilage was obtained from 5 different patients using tissue from knee lateral condyles. After 48h from the start of the co-culture, EVs were isolated from the supernatant and analysed. TEM images showed that small EVs were present in the supernatant (fig. 20). The EVs showed specific rounded morphology and mode size of 164.1 +/- 17.4 nm, as determined by NTA (fig. 21).

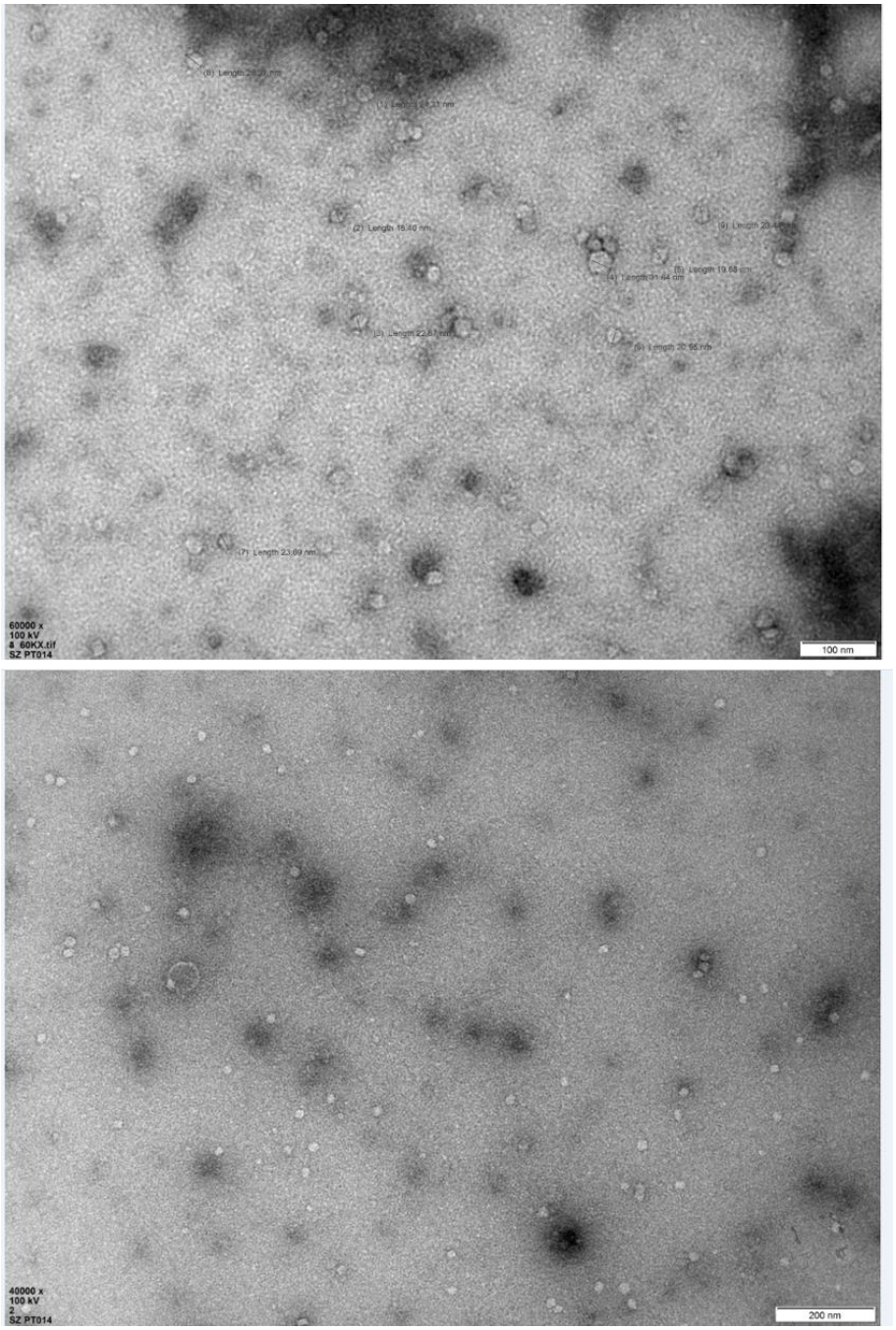

Figure 20 **Characterisation of EVs present in the supernatant of BMSC-Cartilage co-culture.**
Negative contrast micrograph of EVs imaged by T, scale bar 100 nm (upper) and 200 nm (lower).

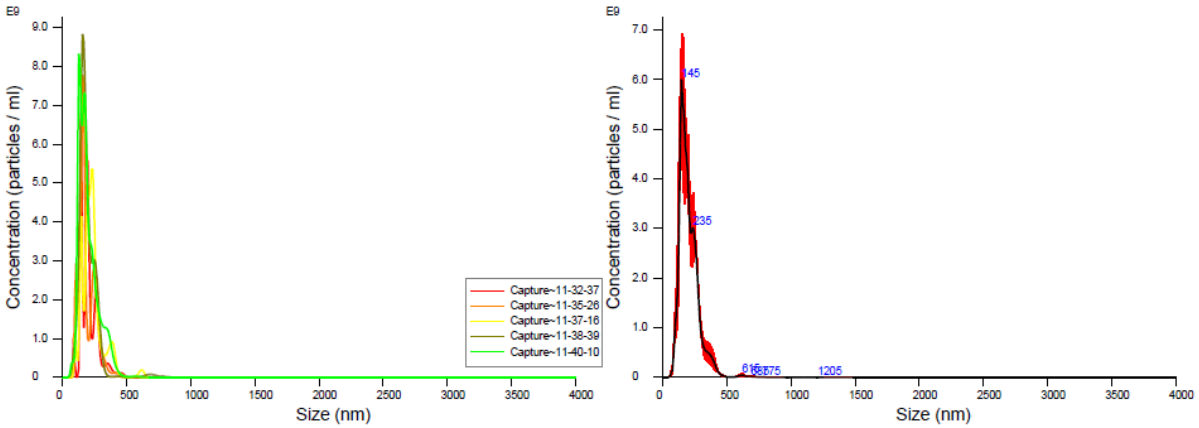

Figure 21 **Characterisation of EVs present in the supernatant of BMSC-Cartilage co-culture.**
Quantification using Nanosight nanoparticle tracking analysis. Averaged Concentration / Size for is reported in the right figure, obtained from 6 measurements (left). Error bars indicate + / -1 standard error of the mean.

To determine the miRNA cargo of isolated EVs, total RNA was isolated from the EVs. As expected, RNA obtained from the EVs was extremely low in concentration and required a Bioanalyser analysis to accurately determine the concentration and purity level. Figure 22 shows representative electrophoretic charts (electropherograms) of two RNA sample pairs out of 5 and includes RNA concentrations and RNA integrity Numbers (RIN). The electropherograms illustrate the quality of total RNA samples and was performed using the RNA 6000 Pico LabChip kit. 5 ng of RNA samples were analysed on the Agilent 2100 bioanalyzer. 18S/28S rRNA peaks are not present (generally seen at 40 and 47 seconds). For the downstream application of isolated total RNA, RINs are generally accepted when above 8. However, because the calculation for RIN is based on ribosomal RNA which is not present in EVs, the RNA was still deemed usable for further analysis based on apparent abundance.

A

Sample ID	RNA (pg/µl)	RIN
MSCs CTRL A	106	2.1
MSCs CTRL B	150	2.4
SZ Pt006	67	1.9
MDZ Pt006	79	1.4
SZ Pt007	44	1.5
MDZ Pt007	325	N/A
SZ Pt011	186	2.8
MDZ Pt011	36	2.3
SZ Pt014	63	1.8
MDZ Pt014	56	1.3
SZ Pt998	471	2.5
MDZ Pt998	240	6.4

B

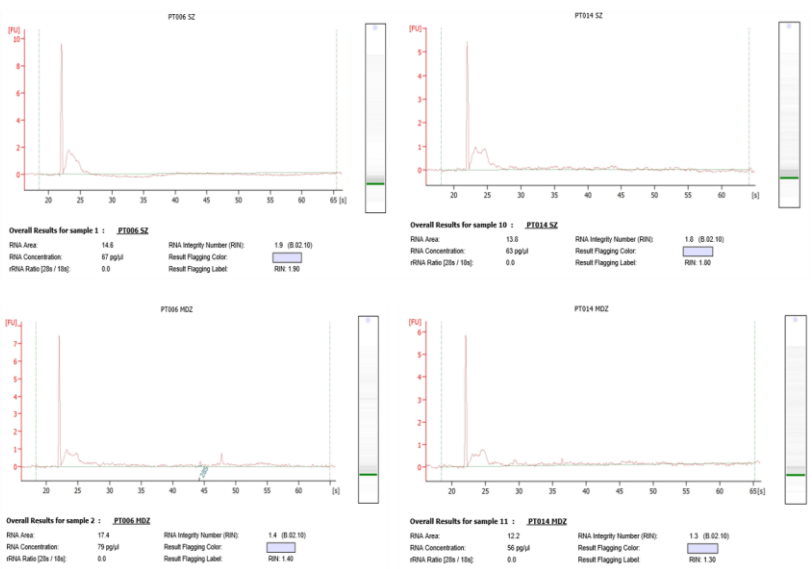

Figure 22 **EVs isolated RNA concentration and quality**.
RNA concentrations (A) from control conditions ('MSCs CTRLA' and 'MSCs CTRL B', EVs isolated from the supernatant of BMSCs culture in basal medium) and experimental conditions (EVs present in the supernatant of MSCs-SZ or -MDZ co-cultures) was determined with RNA 6000 Pico LabChip kit. For all the experiments, BMSCs were from the same pool of BMSCs from 3 healthy donors at passage 5. Experimental conditions are paired as SZ and MDZ cartilage were obtained from the same patient. B) 4 representative electropherograms are shown, obtained by loading 5 ng of RNA in the Agilent 2100 bioanalyzer.

The small amount of RNA isolated from EVs was not a limiting factor for the analysis of miRNAs. Using low total RNA concentration is possible thanks to the higher accuracy of the NanoString technology over RNA sequencing or other gene expression analysis methods. Because techniques like qPCR and RNAseq are reliant on reverse transcription of RNA to cDNA, they are also prone to technical bias. NanoString is based on direct hybridization of reporter molecules to RNA, thus removing the need for reverse transcription. This allows for a direct digital count of tagged labelled barcodes that eliminates background noise, as shown by Prokopev et al. (Prokopec et al., 2013). The multiplex assay selected for the experiment includes 799 mature miRNA and internal control probes against control transcript sequences. Six of these sequences are used as positive hybridization controls: positive controls are used to confirm linear response to input amounts and confirm that low input signal is above background. Eight of the probes are used as negative controls and are used to determine background signal independent of ligation success. This was then used to set a threshold for defining expression of miRNA. Despite the low RNA concentration (the suggested limit to successfully run the analysis by NanoString Technologies is

100 pg/µl), 10 out of 12 samples passed the initials control analysis performed after running a nCounter miRNA expression assay. Two samples from the same donor were flagged by the analysis software quality control for ligation issues and were excluded from further analysis.

The mean of the negative controls and positive control was removed from the sample readout (background subtraction). Only miRNA with a count ≥ 10 in at least one of the samples were included. This step was included to avoid including samples with a low transcript count as the minimum amount of counts was set to 10. Despite the high specificity of nCounter probes, very low levels of non-specific counting are still inherent to any NanoString assay. Thus, very low number of counts for each of the targets in a CodeSet would represent false positives. This analysis identified 38 miRNAs present in isolated EVs. When the miRNAs clusters from each sample were organised in an unsupervised dendrogram (fig.23), patients samples clustered separately following the cartilage zones, and the BMSC only samples clustered separately from SZ and MDZ conditions.

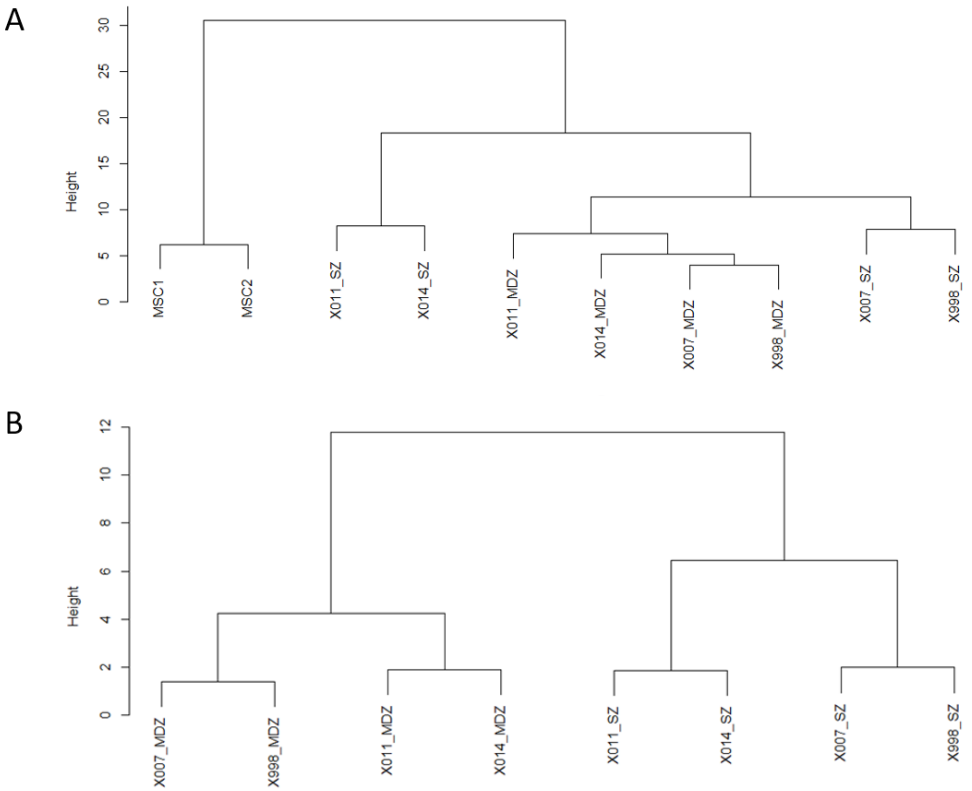

Figure 23 **Unsupervised hierarchical clustering of miRNAs that are present in EVs from BMSC-Cartilage co-cultures supernatant.**
Dendrogram of miRNAs clusters from each sample. Samples having similar miRNAs profiles are closer in the tree. Dendrogram A compares controls (MSC1 and MSC2) and co-cultures conditions. Dendrogram B compares MDZ and SZ conditions.

Among the top 10 miRNAs (those which had the most counts) present in SZ and MDZ conditions, 5 were shared (fig. 24). The top 10 miRNAs for each condition are reported in table 3 alongside their biological role and potential targets. Out of the 38 miRNAs identified, 5 were significantly differentially expressed in SZ and MDZ condition: mir-188-5p, miR-199a-3p, miR23a-3p, miR451a, miR-612 (figure 25). miR-23a-3p was the only miRNA significantly differentially expressed after applying FDR adjustment.

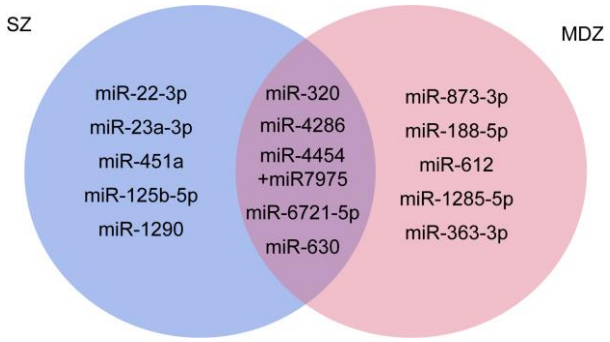

Figure 24 **Venn diagram for the top 10 genes found in EVs from SZ and MDZ samples**.
miRNA with the highest normalised digital count in co-culture BMSC-SZ or -MDZ conditions (N=4) are reported in the diagrams.

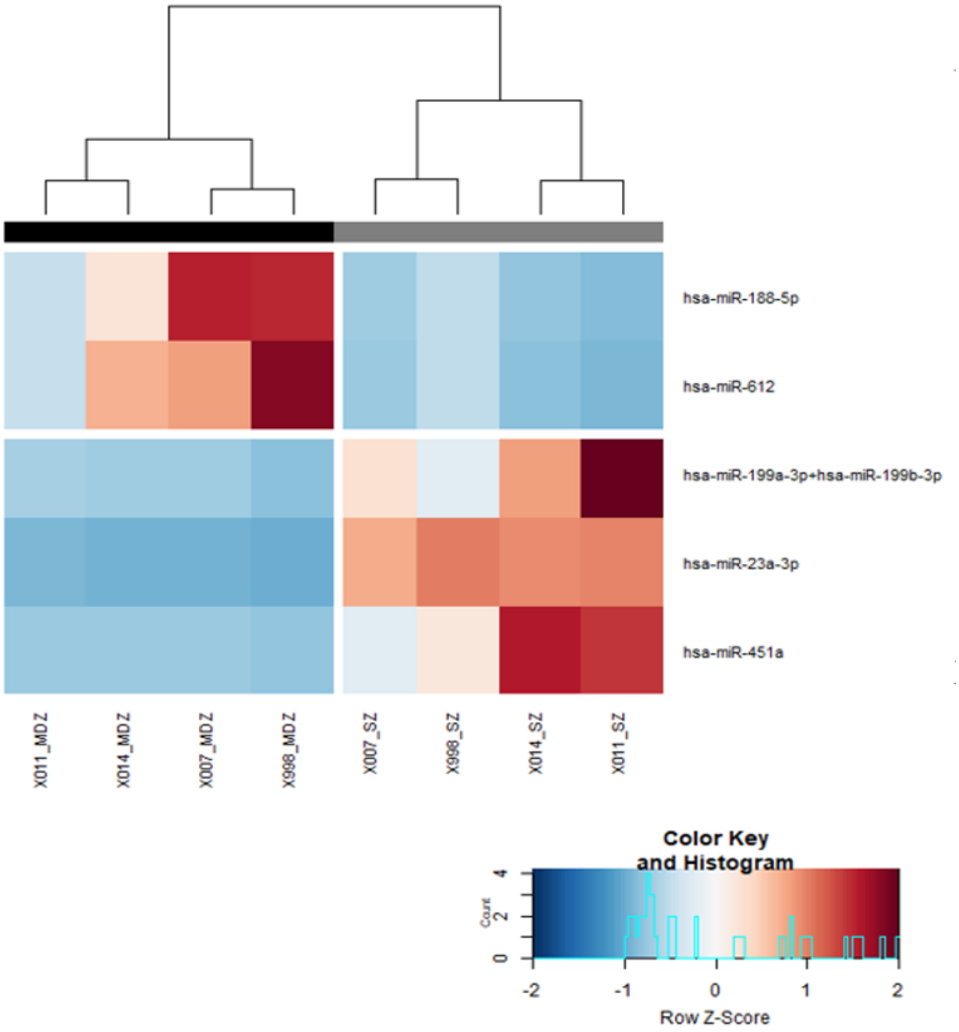

Figure 25 **Heatmap of differentially expressed miRNAs from EVs.**
Heatmap showing hierarchical clustering of significantly differentially expressed microRNAs, based on normalized digital expression counts, in supernatant samples of co-culture of BMSCs-SZ or MDZ cartilage. Each column represents an individual sample. Relative expression changes are indicated by the colour scale (Z-score: red 2; blue -2).

Table 3 **Annotated list of the top 10 miRNAs present in EVs from SZ and MDZ conditions.**

Smpl	miRNA	Biological role	Validated targets	References
SZ	miR-23a	Promotes the development of OA downregulating *COL2* and *ACAN*. Most downregulated	CXCL12, CXCL8, IL6R, LRP5, FRZ5, POU4F2, FOXO3, SMAD3	(Kang et al., 2016) (Prasadam & Xiao, 2018)

		miRNA in OA cartilage. Pharmacological inhibition in normal rats mimicked an OA phenotype. Over-expression of miR-23a-3p suppressed the IL-1β induced catabolic effects.		
	miR-22-3p	Involved in regulating osteogenic differentiation of MSCs.	RAB5B, BMP7, ESR1, WNT1, MMP14 CXCR2, SIRT1, SNAI1	(Thompson, Matsiko, Farrell, Kelly, & O'Brien, 2015)
	miR-451a	Overexpressed in OA cartilage. Found in matrix vesicles in the growth plate.	MIF, MMP2, MMP9, ADAM10, BCL2, MYC, IL6, IL6R, STAT3, FZD	(Coutinho de Almeida et al., 2019) (Z. Lin et al., 2018)
	miR-125b-5p	Regulates inflammation in in stimulated chondrocytes via MIP1α signalling. Regulates aggrecanase-1 expression in OA ACs.	ID1, ID3, ID2, DKK3, E2F2, FZD6, IL6R, MMP13, SIRT7, SMAD4, STAT3, TNF	(Jia et al., 2018) (Matsukawa et al., 2013) (Rasheed, Rasheed, Abdulmonem

		Regulates IL-1β induced inflammatory genes in OA ACs. Promotes apoptosis of synovial cells.		, & Khan, 2019) (Ge, Li, & Yin, 2017)
	miR-1290	Downregulated in de-differentiated chondrocytes.	CTC1, PER1, PRDX3, CLCN6, POP7	(Martinez-Sanchez & Murphy, 2013)
MDZ	miR-873	Regulated in several cancer types.	HES7, KLHL38, UGDH, MIDN, TMC5, ZFX, FZD5,	(Gao et al., 2019; Yu-Hui Li, Zang, & Tian, 2018; Liang et al., 2018)
	miR-188-5p	Down-regulated in RA *in* triggered by inflammation.	FGF5, UBE2I, MTRNR2L3, GREM2, ITGA7, MTRNR2L8, MTRNR2L10, SMAD2	(Ruedel et al., 2015)
	miR-363-3p	Reduced in CD4+ T cells from synovia of arthritis patients.	BCL2L11, CDKN1A, HIVEP1, CASP3, USP28, NOTCH1, SOX4, DUSP5,	(Z. Wang, Guo, Xiao, Qing, & Ma, 2017)
	miR-612	Inhibits dendritic cell growth targeting PRKAR1A.	TP53, AKT2, SP1, GATA6, MRE11, MYH14, DLX6, SBK1	(C.-W. Li, Lee, & Chen, 2016)
	miR-1285-	Regulates cell growth	SEC23B, LRAT,	(Shixia Zhou,

	5p	and migration in cancer through Smad4 and chaderin1.	RBM12B, ZER1, KPNA4, OSBP2, TMEM81, HOXA11	Zhang, Zheng, Zhao, & Han, 2017)
SZ, MDZ	miR-320e*	Influences MSCs adipogenic differentiation. Targets MMP-13 and regulates chondrogenesis.	DCTN5, DDX19A, TXNL1, NPM3, SEMA7A, ZNF275, DUSP19	(Hamam et al., 2014) (Meng et al., 2016)
	miR-4286*	Found in BMSCs-derived EVs.	NSD1, ZNF354B, LDLR, RABGAP1, TRAF3, HSPA4, RRN3, AHSA2	(Horiguchi et al., 2016)
	miR-4454+ mir-7975*	Promotes inflammatory, catabolic, and cell death chondrocytes.	KBTBD8, TRAM2, CASP16P GULP1, TYRP1, SMC1A, GATAD1	(A. Nakamura et al., 2016)
	miR-6721-5p*	-	FBXO41, ZBTB34, ZC3H12B, RPL13A, WAC, CELF1, MBD4, HIVEP3,	-
	miR-630	Upregulated after MSCs chondrogenic differentiation.	BCL2L2, BCL2, IGF1R, SNAI2, FOXM1, IGF1R, YAP1, TP53RK	(Georgi et al., 2015)

Table 3 **Annotated list of the top 10 miRNAs present in EVs from SZ and MDZ conditions**.
miRNAs are described in terms of biological role (with precedence given to studies on musculoskeletal tissues and cells reported in open access papers, when present) and target genes. Target genes were reported from mirTARdatabase

(http://mirtarbase.mbc.nctu.edu.tw). Per each miRNA, the targets that were validated with the most different methods (including qPCR, western blot, Reporter assay, NGS.) or alternatively, reported by the highest number of papers were chosen to be reported on the table. MiRNAs which targets were determined only by NGS are indicated with *.

miRNAs obtained from EVs isolated from the supernatant of BMSCs were analysed as the control condition. SZ and MDZ cartilage alone EVs were not harvested due to the limited number of samples that can be obtained from each patient. Figure 26 shows the heatmaps of hierarchical clustering of miRNAs, comparing differentially expressed genes from the “BMSCs only” condition to SZ or MDZ conditions. For the BMSCs vs SZ comparison, 24 microRNAs were significantly differentially expressed, of which 18 retained significance following FDR adjustment (fig. 27). 22 microRNAs were significantly differentially expressed between BMSC vs. MDZ samples and 20 retained significance. The top 10 miRNAs found in EVs of the different co-culture conditions are reported in figure 27.

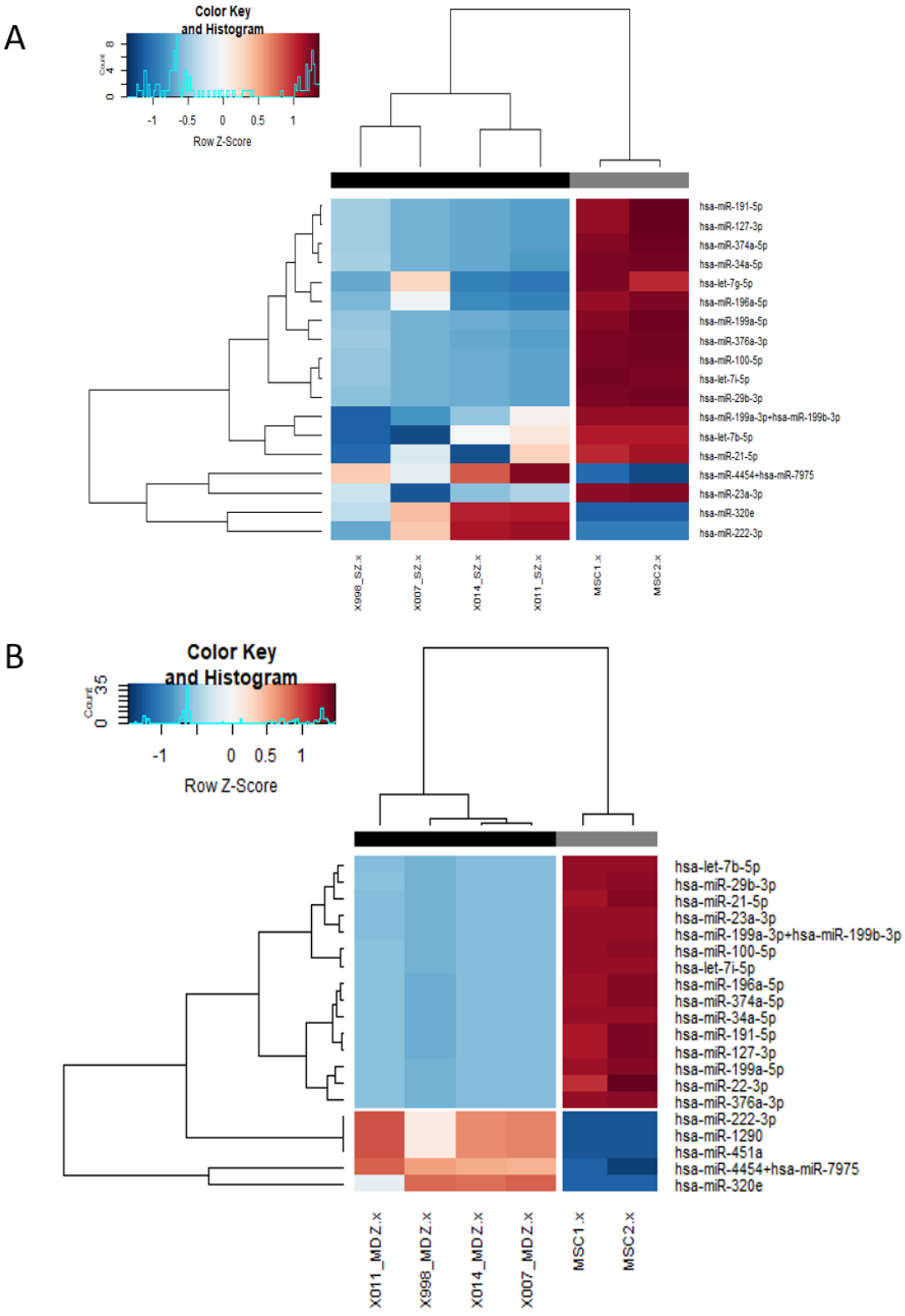

Figure 26 **Dendrograms of differentially expressed miRNAs in EVs from BMSC-SZ and BMSZ-MDZ co-cultures vs BMSCs only**.
Heatmap showing hierarchical clustering of significantly differentially expressed microRNAs, based on normalized digital expression counts, in supernatant samples of co-culture of BMSCs-SZ compared to BMSCs only (A), and BMSCs-MDZ compared

to BMSCs only (B). Each column represents an individual sample. Relative expression changes are indicated by the colour scale (red: high; blue: low).

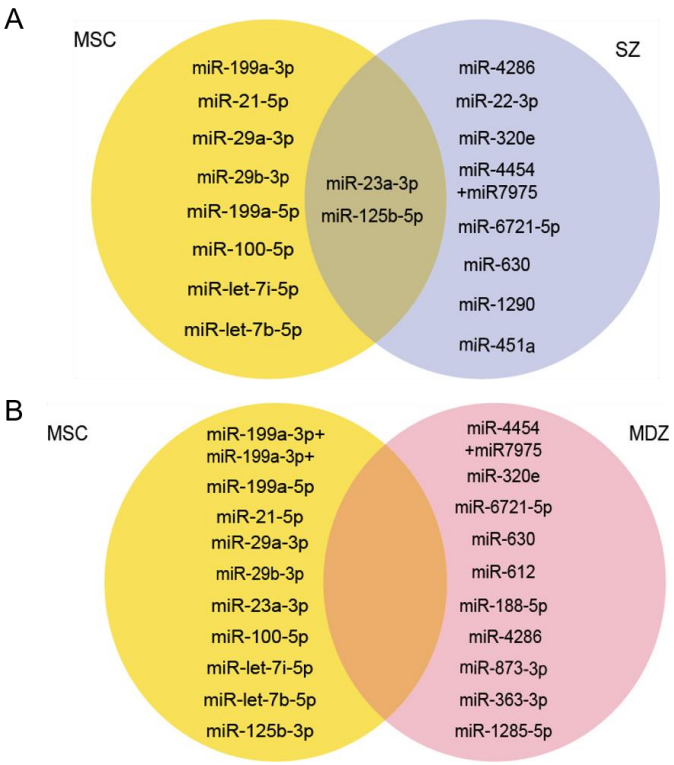

Figure 27 **Venn diagram for the top 10 genes found in EVs from SZ and MDZ vs BMSCs only samples.**
miRNA with the highest normalised digital count in co-cultures BMSC-SZ (A) and BMSCs-MDZ (B) conditions compared to miRNA found in EVs from BMSCs only cultures are reported in the diagrams. BMSCs used across the experiments are from the same donors and passage number. Cartilage from either SZ or MDZ were obtained from 4 different patients (n=4).

4.3 Discussion

The growing number of people affected by cartilage degeneration and related conditions are driving biomedical scientists to find novel approaches for cartilage repair or to improve current cartilage repair methods. Bone marrow stimulation techniques to treat early-stage chondral defects are currently performed but shows variable outcomes in patients regarding the quality of regenerated cartilage. The reasons for such inconsistency are largely unknown. In this work, we hypothesize that resident ACs play a significant role in directing cartilage repair. The aim was, therefore, to describe in more detail which cell populations are present in human articular cartilage obtained from patients undergoing knee replacement and the significance of the

crosstalk between these ACs and BMSCs. More specifically, the goals of this work were to establish a method for isolating articular cartilage cell populations with different characteristics dictated or determined by their zonal origin and describe the different signalling resulting from co-culturing BMSCs with ACs from either SZ or MDZ.

4.3.1 Chondrocyte populations within human articular cartilage and their isolation.

Other groups have published studies describing the use of a dermatome on bovine joint tissue to separate the superficial zone cartilage from the middle and deep zone (Coates & Fisher, 2014a). We used a surgical dermatome on human femoral condyles and obtained three different population of cells that expressed distinct specific gene profiles. Superficial chondrocyte markers such as *PRG4* and *COMP* were more expressed in SZ ACs than MDZ or OAZ ACs, while the expression of markers for differentiated chondrocytes *COL10* and *COL2* was higher for OAZ and MDZ ACs, although not statistically significant. Given the high inter-patient variability of samples isolated from articular cartilage, further patient samples would be needed to confirm or refute the findings. These results were in accordance with previously published data and confirmed that our method was successful for isolating subpopulations with distinct phenotypes. Further substantiating the effectiveness of the method, we observed different cell morphologies when ACs from different layers were imaged under the light microscope. SZ ACs were observed to have an elongated shape, like fibroblasts, whilst MDZ ACs exhibited a rounded morphology more typical of a chondrocyte. ACs are generally considered a poorly proliferative cell population and we observed this when culturing femoral condyle derived ACs. The increased proliferation rate observed for superficial ACs suggests the presence of a subpopulation of more proliferative cells. In line with that observation, CFU efficiency of SZ ACs was always higher than for MDZ. The CFU proliferation assay result was in accordance with work by several researchers that claimed the presence of cells with stem-like properties or progenitor cells in the superficial zone. Although there is evidence of different subpopulations in the SZ there is no consensus in the literature about their exact characteristics. A number of studies have used different markers to identify these cells but the exact identity of this subpopulation remains unknown. The elevated CFU count for OAZ ACs, although smaller than for SZ ACs, is of note. The OAZ ACs are harvested at the adjoining areas of full cartilage thickness damage loss. The harvested chips derived

from both fibrillated and non-normal looking cartilage. The superficial layer of cartilage is the first that is lost in degenerative joint disease, and it is therefore unlikely that the cells with high CFU potential are derived from the SZ of OA cartilage. Fibrillated human cartilage displays a morphological OA hallmark, termed cell clusters. Some studies have suggested the presence of progenitor or stem cell-like cells within the clusters near degenerated cartilage. The high CFU observed in the studies presented here could, therefore, be explained by the presence of such cells, contained in cell clusters. What is the role of cell clusters and why they contain cells with stem-like markers, is currently unknown. One hypothesis is that de-differentiating ACs are presenting stem-cell markers and that the clusters are the result of ACs whose surrounding matrix is degraded in the OA environment. Loss of surrounding matrix could result in the removal of signals that maintains chondrocytes in a differentiated phenotype that once lost induce cells to dedifferentiate. Cell clusters might form or be recruited to the side of degenerated cartilage in the attempt to mediate or contribute to cartilage repair.

4.3.2 Co-culture of cartilage from different zones can affect the chondrogenic differentiation of BMSCs.

Co-culturing with primary ACs has been shown to serve as a chondrogenic inducer for MSCs. In this Chapter the hypothesis that human ACs differentially influence chondrogenic differentiation of BMSCs depending on their zonal origin was tested. A previous study by Coates and Fisher showed how bovine cartilage ACs from the SZ can direct more efficiently the differentiation of bovine MSCs compared to those from the MDZ (Coates & Fisher, 2014). In addition, we wanted to evaluate how the secreted factors from different zonal ACs influenced chondrogenesis in a 3D BMSCs culture, which is the more standard method to evaluate MSCs chondrogenic differentiation *in vitro.* To set up a co-culture experiment with cartilage from different zones and BMSCs we used a transwell system. In this way, the influence of each cell population on the other was determined only by their release of soluble factors. Furthermore, we were able to harvest separately BMSCs and ACs for further analysis. A chemically defined culture medium was used in order to observe strictly the effect of released factors on chondrocyte differentiation. In addition, we decided to use BMSCs from the same donor and at the same passage in all experiments in order to reduce the variability. Despite this experimental design, we still observed variability, in particular with gene expression data, between the three independent co-culture experiments. We observed

that the pellets did not undergo significantly enhanced chondrogenic differentiation according to gene expression analysis. Contrary to observations in young bovine BMSC, the factors released by either of the zonal ACs populations were not able to drive MSC chondrogenic differentiation, as indicated by gene expression of *COL2* and *ACAN* (Coates & Fisher, 2014). However, the high expression of *COL1* in pellets in co-culture with MDZ and OAZ ACs indicates their undifferentiated or fibrotic state, whereas *COL1* expression for SZ condition is low. Lack of correlation between gene expression and histological analysis can be explained by the fact that *COL2* and *COL1* expression rises and falls within three weeks of chondrogenic induction. It is possible that at day 21 when the histology was performed, marker gene expression was falling as the deposition of matrix for the SZ condition was already established as illustrated by the dark purple thionin staining. In contrast, MDZ and OAZ co-culture led to an alternative pattern of gene expression in the BMSC pellets, with transcripts for matrix genes more highly abundant at day 21, perhaps reflecting the early stages of active matrix deposition. The expression of the hypertrophic marker MMP13 was the highest in SZ, then followed by MDZ and OAZ (fig. 15). Expression of metalloproteinases results in cartilage breakdown; however, the histological analysis shows pellet breakdown and reduced thionin staining in pellet cultured with MDZ and OAZ cartilage. Presence of tissue inhibitor of metalloproteinases (TIMPs) in the co-culture could explain this observation (Davidson et al., 2006), which have been shown to act as inhibitors of metalloproteinases and aggrecanases, which could be confirmed by ELISA immunoassay.

From the data, MDZ and OAZ ACs prevent and even have a negative effect on initial chondrogenic differentiation of BMSCs. In data presented here, the AC samples were harvested from the SZ of non-visibly affected cartilage, nonetheless the patients might have much fewer SZ ACs, or altered subpopulations, due to the age-related thinning of the articular cartilage. The experiments performed aimed at understanding the signalling that may underlie the interaction between BMSCs and ACs. It was showed that ACs from MDZ and OAZ cartilage regions can have an anti-chondrogenic effect on BMSCs. To confirm this observation and to determine if the contribution to BMSCs differentiation depends upon the factors released from ACs, cartilage chips could be treated to cause cell death by for example cycles of freeze/thaw and the co-culture experiment then repeated. The relative contribution of released ECM components versus the factors released from ACs of different zones could then be identified.

4.3.3 Signalling between MSCs and cartilage differs in term of miRNAs and cytokine production depending on ACs zonal origin.

MSCs have been injected intra articularly in the knee as a therapeutic strategy to alleviate OA and influence cartilage repair. Cell tracking studies suggest that MSCs only in part act as cartilage building blocks to replenish lost cartilage with new ACs. It is now widely accepted that chondrogenic differentiation is not the main mechanism of action of MSCs in cartilage repair when administered therapeutically (De Bari & Roelofs, 2018). The current hypothesis by which intra-articularly injected MSCs act as a therapy in OA is by modifying the micro-environment through the release of paracrine factors that stimulate locally present progenitor cells, attract other progenitors to the repair region and/or trophic effects on other cells types including immune cells. The work described here showed differences in terms of EV cargo and cytokine production by MSCs and ACs, depending on their origin close to the subchondral bone or the synovial cavity.

4.3.3.1 Cytokine production in BMSCs-cartilage homeostatic and disease conditions.

A commonly described characteristics of MSCs is their ability to be stimulated to produce specific types of cytokines, chemokines, and other factors. For example, MSCs respond to inflammatory stimuli, such as tumour necrosis factor alpha (TNFα) and interferon gamma (IFNγ), by increasing their immunomodulatory properties. Various inflammatory cytokines and growth factors have been proposed to be fundamental in the development of OA and have been targeted for therapeutic intervention. Several studies have shown that IL-6 is one of the cytokines produced in the largest quantities by MSCs (L. Chen, Tredget, Wu, & Wu, 2008). Despite its well documented proinflammatory functions, for example, anti–IL-6 therapy is effective in some diseases, such as rheumatoid arthritis (RA) (Smolen et al., 2013), IL-6 is a pleiotropic cytokine that not only acts on the immune system, but also is involved in various physiologic events, including hematopoietic stem cell proliferation and differentiation, tumorigenesis, proliferation, and differentiation of neural cells (Naka, Nishimoto, & Kishimoto, 2002). IL-6 produced by MSCs contributes to the maintenance of the “stemness” of MSCs and exerts proliferative and antiapoptotic effects by acting as an autocrine/paracrine factor. Determining if IL-6 has a clear

negative or positive role in cartilage repair might depend on target cells. MSCs steadily produce apparently large quantities of IL-6 even under non-stimulatory conditions and it is therefore interesting how, when in the presence of SZ cartilage, its expression is significantly higher in our system (fig. 19), although IL-6 was identified in the supernatant of all co-cultures conditions. These results suggest two possible scenarios: that IL-6 is produced by chondrocytes or that posttranslational regulation results in reduced release of IL-6. Cytokines mRNA turnover is regulated by post-transcriptional mechanisms (White, Brewer, & Wilson, 2013) such as miRNA mediated mRNA degradation and post-translational regulator like ReagnaseA. ReagnaseA is a post-transcriptional regulator of IL-6 expression in human osteoarthritis chondrocytes (Iwasaki et al., 2011; Makki & Haqqi, 2015). miR-9 and miR-139 are an example of miRNAs that by regulating the expression of RagnaseA increased the expression of IL-6 mRNA in OA chondrocytes (Makki & Haqqi, 2015).

CCL2 and CXCL12 , were both present in the supernatant of BMSCs-MDZ co-cultures and transcript levels were higher (p-values just below significant threshold) in MSCs exposed to MDZ cartilage compared to SZ cartilage. CCL2, also referred to as monocyte chemotactic protein 1 (MCP1), is one of the main mediators of monocyte and macrophage migration in cartilage damage. CCL2 presence in the synovial fluid is associated with radiographic OA progression (Longobardi et al., 2018). *Ccl2* expression is rapidly (<6 hours) induced in whole joints upon surgical joint destabilisation in the mouse (Burleigh et al., 2012) and *in vitro* upon mechanical injury of cartilage (Chong et al., 2013). The principal role of CCL2 in the joint may be to recruit leucocytes following joint injury. However, this role is unlikely to be its only action in cartilage, as the tissue is essentially avascular, therefore several other mechanisms for chemokine action might take place. C-X-C motif chemokine 12 (*CXCL12*) codes for the protein also known as stromal cell-derived factor 1 (*SDF1*) and is generally expressed by synovial cells and its receptor (CXCR4) is present on ACs (Kanbe, Takagishi, & Chen, 2002). CXCL12 was shown to have effects on MSC proliferation (X. Liu et al., 2011), on osteogenesis and angiogenesis (Hosogane et al., 2010; Reiter et al., 2017; Sundararaman et al., 2011), as well as a role in OA. On MSCs, CXCL12 prevents apoptosis by protecting from oxidative stress and by activating survival molecular pathways (X. Liu et al., 2011). *Cxcl12* was shown to be upregulated in cartilage and synovial fluid of OA animal models, and to induce MMP13 in ACs (Wei et al., 2012) CXCL12 has a major role in injury and repair of cartilage by acting as a

chemoattractant of cells involved in inflammation and stem cell migration (G. W. Kim et al., 2015; W. Zhang et al., 2013). By blocking Cxcl2, OA progression was halted in a study by Lu et al., in a rat OA model showing direct involvement of this pathway in the progression of post-traumatic OA (Lu et al., 2016). Similarly to CXCL12, CCL2 can act to blocks chondrogenesis thereby limiting MSCs potential for cartilage repair (Harris et al., 2013). The elevated presence of the two cytokines could explain the inability of BMSCs to undergo chondrogenic differentiation as observed in figure 16.

Despite its inability to provide a description of the total protein content of the supernatant, the proteome array used in this study allowed the presence or absence of a relatively large number of cytokines to be determined. Because of the costly nature of the array, the experiment was conceived as an exploratory step to determine which cytokines were present and if a difference between conditions could be observed. A limitation of the experimental setup is the inability to determine which cell population is responsible for the production of the cytokines. It is, however, important to underline that whichever cell is responsible for producing a certain cytokine, it might be doing so as a result of the dynamic cross talk with to the other cell population. Therefore, whilst probing the array with cartilage only or BMSCs only supernatant would have provided baseline information it wouldn't have provided insight into the interplay between the cell types that might occur during disease, repair or regeneration. To try and identify which cells were principally responsible for the combined cytokine profile, gene expression studies for selected transcripts were performed on the co-cultured MSCs only. The analysis was not performed on cartilage because of the difficulty in isolating enough RNA from the cartilage chips retrieved after the co-culture. Furthermore, it should be acknowledged that gene expression does not always directly correlate with the total amounts of cytokines eventually present in the supernatant. Transduction and export of cytokines outside the cell plasma membrane is a tightly post-transcriptionally regulated process (Anderson, 2008).

According to the more recent hypothesis that BMSCs act as immunomodulators to aid cartilage repair when recruited or injected, the fact that CXCL12 and CCL2 diminished in BMSCs when in contact with SZ cartilage is of interest. In homeostatic conditions, knee articular cartilage is intact and predominantly superficial ACs and their extracellular matrix is exposed to the synovial fluid, that contains and acts as a point of contact with synovial MSCs. When damage occurs, MDZ cartilage is exposed and the surface in contact with the synovial fluid is greater. According to the data shown

here, MDZ cartilage in contact with BMSCs results in a greater and more varied production of cytokines, including anti-chondrogenic CXCL12 and CCL2. Such an effect would be important to start a reparative signalling process but if unchecked could perpetuate a catabolic effect on cartilage. MSCs are however releasing trophic factors that contribute to promote cartilage repair alongside, therefore the effects observed are likely nuanced and influenced in the co-culture.

4.3.3.2 EVs: novel means of communication between cartilage and BMSCs

As mentioned earlier, MSCs are considered to act through their production of trophic factors. EVs have been identified to be one of the principal mechanisms mediating MSCs regenerative effects in ischemia and pulmonary hypertension (Lee et al., 2012; Timmers et al., 2008).

EVs have only recently gained attention in the context of joint diseases with synovial fibroblast and MSC produced EVs mostly studied (Zhang et al., 2018). EVs released in the synovial fluid of inflamed joints (both with OA and rheumatoid arthritis) were shown to have a role in disease progression. A few studies have investigated EVs derived from synovial fibroblasts. In a study by Domenicis et al., exosomes derived from advanced OA synovial fibroblasts were added to macrophages, immune cells responsible for cytokine production and involved in inflammatory regulation. After the treatment, macrophages produced chemokines including MMP13, CXCL1, IL-1β that resulted in inflammation and cartilage catabolism (Domenis et al., 2017). This and other studies underline the primary role of EVs as a mean of communication of MSCs in the knee articulation (Kolhe et al., 2017). Vonk et al. recently published a study indicating that when BMSCs-derived EVs are added to OA ACs, the TNFα mediated expression of inflammatory molecules and enzymatic degradation is halted (Vonk et al., 2018). In addition, EVs had an anabolic effect on ACs, promoting proteoglycans and collagen type II production. The results of these *in vitro* studies suggest that EVs hold great promise as a therapeutic strategy for cartilage repair. The advantages in terms of therapeutic usage of EVs over MSCs seem numerous. EVs are easier to obtain, have long shelf life and are not damaged by freeze-thaw cycles. The avoidance of cells also eliminates the immune related issues of allotransplantation (even if MSCs are considered immune privileged), the dangers of ectopic migration and engrafting and their subsequent abnormal cell proliferation. However, the composition of MSC

secretome encompasses cytokines and growth factors, in addition to EVs. Protocols to obtain sufficient amounts of EVs are not yet been satisfactory due to limitations in cell growth and large variations among the donor cell types. Furthermore, using MSCs has the advantage that the cell can respond to environmental cues when delivered to the site of injury, producing regenerative, trophic and anti-inflammatory factors while EVs cargo is stable. Further study of EVs and the cells they are produced by are needed to improve their therapeutic potential. The role and mechanism of EVs produced by ACs, for examples, is largely understudied.

4.3.3.3 EVs contains different miRNA depending on ACs zonal origin.

The content of EVs includes proteins, mRNA, lncRNA, miRNA. These elements are responsible for modulating gene expression resulting in downstream alteration of recipient cell function and consecutively physiological and pathological processes. In this study, miRNAs were the only type of EV cargo studied.

The miRNA content of the EVs was assessed using Nanostring technology that allows simultaneous investigation of about 800 miRNAs that were chosen because of their known biological significance (according to published studies). 38 miRNAs were detected in the EVs isolated in this thesis. The top 10 miRNAs from SZ and MDZ conditions that are reported and described in table 3 shows how the MDZ miRNAs are not well studied in cartilage tissues and cells. The results reported here link for the first time these miRNAs to cartilage and MSCs field of study.

Five miRNAs were significantly differentially expressed between the SZ and MDZ conditions, with mi-R188-5p and miR-612 having significant higher expression in MDZ and miR23a-3p, in particular, having high expression in ZS along with miR-199a/b and miR-451a (fig. 25)

miR-188-5p is located on the X chromosome and has been reported to be present in synovial tissue from RA patients. Downregulation of this miRNA resulted in migration inhibition, and its expression was downregulated by exposure to IL-1β. miR-188 was reported to be found in MSCs-derived EVs (Y. Nakamura et al., 2015). It was also linked to proliferation, migration and invasion of metastatic prostate cancer cells when inhibited (Fang et al., 2015). Targets of miR-188-5p include MMP2 and MMP13: by downregulating MMPs, miR-188-5p prevented the participation of BMSCs in neo-vascularisation of the eye (Hou et al., 2018). There are no studies showing whether

miR-188-5p also target MMPs in cartilage, but such a study would be extremely relevant for therapeutic strategies aimed at blocking cartilage degradation during OA. miR-612 is located on Chromosome 11 and has been shown to target and regulate the Wnt and Naong pathways and has inhibitory effects on cell proliferation, migration, invasion, and metastasis of hepatocellular carcinoma (Y. Liu et al., 2016; J. Tang et al., 2014) No data are present in the literature on the role on miR-612 in cartilage or BMSCs.

miR-451a is a miRNA located on chromosome 17qll.2 whose expression is regulated by hypoxia, and its activity is linked to the proliferation, migration, differentiation and regulation of the haematopoietic system (Altuvia et al., 2005). The target genes of miR-451a include a calcium-binding protein, eukaryotic translation elongation factor, and the F-box protein family, as well as proteins relevant to cartilage degradation (MMP2, MMP9, ADAM10) and inflammation (IL6R). Studies that focus on the role of miR-451a in cartilage show a link to OA. In a recent study, miR451 was detected as a plasma circulating miRNA and could be used as a biomarker for OA (Coutinho de Almeida et al., 2019). miR-451a was also shown to be involved with chondrocyte apoptosis (L. Tang, Ding, Zhou, & Liu, 2018). miR-451 was found in MSCs-derived EVs and to act as a stimulator of cell proliferation and viability in kidney cells (Zhong et al., 2018).

miR-199a-3p is another of the listed miRNA that seems to target and modulate Wnt signalling. miR-199 acts as an activator/inhibitor of endothelial-to-mesenchymal transition, targeting β-catenin in Wnt signalling (Zhao et al., 2014). miR-199a-3p has been reported to negatively regulate chondrogenesis (Lin et al. 2009; Akhtar and Haqqi 2012) and have a role in ACs senescence (Tian, Zhang, & Chen, 2014). miR-199a-3p validated targets that have a relevant role in chondrogenic differentiation including SMAD1 (Lin, Kong, Bai, Luan, & Liu, 2009), CD44 (Henry et al., 2010) and Cyclooxygenase2 (Akhtar & Haqqi, 2012).

Although both miR-612 and miR-199a-3p would be interesting to study further thanks to their role as Wnt pathway modulators, no exhaustive study is available to confirm that these miRNAs are also regulating Wnt in ACs or chondroprogenitor cells.

Finally, miR-23a-3p was identified as differentially expressed between SZ and MDZ conditions in this study, showing higher expression in the SZ samples. miR-23a-3p is located on chromosome 19 and is involved in different cellular processes, including proliferation, senescence and ECM synthesis and is found at increased levels in rheumatoid arthritis cartilage and synovial fluid of OA patients (Hu et al., 2017; Li et al.,

2016). miR-23a-3p targets SMAD3, a TGF-β signalling mediator, which is critical in cartilage development, homeostasis, and repair (Kang et al., 2016). Additionally, miR-23a-3p act to downregulate the expression of COL2 and ACAN (Kang et al., 2016). The suppression of miR-23a-3p in OA ACs enhanced chondrocyte-specific marker expression (Prasadam & Xiao, 2018). Runt-related transcription factor 2 (RUNX2) was identified as a direct target of miR-23a-3p and showed an up-regulation of RUNX2 levels after experimental downregulation of miR-23a-3p (He, Meng, Shao, Wang, & Yang, 2014; Prasadam & Xiao, 2018).

miRNAs detected in EVs from BMSCs alone in culture, cluster separately from miRNAs from either SZ or MDZ conditions, as shown in figure 23. It has been postulated that SZ chondrocytes would resemble MSCs, as PRG4 positive chondrocytes are putative progenitors of ACs. Looking at the overlap between the miRNAs in SZ and BMSCs conditions, 2 miRNAs are present among the top 10 expressed genes, miR-23a-3p and miR-125b-3p. No miRNAs are overlapping between MDZ and BMSCs conditions. As discussed above, miR-23a-3p is also significantly differentially expressed and higher in SZ compared to MDZ conditions, and an interesting miRNA in cartilage homeostasis. miR-125p-5p has recently been reported in different studies to regulate inflammation in OA. It was reported to act through IL-1β to induce the expression of inflammatory genes and cartilage degradation by regulating ADAM4. miR-125p-5p stimulates inflammation in chondrocytes via MIP1α signalling. Interestingly, it was found in the supernatant of BMSCs-OAZ co-cultures, but not in the other two co-culture conditions (fig. 18).

Further experiments studying the relations between miR-23a-3p and miR-125p-5p would help elucidate the different signalling mechanisms between SZ and MDZ ACs, and how this difference is important in term of cartilage repair and OA progression. As SZ cartilage favoured chondrogenesis of BMSCs pellets compared to MDZ and OAZ cartilage in our experiment, miR-23a-3p and miR-199 could potentially be explored as a therapeutic in the contest of cartilage repair and regeneration. A caveat resides in using miR-23a-3p in cartilage where inflammation is present, as it seems to respond to inflammatory stimuli (IL-1β) and potentially having a catabolic effect in OA cartilage (Li et al., 2016). miR-23a-3p could be considered in the context of MSCs differentiation towards chondrocytes, rather than therapeutic in OA context. Given the role of miR-

199 in regulating the Wnt pathway and blocking senescence, this miRNA could be explored as therapeutic.

Promoting apoptosis of synovial cells, and contributing to inflammation via MIPα signalling and aggrecanases expression in OA ACs, miR-125 could be potentially explored as a target in disease.

4.3.4 Limitations of the study

One major limitation of the study is the use of cartilage solely from final stage OA patients with different previous treatment interventions. The cartilage obtained from the macroscopically intact lateral condyle was considered as a “control” but it should be kept in mind that OA is considered a whole joint disease and the tissue from this region could also have been exposed to pathological stimuli in the form of soluble mediators of altered mechanical load. However, also genomic studies use chondrocytes isolated from the lateral condyle as relative control (Tachmazidou et al., 2019). To better represent the potential treatment group, it would be most appropriate to study articular cartilage from younger donors. However, total knee replacement in patients younger than 50 years of age is less common and whilst other orthopaedic procedures may have provided access to human cartilage, they would have been more sporadic or insufficient in terms of tissue amount to enable appropriate studies to be conducted. As an alternative, ovine healthy articular cartilage could be obtained to determine if SZ AC characteristics, with respect to their MDZ counterparts, reflect the results presented here. However, that would limit the observation to an animal model but would permit larger-scale experimentation on tissue more closely matched in terms of age.

In order to study and compare the EVs present in the co-cultures conditions described in this chapter, EVs were isolated with a kit that allowed EVs precipitation. The choice of methodology for EVs isolation depends on the downstream functional study objective. Ultracentrifugation is an effective isolation method that is more cost-efficient and more widely used. However, it is time-consuming and it requires large amounts of cells. It also might damage vesicles and affect their downstream analysis. On the other hand, the method of choice presented here has limited the ability to fully characterise the isolated vesicles. EV characterisation following isolation is generally a necessary step to determine which subtypes of EVs are produced. EVs were characterised here by size and morphology, but it was not possible to obtain a clear description of EVs

biomarkers CD9, CD63 and CD81. However, the study of EVs was focusing on miRNA content, more than their origin derivation, and therefore the exact characterisation of the EVs in this context is secondary. Another limitation is that it is not possible to distinguish from which cell type the EVs are derived because of the co-culture set up. Similar to what was discussed above, the driving hypothesis is that the EVs would be produced by either cell type in response to being exposed to each other. It was therefore not possible to study such EVs without mixing the two cell populations. Theoretically, it might be possible to determine from which cell a subpopulation of EVs is derived. Microvesicles originate from the plasma membrane surface, in contrast to exosomes, which are of endosomal origin. Hence, microvesicles should present superficial markers that reflect their cell of origin, which could be exploited in flow cytometry approaches to achieve sorting. However, several technical limitations are associated with sorting EVs to determine their cell of origin. In addition, markers to discriminate between MSCs and ACs are not well defined in the literature.

Another point to develop further is the characterisation of the EVs studied. MSC-derived EVs are more widely described in the literature than AC-derived EVs. Very few studies have investigated EVs derived from articular ACs either ex vivo or from isolated cells in vitro. A full characterisation of EVs isolated from SZ or MDZ cartilage is not presented here and would be important to further confirm the different nature of regional ACs.

4.4 Summary and future work.

Chondrocytes isolated from different zones of articular cartilage have distinct phenotypes and properties. The influence of resident ACs on cartilage repair is of great relevance not only to surgical techniques like bone marrow recruitment techniques and ACI but to better understand cartilage tissue in homeostasis and disease. A further and deeper analysis of human cartilage layers is required, as they are in fact made up of different cell subpopulations. RNA sequencing or single cell analysis would describe at the molecular level the specific cartilage subpopulation. The outcome of such studies would potentially be a starting point for identifying new cell and molecular mechanisms involved in repair or disease, or for discovering new markers to isolate cell subpopulations within the tissue.

This study further supports the presence of proliferative progenitor cells in the superficial zone. Such progenitor cells would be useful for determining the molecular and transcriptional signatures that cartilage progenitor should possess. Not only would this allow us to pin down which specific subset(s) of cells contribute to cartilage repair and could potentially be targeted by therapeutics, but also those cells that could be specifically isolated for cell therapy.

Cytokines and chemokines are homeostatically present in the synovial fluid in contact with the SZ of knee cartilage and are produced by the heterogeneous population of cells present around the synovial cavity: synovial fibroblast, monocytes and blood-borne cells present in the highly vascularized synovial tissue, fat pad, cartilage. Generally, a low degree of inflammation is considered beneficial and necessary to recruit specialised cells and induce tissue repair (Haseeb & Haqqi, 2013). After cartilage damage, damage-associated molecular pattern (DAMP) endogenous molecules signal to immune and other cells to initiate and contribute to the reparative response. Immune cells respond by, among others, releasing cytokines. Prolonged DAMP signalling may result in overexpression of particular cytokines and induce a catabolic effect in cartilage, instead of promoting its repair. In the study presented here, SZ cartilage is responsible for promoting different signalling to MSCs, and possibly other cell types present in the knee, compared to the MDZ.

Because of the emerging role of EVs in cartilage homeostasis and disease, it is fundamental to improve our understanding of how EVs are involved in the initiation, progression and modulation of cells in the joint system. As MSC-derived EVs are currently being explored and exploited as a therapeutic, it is paramount that a better description of their cargo is available. This study has shown for the first time that miRNA obtained from SZ-BMSCs and MDZ-BMSCs co-cultures are different. Recently, Chen et al. (Y. Chen, Xue, Zhang, Zheng, & Liu, 2018) reported the use of rabbit ACs derived exosomes for promoting in vivo chondrogenic differentiation of cartilage precursors. When comparing exosomes derived from ACs to exosomes derived from BMSCs, the former induced formation of stable cartilage with limited hypertrophic markers, and inhibition of angiogenesis compared to the other condition. This study, therefore, suggests that obtaining EVs from ACs for use in cartilage repair strategies might be more beneficial for cartilage production than EVs from BMSCs. Using EVs from both ACs and BMSCs, either alone or in co-culture from in vitro cell

culture might be of interest to target different aspects of early-stage OA. Combining inflammatory modulation of EVs from BMSCs and anabolic induction molecules to repair cartilage tissues could be an interesting strategy to achieve optimal healing or regeneration. In this situation, the miRNA contained in the EVs isolated in the experiment could be interesting to study further as these EVs are obtained from a co-culture of the two cell types.

This work showed for the first time that depending on its proximity to the bone or the synovial cavity, cartilage signalling varies in terms of EV cargo and cytokine/chemokine production. The different signalling factors produced by these different cartilage regions could explain the differences in chondrogenic differentiation of BMSCs in these studies. Although the observations presented here are only from an in vitro system it does indicate the likelihood of differential contributions of distinct chondrocyte populations during cartilage repair and regeneration.

5 DACT1 and DACT2 in knee joint tissues

5.1 Background and rationale

Further investigation of the events that initiate OA is essential to developing strategies to arrest cartilage degradation that leads to the disease. The thinning of superficial hyaline cartilage is, among other changes including subchondral bone remodelling, one of the identified features of the early stages of OA. The SZ of cartilage has unique mechanical properties resulting from its distinct proteoglycan and molecular content compared to the deeper regions (D. Archer, 1999). Aligned collagen and elastin fibres are arranged parallel to surface, whereas they are perpendicular in the MDZ. The proteoglycan content and density are also different from the deeper zones. ACs in the SZ have an elongated shape and are parallel to the articular surface unlike the more spherical chondrocytes in the deeper zones. MDZ ACs have a lower metabolism, both in producing proteins and in responding to load. The causal link between the loss of SZ and OA initiation has been suggested to be lubricin. Lubricin is encoded by the gene *PRG4* and binds onto cartilage surfaces forming a molecular monolayer that ensures low friction during joint motion, preventing hard contact of the joint extremities. The role of Lubricin was identified by studies that selectively removed by enzymatic cleavage several molecules found at the cartilage surface (Chan, *et al.,* 2010). Furthermore, it was shown in mouse that cartilage containing collagen II positive cells overexpressing *PRG4* is protected from tissue degradation after surgery inducing OA (Ruan et al., 2013). Finally, the observation that *PRG4* expressing cells in the SZ act as chondroprogenitors introduces a new level of complexity in understanding the relevance of SZ loss in OA (Decker et al., 2017; Kozhemyakina et al., 2015). Whether the SZ is a stem or progenitor cell niche that can supply new chondrocytes during adulthood is still unclear.

Mechanical loading, which is pivotal in *PRG4* regulation, regulates Wnt signalling (Brunt, Begg, Kague, Cross, & Hammond, 2017; Ogawa, Kozhemyakina, Hung, Grodzinsky, & Lassar, 2014; Praxenthaler et al., 2018). *PRG4* has been demonstrated to be a transcriptional target of TGFß via activation of Smad3, a transducing protein in the TGF-ß pathway (Chavez, Sohn, & Serra, 2019). Stem cell maintenance and differentiation are regulated by the Wnt and TGFβ pathways (Cleary, van Osch, Brama, Hellingman, & Narcisi, 2015; Narcisi et al., 2015). Because of the close relationship of such processes, studying proteins that regulate Wnt and TGFβ pathways in cartilage

is essential to further our understanding of the part that the SZ plays in cartilage homeostasis and to find potential therapeutic targets.

DACT1, DACT2 and DACT3 are proteins at the intersection of the Wnt and TGFβ pathways. DACTs interact with Dishevelled (Dvl), Casein Kinase δ/ϵ, Vangl, Protein Kinase A and C, (important in the various Wnt pathways), or with the Alk4/5 TGFβ receptors. Dact1 seems to accelerate Dishevelled2 degradation by promoting its ubiquitination leading to aggregate-induced autophagy. As it can bind and facilitate Alk5 degradation, Dact2 has been described to be a suppressor of TGFβ-dependent wound healing and Nodal-dependent mesoderm induction (Y. Su et al., 2007; L. Zhang et al., 2004). These multi-domain proteins are well conserved among bony vertebrates and have been identified in mammals, chicken, frog and zebrafish (Schubert, Sobreira, Janousek, Alvares, & Dietrich, 2014), suggesting that their role is fundamental in developmental processes. Therefore, Dact proteins can positively or negatively regulate the Wnt pathway. In the last few years, a role for DACTs in cartilage has emerged. Using laser microdissection of rat articular cartilage, Mori and colleagues have reported that the expression of Dact2 is significantly (16.5 fold) higher in the superficial zone chondrocytes compared to the articular cartilage (Mori, Chung, Tanaka, & Saito, 2014). Shubert and colleagues (Schubert, *et al.*, 2014) reported that Dact1 and 2 are involved in limb development by integrating Wnt and TGFβ signalling. To date, no thorough study is available on DACT proteins in cartilage homeostasis and disease or description of these proteins in the context of human joints DACT proteins could be interesting mediators of the cartilage reparative process as they are present in the superficial, stem cell/progenitor -enriched zone of articular cartilage in rat. In this chapter, the presence of DACT1 and DACT2 were investigated in mammalian tissues. Human macroscopically normal and OA samples were analysed for gene and protein expression of DACT1 and DACT2. To investigate the presence of DACT during development, mouse embryonic limbs were processed and stained for DACT1 and DACT2.

5.2 Results

5.2.1 DACT1 and DACT2 are present in healthy and OA cartilage.

The presence, role and regulation of DACT proteins in human articular cartilage had not been previously reported, therefore DACT gene expression in the different femoral condyle zones and in osteoarthritic full-thickness cartilage was assessed in samples from four different patients (fig. 28). To investigate *DACT1* and *DACT2* expression, primers were designed. Studying DACT2 at gene expression level in human cartilage was not performed because of inability to design an optimal primer. Primers were tested on the RNA isolated from HEK cells, which express both genes. A ready primer was also purchased from but failed when tested. RT-qPCR analysis revealed that *DACT1* is expressed in human adult cartilage (fig. 28). Matched samples from either the lateral (non-OA “control”) or medial (“OA”) side from each patient shows that *DACT1* expression is reduced in OA cartilage. Overall, *DACT1* Ct values were low, indicating that these genes are likely expressed at a low level in cartilage tissues compared to marker genes such as COL2 or ACAN (data not shown). RNA was isolated directly from cartilage tissue, by pulverising the cartilage in liquid nitrogen and extracting RNA with TriZol reagent. Initially, the experiment was performed on chondrocytes that were isolated from cartilage by overnight collagenase treatment. Enzymatic overnight treatment was considered as possibly disruptive to the original expression of genes as lowly expressed as DACT1. It was decided to opt for a method that would maintain the gene expression profile as close as the (patho)physiological one as possible. Samples were therefore harvested within two hours from surgery and snap-frozen and extracted in liquid nitrogen.

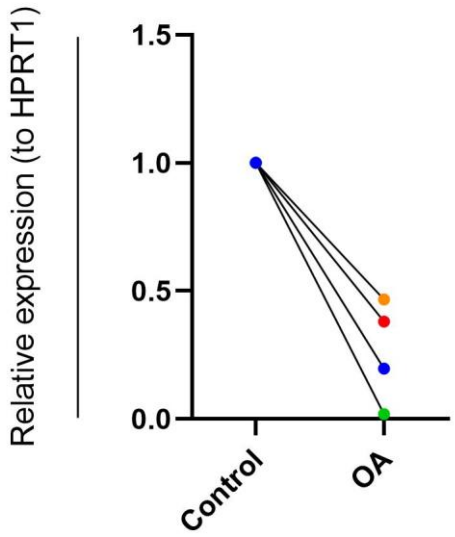

Figure 28 **Gene expression of *DACT1* in matched OA and non-OA samples.** qPCR was performed on cartilage samples from either lateral condyle ("Control") or medial condyle ("OA"), linking line indicates samples from the same patient (N=4).

After observing that *DACT1* are present in cartilage tissue, protein expression was evaluated by immunohistochemistry on cartilage tissue obtained from end-stage OA patients undergoing total knee replacement surgery. Immunohistochemistry does not allow permit real quantification of the protein of interest but offers qualitative information about which cells of the analysed tissue expressed the protein and if it is intracellular or extracellular. DACT1 staining (brown) is mostly localised intracellularly in cells present in the SZ of cartilage harvested from the lateral condyles (fig. 29), while ACs in the MDZ are green (methyl green counterstaining) and show no DACT1 protein. The brown staining region is approximately overlapping to the non-GAG rich SZ identified by the SafraninO/FastGreen staining (blue). DACT1 staining was visible in some of the cells present in the underlying bone. DACT2 was similarly expressed mostly in the SZ of the lateral condyle. Occasionally, brown staining in ACs in the MDZ was detected (fig. 30).

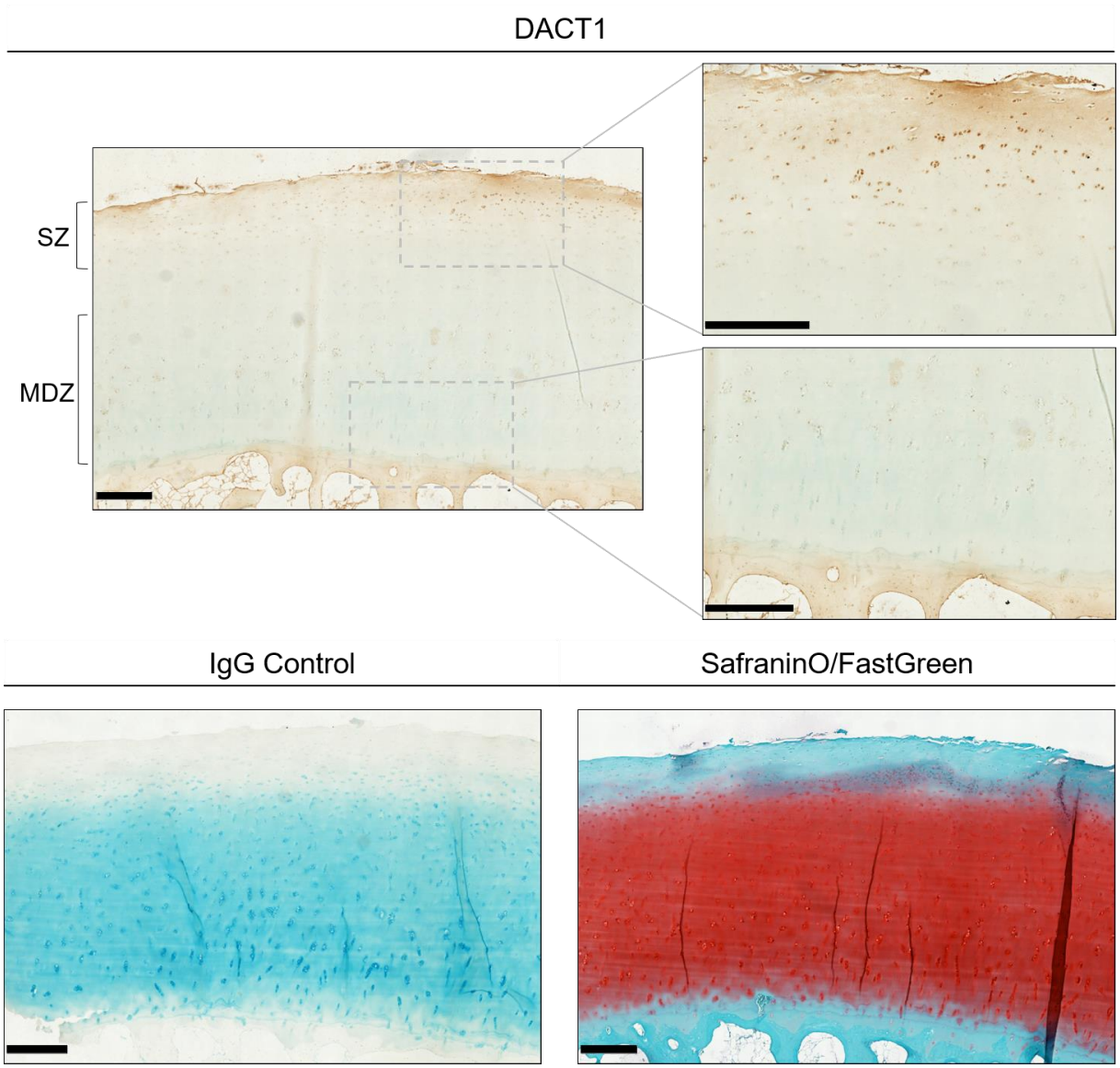

Figure 29 **DACT1 is expressed in the superficial zone of human articular cartilage.** Methylgreen counterstaining and immunohistochemistry with DACT1 antibody performed on 5 µm thick section from paraffin-embedded samples, after 2 weeks de-calcification protocol. Chondrocytes staining for DACT1 are in brown and non-stained appear green. Rabbit IgG was used as a negative control and SafraninO/FastGreen (red: GAGs; light blue: non GAG-rich tissue, bone) to show histomorphology of the non-OA cartilage sample. Representative images are shown, error bars = 0.5 mm. Staining was repeated on samples from different patients (N=5).

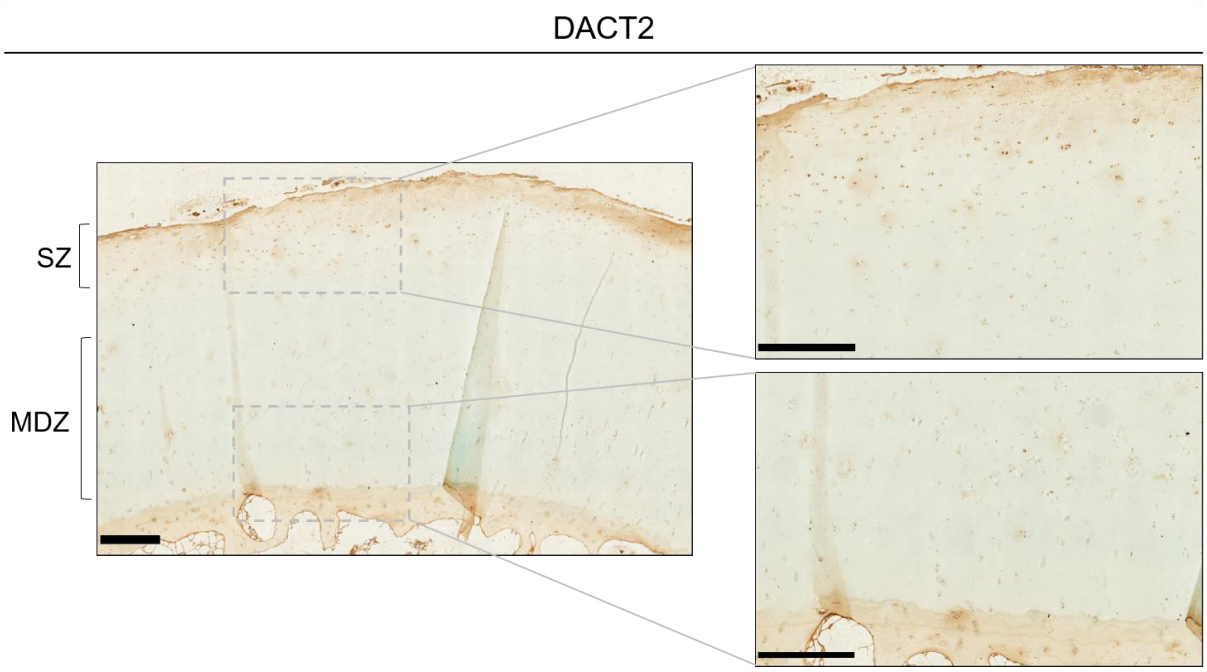

Figure 30 **DACT2 is expressed in the superficial zone of human articular cartilage.** Methylgreen counterstaining and immunohistochemistry with DACT1 antibody performed on 5 µm thick section from paraffin-embedded samples, after 2 weeks de-calcification protocol. Chondrocytes staining for DACT1 are in brown and non-stained appear green. Refer to fig. 29 for controls. Representative images, error bars = 0.5 mm. Staining was repeated on samples from different patients (N=5).

Because of the differential expression of *DACT1* and *DACT2* in the "control" (macroscopically non-osteoarthritic) condition compared to OA cartilage, OA tissue was also assessed with immunohistochemistry. Both DACT1 and DACT2 show staining in the cell clusters present in fibrillated cartilage. As a result of OA, cartilage tissue architecture is compromised with no clear SZ and MDZ (fig. 31), SafraninO/FastGreen).

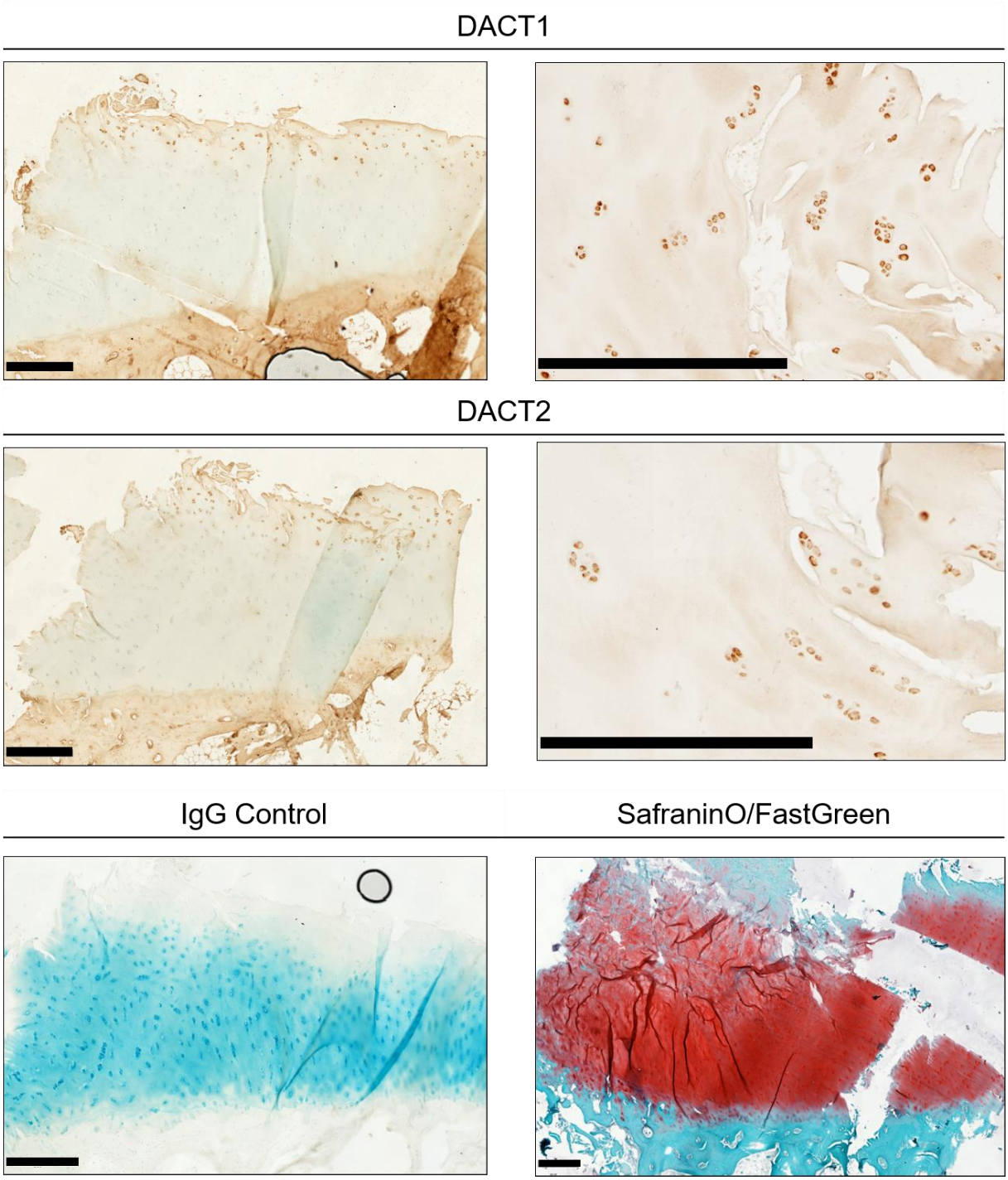

Figure 31 **DACT1 and DACT2 are expressed OA cartilage**.
Methylgreen counterstaining and immunohistochemistry with DACT1 and DACT2 antibody performed on 5 µm thick section from paraffin-embedded samples, after 2 weeks de-calcification protocol. Chondrocytes staining for DACT1 or DACT2 are in brown and non-stained appear green (images on the left, scale bar 0.5 mm). Representative images, staining was repeated on samples from different patients (N=5). Images on the right for DACT1 and DACT2 show details of cell clusters in higher magnification. Scale bar = 0.5 mm). IgG control and SafraninO/Fast Green staining show bone and non-GAG rich tissue, blue and GAGs, red.

To determine the subcellular localisation of DACTs in chondrocytes, ACs were enzymatically isolated from the articular cartilage samples and immunohistochemistry was performed. Confocal microscopy shows that DACT1 and DACT2 are present exclusively in the cell cytoplasm (fig. 32). DACT2 is also highly expressed around the nucleus, probably in the endoplasmatic reticulum (ER) the cellular organelle responsible for protein production, trafficking and cell communication.

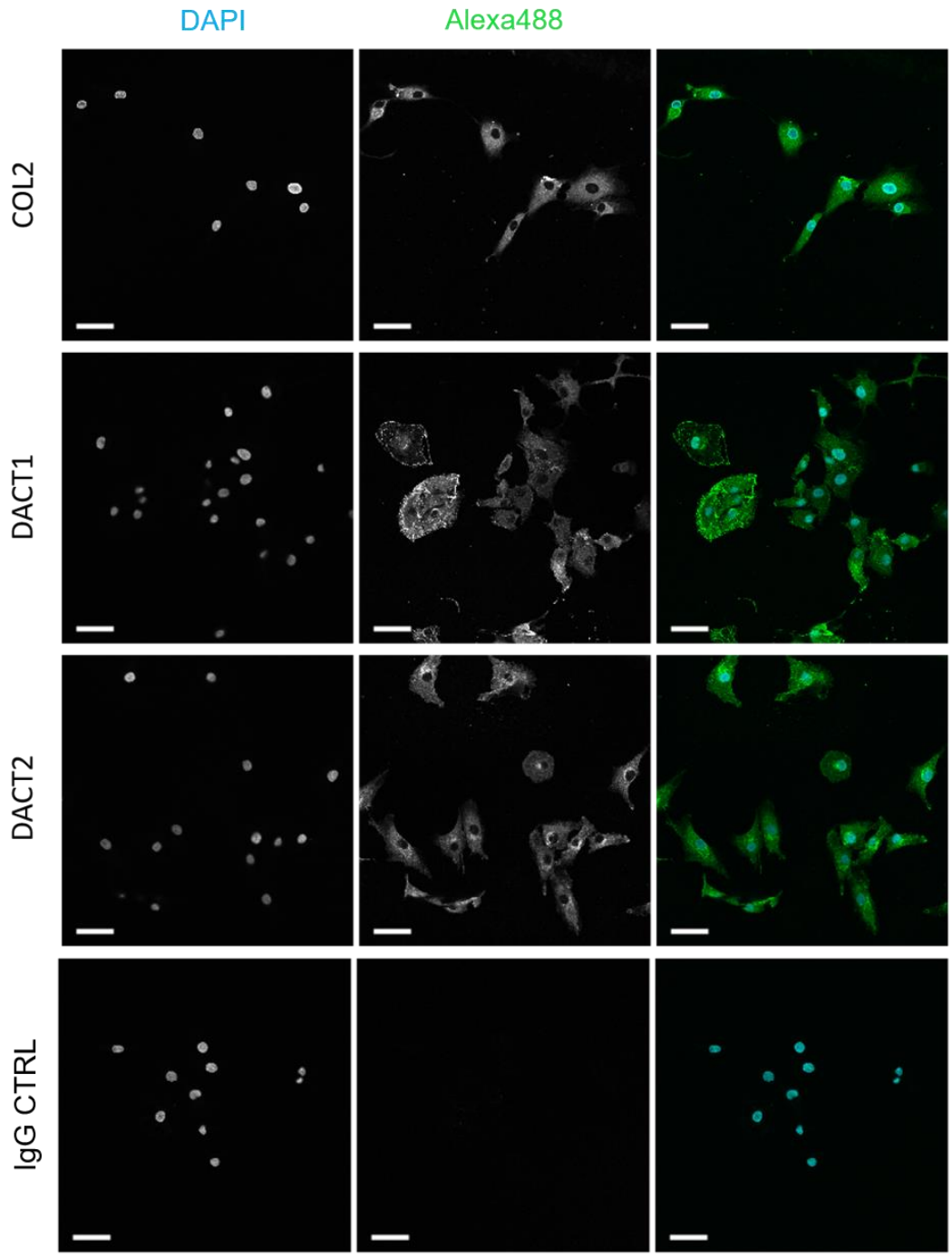

Figure 32 **DACT1 and DACT2 are expressed in the cytoplasm of human chondrocytes.**
Immunohistochemistry was performed on chondrocytes isolated from knee cartilage. Fixed cells were stained for COL2, DACT1 and DACT2 with primary antibodies at concentrations described in table 2.3. Alexa488 secondary antibody (1:1000) was used for all stainings. Imaged by confocal microscopy (40x objective). DACT1/2/COL2, green; nuclei, blue. Scale bar indicates 50 µm.

Developmentally, the articular cartilage and the synovium derive from the same cell precursors (Decker et al., 2017; Koyama et al., 2008; Roelofs et al., 2017). It was

therefore hypothesised that DACT1 and DACT2 could also be expressed in the synovium. Sections of the synovial membrane obtained from patients undergoing total knee replacement were analysed for the expression of DACT1 and DACT2. Synovial samples were isolated from the parapatellar region of the knee joint (fig 33). The synovial lining cell layer is enlarged, as expected from a sample isolated from a patient with advanced OA.

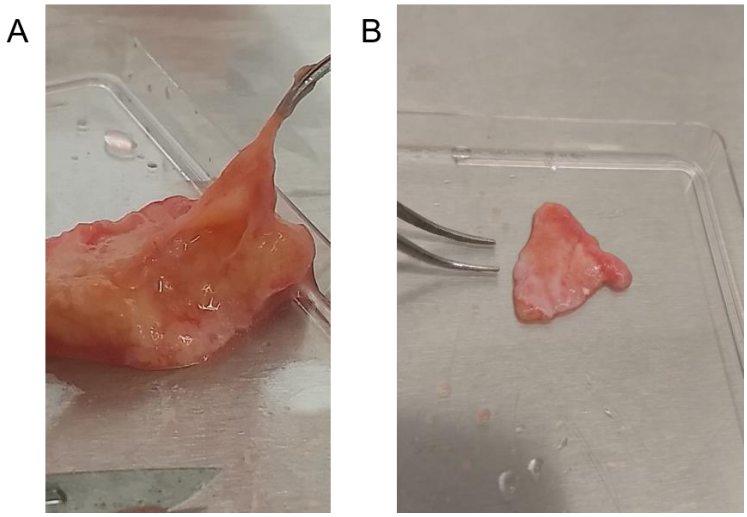

Figure 33 **Synovial membrane isolated from parapatellar region of human knee joints**.
Section of the fat pad and attached synovial membrane are removed during total knee replacement by the orthopaedic surgeon (A). Using tweezers and scalpel, the synovial membrane (B) is then separated from the fat tissue and processed for histological analysis or treated to isolate SynMSCs.

Figure 34 shows immunohistochemistry for DACT1 and DACT2 on the synovium obtained from a patient undergoing total knee replacement. The synovium is rich in small blood vessels (indicated by arrows) and the synovial lining, which is the side in contact with the joint cavity, is visible at the upper end of the images. DACT1 and DACT2 (in brown) are mostly staining the same regions: endothelial cells around blood vessels, the cytoplasm of cells at the synovial lining.

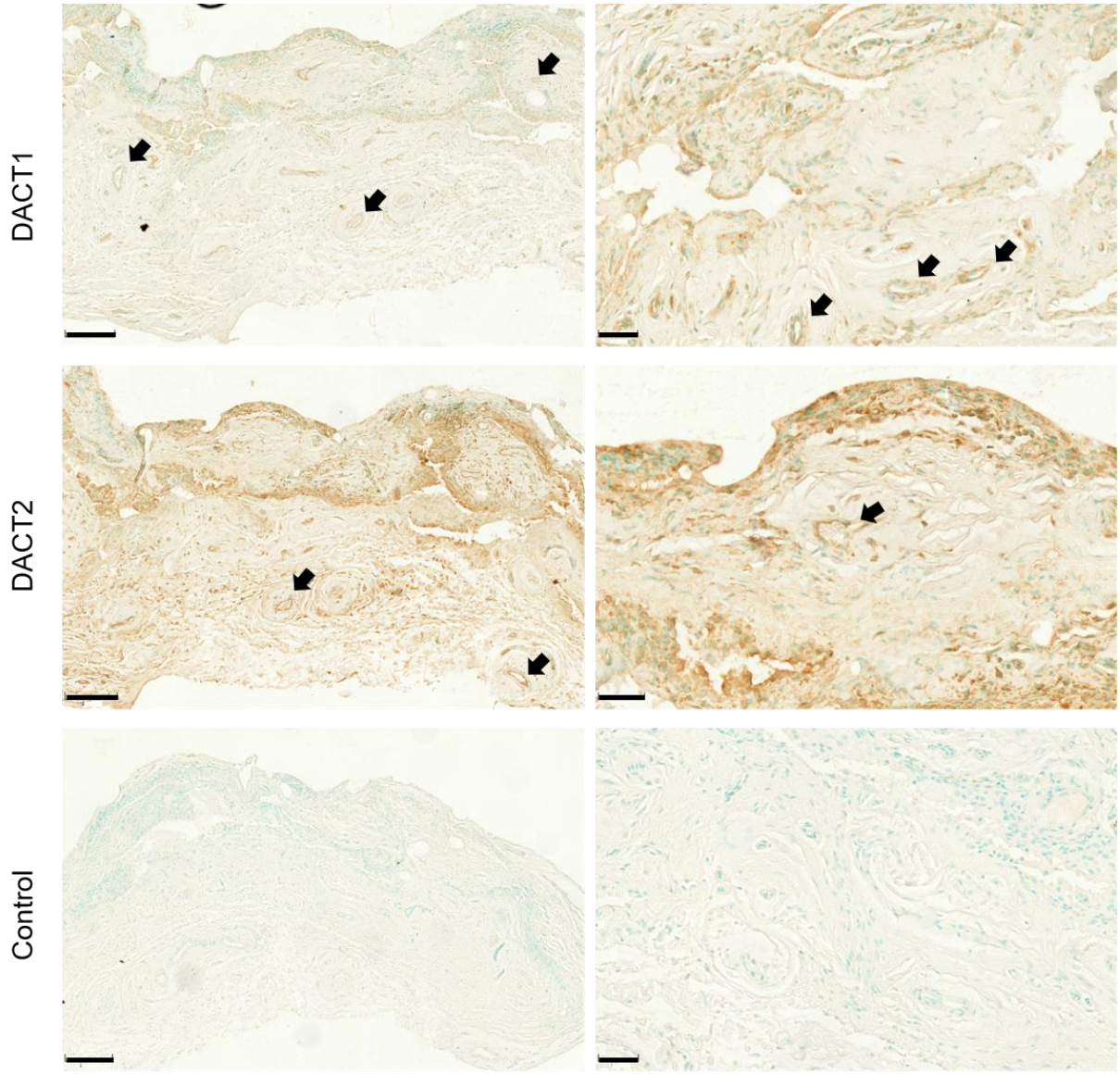

Figure 34 **DACT1 and DACT2 are expressed in human synovial tissue**.
Methylgreen counterstaining and immunohistochemistry with DACT1 and DACT2 antibody performed on 5 µm thick section from paraffin-embedded synovial membrane samples. Brown DAB staining indicates DACT1 and DACT2 protein and non-stained cells appear green. Representative images, staining was repeated on samples from different patients (N=3). Control condition used Rabbit IgG and then DAB was applied for 20 seconds, as for the other conditions. Scale bars for images on the left, 500 µm; Scale bar for images on the right, 50 µm.

5.2.2 Dact2 is expressed in the developing synovial joints of mouse

Mesenchymal cell condensation at the site of a future joint is a key step in synovial joint formation, which is visible from E13.5 (Shwartz et al., 2016) and proceeds to joint cavitation development at E14.5 and E15.5. The cells in the prechondrogenic space were shown to be GDF5^{+}, the earliest marker of joint formation (Koyama et al., 2008). GDF5 expressing cells give rise or contribute to the formation of superficial cartilage,

menisci, ligaments and synovium. Because of this common progenitor and the observation that DACT1 and DACT2 are expressed in GDF5 derived adult synovial joint tissues, DACT1 and DACT2 expression during limb development was examined. Limbs were obtained from mouse embryos at embryonic day (E) 13.5, 14.5, and 15.5 and analysed by immunohistochemistry to describe the expression of Dact1 and Dact2 in the developing limbs.

The interzone is visible at E13.5 at the prospective metacarpal-phalangeal and interphalangeal joint sites (fig. 35, large arrows). DACT1 staining is not present on E13.5 mouse limbs. DACT2 is present on the endothelial cells around blood vessels (fig. 37, black arrow heads), and possibly a very weak signal is detected at the Interzone.

At E14.5 the Interzone is still present and the cavitation phase has not yet started. DACT1 is not expressed at the interzone, as well as DACT2, which continues to be only present around blood vessels (fig. 36, black arrow heads).

Staining for DACT2 is clearly visible (fig. 37, black arrows) at day E15.5 when joint cavitation has begun, and DACT1 and DACT2 are also present on the endothelial lining of vessels around the digits. DACT2 staining is also visible at all three stages in the developing tendons and skeletal muscles (indicated by *) of the limb.

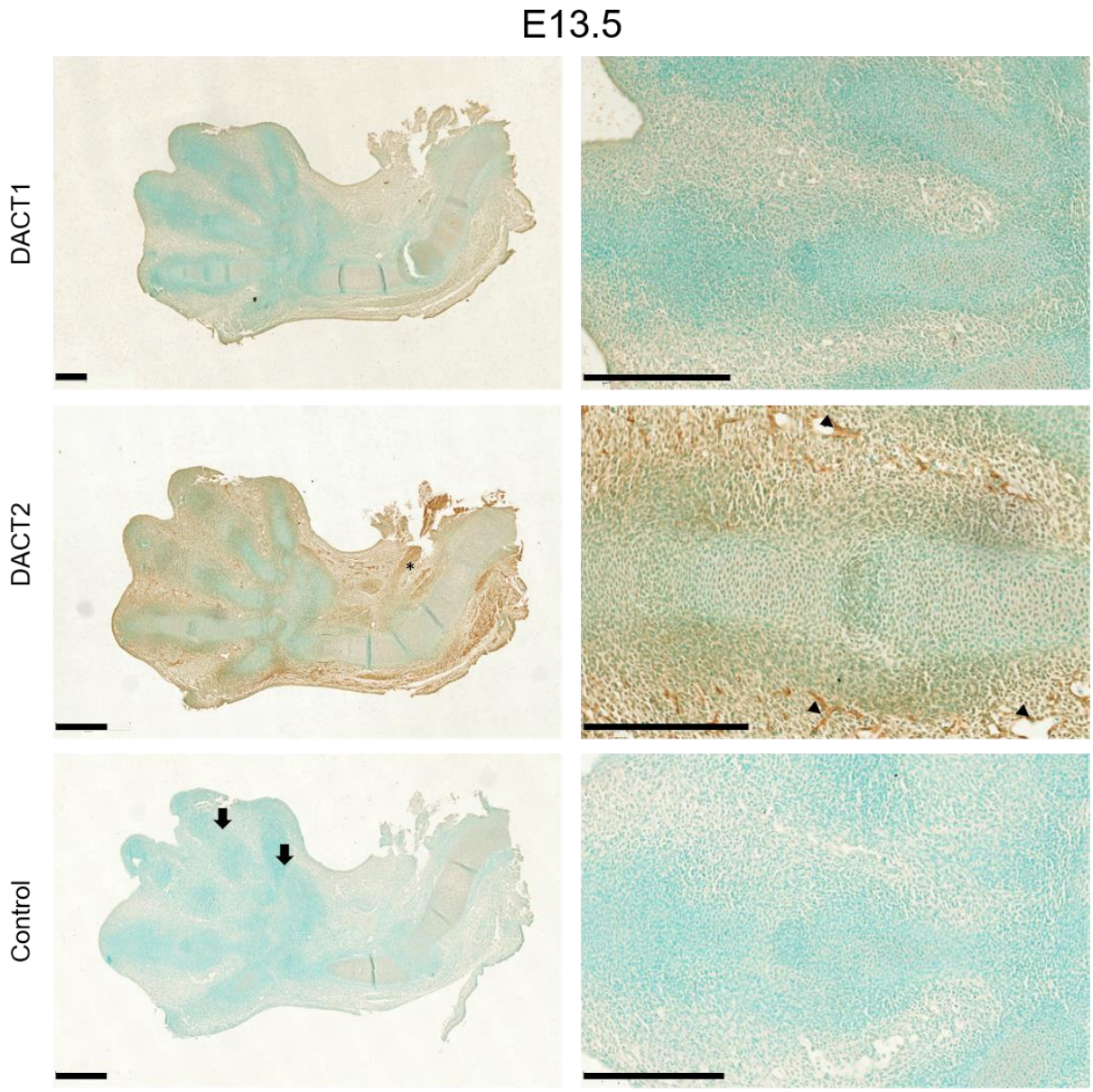

Figure 35 **Dact1 and Dact2 expression in developing mouse limb at E13.5.** Immunohistochemistry with Dact1 and Dact2 antibody performed on 5 µm thick section from paraffin-embedded limb of E13.5 C57BL/6J mice. Methylgreen was used as counterstain. Brown DAB staining indicates Dact1 and Dact2 protein and non-stained cells appear green. Black arrow heads indicate positive staining. Control condition used Rabbit IgG and then DAB was applied for 30 seconds, as for the other conditions. Images on the left shows the whole embryo limb, images on the right show a higher magnification of the phalangeal joint site. Large arrows: interzone sites; arrow heads: endothelial cells. Scale bars = 0.5 mm.

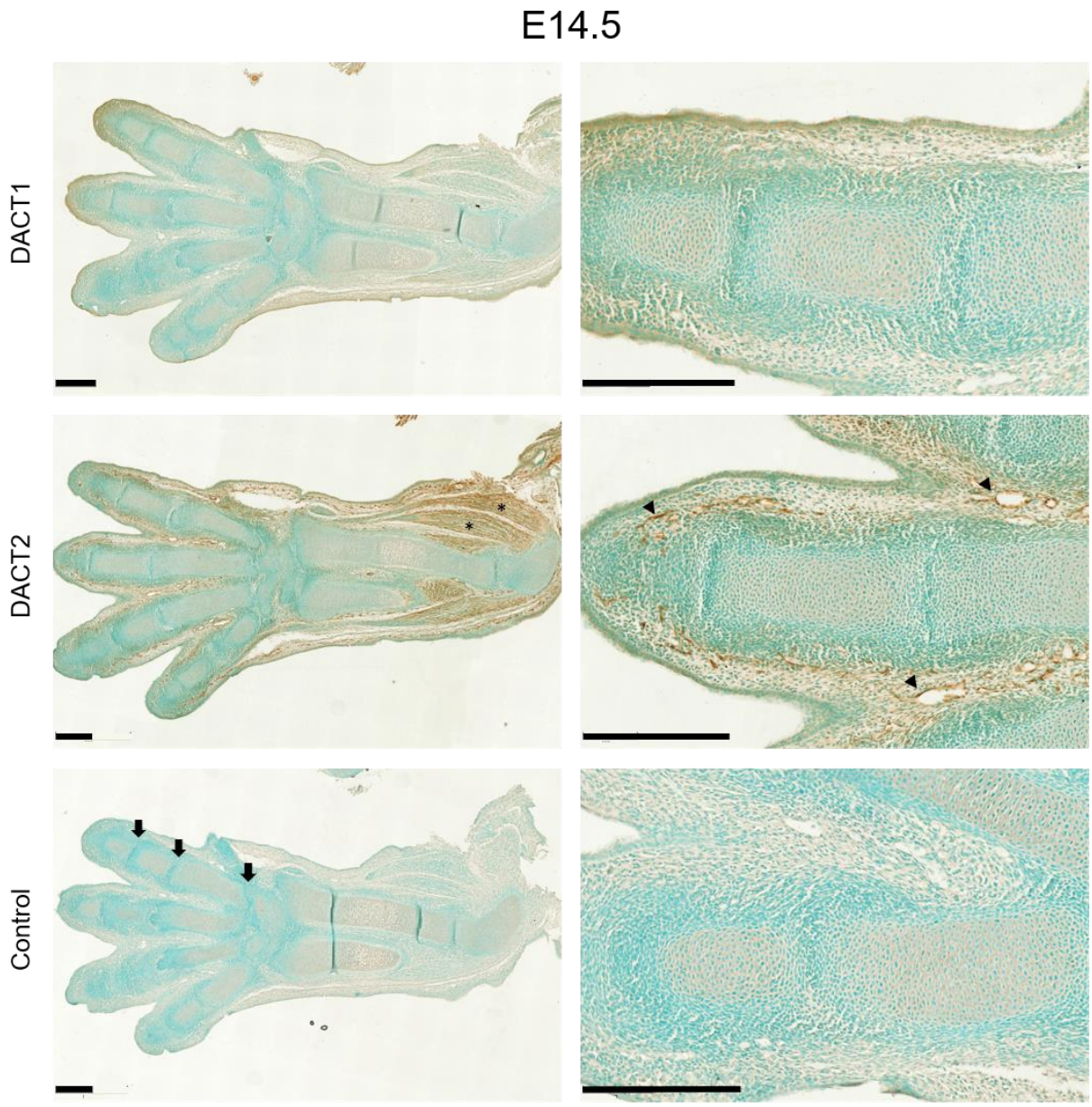

Figure 36 **Dact1 and Dact2 expression in developing mouse limb at E14.5.** Immunohistochemistry with Dact1 and Dact2 antibody performed on 5 µm thick section from paraffin-embedded limb of E14.5 C57BL/6J mice. Methylgreen was used as counterstain. Brown DAB staining indicates Dact1 and Dact2 protein and non-stained cells appear green. Black arrow heads indicate positive staining. Control condition used Rabbit IgG and then DAB was applied for 30 seconds, as for the other conditions. Images on the left shows the whole embryo limb, images on the right show a higher magnification of the phalangeal joint site. Large arrows: Interzone sites; arrow heads: endothelial cells; stars: tendons and skeletal muscle. Scale bars = 0.5 mm.

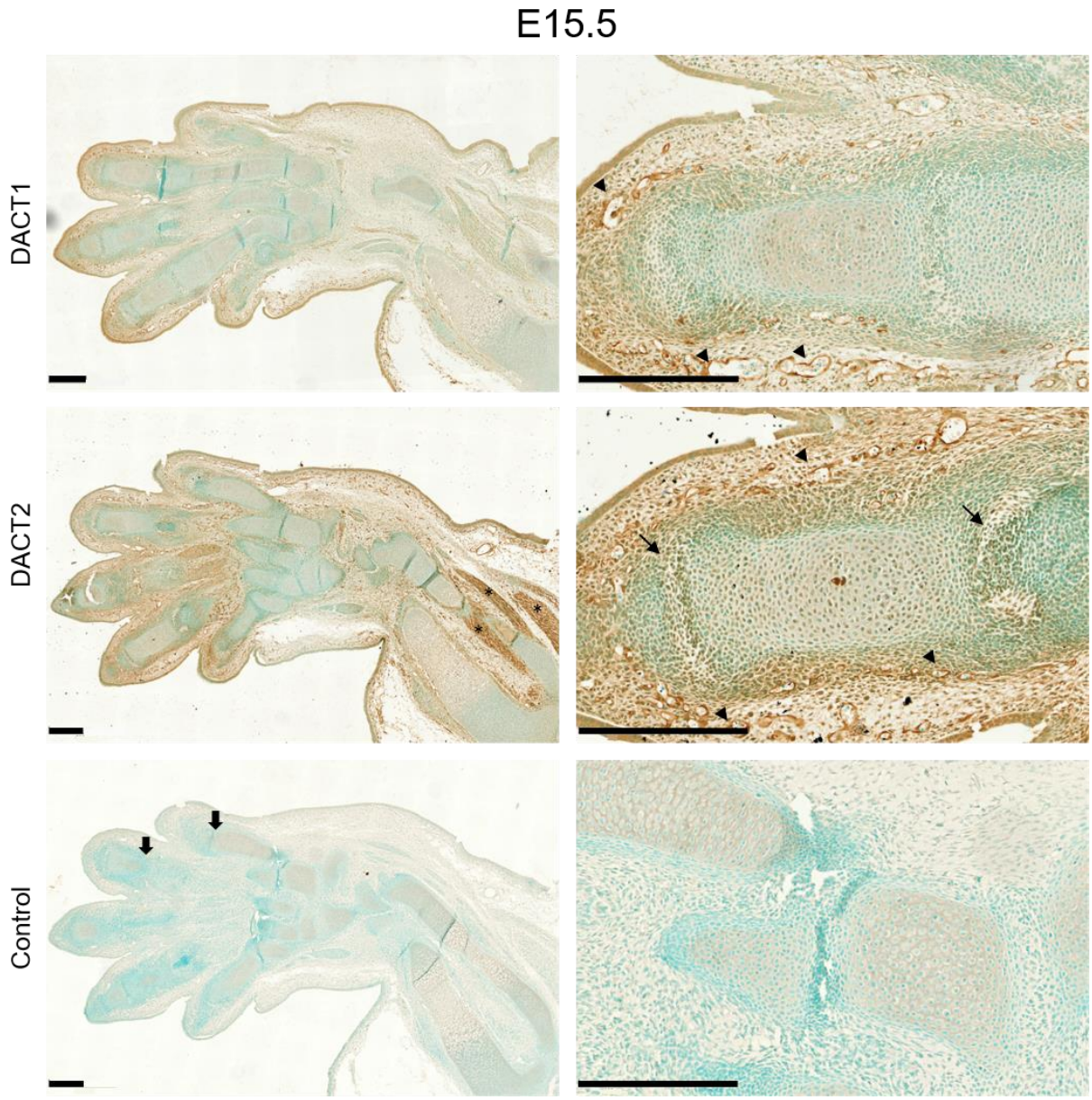

Figure 37 **Dact1 and Dact2 expression in developing mouse limb at E15.5**. Immunohistochemistry with DACT1 and DACT2 antibody performed on 5 µm thick section from paraffin embedded limb of E16.5 C57BL/6J mice. Methylgreen was used as counterstain. Brown DAB staining indicates Dact1 and Dact2 protein and non-stained cells appear green. Black arrow heads indicate positive staining. Control condition used Rabbit IgG and then DAB was applied for 30 seconds, as for the other conditions. Images on the left shows the whole embryo limb, images on the right show a higher magnification of the phalangeal joint site. Large arrows: interzone sites; small arrows: cells at the cavitation zone; arrow heads: endothelial cells; stars: tendons and skeletal muscle. Scale bars = 0.5 mm.

5.2.3 Dact1 and Dact2 are expressed in the mouse knee

Descriptive studies of Dact1 and Dact2 in mouse adult synovial joints have not been previously described in the literature. To explore the expression of the two proteins,

mouse limbs were obtained from 2 weeks old C57BL/6J mice and processed for immunohistological analysis. Dact1 expression is weakly present at the cartilage surface and in bone marrow cells (fig. 38, black arrow heads), synovial lining (fig. 38, arrows) and menisci (fig. 38, blue arrow heads). Dact2 expression reflects Dact1, although its staining appears more intense.

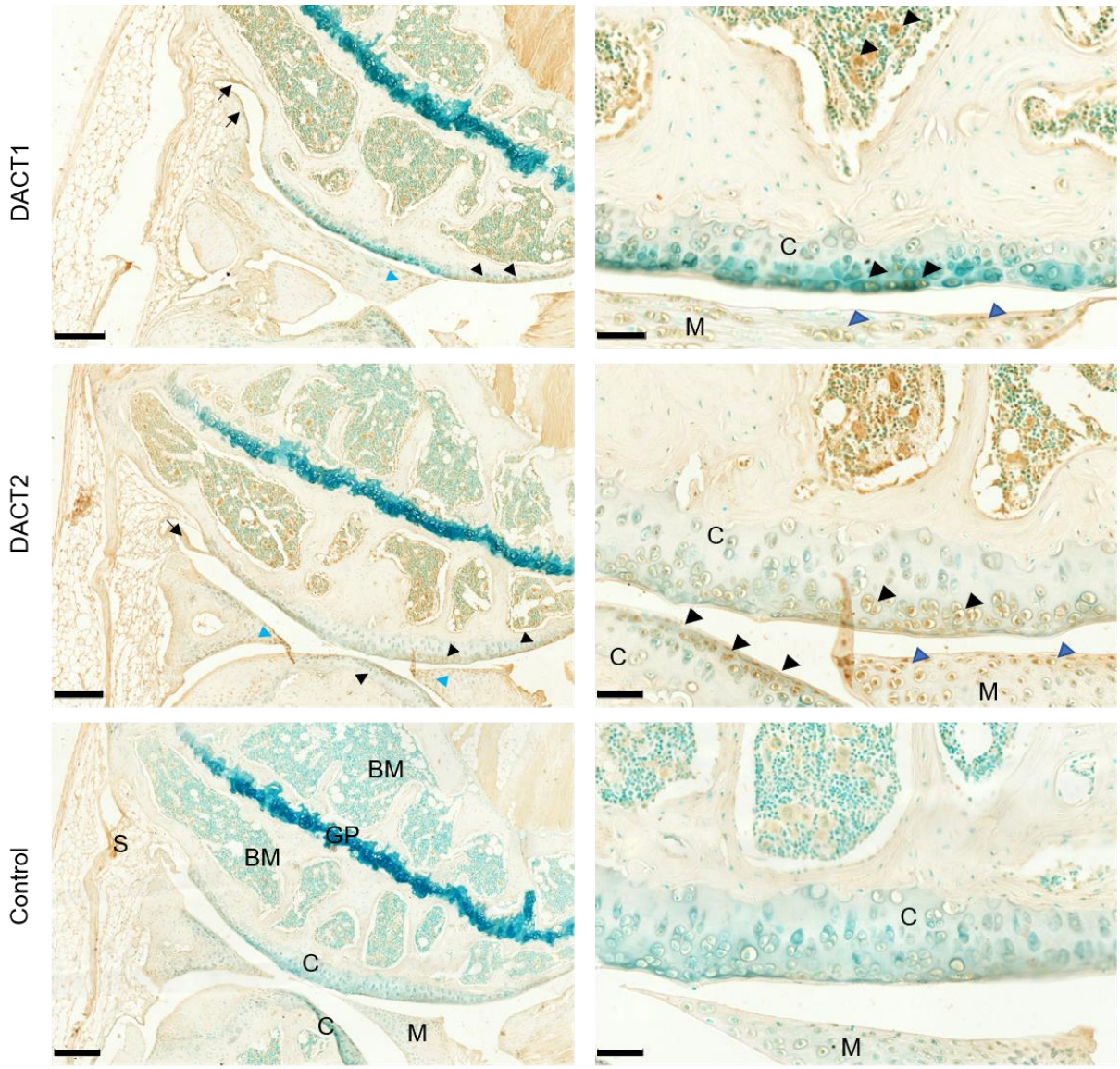

Figure 38 **Dact1 and Dact2 are expressed in adult mouse knee.**
Methylgreen counterstaining and immunohistochemistry with Dact1 and Dact2 antibody performed on 5 µm thick section from paraffin-embedded knees of 2 weeks old C57BL/6J, after decalcification protocol. Brown DAB staining indicates Dact1 and Dact2 protein and non-stained cells, and cartilage tissue appear green. Black arrow heads indicate positive staining in the cartilage tissue, blue arrow heads in the meniscus, black arrow in the synoviual lining. Control condition used Rabbit IgG and then DAB was applied for 15 seconds, as for the other conditions. Scale bars for images on the left, 200 µm; Scale bar for images on the right, 50 µm. BM: bone marrow; C:cartilage; M: meniscus; S: synovium, GP: growth plate.

Immunocytochemistry of ACs isolated from one-week-old mouse femur heads shows Dact2 expression in the cytoplasm of the cells (fig. 39). As described for figure 32, Dact2 signal is particularly strong on around the nucleus, probably in the ER. Dact1 showed no expression in mouse chondrocytes.

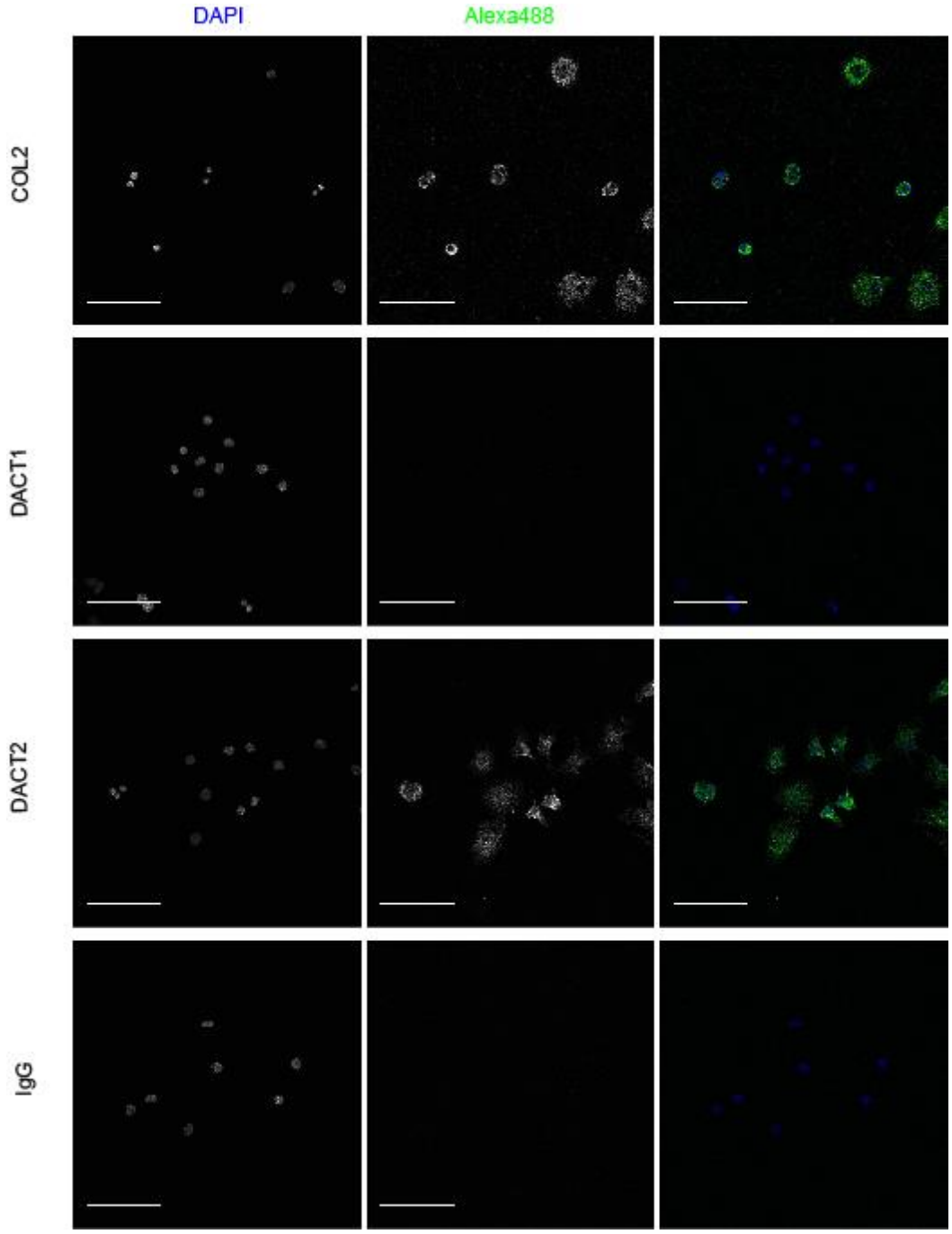

Figure 39 **Dact2, but not Dact1, is expressed in the cytoplasm of mouse chondrocytes.**
Immunohistochemistry was performed on mouse chondrocytes isolated from the hip cartilage. Fixed cells were stained for Col2, Dact1 and Dact2 with primary antibodies at concentrations described in table 2.3. Alexa488 secondary antibody (1:1000) was

used for all stainings. Imaged by confocal microscopy (40x objective). Dact1/2/Col2, green; nuclei, blue. Scale bar indicates 50 µm.

5.2.4 DACT1 and DACT2 are expressed in Synovial- and Bone Marrow-derived MSCs.

Because of the presence of DACT2 in the sites of early synovial joint formation in mouse, it was hypothesised that adult mesenchymal MSCs may express DACT proteins. Immunocytochemistry of MSCs isolated from the bone marrow of healthy donors (purchased from and previously characterised by Lonza) was performed. Figures 40 and 41 show DACT1 and DACT2 expression in BMSCs and SynMSCs respectively. Both proteins appear mostly expressed in the cytoplasm, which support the role in signalling transduction observed in other cell types. DACT1, in particular, localises on the side of the nucleus, probably in the ER.

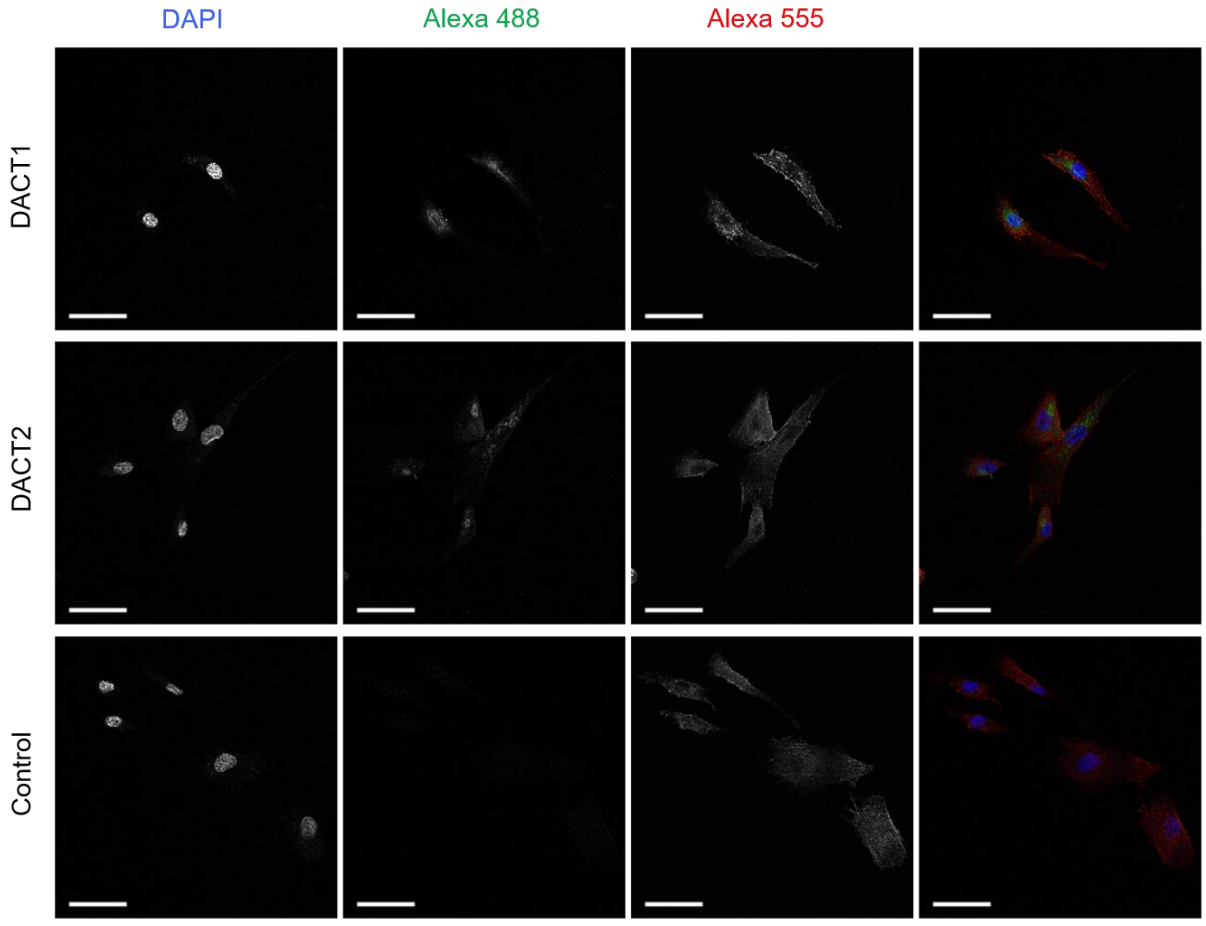

Figure 40 **DACT2 and DACT1 are expressed in the cytoplasm of human BMSCs.** Immunohistochemistry was performed on MSCs derived from bone marrow of healthy donors, passage 4 (Lonza). Fixed cells were stained for DACT1 and DACT2 with primary antibodies at concentrations described in table 2.3. Alexa488 was used as

secondary antibody (1:1000) and Phalloidin-Alexa555 (1:40,000) was used to stain actin filaments. Rabbit IgG used as a negative control (“Control”). Imaged by confocal microscopy (40x objective). DACT1/2, green; actin filaments: red; nuclei, blue. Scale bar indicates 50 µm.

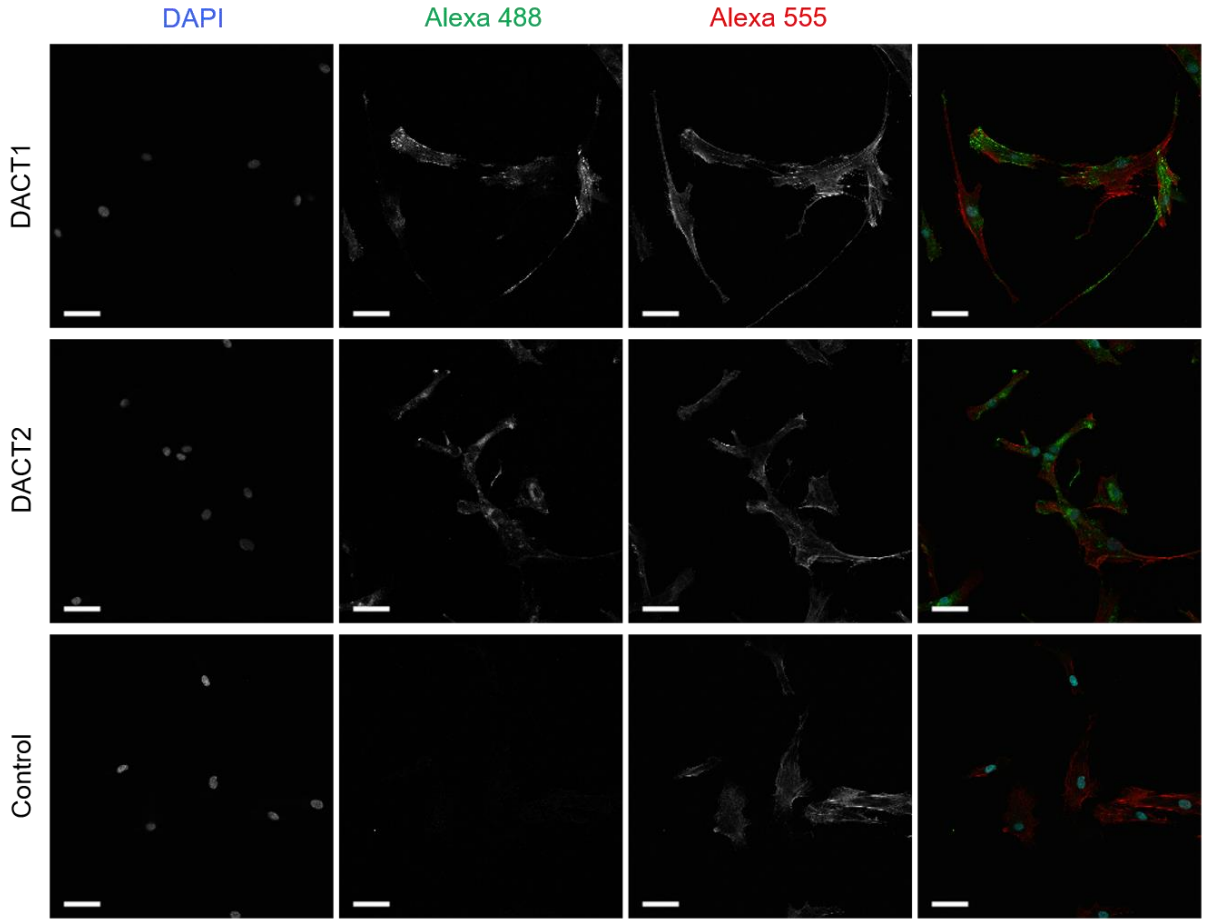

Figure 41 **DACT2 and DACT1 are expressed in cytoplasm of human SynMSCs.** Immunohistochemestry was performed on MSCs derived from MSCs isolated from the synovial membrane of patients undergoing knee replacement.bone marrow of healthy donors (passage 1). Fixed cells were stained for DACT1 and DACT2 with primary antibodyes at concentrations described in table 2.3. Alexa488 secondary antibody (1:1000) was used for all stainings. Phalloidin-Alexa555 (1:40,000) was used to stain actin filaments. Rabbit IgG used as a negative control (“Control”). Imaged by confocal microscopy (40x objective). DACT1/2, green; actin filaments: red; nucles, blue. Scale bar indiates 50 µm.

5.3 Discussion

5.3.1 DACT1 and DACT2 are expressed in human and mouse knee joints and are modulated in human OA cartilage.

DACT proteins are known regulators of two of the most important pathways in cartilage development and homeostasis, Wnt and TGFβ pathways (C. W. Archer, Dowthwaite, & Francis-west, 2003). The involvement of the Wnt pathway in cartilage development and the pathogenesis of OA has been investigated and described in many animal models. TGFβ signalling is extensively studied for its role in regulating all stages of differentiation of chondrocytes, as well as chondrogenic and osteogenic differentiation of mesenchymal cells. For example, the potential of BMPs (members of the TGFβ superfamily) to induce cartilage formation has been explored in several pre-clinical studies (reviewed by (Deng, Li, Gao, Lei, & Huard, 2018). Recent interesting studies have begun to recognise how in joint development the two pathways are interconnected. When Wnt and BMP signalling are misregulated following lack of mechanical stimuli, β-catenin activation is reduced and concomitantly pSMAD1/5/8 signalling is upregulated and the joint then develops abnormally (Singh et al., 2018). The interplay between Wnt and TGFβ pathways seems to regulate the fate decision of progenitors to cartilage differentiation: the activation of Wnt/β-catenin signalling is concomitant to downregulation of BMP signalling. The two pathways are involved in movement-induced development of joints and this regulation is conserved across vertebrate species.

The studies presented here show, for the first time, the expression of DACT1 in human articular cartilage, both at gene and protein level. The expression of DACT1 in articular cartilage suggests that it may act as a modulator of cartilage homeostasis and development. In human articular cartilage, DACT1 and DACT2 are more expressed in SZ compared to MDZ (fig. 29 and 30). In the adult mouse knee, Dact2 is also clearly expressed in the SZ of articular cartilage. This result mirrors what has been reported by Mori and colleagues (Mori et al., 2014) in rat articular cartilage. Data described here show that Dact1 expression in mouse chondrocytes (fig. 39) is not conclusive. Immunohistochemistry is negative for Dact1 in chondrocytes isolated from 1-week old mouse hip cartilage, and the staining in adult knee is weak. The antibody purchased for visualising DACT1 recognises both human and mouse (*DACT1* is very well conserved across vertebrates), but a different antibody for DACT1 could potentially

confirm the expression of Dact1 in mouse cartilage. Another reason for the weak staining observed could be low expression of Dact1. According to the online Human Protein Atlas website (Uhlén et al., 2015), DACT1 is mostly expressed in the brain and only very weak expression is found in other organs, particularly those of mesodermal origin (kidney, urogenital and lymphatic tissues). Histological samples reported in the atlas, show DACT1 is often clearly visible in endothelial tissues, like the inner layer of vessels, which is also clearly observable in figure 34. Similar to that reported in this chapter, studies by Sensiate *et al*. and Shubert et *al.* on DACTs during chick embryo limb development show that *Dact2* appears more expressed than *Dact1* in the interphalangeal and metacarpal-phalangeal joints (Schubert et al., 2014; Sensiate et al., 2014).

Since the start of this investigation on the presence of DACT1 and DACT2 in human cartilage, one paper was published that reported the presence of Dact1 in human cartilage. Chou and colleagues (2015) compared gene expression between the medial and lateral compartment of OA knees to identify severity associated genes. DACT1 was identified, both by array and qPCR, to be one of the top down-regulated genes in severely damaged cartilage across 42 human samples. However, this study does not provide information about the protein expression of DACT1, nor offer a description of the molecular mechanism of DACT1 in OA chondrocytes.

Gene expression data on DACT1 showed a reduction in gene expression of *DACT1* (fig. 28). Post-translational regulation might explain the strong protein expression of DACT1 and DACT2 localised to cells in OA cell clusters at the edge of fibrillated cartilage (fig. 31). Cell clusters are defined as 6 or more cartilage cells residing in one large lacuna and their role or significance is still not fully understood (Lotz et al., 2010). This type of cell organization is well described in OA cartilage and it is thought to result through cells migrating from degrading matrix and then proliferating (Graverand et al., 2001; Lee, Paul, Slabaugh, & Kelley, 2000; Pfander, Swoboda, & Kirsch, 2001). The phenotype of the cells residing in cartilage clusters have not been thoroughly delineated, so it is not known if clusters are composed of clonal cell populations or heterogeneous chondrocytes and whether they include cartilage progenitors. As a consequence, it is not fully understood if cell clusters are simply the result of cell migration in response to damage or if they have a role in cartilage repair (Lotz et al., 2010). A recent study on human tissue has suggested that cartilage cell clusters present in late OA include cells with stem-like progenitor properties (Hoshiyama et al.,

2015). More studies have since used CD146 as a marker to identify OA-MSCs (X. Su et al., 2015). This marker was shown to be expressed on some of the cells contained in OA clusters, arguing that OA cell clusters contain both stem and differentiated chondrocytes (Jayasuriya et al., 2018). Elucidating further the role of DACT1 and DACT2 in ACs biology could extend our understanding of the origin and purpose of cell clusters.

5.3.2 Dact2 is found at the Interzone of developing mouse joints.

Limb development has been studied in mouse and chick embryos to identify the molecular pathways governing bone and cartilage formation in joints (Pitsillides & Ashhurst, 2008). As previously described, following the formation of the limb bud, a condensation of mesenchymal cells start differentiating into chondrocytes and all the cells that form the limb (Kronenberg, 2003). The stages of rodent limb embryonic development are well characterised with the stages at which joint structure start forming well documented (P. Martin, 1990; Mitrovic, 1978). Around day 14.5, the cartilaginous template starts to get replaced by bone. Muscle myosin chains are present in the limbs from day 11.5, and by day 14.5 muscle and nerves in the limbs are mature. From E13.5 the interzone forms, and by E15.5 the distal phalanges are also developed. By the later phases of embryogenesis, the interzone begins to cavitate, forming two separated articular surfaces joined by synovial fluid (Koyama et al., 2008). Cavitation occurs in a proximal to distal fashion as limb joints develop, with the most distal phalangeal joints initiating cavitation by late embryogenesis, and completed in early postnatal life (Mitrovic, 1978).

In the data presented here, Dact2 starts to be expressed in the interzone, although only weak signal is detected, and this becomes clearer when cavitation starts. Dact1 signal is not convincingly detected in these stages of the developing joint. To more broadly compare these results, the MGI online database was consulted (Bult et al., 2019). This specific database indicates that D*act1* and *Dact2* genes are expressed in the mouse, including in the “musculoskeletal system”. The database also includes developmental analysis of genes. *In situ* hybridisation shows that *dact1* is more expressed than *dact2* in the interdigital joint space and the metacarpal-phalangeal joints (fig. 42). In the developing chick however *dact2* appears more expressed and also to be localised in the limb developing joint interspace (Sensiate et al., 2014). The

chick embryo studies were primarily exploring limbs, whereas the mouse embryo database reports a whole-mount histology, with limbs not being in the most optimal position to investigate gene expression in the limb. For that reason, the chick embryo study might be more indicative of gene expression of Dact2. As previously discussed, a different antibody for Dact1 should be considered to confirm protein expression in the developing joints.

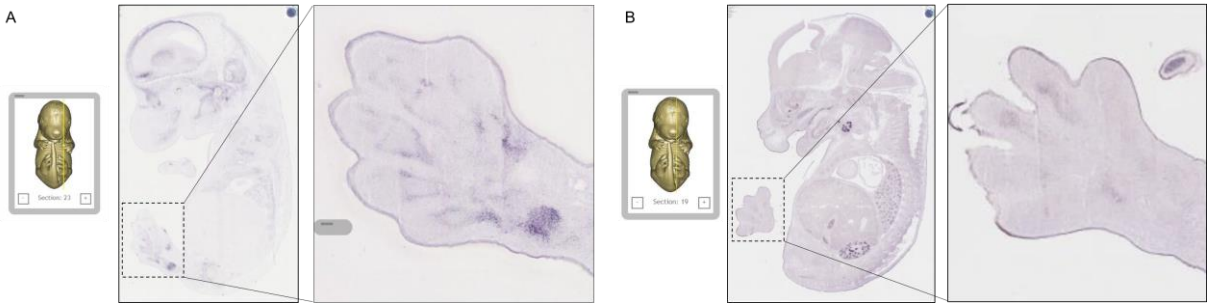

Figure 42 **Whole embryo *in situ* hybridisation of Dact1 and Dact2.**
Figures were obtained from the International Database Resource for the Laboratory Mouse. *In situ* hybridisation was performed for *Dact1* and *Dact2* mRNA on mouse embryos E14.5 (The jackson laboratory, n.d.).

Taken together, these studies suggest a link between Dact1 and Dact2 and joint development. The data reported in this chapter shows that Dact2 is present at protein level in the prospective joint space and might, therefore, be playing a role in the regulation of joint formation in the mouse.

5.3.3 DACT1 and DACT2 are expressed in BMSCs and SynMSCs.

Recent evidence in mouse and humans shows that cells residing in the SZ of cartilage are different from the chondrocytes in the MDZ of articular cartilage. Lineage tracing studies following the progeny of Gdf5-expressing cells have shown that articular cartilage and synovium have a common progenitor as cells that have expressed GDF5 go on to express PRG4 (Roelofs et al., 2017). Because cells of the progenitor lineage are both present in the cartilage SZ and synovial membrane, and both DACT1 and DACT2 are present in the SZ, the expression of DACT1 and DACT2 was investigated in the synovium. The knee joint relies on the synovium for nutrients and removal of waste product from chondrocytes metabolism and articular matrix turnover. The synovium is rich in blood vessels and acts as a semipermeable membrane allowing molecular and nutrient exchange with the synovial fluid to maintain the articulation physiological state. Both DACT1 and DACT2 are expressed in the synovium, in

particular in the synovial lining layer. Most cells present in the lining layer are of fibroblastic and macrophage origin. Macrophages are responsible for removing by phagocytosis damaged cells. In a recent paper, Culemann and colleagues showed that another role for the macrophages in the synovial lining is to create an immunological barrier to between the inflamed joint and the bloodstream (Culemann et al., 2019). Whether DACT proteins are also expressed by these tissue-specific macrophages is not known.

As MSCs differentiation potential and maintenance are well known to be regulated by Wnt and TGFβ pathways, it was hypothesised that MSCs would express DACT1 and DACT2. In addition to bone marrow, the synovium is also a source MSCs. SynMSCs display excellent chondrogenic differentiation potential *in vitro* and are thought to participate in cartilage repair (Roelofs et al., 2017). MSCs isolated from the synovium, as well as BMSCs, show expression of both DACT1 and DACT2. DACT1 was described to be part of Wnt signalling in regulating adipose differentiation and general fate determination of C3H10T1/2 (Zhou et al., 2016). There is however no information available on the presence and role of DACT1 and DACT2 in primary MSCs.

5.3.4 Limitations of the study.

Despite having shown that in four different patients DACT1 and DACT2 are modulated by OA, more samples are needed to reach a statistically significant result because of interpatient variation. In addition, because the control samples are collected from patients with end-stage osteoarthritis, proper control would possibly provide a clearer difference in expression between OA and normal tissue. To confirm the differential gene expression at protein level, further analysis should be performed. Isolating protein from cartilage tissues has proven difficult without enzymatic digestion of the matrix to obtain single cell chondrocytes. It should be then ensured that the low expression/presence of DACT1 and DACT2 in chondrocytes would not be altered by such overnight enzymatic digestion and cell culture. Due to inter-patient variability and the low amount of sample, it was not possible to isolate RNA from SZ and MDZ chips to analyse *DACT1* and *DACT2* expression in different zones. Histological analysis of the proteins across more than 6 patients showed a constant zonal expression of DACT1.

Information about the expression of DACT1 and DACT2 in cartilage that is not exposed to mechanical loading is missing, as samples analysed here were obtained from the knee condyles. The Wnt pathway is known to be regulated by mechanical loading and a study of DACT1 and DACT2 expression in cartilage from different location would shed light on their regulation.

Despite the obvious limitation of using mouse for modelling and studying genes that affect human limb development, mouse embryo histology was able to provide information on DACTs expression in limb development. Whereas organoid cultures of other organ/tissues (such as intestine and liver) are allowing study of patterning and signalling pathways on human tissue, knee osteochondral organoid or cartilage/bone differentiated iPSCs technology are not readily available. Human samples to study limb development are generally difficult to obtain. DACT genes have a high degree of evolutionary conservation, not just in mammals, but in all vertebrates (Schubert et al., 2014). It therefore likely that DACTs developmental mechanism extrapolated from mouse would be similar in human. In support of this claim, data reported in this chapter shows parallel expression of both proteins in mouse and human adult cartilage tissues.

5.4 Summary and future work.

The SZ of articular cartilage is believed to host a subpopulation of chondrocyte progenitors that regulate tissue homeostasis and might be involved with cartilage repair and OA progression. In order to develop therapeutic strategies to heal cartilage damage, resident cartilage progenitors were explored by studying the presence of Wnt and TGFβ signalling modulators DACT1 and DACT2. Both are present at gene and protein level in adult human cartilage and synovium, and in OA their expression is altered. Despite the consensus in the literature about DACT1 and DACT2 being part of the molecular mechanisms involved in Wnt and TGFβ signalling pathways, upstream regulators or signals determining their gene transcription are unknown. One approach to investigating what might regulate *DACT1* and *DACT2* during OA progression could be to understand if inflammatory cytokines influence either MSC or chondrocyte expression of these genes.

It was also shown in this chapter that DACT1 and DACT2 are present in mouse developing limbs, with DACT2 present at the site of prospective joints. Both proteins

are also present in human SynMSCs and BMSCs. The implications of a link between progenitors (either during development or in adult tissues) and DACT proteins are a strong motivation to continue investigating the role of DACT in articular cartilage. Although the role of DACT1 and DACT2 has been described in the literature, particularly in cancer cells, no information about the specific role in chondrocytes or MSCs is available. Shedding light on the role of DACT1 and DACT2 would be advantageous to cartilage repair and regeneration strategies. DACTs role in cartilage could also help to define the molecular mechanisms underlying osteoarthritis (OA). Notably, activation of β-catenin in ACs in adult mice led to the development of an OA-like phenotype (Zhu et al., 2009). β-catenin levels are increased in human OA sample and variants of the FRZB gene are associated with OA (Loughlin et al., 2004). Initial investigation about the role of these proteins in MSCs and ACs will be explored in the next chapter.

6 Investigating the role and mechanism of DACT1 and DACT2 in MSCs.

6.1 Background and rationale

Canonical Wnt signalling is believed to play a central role in the progression of OA and is involved in many aspects of cartilage development and homeostasis. In parallel, the TGFβ pathway has been shown to actively contribute to the regulation of joint maintenance and to be deregulated in various tissues suffering from OA.

Depending on the receptor activated and intracellular signalling molecules, different Wnt signalling pathways can be activated: the planar cell polarity (PCP) and Wnt/β-catenin pathways often referred to as 'canonical', are the best described. DACTs proteins are primarily known to bind to DVL, which is the first signal transduction protein of the three Wnt pathways. In the canonical pathway, DVL causes the disruption of the GSK3β-Axin-β-catenin complex by inhibiting GSK3β. β-catenin is then not phosphorylated, and therefore destroyed, but can accumulate and be transported to the nucleus where it activates target gene expression (fig. 43). The PCP pathway is less well characterized than the canonical pathway and also relies on DVL interaction with downstream effectors after Wnt binding to the FZD receptor. In the PCP pathway, downstream effectors of DVL include the small GTPases RHO and RAC (fig. 43). At the same time, DVL also influences the degradation of the alternative receptor to FZD, Pk. DVL binds to the ubiquitin ligase SMURF to promote the ubiquitination of Pk that gets then degraded (Narimatsu et al., 2009). How the common FZD-DVL distinguishes among different Wnt pathways is unclear.

The TGFβ signalling pathway relies on transmembrane type I and type II serine/threonine kinase receptors to transmit signals to the intracellular effector SMAD proteins. Seven different receptors, activin receptor-like kinases (ALKs) exist that selectively phosphorylate different complexes of SMADs. Upon BMP binding to ALK 1, 2, 3 and 6, SMAD 1/5/8 are phosphorylated. In contrast, TGFβ binds ALK 4, 5, and 7 which signals through activation of SMAD 2/3. BMPs are regulated by different inhibitors that by competitively interacting with them blocks their binding to the receptor. These inhibitors include Noggin, inhibitory SMADs (SMAD6 and SMAD7), and SMURFs (Itoh et al., 2001; Neul & Ferguson, 1998; H. Zhu et al., 1999).

The cross-talk between the Wnt and TGFβ pathways has been reported in several cartilage studies. For examples, BMP-2 enhanced mesenchymal differentiation to the cartilage lineage through upregulation of master regulator of chondrogenesis SOX9 (Jin et al., 2006). This is achieved by downregulating Wnt/β-catenin expression as overexpression of β-catenin results in proteasome degradation of Sox9 via ubiquitination. Another example of the interconnection of the two pathways is the number of shared receptors and ligands such as sclerostin (Wnt antagonist that competitively binds to LRP5/6 receptor and modulates BMP signalling (Xiaofeng Li et al., 2005; Winkler et al., 2005)) and CTGF (regulated by WNT3a and BMP-9, and can bind to BMP-4 and TGFβ (J. G. Abreu, Ketpura, Reversade, & De Robertis, 2002). A third example is the complex interaction of cytoplasmic proteins belonging to each pathway. Synergistic signalling between Wnt and TGFβ pathway proteins results in enhanced chondrogenic differentiation (Im & Quan, 2010; Narcisi et al., 2015; Shuanhu Zhou, Eid, & Glowacki, 2004). Due to the complex interactions of Wnt and TGFβ pathways, the exact underlying molecular mechanisms linking the two pathways remains elusive, but its relevance to better understanding cartilage disorders and its regeneration appears clear.

DACT1 and DACT2 act on both Wnt and TGFβ pathways (Y. Su et al., 2007). The cytoplasmic form of DACT1 can induce DVL degradation via a lysosome-dependent mechanism. In the nucleus, DACT1 can prevent the formation of LEF1:β-catenin complexes at target gene promoters (X. Gao et al., 2008). In both these cases DACT1 acts as a Wnt signalling antagonist. DACT2 has also been shown to have a negative effect on Wnt canonical pathway (S. Wang et al., 2015). DACT2 overexpression negatively regulates TGFβ signalling by binding and targeting ALK4 and ALK5 for degradation (Y. Su et al., 2007; L. Zhang et al., 2004). Other studies report DACT1 and DACT2 as positive regulators of the Wnt pathway (Waxman, Hocking, Stoick, & Moon, 2004). DACT1 was proposed to inhibit GSK3β, which results in increased intracellular β-catenin levels ensuring activation of target genes (Yuan et al., 2012). The double regulation has been clear since the earliest reports of DACTs (Cheyette et al., 2002). The ability to act both as positive and negative regulator seems to be dependent on the phosphorylation state of DACT1: DACT1 take on an inhibitory role when unphosphorylated, and promotes Wnt signalling when phosphorylated (Teran, Branscomb, & Seeling, 2009). As previously discussed, which pathways DACT1 and DACT2 regulate in MSCs and cartilage, and their molecular mechanism is unknown.

Biochemical studies have shown that the PCP pathways is regulated by DACT1 by its binding to DVL, as it is disrupted in the developing tissues of mouse Dact1 KO (Suriben, Kivimäe, Fisher, Moon, & Cheyette, 2009; Wen et al., 2010).

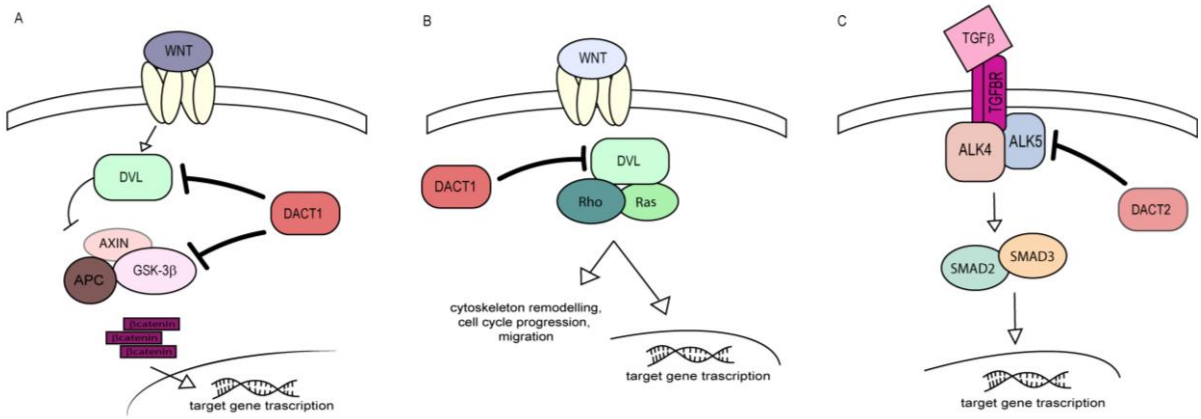

Figure 43 **DACT1 modulates Wnt and TGFβ pathways.**
In the canonical Wnt pathway (A) and PCP/Wnt pathway (B) DACT1 can activate gene expression by either binding to DVL, that results in the degradation of GSK3β-Axin- β-catenin complex, or by inhibiting GSK3β. β-catenin is then not phosphorylated but can accumulate and be transported to the nucleus where it activates target gene expression. In the TGFβ pathway (C), DACT2 targets ALK4/5 for degradation blocking SMAD2/3 activation. Original work.

Because of the relevance of Wnt and TGFβ pathways in both MSCs and chondrocytes, it was hypothesised that DACT1 and DACT2 would act as a mediator in these pathways. In this chapter, DACT1 and DACT2 silencing through RNAi were performed on MSCs and ACs to investigate their role. After observing a clear effect of DACT1 knockdown on cell survival, Wnt target genes upon DACT1 silencing were tested. WNT3a and inhGSK3β were then used to determine if the phenotype of DACT1 silenced MSCs could be rescued. Finally, an RNA sequencing study on DACT1 silenced MSCs was performed in the attempt to determine DACT1 targets molecules and pathways.

6.2 Results

6.2.1 DACT1 knockdown in MSCs and ACs results in cell death.

To investigate the role of DACT1 and DACT2 on MSC *in vitro*, RNAi was performed. RNAi on BMSCs, SynMSCs and ACs, was optimised using GAPDH siRNA as a positive control where cell seeding density and lipofectamine volume was varied to

determine the optimal RNA interference conditions (data not shown). Despite the use of primary cells, effective silencing (>75%) was achieved in all cells (figure 44). Control cells were included in all silencing experiments, transfected with negative control siRNA (siCTRL). The conditions that were used throughout this chapter were 10 µM siRNA mixed with 2.55 µL of lipofectamine per mL of media, and a seeding density of MSCs 8000 cells/cm^2, such that cells were around 50–60% confluent upon transfection applied on the following day. Seeding conditions for chondrocytes were about 10,000 cells/cm^2. In order to determine the efficiency of the knockdown performed with RNAi, qPCR primers were designed for *DACT1* and *DACT2*. *DACT1* primers were identified and successfully tested for efficiency on RNA from isolated chondrocytes. DACT2 primers were designed or taken from publications but failed to prove efficient for RT-qPCR analysis. It was then decided to continue the study primarily on DACT1.

MSCs were incubated with either a negative control siRNA or target siRNA (siDACT1) for 1 day or 5 days before mRNA was harvested and amplified by RT-qPCR (fig. 44). Images of the cells were taken each day with a light microscope to assess the effect of the silencing on cell morphology. The results show that after normalising to the housekeeping gene HPRT1, there was a significant reduction in DACT1 mRNA expression levels (81±18 % after 24 hours and 93±3 % after 5 days) relative to the control conditions.

The silencing was also performed on chondrocytes isolated from knee condyle tissue by enzymatic digestion (passage 1). Although tested on only one patient sample, silencing showed high efficiency both after one day following silencing, as well as 5 days after. Due to larger inter-patient variability and inconsistent accessibility to donor tissue, as well as a consequence difficulty in performing parallel and relative experiments on passage one ACs, further studies on DACT1 were conducted in BMSCs and SynMSCs only.

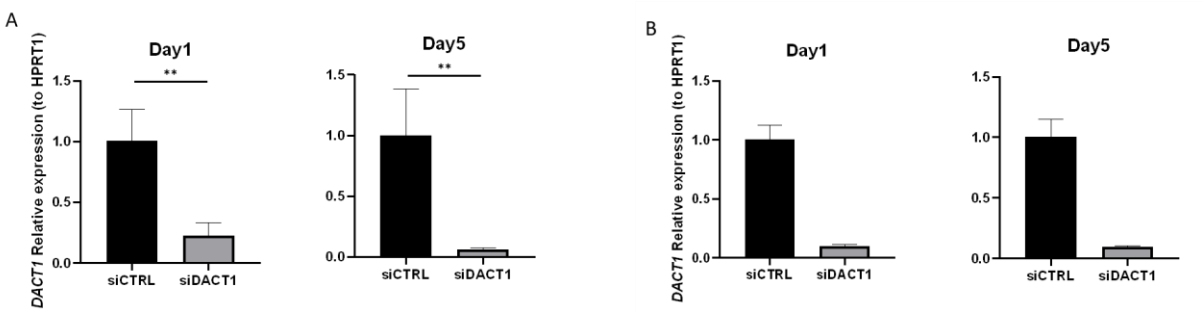

Figure 44 **Silencing efficiency of DACT1 in MSCs and ACs**.
qPCR was performed on A) patient derived MSCs (N=7 for Day1, N=3 for day 5) and B) ACs (N=1, error bars indicate the SD of technical replicates). Silencing was performed on ACs at passage one, and BMScs at passage 4-5. Relative expression was calculated with 2^-ΔΔCt method. (Mann-Whitney non-parametric test was performed on the data, ** indicates $p < 0.01$).

Light microscopy of silenced BMSCs and SynMSCs did not show detectable morphological differences at day 1 after silencing (fig.45 and 46). The siCTRL condition shows after 5 days an expected level of proliferation and cells appear fibroblastic and healthy, without evident morphological differences to normal untreated cells. That indicates that the amount of lipofectamine used was not toxic to the cells. siGAPDH showed similar results. 5 days after transfecting with siDACT1, both BMSCs and SynMSCs showed not only lack of proliferation, but fewer cells were present in the wells. Few cells remained attached to the well and floating (rounder cells) cells were visible in the media. The siDACT2 condition showed no evident differences in morphology and proliferation and was comparable to the control condition.

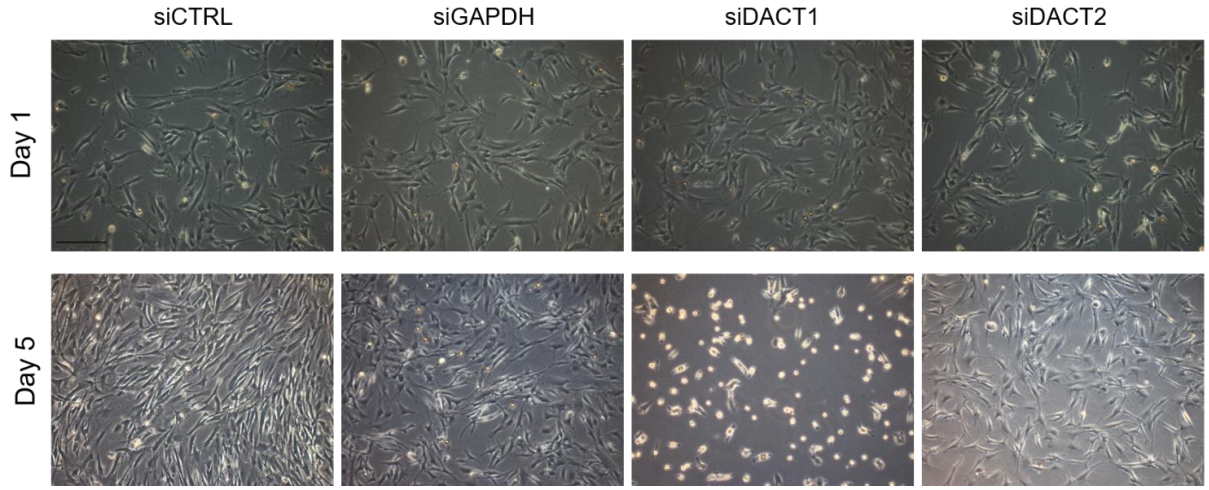

Figure 45 **BMSCs silencing of DACT1 affects cell proliferation and survival.**
Light microscopy pictures of BMSCs passage 4-5, isolated from BM healthy donors (Lonza). Silencing was applied the day following seeding at 60-70% confluence (N=4). In siCTRL condition a scrambled miRNA was transfected as a negative control, siGAPDH was transfected as a positive control. Scale bar = 200 µm.

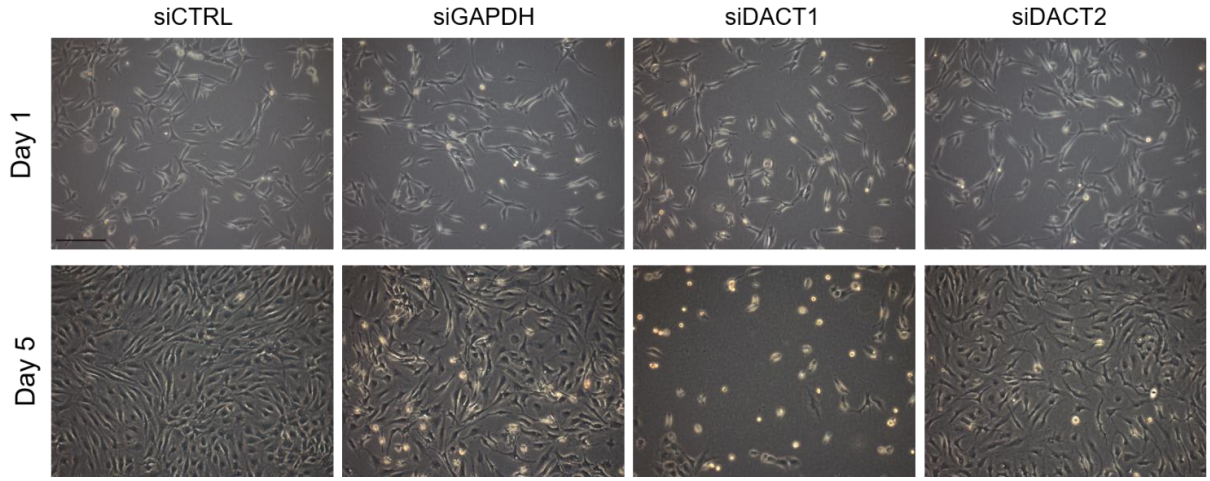

Figure 46 **SynMSCs silencing of DACT1 affects cell proliferation and survival.** Light microscopy pictures of SynMSCs passage 1, isolated from the synovium of patients undergoing total knee replacement. Silencing was performed on the day following seeding at 60-70% confluence (N=3). In siCTRL condition a scrambled miRNA was transfected as a negative control, siGAPDH was transfected as a positive control. Scale bar = 200 µm.

Plated chondrocytes were smaller and rounder in morphology two days after plating (fig. 47, day 1). Proliferation after 7 days was limited, as expected for slow cycling chondrocytes. After one day from applying the silencing, cells show no visible morphological differences. To clearly observe the same anti-proliferative effect and reduction of cells, more time was needed in comparison to the more metabolically active MSCs. Similarly to that observed in BMSCs and SynMSCs, the siDACT2 condition showed no clear differences in morphology or cell numbers from the control condition.

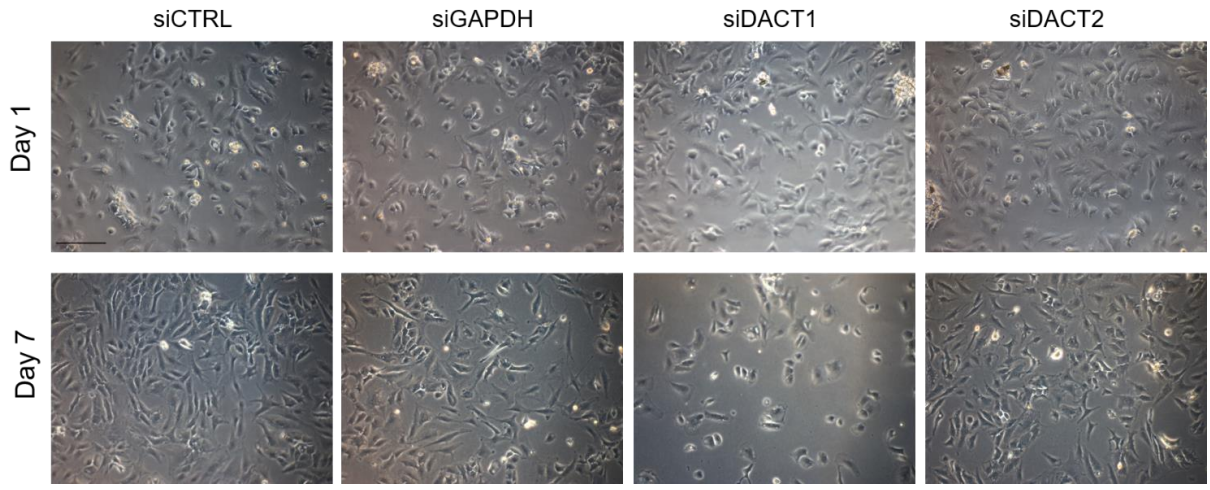

Figure 47 **ACs silencing of DACT1 affects cell proliferation and survival.**
Light microscopy pictures of ACs passage 1, isolated from lateral knee condyle cartilage of patients undergoing total knee replacement. Silencing was performed on the day following seeding 80% confluence (N=2). In the siCTRL condition, a scrambled miRNA was transfected as a negative control, siGAPDH was transfected as a positive control. Scale bar = 200 µm.

The effect on proliferation and survival of BMSCs was further investigated with two different assays. The proliferation of cells was observed 72 hours from silencing and showed that by 48 hours from silencing, the cells were still attached to the well were fewer than at the time of silencing (fig. 48). Treatment with siDACT2, on the other hand, showed an identical trend in proliferation to the control condition.

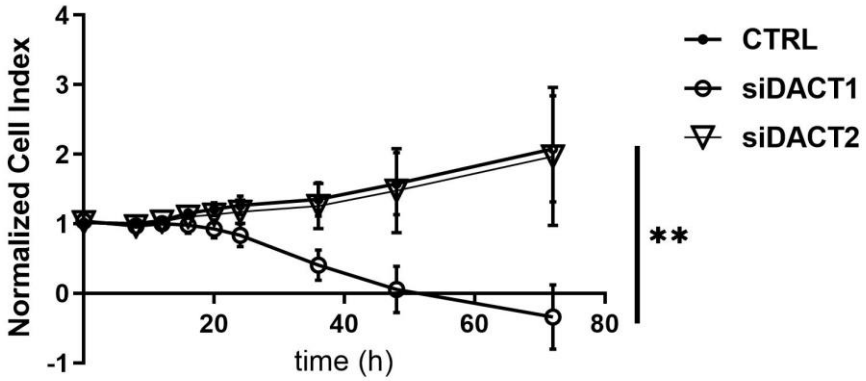

Figure 48 **Real-time effect of DACT1 silencing on BMSCs proliferation and survival over 72 hours.**
BMSCs from healthy donors (Lonza) were seeded in XCELLigence E-plates and their impendence measured every 15 minutes by XCELLigence RTCA (N=4). Cell Index measurements were normalised to the time of silencing. The control condition was transfected with a scrambled miRNA (Non-parametric Kruskal-Wallis test was performed on the measurements at 72 hours, ** = $p<0.01$).

To determine if the observed effect of siDACT1 was, in fact, caused by cell death, the CyQUANT® Direct assay was performed on silenced cells 48 hours after silencing. The assay uses a cell-permeable dye that binds to DNA to quantify the cells present in a well. The reagent was added to the well without removing the media (where cells affected by the DACT1 silencing were by then potentially floating). The added reagent includes a masking dye that blocks staining of dead cells or cells with compromised cell membranes resulting in only healthy cells being stained. The masking dye allows a measure of cell death. The significant reduction registered in the siDACT1 condition is clearly the result of cell death (fig. 49). siDACT2 showed no significant difference from the control condition (fig.49).

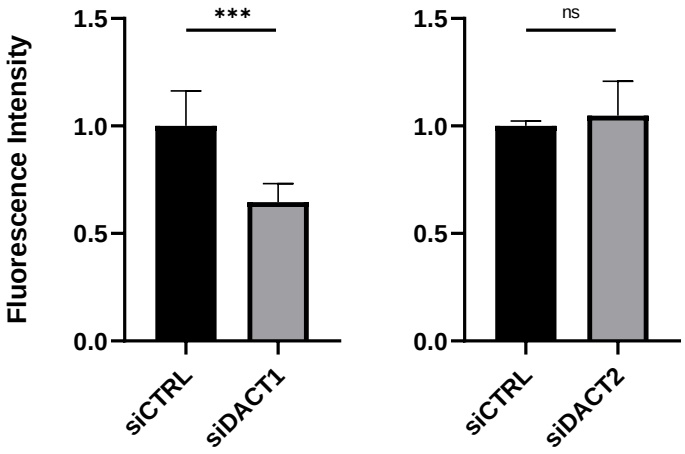

Figure 49 **CyQuant assay shows reduced BMSCs 48 hours after DACT1 silencing.** BMSCs from healthy donors (Lonza) were transfected with siDACT1 or siDACT2. The control condition was transfected with a scrambled miRNA (siCTRL). The assay was performed at 48 hours after silencing. CyQUANT® Direct 2X detection reagent was added to adherent cells in culture media, and the fluorescence was read 30 minutes after reagent addition. (Non-parametric Mann-Whitney test was performed, *** = $p<0.001$, N=3).

Morphological changes of the dying cell are similar across all cell types and display specific hallmark features (Hacker, 2000). Cell shrinkage is probably one of the earliest and easiest to observe changes. Confocal fluorescence imaging of immunocytochemistry for DACT1 and actin filaments shows cell shrinkage after 16h of DACT1 silencing. Normally elongated and fibroblastic-like BMSC morphology is lost and the nuclei show initial pyknosis (nuclear shrinkage due to DNA condensation in preparation for nuclear fragmentation) (fig. 50). DACT1 silencing at the protein level is also observed in the reduced intensity of Alexa488 (fig. 50). To further confirm cell

death assessment of DNA laddering by agarose gel electrophoresis could be used as a semiquantitative method to detect apoptosis.

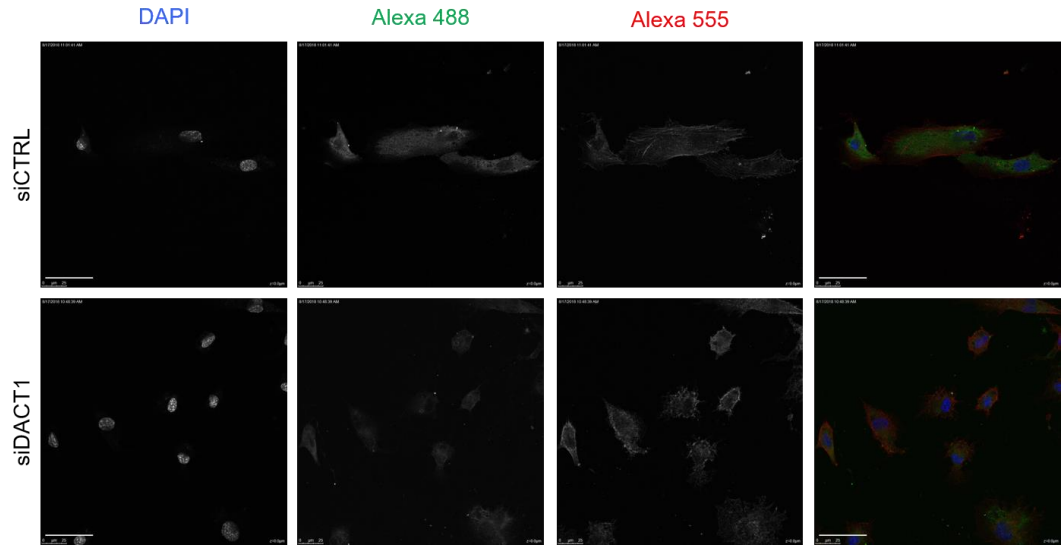

Figure 50 **Protein knockdown of DACT1 result in BMSCs death**. immunohistochemistry was performed on BMSCs passage 5-6 isolated from healthy donor bone marrow (Lonza). Fixed cells were stained DACT1 (1:500) and Alexa488 secondary antibody (1:1000). Phalloidin-Alexa555 (1:40,000) was used to stain actin filaments. Imaged by confocal microscopy (40x objective). The control condition was transfected with a scrambled miRNA (siCTRL). Representative images from one of four independent experiments with BMSCs and SynMSCs are shown. DACT1 green; actin: red, nucleus, blue. Scale bar indicates 50 µm.

6.2.2 Transcriptomic analysis to identify DACT1 targets in BMSCs.

As described here, the influence of DACT1 and its likely mechanism of action is highly dependent on the cell type where it is expressed and largely undescribed in cartilage and mesenchymal progenitors. After observing a very clear phenotype upon knockdown of DACT1, an RNAseq study was performed on BMSCs from 4 different healthy and young patients that were silenced for DACT1. As can be observed in figure 48, at about 20 hours cell death starts, which suggests an upstream and early effect of DACT1 silencing on cell homeostasis. A time point of 16 hours after silencing was then chosen to harvest RNA to observe which genes are affected by DACT1 knockdown.

Before submitting for sequencing, the harvested RNA was retrotranscribed to cDNA determine if DACT1 had been significantly silenced and illustrate if the RNA quality was sufficient to perform the deep sequencing. The average DACT1 knockdown was 87±4 % relative to the control condition (fig. 51A). The RNA quality was further

assessed with a Bioanalyzer. For 3 of the 8 samples, the RIN numbers were not available. Electropherograms samples with RIN = 10 were comparable to those with RIN N/A (fig. 51B and C), therefore, it was concluded that RNA quality was for all samples of a high standard to continue the experiment.

A

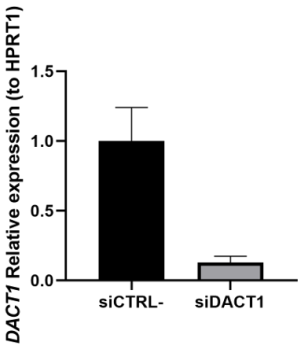

B

Sample ID	RNA (ng/µl)	RIN
siCTRL 29518	51	10
siDACT1 29518	48	10
siCTRL 31177	45	N/A
siDACT1 31177	44	10
siCTRL 30654	40	N/A
siDACT1 30654	51	10
siCTRL 29672	48	N/A
siDACT1 29672	58	10

C

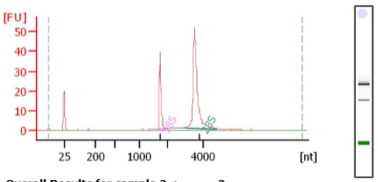

Overall Results for sample 2 : 2

RNA Area:	163.6
RNA Concentration:	48 ng/µl
rRNA Ratio [28s / 18s]:	2.8
RNA Integrity Number (RIN):	10 (B.02.07)
Result Flagging Color:	
Result Flagging Label:	RIN:10

Fragment table for sample 2 : 2

Name	Start Size [nt]	End Size [nt]	Area	% of total Area
18S	1,613	1,910	34.7	21.2
28S	2,897	4,768	98.0	59.9

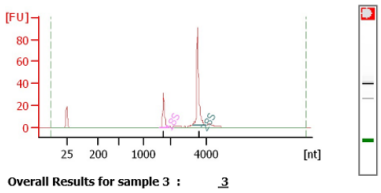

Overall Results for sample 3 : 3

RNA Area:	153.2
RNA Concentration:	45 ng/µl
rRNA Ratio [28s / 18s]:	3.0
RNA Integrity Number (RIN):	N/A (B.02.07)
Result Flagging Color:	
Result Flagging Label:	RIN N/A

Fragment table for sample 3 : 3

Name	Start Size [nt]	End Size [nt]	Area	% of total Area
18S	1,596	1,902	28.3	18.5
28S	3,183	3,959	84.6	55.2

Figure 51 **RNA of DACT1 silenced BMSCs concentration and quality for RNA sequencing.**
RNA was isolated from BMSCs after 16 hours from siDACT1 transfection. The control condition was transfected with a scrambled miRNA (siCTRL). A) qPCR was performed to verify *DACT1* silencing. Relative expression was calculated with 2^-ΔΔCt method. Agilent 2100 bioanalyzer was used to determine RNA quality B) RNA concentration and RIN of experimental conditions are reported. C) Two representative electropherograms and overall results from two of the samples are shown.

RNA sequencing detected 5624 differentially expressed genes between DACT1 knockdown and control BMSCs, of which 1330 were significant using <10 % FDR threshold set for all the differentially expressed and < 0.05% p-value (figure 52). Tables 4 and 5 report respectively the top 10 up (A) and down (B) regulated genes and their biological role following DACT1 knockdown. Unsurprisingly, the pre-apoptotic gene ATP-dependent RNA helicase (AIF4A1) is among the top upregulated ones. DACT1 is the top hit of the downregulated genes, confirming the qRT-PCR result in fig. 53A. Several of the top downregulated proteins are associated with the Wnt/PCP pathway: Ras Association Domain Family Member 3 (RASSF3), a RAS binding protein

involved in the regulation of apoptosis and signal transduction. Another protein that is known for its role in the Wnt/PCP pathway, as well as SMAD regulator, is SMURF2. Ring Finger Protein 130 (RNF130), another ubiquitin ligase like SMURF, is also among the top downregulated genes. Ubiquitin Specific Peptidase 46 (USP46), which is part of ubiquitin-proteasome system, is responsible for dynamic cellular processes such as the regulation of cell cycle and proliferation. USP46 might also be a protein involved in Wnt signalling (X. Li et al., 2013; Shi et al., 2015). In general, several proteins involved in ubiquitination (LON Peptidase N-Terminal Domain And Ring Finger 1 - LONRF1, SMURF2, RNF130, USP46) are represented in the top affected genes. Another pathway seems to frequently appear in the biological functions of the top differentially expressed genes reported in the tables is apoptosis (AIF4A1, RNF130, Cyclin Dependent Kinase 6 - CDK6, RASSF3).

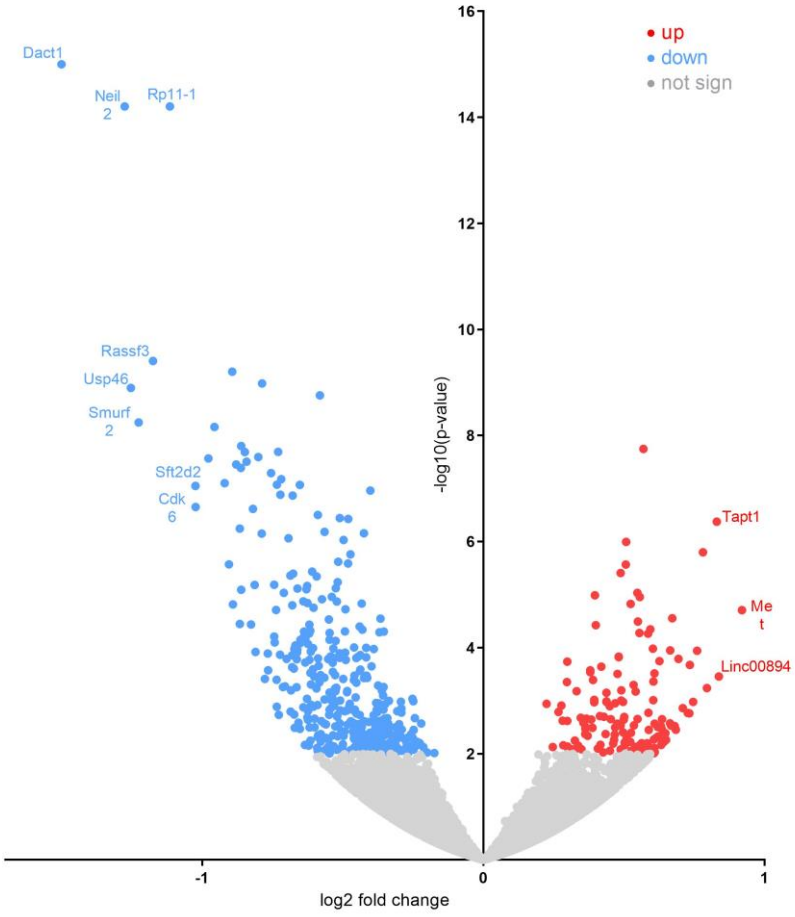

Figure 52 **Volcano plot of the fold change of differentially expressed genes in DACT1 silenced BMSCs.**
5624 genes were differentially expressed, 1330 of which were significant. Each gene is represented by one point on the graph, in grey are plotted non statistically significant differentially expressed genes, in red the upregulated genes and in blue the

downregulated genes. The horizontal axis is the log2 fold change between siDACT1 and siCTRL conditions. The negative log10 of the p-value is plotted on the vertical axis. The control condition was transfected with a scrambled miRNA (siCTRL) (N=4)

Table 4 **List of the top 10 up-regulated genes siDACT1 vs siCTRL BMSCs.**

Fold Change	Molecules	ID	Biological Role
0.920	MET	Hepatocyte growth factor receptor	Wnt-protein binding participates in wound healing as well as organ regeneration and tissue remodelling. May regulate cortical bone osteogenesis.
0.837	LINCO0894	N/A	
0.830	TAPT1	Transmembrane anterior posterior transformation 1	Primary cilia formation. Downstream effector of HOXC8 transmitting extracellular information for axial skeletal patterning. Involved in cartilage and bone development.
0.795	SLC26A10	Solute carrier family 26 member 10	Chloride/bicarbonate exchanger, may be a pseudogene.
0.781	PTPMT1	Phosphatidylglycerophosphatase and protein-tyrosine phosphatase 1	Lipid phosphatase, biosynthetic pathway of cardiolipin. Mediates dephosphorylation of mitochondrial proteins.
0.760	ANKRD20A5P	Putative ankyrin repeat domain-containing protein 20A5	Pseudogene
0.733	CA2	Carbonic anhydrase 2	Essential for bone resorption and osteoclast differentiation. Reversible hydration of carbon dioxide.
0.709	SLC36A1	Proton-coupled amino acid transporter 1	Neutral amino acid/proton symporter.
0.672	FAM49B	Protein FAM49B	Activation of platelets and immune cells.
0.668	AIF4A1	Apoptosis-inducing factor 4A1	Proapoptotic factor in a caspase-independent pathway.

Table 5 List of the top 10 down-regulated genes siDACT1 vs siCTRL BMSCs.

Fold Change	Molecules	ID	Biological Role
-2.078	DACT1	Dapper antagonist of catenin 1	Regulation of intracellular signalling pathways during development: canonical and/or non-canonical Wnt pathways through interaction with DVL.
-1.276	NEIL2	Endonuclease 8-like 2	Involved in base excision repair of DNA damaged by oxidation or by mutagenic agents.
-1.226	LONRF1	LON peptidase N-terminal domain and RING finger protein 1	Protein polyubiquitination. Involved in ubiquitination & Proteasome degradation pathways.
-1.175	RASSF3	Ras association domain family member 3	Regulation of apoptosis and signal transduction.
-1.114	SFT2D2	SFT2 domain containing 2	Fusion of retrograde transport vesicles derived from an endocytic compartment with the Golgi complex.
-1.024	USP46	Ubiquitin specific peptidase 46	GTPase-activating protein for RAB5A and RAB43. Receptor trafficking. In complex with EPS8 inhibits internalization of EGFR.
-1.023	CDK6	Cyclin dependent kinase 6	Serine/threonine-protein controlling cell cycle and differentiation; promotes G1/S transition.
-0.977	VAMP3	Vesicle-associated membrane protein 3	SNARE involved in vesicular transport from the late endosomes to the trans-Golgi network.
-0.956	SMURF2	SMAD specific E3 ubiquitin protein ligase 2	Regulate ubiquitination-mediated protein degradation
-0.920	RNF130	E3 ubiquitin-protein ligase RNF130	Acts as an E3 ubiquitin-protein ligase. Involved in programmed cell death of hematopoietic cells.

To confirm the RNAseq results, primers for 4 of the top up- and down-regulated genes were designed and tested. The expression of the genes of interested was quantified on RNA isolated from BMSCs after 24 hours of silencing. The 24 hours and not 16 hours time point was selected to confirm continued patterns of differentialexpression (as a quick confirmation of the sequencing data). The genes tested show consistent results with what shown by the RNA sequencing. TAPT1 was upregulated 4-fold, while

DACT1, USP6, CDK6 and SMURF2 show decreased expression in DACT1 knockdown BMSCs (fig. 53). At 24 hours after silencing, the selected genes showed increased fold change compared to 16 hours, further confirmation that their differential expression is caused by DACT1 silencing.

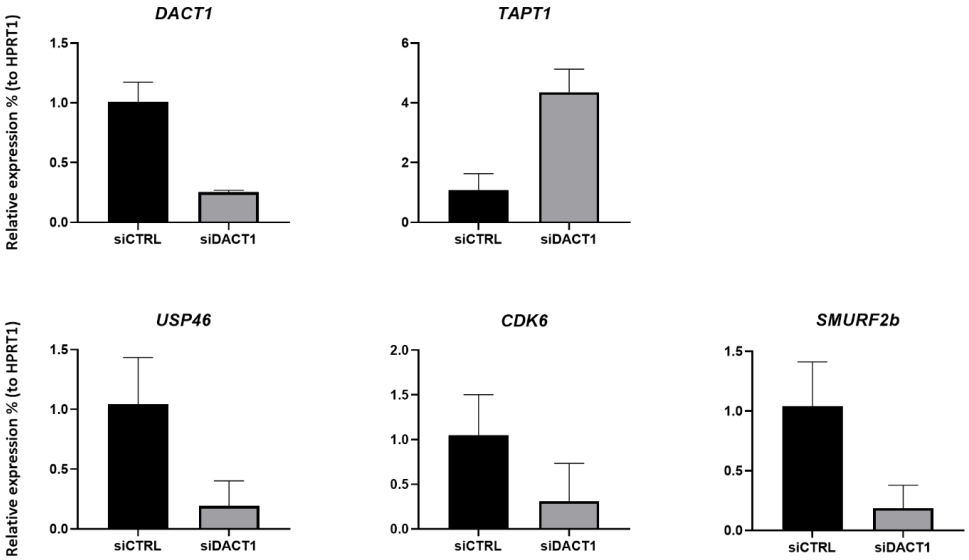

Figure 53 **RNAseq data validation by RT-qPCR.**
5 genes among the top up and downregulated from the RNA sequencing analysis were validated in a sample after 24 hours from silencing. Relative expression was calculated with the formula 2^-ΔΔCt. The control condition was transfected with a scrambled miRNA (siCTRL). Error bars indicated the standard deviation of the mean of technical replicates, N=1.

Top 300 differentially expressed genes were analysed with Ingenuity Pathway Analysis (IPA, Qiagen), a bioinformatics software for the analysis and integration of 'omics data. The software analysis identified canonical pathways (fig. 54), diseases and biological functions (fig. 55), and gene networks and regulators (fig. 56) that are most significant to the uploaded data.

Figure 54 shows the known biological pathways that appear most significantly affected by the genes in the uploaded data set. As expected, "Cell Cycle G1/S checkpoint regulation", in white, meaning that the pathway is activated upon DACT1 knockdown, and "GADD45 signalling" (grey, activation unknown) are highlighted, as they are both linked to cell cycle control and apoptosis. Growth arrest and DNA-damage-inducible, alpha (GADD45) encodes for a protein induced by DNA damage and other stress signals associated with growth arrest and apoptosis (Salvador, Brown-Clay, & Fornace, 2013). Worth noting is the Sirtuin negative pathway, as Sirtuin has been

reported to affect DACT1 expression in BMSCs (Zhou et al., 2016). The Sirtuin pathway shows a negative z-score. This would indicate that DACT1 knockdown inhibits the transcriptional activation of the Sirtuin pathway. Most of the reported pathways, however, are not obviously relevant to musculoskeletal tissues, such as “hereditary breast cancer signalling”, “oleate biosynthesis” or “Estrogen receptor signalling”.

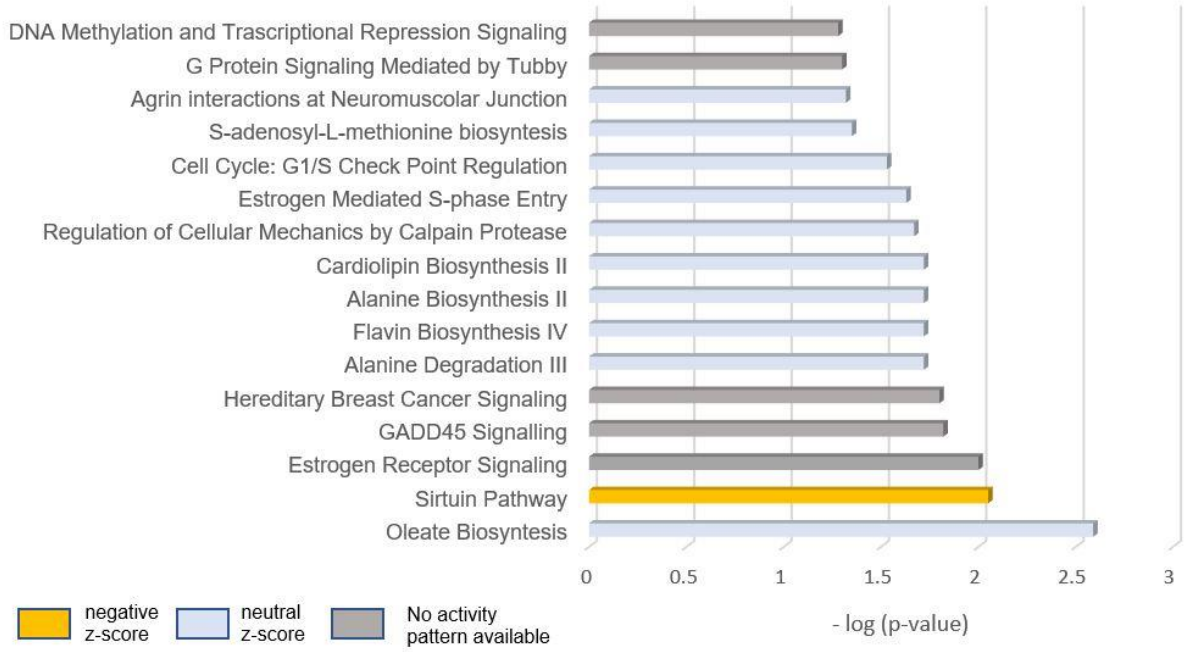

Figure 54 **Top enriched canonical pathways following DACT1 silencing in BMSCs.**
The pathway that shows significant enrichment for a set of top 300 genes from the RNA sequencing analysis is reported. The x-axis reports the top function as calculated by IPA based on the 300 differentially expressed genes uploaded from the RNA sequencing analysis siDACT1 vs siCTRL. The y-axis represents the ratio of the number of genes from the dataset that map the to the pathway and the number of all genes ascribed to that pathway. The vertical yellow line represents the threshold p-value (calculated by Fisher’s test). According to the expression value of each gene, IPA determines per each reported pathway if they are activated or not (z-score). In yellow are activated pathways, in blue non activated, in white could be either and in grey are pathways for which data activity pattern is not available.

Differentially expressed genes were also categorized to diseases and functions (fig. 55). Consistent with the results of canonical pathway analysis following DACT1 silencing, cancer, reproductive system disease, endocrine system disorders appear linked to the 300 genes updated that were differentially expressed after DACT1 knockdown. “Cell growth and proliferation”, “cell movement”, “embryonic development”, “organ development” are all biological functions that fit in with the hypothesis that DACT1 modulates WNT and TFGβ pathways.

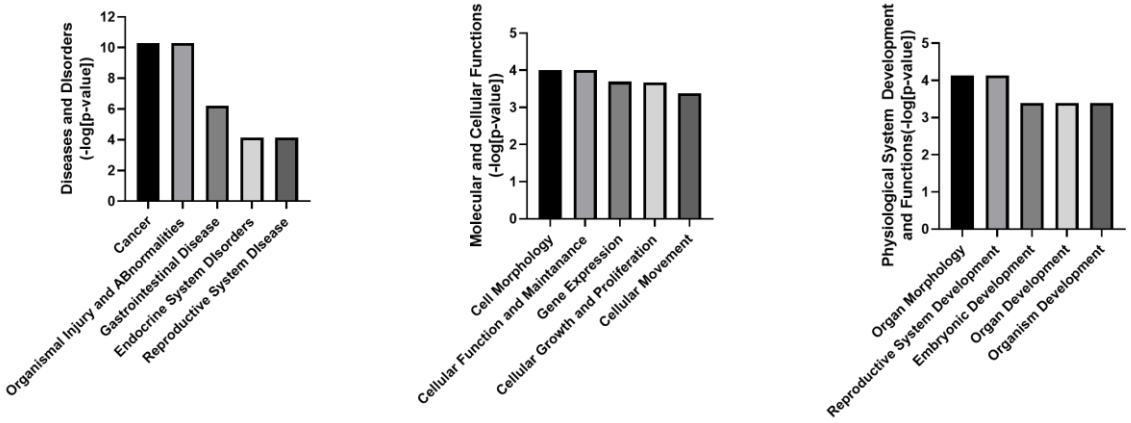

Figure 55 **Summary of key biological processes and diseases influenced by differentially expressed genes.**
The top 5 “disease and disorders”, “molecular and cellular functions” and “physiological system development and functions” associated with the top 300 differentially expressed genes resulting from DACT1 silencing. Y-axis reports the negative logarithm of the p-value calculated by IPA.

Besides the predominant pathways and cellular functions, gene networks were built to connect genes and enriched categories of diseases and functions based on the correlation between differentially expressed genes. It is worth noting that WNT3a appeared among the top regulators of the networks. That is consistent with its role in cell cycle progression and the link between DACT1 and Wnt pathways, of which WNT3a is a prime ligand and signalling molecule. WNT3a activates both canonical and non-canonical Wnt pathways in BMSCs (Qiu, Chen, & Kassem, 2011), and has been shown to sustain BMSCs proliferation and chondrogenic potential (Narcisi et al., 2015). Again, the network function relates back to developmental disorders and embryonic development, cell cycle and cellular growth and proliferation (fig. 56). The networks linking different genes further highlighted interesting links between certain proteins of interest such as SMURF2, miR-221, RUNX1, ID4.

In network 4 “Cellular development, cell growth and proliferation, cell cycle” miR-221 (in red, upregulated) is present, forming links with MAPK1/2, MET (also upregulated, and a top hit of upregulated genes) and PDF. MAP kinases in WNT signal transduction bind to AXIN and E3 ligases to regulate β-catenin activity. Mir-221 was reported to behave as an anti-chondrogenic regulator in MSCs. Upon silencing of miR-221, MSCs undergo chondrogenic differentiation in the absence of TGBβ signalling (Lolli et al., 2016).

RUNX1 Partner Transcriptional Co-Repressor 1 (RUNX1T1) is an important protein in BMSCs fate determination present in one of the networks (number 5, “Embryonic development, Nervous System Development and Function, Organ Development”) displayed in figure 56. RUNX1T1 is reported to act as a negative regulator of adipogenesis and is downregulated alongside DACT1 silencing. In the network, it is connected to inhibitor of DNA binding protein 4 (ID4), a gene encoding for a member of the inhibitor of DNA binding (ID) protein family. Downregulation of ID proteins, orchestrated by SMAD proteins, is a pathway by which TGF-β signalling could arrest the cell cycle (Kowanetz, Valcourt, Bergström, Heldin, & Moustakas, 2004). These networks collectively provide a valuable list of proteins that are known to be important in MSCs regulation and chondrogenesis. The identified networks also provide putative proteins and molecules which effects have not been investigated in the musculoskeletal context.

Figure 56 **List of top regulators and networks of siDACT1 300 genes.**
Reported upstream regulators can elicit the gene expression changes observed in the provided data set. To build the networks, IPA uses the upstream regulator and computationally seek pairs of regulators predicted to affect the expression of a similar set of genes and repeats it. The genes shaded in red are upregulated, and the genes shaded green are downregulated. Legend at the lower right explains the relationship arrows and shapes utilized in the networks.

Top Regulator Effect Networks

ID	Regulators	Diseases & Functions	Consistency Score
1	TP73	Phosphorylation of protein	-7.0
2	miR-124-3p (and other miRNAs w/seed AAGGCAC)	Cell cycle progression	-7.5
3	WNT3A	Cell cycle progression	-8.66

Top Networks

ID	Associated Network Functions	Score
1	Developmental Disorder, Hereditary Disorder, Metabolic Disease	49
2	Embryonic Development, Organismal Development, Reproductive System Development and Function	46
3	Embryonic Development, Nervous System Development and Function, Organ Development	44
4	Cellular Development, Cellular Growth and Proliferation, Cell Cycle	29
5	Developmental Disorder, Hereditary Disorder, Neurological Disease	25

Network 1 : CTRLvsDACT1 - 2018-08-24 04:25 PM : CTRLvsDACT1 : CTRLvsDACT1 - 2018-08-24 04:25 PM

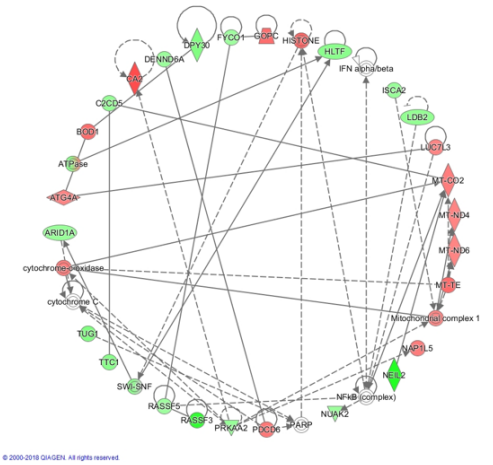

Network 2 : CTRLvsDACT1 - 2018-08-24 04:25 PM : CTRLvsDACT1 : CTRLvsDACT1 - 2018-08-24 04:25 PM

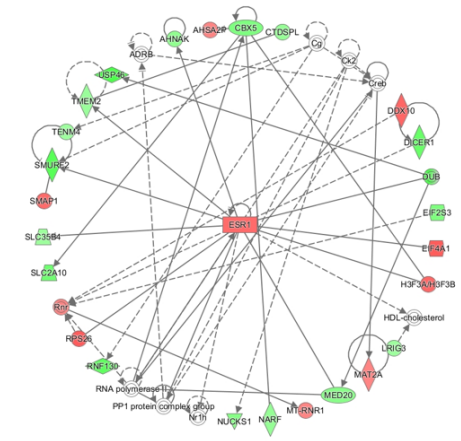

Network 3 : CTRLvsDACT1 - 2018-08-24 04:25 PM : CTRLvsDACT1 : CTRLvsDACT1 - 2018-08-24 04:25 PM

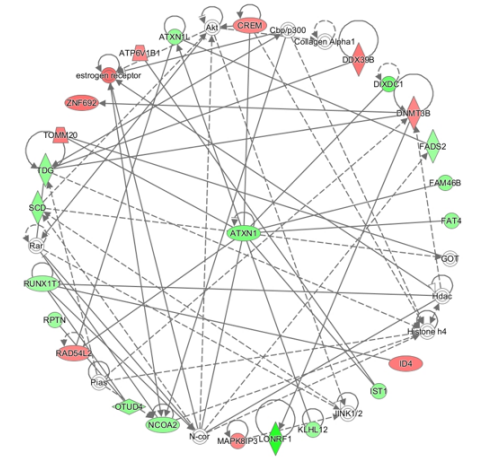

Network 4 : CTRLvsDACT1 - 2018-08-24 04:25 PM : CTRLvsDACT1 - 2018-08-24 04:25 PM

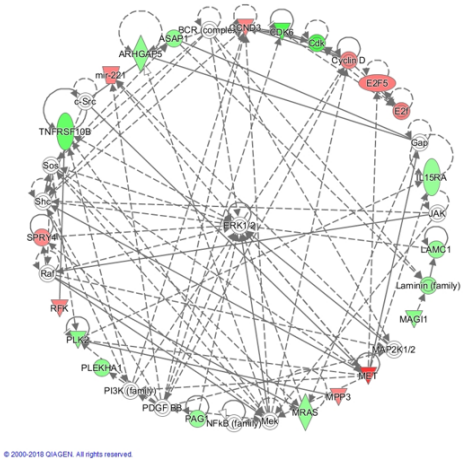

Network 5 : CTRLvsDACT1 - 2018-08-24 04:25 PM : CTRLvsDACT1 - 2018-08-24 04:25 PM

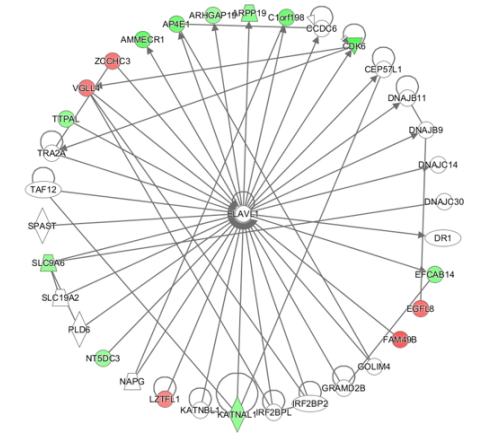

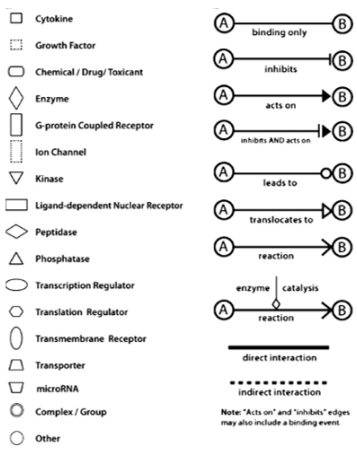

6.2.3 DACT1 could be involved in the canonical Wnt pathway in BMSCs.

Wnt pathways are known for their role in regulating MSCs proliferation. Wnt signalling target genes include CMYC and CCND1, important for cell proliferation. Several Wnt pathway proteins were identified to be linked to DACT1 from the data resulting from the sequencing of DACT1 silenced cells. Wnt gene targets were selected and their expression was studied after DACT1 silencing to establish if they were modulated by DACT1 loss. siDACT1 was applied to SynMSCs from three different patients and after 24 hours the expression of Wnt target genes *CCND1*, *JAG1*, *ID1*, *SOX9* and *FZD* was determined by RT-qPCR. Cyclin-dependent kinase D1 (CCND1) is a protein that integrates Shh and Wnt activities and is a cell cycle regulator. *CCND1* is a direct target gene of the Wnt canonical pathway: TCF consensus binding sites are present in the *CCND* promoter. Jagged 1 (JAG1) is β-catenin target gene that acts as a ligand for the NOTCH pathway (Estrach, Ambler, Lo Celso, Hozumi, & Watt, 2006). NOTCH signalling has an important role in cell growth and differentiation (Artavanis-Tsakonas, Rand, & Lake, 1999; Fortini, 2009). ID1 is a protein regulating both Wnt and TGFβ pathways (Järvinen, Shimomura-Kuroki, Balic, Jussila, & Thesleff, 2018; Nakashima, Katagiri, & Tamura, 2005). FRZB is a Wnt receptor that transmits the signalling in the PCP and canonical Wnt pathway, as previously described.

Firstly, *DACT1* was consistently silenced in all SynMSCs after 24 hours. *JAG1* and *SOX9* showed up-regulation following DACT1 silencing and *CCND1* expression was also increased, around 2-fold in all samples. *ID1* expression was concomitantly reduced alongside *DACT1*. *FZD* expression was not consistent across the samples and therefore difficult to interpret (fig. 57). The data suggest that DACT1 acts as an inhibitor of the Wnt pathway.

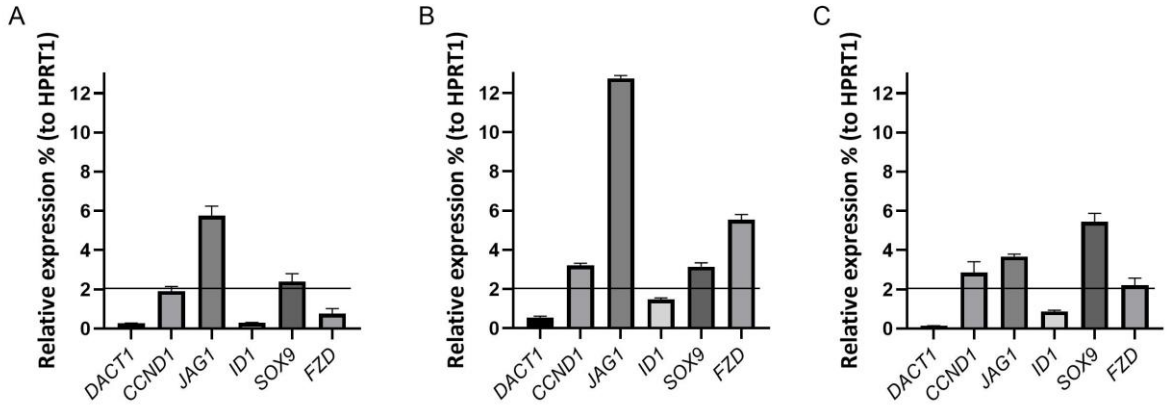

Figure 57 **WNT target genes affected by DACT1 silencing in BMSCs.**
Expression of 5 targets gene of the canonical WNT pathway was determined by RT-qPCR after 24 hours DACT1 silencing of SYnMSCs. Relative expression was calculated with the formula 2^-ΔΔCt. The control condition was transfected with a scrambled miRNA (siCTRL) (N=3). Error bars refer to the standard deviation of technical replicates.

WNT3a was suggested to be an upstream network regulator according to IPA analysis and the expression of *SOX9*, *CCND1* and *JAG1* canonical Wnt target genes were upregulated following DACT1 silencing. It was hypothesised that by adding a Wnt pathway activator such as CHIR-99021 (which is a potent GSK3β inhibitor, subsequently referred to as inhGSK3β), we would be able to mimic all or part of the DACT1 silencing effects in MSCs and gain an insight into the balance that DACT1 may have on canonical and non-canonical Wnt signalling in DACT1 silenced cells.

Because of cell death resulting from DACT1 silencing, it was not possible to test if DACT1 silencing causes an increase or a reduction of nuclear β-catenin. GSK3β phosphorylates highly conserved serine (Ser) and threonine (Thr) residues (Ser 33, Ser 37, Thr 41, and Ser 45) at the N-terminus of β-catenin and targets β-catenin for degradation. Different antibodies were used to identify unphosphorylated β-catenin (ABC, in red), and a different antibody that binds to phosphorylated β-catenin was also used (in green, Alexa488). In the presence of Wnt signalling, the destruction complex is inactivated resulting in the cytoplasmic accumulation of β-catenin and its subsequent translocation to the nucleus. Similar nuclear localisation of active-β-catenin (ABC) was expected in both conditions where WNT3a and inhGSK3β were added to the cells, or when the two were both added to the BMSCs. After overnight serum starvation, BMSCs were treated with WNT3a, inhGSK3β or both overnight. In figure 58 fluorescence miscopy images of BMSCs after overnight serum starvation shows no

ABC localisation in the nucleus. Limited phosphorylated β-catenin is present in the plasma membrane. BMSCs treated with canonical Wnt activators WNT3a and inhGSK3β show nuclear localisation of ABC.

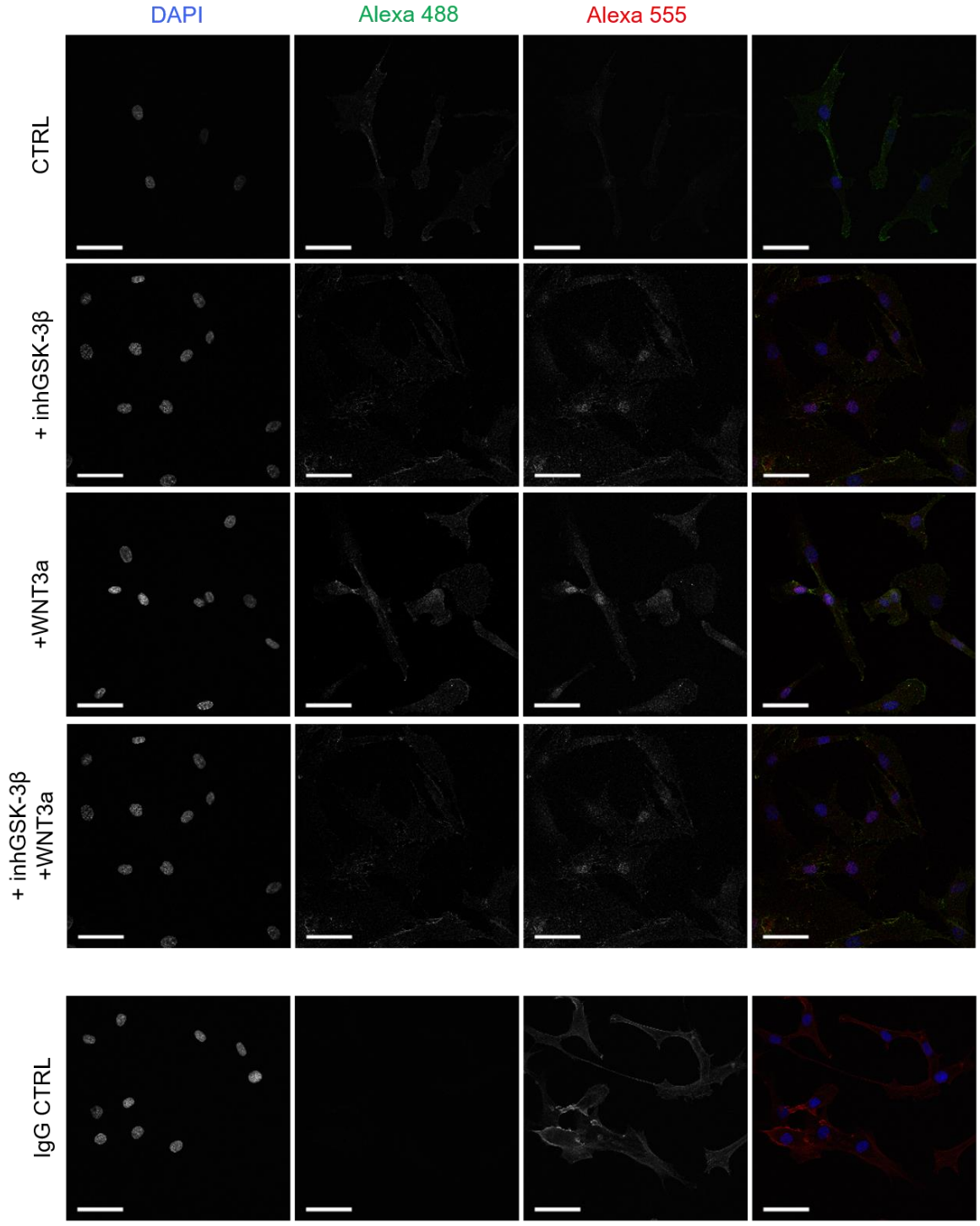

Figure 58 **WNT3a and GSK3b inhibitor treatments cause nuclear localisation of active-β-catenin.**
Anti-β-catenin (in green, Alexa488) and anti-ABC (in red, Alexa555) antibodies (1:500) staining on BMSCs, after overnight serum starvation, that were treated with WNT3a,

2.5 µM inhGSK3β or both overnight before fixation. In the IgG CTRL condition, phalloidin-Alexa555 was used to show cytoskeletal actin filaments. Representative images from one of two independent experiments with BMSCs are shown (N=2). β-catenin: green; red: active-β-catenin; nucleus: blue Scale bar: 50 µm.

After ensuring that WNT3a and inhGSK3β acted on BMSCs as expected, the two molecules were added before treatment with siDACT1.

First, GSK3β inhibitor (Wnt activator) was tested alone and in combination with siDACT1, and compared to the siDACT1 alone condition, on BMSCs (fig. 59). The experimental hypothesis was that GSK3β inhibitor would mimic the effect of DACT1 silencing if DACT1 was modulating only the Wnt pathway. After one day from applying the silencing, siDACT1 and inhGSK3β conditions showed no significant difference in cell index values. At day 2 and 3 statistically significant differences arose between the two conditions. In addition, siDACT1 alone had a similar effect to what observed in the GSK3β+siDACT1 condition. At day 2 and day 3 the difference between GSK3β+siDACT1 and the control was not statistically significant, whereas with siDACT1 there continued to be have significant influence. The experiment showed that DACT1 silencing was not exactly mimicked by adding a Wnt pathway activator.

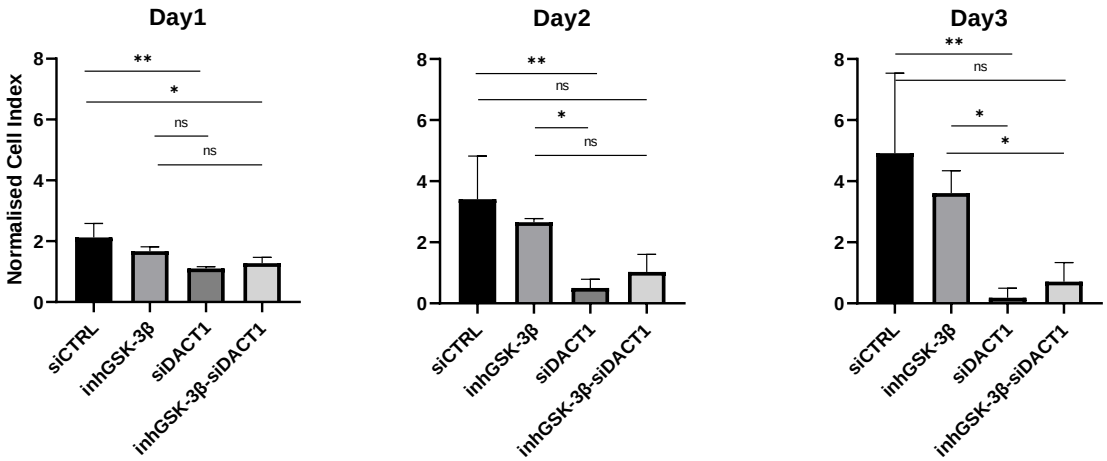

Figure 59 **Real-time effect of inhGSK3β on siDACT1 BMSCs over 72 hours.** BMSCs from healthy donors (Lonza) were seeded in XCELLigence E-plates and their impendence measured every 15 minutes by XCELLigence RTCA. Cell Index measurements were normalised to the time of silencing. The control condition was transfected with a scrambled miRNA. 2.5 µM GSK3β inhibitor was added to cells 5 hours before applying the silencing (Kruskal-Wallis non-parametric test was performed on the measurements at 24, 48, and 72 hours, *= $p<0.05$, ** = $p<0.01$, N=3).

The CyQUANT® Direct assay was performed after 48 hours to determine the effect of WNT3a and GSK3β inhibitor on unsilenced and DACT1 silenced cells (fig. 60). As

previously determined, siDACT1 caused a significant reduction in cell numbers compared to the control conditions after 48 hours. The addition of inhGSK3β to the cells did not have a significant effect on cell numbers compared to untreated control. By adding WNT3a or inhGSK3β to the cells before transfecting with siDACT1, a similar resulted to siDACT1 condition was observed. siDACT1, Wnt3a and nhGSK3β conditions showed no statistically significant difference. Treatment with inhGSKb or Wnt3a reproduces siDACT1 results partially, which indicate that potentially DACT1 impact Wnt pathway. However, given the results obtained in figure 59, a more plausible explanation would be that DACT1 impact on other pathways (non-canonical & TGFb) that support cell survival (as well as canonical Wnt signalling). Further study are however necessary to confirm these observations.

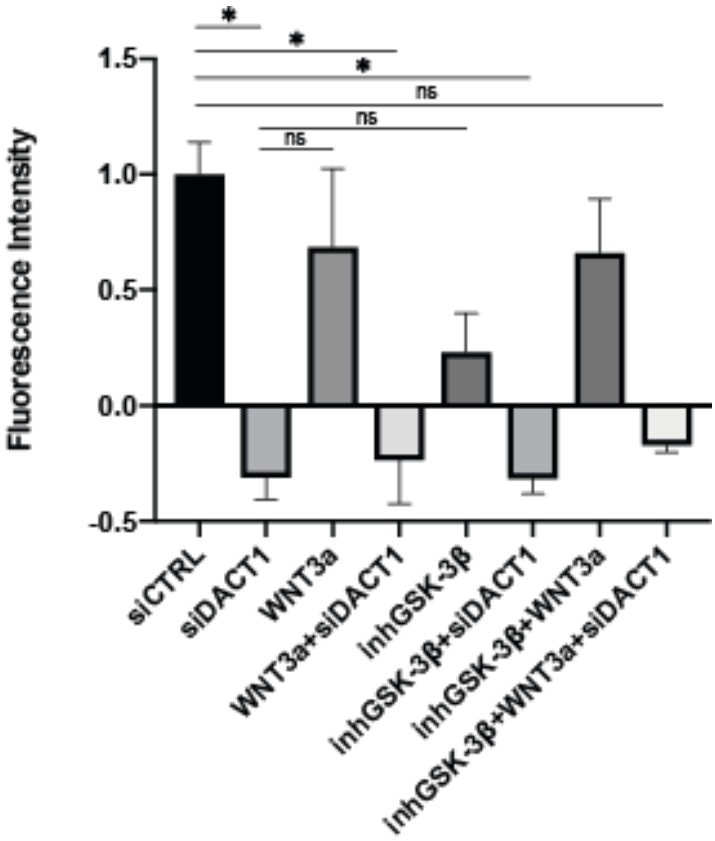

Figure 60 **Effect of WNT3a and inhGSK3β on DACT1 silenced cell survival and proliferation.**
CyQUANT® Direct assay was performed after 48 hours of DACT1 silencing. BMSCs from three healthy donors (Lonza) were transfected with siDACT1 5 hours after administering WNT3a, or 2.5 μM inhGSK3β or both. The control condition was transfected with a scrambled miRNA (siCTRL) (Kruskal-Wallis non-parametric test was performed on the measurements, * = $p<0.05$, N=3).

6.2.4 Preliminary work suggests a role for DACT1 in regulating protein ubiquitination.

The RNAseq data suggested that several genes encoding for proteins involved in ubiquitination are affected by DACT1 silencing in BMSCs. Ubiquitination is a simple and versatile protein modification that can impart different signalling consequences. Ubiquitin is a small protein that is covalently attached to target protein by a process involving three different enzymes E1, E2 and E3 and can also be conjugated to other substrate proteins. Ubiquitin modification controls signalling pathways by influencing both proteolytic and nonproteolytic functions, such as control of protein activity and subcellular localisation. Because several ubiquitin-related genes are downregulated after DACT1 knockdown, it was hypothesised that ubiquitinated protein levels in silenced cells would be higher than the control condition. Western blot analysis probing for ubiquitin in the protein lysate obtained from BMSCs after 6 h or 24 h following DACT1 silencing was performed. After 6 h no ubiquitination was detectable and no difference between the two conditions was visible. After 24h, siDACT1 showed bands at several heights suggesting a higher number of ubiquitinated proteins than in siCTRL condition at the same time point. This result supports the hypothesis that DACT1 may be involved in regulating protein ubiquitination

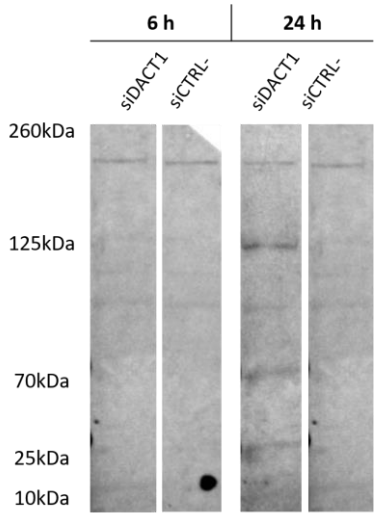

Figure 61 **DACT1 knockdown increases ubiquitination in BMSCs.**
BMSCs from healthy donor (Lonza) were transfected with siDACT1 or scramble miRNA (siCTRL) and harvested for protein analysis at 6 hours or 24 hours after silencing. Total protein was quantified, and the same amount was loaded in each lane. Anti-ubiquitin antibody (1:500) was used to detect ubiquitinated protein present in each sample. N=1.

6.3 Discussion

6.3.1 DACT1 knockdown influences BMSC survival by activating apoptotic and cell cycle pathways.

siDACT1 transfection has been performed previously in colon cancer cell lines without resulting in the apoptosis of the silenced cells. In three cancer cell line cells, siDACT1 reduced migratory potential and downregulated protein levels of β-catenin, cyclin D1 and c-Myc (Yuan et al., 2012). The same study reports that overexpression of DACT1 enhances cell proliferation. This results from DACT1 inhibiting GSK3β and consequent resulting in β-catenin stabilisation (Yuan et al., 2012).

Two other studies investigating DACT1 in different cancer cell lines reported opposite observations relative to cell growth and proliferation, but still describe DACT1 regulation of these proliferative and apoptotic pathways through WNT signalling. Yin et al. showed that in breast cancer cells, DACT1 overexpression results in apoptosis by negative regulation of the canonical Wnt pathway -by decreasing β-catenin activity (Yin et al., 2013). Analogous to what was described in breast cancer cells, in a leukaemia cell line, DACT1 was reported to influence not only cell growth and proliferation but also apoptosis. DACT1 overexpression arrested leukaemia cells in G0/G1 and induced apoptosis (K. Zhu, Jiang, Yang, Hu, & Liu, 2017).

In this chapter, silencing of DACT1 by RNAi suggests that in response BMSCs and SynMSCs undergo cell death. Transcriptome analysis showed that the apoptotic pathway was activated following DACT1 downregulation, corroborating what was observed morphologically (fig. 50) and functionally (fig. 48 and 49). To support this observation, a TUNEL assay or an agarose gel electrophoresis showing DNA laddering should be performed. In order to exclude the possibility that the specific sequence of miRNA used in these experiments had unforeseen off-target toxic effects, a different siDACT1 (with different miRNA sequence that still targets *DACT1* mRNA) was purchased and tested. The same cell phenotype was observed in silenced MSCs with the different siDACT1 molecules, suggesting that effects are specific to DACT1 knockdown.

A similar apoptotic effect following DACT1 silencing was observed in cultured ACs although further studies need to be performed to confirm that the same pathways are activated in this cell type.

6.3.2 Transcriptome analysis of DACT1 silenced cells reveals an interesting connection to ubiquitination and Wnt pathways.

Transcriptome analysis of DACT1 silenced cells was performed and the list of genes identified by the RNA sequencing highlighted several interesting genes that are linked to DACT1 in BMSCs.

This is the first report of a link between DACT1 and SMURF2. SMURF2 downregulation following DACT1 knockdown was significant after 24 hours, as shown by RT-qPCR (fig. 44). SMURF2 is an E3 ubiquitin ligase that selectively interacts with SMADs and is known to target SMAD1 for ubiquitination, determining its degradation by the proteome. Vertebrates express two *SMURF* genes: *SMURF1* and *SMURF2*. The two genes possess similar expression patterns, and probably have partially redundant functions as double Smurf1−/−; Smurf2−/− (Smurf DKO) mice are embryonic lethal at around E12.5 (Narimatsu et al., 2009). If only one of the two genes is knockout, mice survive. Both proteins are expressed by osteoblasts and proliferating chondrocytes (Wu et al., 2009; Yamashita et al., 2005). In chondrocytes, SMURF2 mediates GSK3β ubiquitination and its degradation by the proteome, resulting in upregulation of β-catenin. It has been suggested that this is possibly a starting signalling that contributes to the initiation of OA (Wu et al., 2009). Recently, Huang et al. reported that when SMURF2 is overexpressed under the COL2 promoter, it starts a signalling cascade that initiates OA development (H. Huang, Veien, Zhang, Ayers, & Song, 2016). TGFβ signalling can elicit cell proliferation, differentiation and apoptosis through SMAD mediators. SMAD3 can be targeted for phosphorylation by GSK3β that results in ubiquitin-mediated degradation of SMAD3 (Xing Guo et al., 2008). DACT1 knockdown affected genes regulating both ubiquitination and phosphorylation, indicating that DACT1 might act to integrate the TGFβ and WNT pathways by regulating the stability of central mediators of these pathways such as GSK3β and SMADs.

LONRF1, RNF130, and USP46 are genes identified by RNA sequencing linked with ubiquitination, as pointed out in tables 4 and 5. The downregulation of these genes alongside *DACT1* suggests a role for DACT1 as a signal mediator in the pathways where it is involved through ubiquitination. To support this hypothesis, a preliminary experiment showed increased protein ubiquitination 24 hours after DACT1 silencing of BMSCs (fig. 61).

Among the top upregulated genes, TAPT1 has never before been associated with DACT1 and would make an interesting gene to further investigate because of its link to cartilage. In the mouse embryo, TAPT1 is involved in the development of the axial skeleton, and mutation in this gene leads to a complex lethal osteochondrodysplasia (Howell et al., 2007; Symoens et al., 2015). TAPT1 is a positive regulator of cartilage development.

MET, which encodes for the receptor of the hepatocyte growth factor (HGF), is the top upregulated gene following DACT1 silencing. Although no previous work has been reported that links DACT1 and MET, *DACT1* is downregulated in hepatocellular carcinoma (Yau et al., 2005). HGF was shown to have a role in the proliferation of mesenchymal cells and to regulate limb dub development. The protein expression pattern of MET is however very interesting and relevant to the consideration of the data presented in Chapter 5 and 6. Immunohistochemistry shows the presence of MET in the deep zone of normal cartilage. In addition, only a small number of chondrocytes in the superficial and intermediate zone showed MET staining. Additionally, in OA cartilage, and in contrast to normal cartilage, MET was identified using immunohistochemistry in all OA chondrocytes (Pfander et al., 1999). From the immunohistochemical pictures reported by Pfander and colleagues, MET seems to have exactly the opposite expression pattern to DACT1 (Chapter 5). Further analysis is needed to determine if the gradient formed by these two proteins is instrumental in maintaining cell phenotype in either zone of articular cartilage.

6.3.3 DACT1 as a modulator of the WNT signalling in BMSCs.

The data described in this thesis does not unambiguously clarify whether the canonical Wnt pathways is the only one where DACT1 is involved. On one hand, DACT1 knockdown alters the expression of known Wnt targets such as *CCND1*, *SOX9*, and *JAG1*. However, the addition of WNT3a and GSK3b inhibitor is not able to completely reproduce the siDACT1 phenotype. WNT3a signals via the canonical WNT pathway and inhibits hypertrophic differentiation of BMSCs, as well as maintaining proliferation and chondrogenic potential (Narcisi et al., 2015). Recently, a paper reported that WNT3a did not affect *DACT1* expression in intestinal epithelial cells and that TGFβ instead can regulate *DACT1* expression (Wang et al., 2018). The combination of both WNT3a and GSK3β, however, resulted in a small reduction in cell death (fig. 59 and

fig. 60). As the presence of WNT3a and inhGSK3β result in increased MSCs proliferation, it is possible that the “rescue” effect was determined by the proliferation of non silenced cells. Further analysis is necessary to determine the percentage of DACT1 which is effectively knockdown after 48 hours in that condition. However, because of the high silencing efficiency already at 24 hours (fig. 44), it is unlikely that the proliferation of a few cells can determine the partial rescue effect detected. More likely, DACT1 regulates Wnt canonical pathway in BMSCs, but that is not the only pathways where is has regulatory effects.

If the canonical Wnt pathway is only one of the signalling networks in which DACT1 is involved, the genes detected by the RNA sequencing can be instrumental in identifying other candidates. Top downregulated genes *SMURF2* and *RASSF3* code for proteins that are involved in the regulation of the PCP signalling pathway.

PCP regulates the polarisation of cells in tissue and their migration. PCP proteins in embryos have important roles in epithelial cells, mesenchymal cells, and neurons. In adults, Wnt regulation of RHO and other PCP pathway proteins respond to and transduce mechanical stimuli (Abuammah et al., 2018). The Wnt co-receptor LRP5, for example, is required for strain-induced mechanotransduction in osteoblasts and is involved in both canonical and PCP pathways (Bryja et al., 2009). Mechanical signals that regulate cartilage repair remain poorly understood but may well share similar pathways and relevant molecules to osteoblasts. A study on the effect of PCP pathway inhibitors such as Y-67632, a ROCK inhibitor, might be a possible avenue to further elucidate which pathway is influenced by DACT1

Among the top pathways suggested by IPA analysis, Sirtuin is of interest because of its link to OA and cartilage. Sirtuins are a family of proteins that regulate longevity and ageing in several tissues, including cartilage, and are associated to cellular functions such as inflammation, senescence, autophagy and apoptosis (Kida & Goligorsky, 2016; Yacoub, Lee, & He, 2014). Sirtuins are deacetylases that act on histones to modulate transcription but were shown to have a general role to modify protein stability, catalytic activity and binding properties. SIRT1 is expressed in chondrocytes and downregulated in OA cartilage. SIRT1 knockdown results in ACAN downregulation and upregulation of OA marker genes such as COL10 and ADAMTS-5 (Fujita et al., 2011). In a cartilage-specific conditional Sirt1-knockdown, OA was surgically induced and loss of Sirt1 in chondrocytes led to the accelerated development of OA, suggesting that SIRT1 has a preventive role against the development of OA (Matsuzaki et al., 2014).

In agreement with the study published by Matsuzaki et al. intra-articular injections of SIRT1 activator, resveratrol, were able to preserve cartilage from developing OA in mice (W. Li, Cai, Zhang, Cui, & Shen, 2015). Zhou et al., suggest in their study on MSCs that resveratrol treatment increases DACT1 expression. They proposed that SIRT1 acts as an adipogenesis inhibitor in MSCs by inhibiting DACT1 (Zhou et al., 2016). Taken together these studies show that SIRT1 has an important role in regulating survival and senescence of chondrocytes and its function is lost in OA.

6.3.4 Limitations of the study

The transcriptome analysis described in this Chapter was performed on DACT1 silenced BMSCs obtained from 4 young and healthy donors. The time point selected for the study was 16 hours after silencing based upon the observation that a clear phenotypic effect (cell death) was initiated on average around 20 hours from silencing. In each of the different donors, the decline in cell number started between 15 hours and 20 hours after silencing. Despite the small number of samples and the apparent differences in time of response to silencing, 1330 genes showed statistically significant differential expression following DACT1 knockdown. Indeed, it is expected that more statistically significant genes might be detected by increasing the number of biological samples

The analysis performed by IPA on the top 300 genes differentially expressed following DACT1 knockdown has some limitations. IPA interprets the patterns of differentially expressed genes by grouping them into functional categories and pathways and then scores them with statistical analysis. The statistical analysis indicates the likelihood that the pathways are not detected by chance. Due to the small number of samples, and the low fold change, the pathways suggested by IPA should be confirmed by independent experiments. The genes uploaded were also filtered: only the top 150 upregulated and the top 150 downregulated (fold change) genes were selected. This limited selection assumes that only changes resulting in high fold change expression are relevant, so nuanced responses may be lost in this analysis.

Another imitation of the IPA analysis is the bias due to its reliance on published and available material on the uploaded genes. Because the information on DACT1 is limited in the literature, it is likely that many connections to this protein have not been made yet. For example, none of the 300 differentially expressed genes uploaded were

among the genes connected to DACT1 in the manually updated database in the IPA software. IPA results should, therefore, be considered as an explorative tool to be confirmed by other experiments.

6.4 Summary and future studies

The results presented and discussed in this chapter represent the first study on the function of DACT1 in human primary MSCs and the first transcriptome analysis on DACT1 silenced cells. The RNA sequencing study provides a list of potential target genes influenced by DACT1 and interacting pathways. A few genes give a glimpse of the potential molecular mechanisms of DACT1. SMURF2 acts on both WNT and TGFβ pathways in close relation to DVL. SMURF2 is expressed in cartilage and involved in early OA development. This study links for the first time DACT1 with SMURF2 which could help dissect the double role of DACT1 in WNT and TGFβ pathways. SMURF2 and three more downregulated genes (*LONRF1*, *RNF130*, and *USP46)* are involved in protein ubiquitination, suggesting a role of DACT1 in ubiquitin signalling. Another interesting identified target gene is *MET*. Coding for the receptor of HGF, MET has a mutually exclusive expression pattern with DACT1 in articular cartilage, as described in chapter 5, and is overexpressed in OA cartilage. A follow-up analysis of modulated genes found in this study might be useful for acquiring a deeper understanding of pathological changes in OA.

It was demonstrated with different experiments that DACT1 knockdown leads to apoptosis of BMSCs. The data presented in this chapter suggests that WNT pathways (canonical and perhaps PCP) might be regulated by DACT1. The DACT1 link to the WNT/β-catenin pathway was assessed by administering a Wnt3a or a GSK3β inhibitor to investigate their potential to mimic the effect of siDACT1 on BMSC apoptosis. Partial but not complete reproduction of the phenotype was observed, which may indicate that DACT1 knockdown triggers apoptotic signals through multiple different pathways and not just canonical/non-canonical Wnt signalling. An overexpression of DACT1 study is necessary to further determine its role in BMSCs and ACs. DACT1 overexpression could have a protective effect on BMSCs. In support of this hypothesis are the recent data from phase 3 WNT inhibitor drug developed by Samumed. In the work published by Deshmukh and colleagues, SM04690 was able to drive chondrogenic differentiation

of BMSCs and when injected into a rat OA model showed cartilage regeneration (Deshmukh, Seo, Swearingen, & Yazici, 2018). SM04690 was also showed to help cartilage regeneration and reduce synovial inflammation. The Wnt pathway inhibitor SM04690 acts by targeting two kinases, CLK2 and DYRK1A, which result in the upregulation of DACT1 (Deshmukh, Seo, Swearingen, & Yazici, 2018). These data suggest that a higher expression of DACT1 can be beneficial for cartilage repair and block the progression of OA.

The results reported here have led to other questions on the role of DACTs. It was shown in chapter 5 that *DACT1* expression is reduced in OA cartilage samples (data reported also in another study (Chou et al., 2015)), which suggest that this intracellular signalling modulator may have an important role in cartilage homeostasis. To further explore the role of DACT1 *in vivo,* mouse models could be used. If DACT1 expression is important for repair, a cell-specific DACT1 knockout in chondrocytes or MSCs should affect repair after chondral damage or its ability to prevent synovial joint tissue damage development in an OA model.

Another interesting question is what molecules regulate DACT1. The sirtuin pathway was identified by IPA analysis and was reported to modulate DACT1 expression in MSCs. Sirtuin has a role in cell senescence and not only shows downregulation in cartilage (like DACT1) but, when silenced, initiates OA development in the mouse. Further studies to investigate DACT1 regulation by SIRT1 could improve our understanding of OA progression.

Although limited experiments were performed with DACT2 knockdown cells, we observed that DACT2 knockdown had no effect on apoptosis or cell proliferation, in complete contrast to DACT1 knockdown. Further studies on DACT2 could give an interesting insight into the regulation of TGFβ signalling. A mouse Dact2 knockout model is available (Sanger Institute, UK) and although it shows no abnormal musculoskeletal features, no studies have been performed on adult and older mice. Histological analysis in older mice could unveil the effect of DACT2 knockdown on cartilage tissue. Alternatively, a cartilage damage model with this knockdown would inform us of the importance of DACT2 on osteochondral repair.

To conclude, it can be hypothesised, that DACT1 acts on cell survival and proliferation by modulating phosphorylation and ubiquitination of proteins of both WNT and TGFβ pathways, possibly through SMURF2, USP46 and RNF130 (fig. 62).

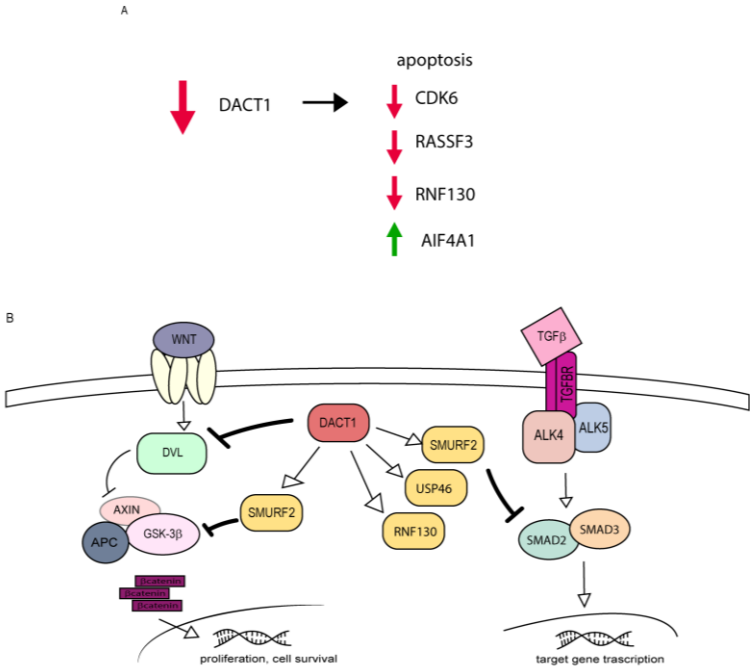

Figure 62 **DACT1 act on BMSCs survival and proliferation by modulating TGFβ and WNT pathways.**
DACT1 knockdown results in BMSCs apoptosis through downregulation of CDK6, RASSF3 and RNF130, and by upregulating AIF4A1 (A). DACT1 might integrate the two pathways through modulating phosphorylation and ubiquitination through SMURF2, USP46 and RNF130 (B).

7 Summary and conclusion

The aim of this body of work has been to extend our knowledge of the phenotypic differences between chondrocytes from different regions of articular cartilage. The existence of chondrogenic stem progenitor cells in the superficial zone of articular cartilage has been suggested (by others and by the data presented in this thesis and by others) based on their adhesion properties, expression of stem-cell markers, CFU potential, and ability to differentiate into chondrocytes *in vitro.* Recent murine genetic lineage tracing experiments have been able to confirm in vivo the presence of progenitors in the SZ of articular cartilage (Decker et al., 2017; Kozhemyakina et al., 2015; L. Li et al., 2017). The identified SZ cartilage progenitors form the entire adult articular cartilage *in vivo* and might take part in the healing of small cartilage defects. Questions remain on whether this cell population is present in adult human tissue and how it may take part in repairing cartilage damage during injury and disease. To further our understanding of how distinct chondrocyte populations might contribute during cartilage repair and regeneration, this thesis explored the signalling between the different regions of articular cartilage in terms of cytokine production and EVs-miRNA content. Understanding the differences between different subpopulations were also investigated in terms of DACT1 expression. DACT1 has been reported to be a modulator of both WNT and TGFβ pathways, but its role has not been explored extensively in cartilage.

7.1 Summary of the key findings

7.1.1 Bi-directional signalling between BMSCs and cartilage differs

The influence of resident ACs on cartilage repair is of great relevance not only to surgical techniques like microfracture and ACI but also to better understand cartilage tissue in homeostasis and disease. To study what determines a difference in modulating MSCs trophic and immunomodulatory action, a deeper analysis of human cartilage layers is required. In chapter 4, the crosstalk in terms of cytokine production and miRNA present in EVs was shown to be different when BMSCs are co-cultures with SZ or MDZ cartilage. MDZ-BMSCs co-cultures resulted in a larger array of cytokine production compared to SZ-BMSC condition. EVs isolated from either BMSCs-SZ cartilage or BMSCs-MDZ cartilage co-cultures carried different miRNAs. 38 miRNAs were identified in EVs obtained from co-culture supernatants, 5 were significantly differentially expressed in SZ and MDZ condition: mir-188-5p, miR-199a-3p, miR23a-3p, miR451a, miR-612. miR-23a-3p were

the only miRNA significantly differentially expressed after applying FDR (multiple testing correction) adjustments. miR-23a-3p is present in significantly higher quantities in EVs from the BMSCs-SZ condition. Targeting SMAD3 and RUNX2, and downregulating the expression of COL2 and ACAN, miR-23a-3p is a well-known regulator of cartilage. When compared the miRNAs carried by EVs obtained from BMSC not co-cultured with cartilage to BMSCs-SZ conditions, miR23a-3p and miR-125b-5p were present in both. That might suggest that BMSCs produce more miR23a-3p and miR-125b-5p when in contact with SZ, or that both cell types produce these miRNAs when in the presence of each other. miR-125p-5p regulates inflammation in OA by acting through IL-1β to induce the expression of inflammatory genes and cartilage degradation by regulating ADAMTS4. On the other hand, no overlapping in miRNAs was detected between BMSCs only and BMSCs-MDZ conditions.

Although the data presented here is obtained from in vitro experiments, it is indicative of the large differences in AC phenotype within cartilage tissue. What the data also suggest is that the signalling of superficial zone chondrocytes to surrounding cells in the knee joint might be an interesting avenue to explore with the aim of identifying novel mechanisms and targets for cartilage repair.

7.1.2 DACTs are found in human joints and regulate BMSC apoptosis and proliferation through the canonical Wnt pathway.

DACT1 was found to be expressed in the SZ of articular cartilage, which has been shown to host a subpopulation of chondrocyte progenitors that regulate tissue homeostasis and might be involved in cartilage repair and OA progression. It was shown here and by others that DACT1 is downregulated in OA. DACT1 and DACT2 are present at gene and protein level in adult human cartilage and synovium. DACT2 was identified in adult cartilage and during development, specifically in the Interzone, a region of condensed mesenchymal cells that give rise to the joint. Both proteins are also present in human SynMSCs and BMSCs. DACT1 knockdown in BMSCs induces apoptosis, as confirmed by the differential expression detected by transcriptomic analysis of genes involved in apoptosis. As DACT1 is almost exclusively expressed in the SZ and downregulated in OA, and its knockdown in MSCs results in cell death, it can be hypothesised that a loss of superficial chondrocytes is linked to OA development. When SZ cartilage loses its stable state, it would be expected that response to mechanical loading is altered resulting in cartilage and subchondral bone remodelling. Perhaps together with a concomitant inflammatory state of synovial tissue

and fluid, OA changes are initiated. miR-125b-5p is one of the miRNAs identified in EVs isolated from BMSCs alone and when cultured with SZ cartilage, which has been reported to have an inhibitory effect on DACT1 expression. miR-125b-5p downregulation of DACT1 resulted in inhibition of cell proliferation and promoted cell apoptosis (Yu, Yang, & Rui, 2019). Further studies to dissect the regulation of DACT1 expression could give valuable insight to OA development.

7.2 Conclusion

OA is a musculoskeletal disease that affects millions of people across the world and is a leading cause of disability, heavily affecting the quality of life and wellbeing. Understanding cartilage progenitors both in terms of how they are regulated and how they communicate with other cell types in the joint, is paramount to understand and develop novel therapies to treat early cartilage defects and so help slow or prevent the development of OA. The articular surface is home to cartilage progenitors. Elucidating the signalling between SZ cartilage and BMSCs would be beneficial to improve our drug/biomolecule treatment, cell therapy and surgical intervention for cartilage repair. This study shows how the interaction between BMSCs and SZ cartilage produces a specific cytokine response. The crosstalk between cartilage and BMSCs may also be based on signalling through EVs. In experiments presented here, EVs were found to have different miRNA profiles depending on whether BMSCs were cocultured alone or with SZ or MDZ cartilage. A list of differentially expressed EV-derived miRNA was identified and could be further investigated to understand how resident chondrocytes might interact to repair cartilage in MSC therapy. This thesis presents a novel study on a Wnt regulator, DACT1, in cartilage and MSCs. Collectively, the data suggest a role in apoptosis and senescence for DACT1 in BMSCs. Further study on DACT1 and its downregulation could help provide a possible link between senescence of SZ progenitors and OA development. Overexpression of DACT1 could potentially have a protective role in cartilage and should be considered as a target for therapeutic strategies.

8 References

Abreu, J. G., Ketpura, N. I., Reversade, B., & De Robertis, E. M. (2002). Connective-tissue growth factor (CTGF) modulates cell signalling by BMP and TGF-beta. *Nature Cell Biology*, *4*(8), 599–604. https://doi.org/10.1038/ncb826

Abreu, S. C., Weiss, D. J., & Rocco, P. R. M. (2016). Extracellular vesicles derived from mesenchymal stromal cells: a therapeutic option in respiratory diseases? *Stem Cell Research & Therapy*, *7*(1), 53. https://doi.org/10.1186/s13287-016-0317-0

Abuammah, A., Maimari, N., Towhidi, L., Frueh, J., Chooi, K. Y., Warboys, C., & Krams, R. (2018). New developments in mechanotransduction: Cross talk of the Wnt, TGF-β and Notch signalling pathways in reaction to shear stress. *Current Opinion in Biomedical Engineering*, *5*, 96–104. https://doi.org/10.1016/j.cobme.2018.03.003

Akhtar, N., & Haqqi, T. M. (2012). MicroRNA-199a* regulates the expression of cyclooxygenase-2 in human chondrocytes. *Annals of the Rheumatic Diseases*, *71*(6), 1073–1080. https://doi.org/10.1136/annrheumdis-2011-200519

Altuvia, Y., Landgraf, P., Lithwick, G., Elefant, N., Pfeffer, S., Aravin, A., … Margalit, H. (2005). Clustering and conservation patterns of human microRNAs. *Nucleic Acids Research*, *33*(8), 2697–2706. https://doi.org/10.1093/nar/gki567

Anderson, P. (2008). Post-transcriptional control of cytokine production. *Nature Immunology*, *9*(4), 353–359. https://doi.org/10.1038/ni1584

Aoyama, E., Hattori, T., Hoshijima, M., Araki, D., Nishida, T., Kubota, S.,

& Takigawa, M. (2009). N-terminal domains of CCN family 2/connective tissue growth factor bind to aggrecan. *The Biochemical Journal*, *420*(3), 413–420. https://doi.org/10.1042/BJ20081991

Archer, C. W., Dowthwaite, G. P., & Francis-west, P. (2003). *Development of Synovial Joints*. *155*(Part C), 144–155. https://doi.org/10.1002/bdrc.10015

Archer, D. (1999). *Biology of the synovial joint*.

Artavanis-Tsakonas, S., Rand, M. D., & Lake, R. J. (1999). Notch signaling: cell fate control and signal integration in development. *Science (New York, N.Y.)*, *284*(5415), 770–776. https://doi.org/10.1126/science.284.5415.770

Bach, F. C., Rutten, K., Hendriks, K., Riemers, F. M., Cornelissen, P., de Bruin, A., … Tryfonidou, M. A. (2014). The Paracrine Feedback Loop Between Vitamin D $_3$ (1,25(OH) $_2$ D $_3$) and PTHrP in Prehypertrophic Chondrocytes. *Journal of Cellular Physiology*, *229*(12), 1999–2014. https://doi.org/10.1002/jcp.24658

Becerra, J., Andrades, J. A., Guerado, E., Zamora-Navas, P., López-Puertas, J. M., & Reddi, A. H. (2010). Articular Cartilage: Structure and Regeneration. *Tissue Engineering Part B: Reviews*, *16*(6), 617–627. https://doi.org/10.1089/ten.teb.2010.0191

Brunt, L. H., Begg, K., Kague, E., Cross, S., & Hammond, C. L. (2017). Wnt signalling controls the response to mechanical loading during zebrafish joint development. *Development*. https://doi.org/10.1242/dev.153528

Bryja, V., Andersson, E. R., Schambony, A., Esner, M., Bryjová, L., Bins,

K. K., … Arenas, E. (2009). The extracellular domain of Lrp5/6 inhibits noncanonical Wnt signaling in vivo. *Molecular Biology of the Cell*, *20*(3), 924–936. https://doi.org/10.1091/mbc.E08-07-0711

Bult, C. J., Blake, J. A., Smith, C. L., Kadin, J. A., Richardson, J. E., Anagnostopoulos, A., … Zhu, Y. (2019). Mouse Genome Database (MGD) 2019. *Nucleic Acids Research*, *47*(D1), D801–D806. https://doi.org/10.1093/nar/gky1056

Burleigh, A., Chanalaris, A., Gardiner, M. D., Driscoll, C., Boruc, O., Saklatvala, J., & Vincent, T. L. (2012). Joint immobilization prevents murine osteoarthritis and reveals the highly mechanosensitive nature of protease expression in vivo. *Arthritis & Rheumatism*, *64*(7), 2278–2288. https://doi.org/10.1002/art.34420

Cantaluppi, V., Gatti, S., Medica, D., Figliolini, F., Bruno, S., Deregibus, M. C., … Camussi, G. (2012). Microvesicles derived from endothelial progenitor cells protect the kidney from ischemia–reperfusion injury by microRNA-dependent reprogramming of resident renal cells. *Kidney International*, *82*(4), 412–427. https://doi.org/10.1038/ki.2012.105

Carthew, R. W., & Sontheimer, E. J. (2009). Origins and Mechanisms of miRNAs and siRNAs. *Cell*, *136*(4), 642–655. https://doi.org/10.1016/j.cell.2009.01.035

Chan, S., Neu, C., DuRaine, G., … K. K.-O. and, & 2010, undefined. (n.d.). Atomic force microscope investigation of the boundary-lubricant layer in articular cartilage. *Elsevier*. Retrieved from https://www.sciencedirect.com/science/article/pii/S1063458410001123

Chavez, R. D., Sohn, P., & Serra, R. (2019). Prg4 prevents osteoarthritis

induced by dominant-negative interference of TGF-ß signaling in mice. *PLoS ONE*. https://doi.org/10.1371/journal.pone.0210601

Chen, L., Tredget, E. E., Wu, P. Y. G., & Wu, Y. (2008). Paracrine Factors of Mesenchymal Stem Cells Recruit Macrophages and Endothelial Lineage Cells and Enhance Wound Healing. *PLoS ONE*, *3*(4), e1886. https://doi.org/10.1371/journal.pone.0001886

Chen, Y., Xue, K., Zhang, X., Zheng, Z., & Liu, K. (2018). Exosomes derived from mature chondrocytes facilitate subcutaneous stable ectopic chondrogenesis of cartilage progenitor cells. *Stem Cell Research & Therapy*, *9*(1), 318. https://doi.org/10.1186/s13287-018-1047-2

Cheyette, B. N. R., Waxman, J. S., Miller, J. R., Takemaru, K.-I., Sheldahl, L. C., Khlebtsova, N., … Moon, R. T. (2002). Dapper, a Dishevelled-Associated Antagonist of β-Catenin and JNK Signaling, Is Required for Notochord Formation. *Developmental Cell*, *2*(4), 449–461. https://doi.org/10.1016/S1534-5807(02)00140-5

Chia, S.-L., Sawaji, Y., Burleigh, A., McLean, C., Inglis, J., Saklatvala, J., & Vincent, T. (2009). Fibroblast growth factor 2 is an intrinsic chondroprotective agent that suppresses ADAMTS-5 and delays cartilage degradation in murine osteoarthritis. *Arthritis and Rheumatism*, *60*(7), 2019–2027. https://doi.org/10.1002/art.24654

Chong, K.-W., Chanalaris, A., Burleigh, A., Jin, H., Watt, F. E., Saklatvala, J., & Vincent, T. L. (2013). Fibroblast Growth Factor 2 Drives Changes in Gene Expression Following Injury to Murine Cartilage In Vitro and In Vivo. *Arthritis & Rheumatism*, *65*(9), 2346–2355. https://doi.org/10.1002/art.38039

Chou, C.-H., Lee, M. T. M., Song, I.-W., Lu, L.-S., Shen, H.-C., Lee, C.-H., … Wu, C.-C. (2015). Insights into osteoarthritis progression revealed by analyses of both knee tibiofemoral compartments. *Osteoarthritis and Cartilage*, *23*(4), 571–580. https://doi.org/10.1016/j.joca.2014.12.020

Cleary, M. A., van Osch, G. J. V. M., Brama, P. A., Hellingman, C. A., & Narcisi, R. (2015). FGF, TGFβ and Wnt crosstalk: embryonic to in vitro cartilage development from mesenchymal stem cells. *Journal of Tissue Engineering and Regenerative Medicine*, *9*(4), 332–342. https://doi.org/10.1002/term.1744

Coates, E. E., & Fisher, J. P. (2014). Engineering superficial zone chondrocytes from mesenchymal stem cells. *Tissue Engineering. Part C, Methods*, *20*(8), 630–640. https://doi.org/10.1089/ten.TEC.2013.0224

Coumans, F. A. W., Brisson, A. R., Buzas, E. I., Dignat-George, F., Drees, E. E. E., El-Andaloussi, S., … Nieuwland, R. (2017). Methodological Guidelines to Study Extracellular Vesicles. *Circulation Research*, *120*(10), 1632–1648. https://doi.org/10.1161/CIRCRESAHA.117.309417

Coutinho de Almeida, R., Ramos, Y. F. M., Mahfouz, A., den Hollander, W., Lakenberg, N., Houtman, E., … Meulenbelt, I. (2019). RNA sequencing data integration reveals an miRNA interactome of osteoarthritis cartilage. *Annals of the Rheumatic Diseases*, *78*(2), 270–277. https://doi.org/10.1136/annrheumdis-2018-213882

Culemann, S., Grüneboom, A., Nicolás-Ávila, J. Á., Weidner, D., Lämmle, K. F., Rothe, T., … Krönke, G. (2019). Locally renewing resident

synovial macrophages provide a protective barrier for the joint. *Nature*. https://doi.org/10.1038/s41586-019-1471-1

Darling, E. M., Hu, J. C. Y., & Athanasiou, K. A. (2004). Zonal and topographical differences in articular cartilage gene expression. *Journal of Orthopaedic Research*, *22*(6), 1182–1187. https://doi.org/10.1016/j.orthres.2004.03.001

Davidson, R. K., Waters, J. G., Kevorkian, L., Darrah, C., Cooper, A., Donell, S. T., & Clark, I. M. (2006). Expression profiling of metalloproteinases and their inhibitors in synovium and cartilage. *Arthritis Research and Therapy*, *8*(4). https://doi.org/10.1186/ar2013

De Bari, C., & Roelofs, A. J. (2018). Stem cell-based therapeutic strategies for cartilage defects and osteoarthritis. *Current Opinion in Pharmacology*, *40*, 74–80. https://doi.org/10.1016/j.coph.2018.03.009

Decker, R. S., Koyama, E., & Pacifici, M. (2014). Genesis and morphogenesis of limb synovial joints and articular cartilage. *Matrix Biology : Journal of the International Society for Matrix Biology*, *39*, 5–10. https://doi.org/10.1016/j.matbio.2014.08.006

Decker, R. S., Um, H.-B., Dyment, N. A., Cottingham, N., Usami, Y., Enomoto-Iwamoto, M., … Pacifici, M. (2017). Cell origin, volume and arrangement are drivers of articular cartilage formation, morphogenesis and response to injury in mouse limbs. *Developmental Biology*, *426*(1), 56–68. https://doi.org/10.1016/j.ydbio.2017.04.006

Deng, Z. H., Li, Y. S., Gao, X., Lei, G. H., & Huard, J. (2018, September 1). Bone morphogenetic proteins for articular cartilage regeneration. *Osteoarthritis and Cartilage*, Vol. 26, pp. 1153–1161. https://doi.org/10.1016/j.joca.2018.03.007

Deshmukh, V., Seo, T., Swearingen, C. J., & Yazici, Y. (2018). SM04690, a WNT pathway inhibitor: anti-inflammatory and cartilage protective effects in preclinical osteoarthritis models. *Osteoarthritis and Cartilage*, *26*, S64. https://doi.org/10.1016/j.joca.2018.02.136

Desvignes, T., Batzel, P., Berezikov, E., Eilbeck, K., Eppig, J. T., McAndrews, M. S., … Postlethwait, J. H. (2015). miRNA Nomenclature: A View Incorporating Genetic Origins, Biosynthetic Pathways, and Sequence Variants. *Trends in Genetics : TIG*, *31*(11), 613–626. https://doi.org/10.1016/j.tig.2015.09.002

Ducy, P., & Karsenty, G. (2000). The family of bone morphogenetic proteins. *Kidney International*, *57*(6), 2207–2214. https://doi.org/10.1046/j.1523-1755.2000.00081.x

Estes, B. T., Wu, A. W., & Guilak, F. (2006). Potent induction of chondrocytic differentiation of human adipose-derived adult stem cells by bone morphogenetic protein 6. *Arthritis and Rheumatism*, *54*(4), 1222–1232. https://doi.org/10.1002/art.21779

Estrach, S., Ambler, C. A., Lo Celso, C., Hozumi, K., & Watt, F. M. (2006). Jagged 1 is a β-catenin target gene required for ectopic hair follicle formation in adult epidermis. *Development*, *133*(22), 4427–4438. https://doi.org/10.1242/dev.02644

Fang, F., Chang, R., Yu, L., Lei, X., Xiao, S., Yang, H., & Yang, L.-Y. (2015). MicroRNA-188-5p suppresses tumor cell proliferation and metastasis by directly targeting FGF5 in hepatocellular carcinoma. *Journal of Hepatology*, *63*(4), 874–885. https://doi.org/10.1016/J.JHEP.2015.05.008

Fischer, J., Ortel, M., Hagmann, S., Hoeflich, A., & Richter, W. (2016).

Role of PTHrP(1-34) Pulse Frequency Versus Pulse Duration to Enhance Mesenchymal Stromal Cell Chondrogenesis. *Journal of Cellular Physiology*, *231*(12), 2673–2681. https://doi.org/10.1002/jcp.25369

Fisher, D. A., Kivimäe, S., Hoshino, J., Suriben, R., Martin, P.-M., Baxter, N., & Cheyette, B. N. R. (2006). Three Dact gene family members are expressed during embryonic development and in the adult brains of mice. *Developmental Dynamics*, *235*(9), 2620–2630. https://doi.org/10.1002/dvdy.20917

Flandry, F., & Hommel, G. (2011). Normal anatomy and biomechanics of the knee. *Sports Medicine and Arthroscopy Review*, *19*(2), 82–92. https://doi.org/10.1097/JSA.0b013e318210c0aa

Fortini, M. E. (2009). Notch signaling: the core pathway and its posttranslational regulation. *Developmental Cell*, *16*(5), 633–647. https://doi.org/10.1016/j.devcel.2009.03.010

Fujita, N., Matsushita, T., Ishida, K., Kubo, S., Matsumoto, T., Takayama, K., … Kuroda, R. (2011). Potential involvement of SIRT1 in the pathogenesis of osteoarthritis through the modulation of chondrocyte gene expressions. *Journal of Orthopaedic Research : Official Publication of the Orthopaedic Research Society*, *29*(4), 511–515. https://doi.org/10.1002/jor.21284

Fukui, N., Miyamoto, Y., Nakajima, M., Ikeda, Y., Hikita, A., Furukawa, H., … Ikegawa, S. (2008). Zonal gene expression of chondrocytes in osteoarthritic cartilage. *Arthritis & Rheumatism*, *58*(12), 3843–3853. https://doi.org/10.1002/art.24036

Gao, L., Guo, Q., Li, X., Yang, X., Ni, H., Wang, T., … Zheng, L. (2019).

MiR-873/PD-L1 axis regulates the stemness of breast cancer cells. *EBioMedicine*, *41*, 395–407. https://doi.org/10.1016/j.ebiom.2019.02.034

Gao, X., Wen, J., Zhang, L., Li, X., Ning, Y., Meng, A., & Chen, Y.-G. (2008). Dapper1 is a nucleocytoplasmic shuttling protein that negatively modulates Wnt signaling in the nucleus. *The Journal of Biological Chemistry*, *283*(51), 35679–35688. https://doi.org/10.1074/jbc.M804088200

Ge, F. X., Li, H., & Yin, X. (2017). Upregulation of microRNA-125b-5p is involved in the pathogenesis of osteoarthritis by downregulating SYVN1. *Oncology Reports*. https://doi.org/10.3892/or.2017.5475

Georgi, N., Taipaleenmaki, H., Raiss, C. C., Groen, N., Portalska, K. J., van Blitterswijk, C., … Karperien, M. (2015). MicroRNA Levels as Prognostic Markers for the Differentiation Potential of Human Mesenchymal Stromal Cell Donors. *Stem Cells and Development*. https://doi.org/10.1089/scd.2014.0534

Griffiths-Jones, S., Saini, H. K., van Dongen, S., & Enright, A. J. (2007). miRBase: tools for microRNA genomics. *Nucleic Acids Research*, *36*(Database), D154–D158. https://doi.org/10.1093/nar/gkm952

Guo, Xing, Ramirez, A., Waddell, D. S., Li, Z., Liu, X., & Wang, X.-F. (2008). Axin and GSK3- control Smad3 protein stability and modulate TGF- signaling. *Genes & Development*, *22*(1), 106–120. https://doi.org/10.1101/gad.1590908

Guo, Xizhi, Day, T. F., Jiang, X., Garrett-Beal, L., Topol, L., & Yang, Y. (2004). Wnt/β-catenin signaling is sufficient and necessary for synovial joint formation. *Genes and Development*, *18*(19), 2404–2417.

https://doi.org/10.1101/gad.1230704

Hacker, G. (2000). The morphology of apoptosis. Cell Tissue Res. *Cell Tissue Res*, *301*, 5–17. https://doi.org/10.1007/s004410000193

Hamam, D., Ali, D., Vishnubalaji, R., Hamam, R., Al-Nbaheen, M., Chen, L., … Alajez, N. M. (2014). MicroRNA-320/RUNX2 axis regulates adipocytic differentiation of human mesenchymal (skeletal) stem cells. *Cell Death and Disease*. https://doi.org/10.1038/cddis.2014.462

Harris, Q., Seto, J., O'Brien, K., Lee, P. S., Kondo, C., Heard, B. J., … Krawetz, R. J. (2013). Monocyte chemotactic protein-1 inhibits chondrogenesis of synovial mesenchymal progenitor cells: An in vitro study. *Stem Cells*, *31*(10), 2253–2265. https://doi.org/10.1002/stem.1477

Hartmann, C., & Tabin, C. J. (2001). Wnt-14 plays a pivotal role in inducing synovial joint formation in the developing appendicular skeleton. *Cell*, *104*(3), 341–351. https://doi.org/10.1016/S0092-8674(01)00222-7

Haseeb, A., & Haqqi, T. M. (2013). Immunopathogenesis of osteoarthritis. *Clinical Immunology*, *146*(3), 185–196. https://doi.org/10.1016/j.clim.2012.12.011

He, Y., Meng, C., Shao, Z., Wang, H., & Yang, S. (2014). MiR-23a functions as a tumor suppressor in osteosarcoma. *Cellular Physiology and Biochemistry*, *34*(5), 1485–1496. https://doi.org/10.1159/000366353

Hellio Le Graverand, M. P., Sciore, P., Eggerer, J., Rattner, J. P., Vignon, E., Barclay, L., … Rattner, J. B. (2001). Formation and phenotype of cell clusters in osteoarthritic meniscus. *Arthritis and Rheumatism*,

44(8), 1808–1818. https://doi.org/10.1002/1529-0131(200108)44:8<1808::AID-ART318>3.0.CO;2-B

Henry, J. C., Park, J.-K., Jiang, J., Kim, J. H., Nagorney, D. M., Roberts, L. R., … Schmittgen, T. D. (2010). miR-199a-3p targets CD44 and reduces proliferation of CD44 positive hepatocellular carcinoma cell lines. *Biochemical and Biophysical Research Communications*, *403*(1), 120–125. https://doi.org/10.1016/j.bbrc.2010.10.130

Holder, N. (1977). An experimental investigation into the early development of the chick elbow joint. In *Embryol. exp. Morph* (Vol. 39).

Horiguchi, H., Kobune, M., Kikuchi, S., Yoshida, M., Murata, M., Murase, K., … Kato, J. (2016). Extracellular vesicle miR-7977 is involved in hematopoietic dysfunction of mesenchymal stromal cells via poly(rC) binding protein 1 reduction in myeloid neoplasms. *Haematologica*. https://doi.org/10.3324/haematol.2015.134932

Hoshiyama, Y., Otsuki, S., Oda, S., Kurokawa, Y., Nakajima, M., Jotoku, T., … Neo, M. (2015). Chondrocyte clusters adjacent to sites of cartilage degeneration have characteristics of progenitor cells. *Journal of Orthopaedic Research : Official Publication of the Orthopaedic Research Society*, *33*(4), 548–555. https://doi.org/10.1002/jor.22782

Hosogane, N., Huang, Z., Rawlins, B. A., Liu, X., Boachie-Adjei, O., Boskey, A. L., & Zhu, W. (2010). Stromal derived factor-1 regulates bone morphogenetic protein 2-induced osteogenic differentiation of primary mesenchymal stem cells. *International Journal of Biochemistry and Cell Biology*, *42*(7), 1132–1141. https://doi.org/10.1016/j.biocel.2010.03.020

Hou, H., Gao, F., Liang, H., Lv, Y., Li, M., Yao, L., … Wang, Y. (2018).

MicroRNA-188-5p regulates contribution of bone marrow-derived cells to choroidal neovascularization development by targeting MMP-2/13. *Experimental Eye Research*, *175*, 115–123. https://doi.org/10.1016/J.EXER.2018.06.010

Howell, G. R., Shindo, M., Murray, S., Gridley, T., Wilson, L. A., & Schimenti, J. C. (2007). Mutation of a ubiquitously expressed mouse transmembrane protein (Tapt1) causes specific skeletal homeotic transformations. *Genetics*, *175*(2), 699–707. https://doi.org/10.1534/genetics.106.065177

Hu, J., Zhai, C., Hu, J., Li, Z., Fei, H., Wang, Z., & Fan, W. (2017). MiR-23a inhibited IL-17-mediated proinflammatory mediators expression via targeting IKKα in articular chondrocytes. *International Immunopharmacology*, *43*, 1–6. https://doi.org/10.1016/j.intimp.2016.11.031

Huang, H., Veien, E. S., Zhang, H., Ayers, D. C., & Song, J. (2016). Skeletal Characterization of Smurf2-Deficient Mice and In Vitro Analysis of Smurf2-Deficient Chondrocytes. *PloS One*, *11*(1), e0148088. https://doi.org/10.1371/journal.pone.0148088

Huang, X., Zhong, L., Post, J. N., & Karperien, M. (2018). Co-treatment of TGF-β3 and BMP7 is superior in stimulating chondrocyte redifferentiation in both hypoxia and normoxia compared to single treatments. *Scientific Reports*, *8*(1). https://doi.org/10.1038/s41598-018-27602-y

Im, G.-I., & Quan, Z. (2010). The effects of Wnt inhibitors on the chondrogenesis of human mesenchymal stem cells. *Tissue Engineering. Part A*, *16*(7), 2405–2413.

https://doi.org/10.1089/ten.TEA.2009.0359

Im, H.-J., Muddasani, P., Natarajan, V., Schmid, T. M., Block, J. A., Davis, F., … Loeser, R. F. (2007). Basic fibroblast growth factor stimulates matrix metalloproteinase-13 via the molecular cross-talk between the mitogen-activated protein kinases and protein kinase Cdelta pathways in human adult articular chondrocytes. *The Journal of Biological Chemistry*, *282*(15), 11110–11121. https://doi.org/10.1074/jbc.M609040200

Imhof, H., Sulzbacher, I., Grampp, S., Czerny, C., Youssefzadeh, S., & Kainberger, F. (2000). Subchondral bone and cartilage disease: a rediscovered functional unit. *Investigative Radiology*, *35*(10), 581–588. Retrieved from http://www.ncbi.nlm.nih.gov/pubmed/11041152

Itoh, F., Asao, H., Sugamura, K., Heldin, C. H., ten Dijke, P., & Itoh, S. (2001). Promoting bone morphogenetic protein signaling through negative regulation of inhibitory Smads. *The EMBO Journal*, *20*(15), 4132–4142. https://doi.org/10.1093/emboj/20.15.4132

Ivkovic, S., Yoon, B. S., Popoff, S. N., Safadi, F. F., Libuda, D. E., Stephenson, R. C., … Lyons, K. M. (2003). Connective tissue growth factor coordinates chondrogenesis and angiogenesis during skeletal development. *Development (Cambridge, England)*, *130*(12), 2779–2791. https://doi.org/10.1242/dev.00505

Iwasaki, H., Takeuchi, O., Teraguchi, S., Matsushita, K., Uehata, T., Kuniyoshi, K., … Akira, S. (2011). The IκB kinase complex regulates the stability of cytokine-encoding mRNA induced by TLR-IL-1R by controlling degradation of regnase-1. *Nature Immunology*, *12*(12), 1167–1175. https://doi.org/10.1038/ni.2137

Järvinen, E., Shimomura-Kuroki, J., Balic, A., Jussila, M., & Thesleff, I. (2018). Mesenchymal Wnt/β-catenin signaling limits tooth number. *Development (Cambridge)*, *145*(4). https://doi.org/10.1242/dev.158048

Jay, G. D., Tantravahi, U., Britt, D. E., Barrach, H. J., & Cha, C. J. (2001). Homology of lubricin and superficial zone protein (SZP): Products of megakaryocyte stimulating factor (MSF) gene expression by human synovial fibroblasts and articular chondrocytes localized to chromosome 1q25. *Journal of Orthopaedic Research*, *19*(4), 677–687. https://doi.org/10.1016/S0736-0266(00)00040-1

Jay, G., rheumatology, C. C.-T. J. of, & 1999, undefined. (n.d.). The effect of phospholipase digestion upon the boundary lubricating ability of synovial fluid. *Europepmc.Org*. Retrieved from https://europepmc.org/abstract/med/10555909

Jayasuriya, C. T., Hu, N., Li, J., Lemme, N., Terek, R., Ehrlich, M. G., & Chen, Q. (2018). Molecular characterization of mesenchymal stem cells in human osteoarthritis cartilage reveals contribution to the OA phenotype. *Scientific Reports*, *8*(1). https://doi.org/10.1038/s41598-018-25395-8

Ji, H., Chen, M., Greening, D. W., He, W., Rai, A., Zhang, W., & Simpson, R. J. (2014). Deep sequencing of RNA from three different extracellular vesicle (EV) subtypes released from the human LIM1863 colon cancer cell line uncovers distinct mirna-enrichment signatures. *PLoS ONE*. https://doi.org/10.1371/journal.pone.0110314

Jia, J., Wang, J., Zhang, J., Cui, M., Sun, X., Li, Q., & Zhao, B. (2018). MiR-125b Inhibits LPS-Induced Inflammatory Injury via Targeting MIP-

1α in Chondrogenic Cell ATDC5. *Cellular Physiology and Biochemistry*. https://doi.org/10.1159/000488178

Jiang, X., Tan, J., Li, J., Kivimäe, S., Yang, X., Zhuang, L., … Yu, Q. (2008). DACT3 Is an Epigenetic Regulator of Wnt/β-Catenin Signaling in Colorectal Cancer and Is a Therapeutic Target of Histone Modifications. *Cancer Cell*, *13*(6), 529–541. https://doi.org/10.1016/j.ccr.2008.04.019

Jin, E.-J., Lee, S.-Y., Choi, Y.-A., Jung, J.-C., Bang, O.-S., & Kang, S.-S. (2006). BMP-2-enhanced chondrogenesis involves p38 MAPK-mediated down-regulation of Wnt-7a pathway. *Molecules and Cells*, *22*(3), 353–359. Retrieved from http://www.ncbi.nlm.nih.gov/pubmed/17202865

Johnstone, B., Hering, T. M., Caplan, A. I., Goldberg, V. M., & Yoo, J. U. (1998). In vitro chondrogenesis of bone marrow-derived mesenchymal progenitor cells. *Experimental Cell Research*, *238*(1), 265–272. https://doi.org/10.1006/excr.1997.3858

Kafienah, W., Mistry, S., Dickinson, S. C., Sims, T. J., Learmonth, I., & Hollander, A. P. (2007). Three-dimensional cartilage tissue engineering using adult stem cells from osteoarthritis patients. *Arthritis & Rheumatism*, *56*(1), 177–187. https://doi.org/10.1002/art.22285

Kanbe, K., Takagishi, K., & Chen, Q. (2002). Stimulation of matrix metalloprotease 3 release from human chondrocytes by the interaction of stromal cell-derived factor 1 and CXC chemokine receptor 4. *Arthritis and Rheumatism*, *46*(1), 130–137. Retrieved from http://www.ncbi.nlm.nih.gov/pubmed/11817585

Kang, L., Yang, C., Song, Y., Liu, W., Wang, K., Li, S., & Zhang, Y. (2016).

MicroRNA-23a-3p promotes the development of osteoarthritis by directly targeting SMAD3 in chondrocytes. *Biochemical and Biophysical Research Communications*, *478*(1), 467–473. Retrieved from https://www.sciencedirect.com/science/article/pii/S0006291X16309895?via%3Dihub

Kida, Y., & Goligorsky, M. S. (2016). Sirtuins, Cell Senescence, and Vascular Aging. *The Canadian Journal of Cardiology*, *32*(5), 634–641. https://doi.org/10.1016/j.cjca.2015.11.022

Kim, G. W., Han, M. S., Park, H. R., Lee, E. J., Jung, Y. K., Usmani, S. E., … Beier, F. (2015). CXC chemokine ligand 12a enhances chondrocyte proliferation and maturation during endochondral bone formation. *Osteoarthritis and Cartilage*, *23*(6), 966–974. https://doi.org/10.1016/j.joca.2015.01.016

Kim, Y.-K., Yu, J., Han, T. S., Park, S.-Y., Namkoong, B., Kim, D. H., … Kim, V. N. (2009). Functional links between clustered microRNAs: suppression of cell-cycle inhibitors by microRNA clusters in gastric cancer. *Nucleic Acids Research*, *37*(5), 1672–1681. https://doi.org/10.1093/nar/gkp002

Knutsen, G., Drogset, J. O., Engebretsen, L., Grøntvedt, T., Isaksen, V., Ludvigsen, T. C., … Johansen, O. (2007). A randomized trial comparing autologous chondrocyte implantation with microfracture: Findings at five years. *Journal of Bone and Joint Surgery - Series A*, *89*(10), 2105–2112. https://doi.org/10.2106/JBJS.G.00003

Knutsen, G., Drogset, J. O., Engebretsen, L., Grontvedt, T., Ludvigsen, T. C., Loken, S., … Johansen, O. (2016). A randomized multicenter trial

comparing autologous chondrocyte implantation with microfracture: Long-Term Follow-up at 14 to 15 Years. *Journal of Bone and Joint Surgery - American Volume*, Vol. 98, pp. 1332–1339. https://doi.org/10.2106/JBJS.15.01208

Kovermann, N. J., Basoli, V., Della Bella, E., Alini, M., Lischer, C., Schmal, H., … Stoddart, M. J. (2019). BMP2 and TGF-β Cooperate Differently during Synovial-Derived Stem-Cell Chondrogenesis in a Dexamethasone-Dependent Manner. *Cells*, *8*(6). https://doi.org/10.3390/cells8060636

Kowanetz, M., Valcourt, U., Bergström, R., Heldin, C.-H., & Moustakas, A. (2004). Id2 and Id3 define the potency of cell proliferation and differentiation responses to transforming growth factor beta and bone morphogenetic protein. *Molecular and Cellular Biology*, *24*(10), 4241–4254. https://doi.org/10.1128/mcb.24.10.4241-4254.2004

Koyama, E., Ochiai, T., Rountree, R. B., Kingsley, D. M., Enomoto-Iwamoto, M., Iwamoto, M., & Pacifici, M. (2007). Synovial joint formation during mouse limb skeletogenesis: Roles of Indian hedgehog signaling. *Annals of the New York Academy of Sciences*, *1116*, 100–112. https://doi.org/10.1196/annals.1402.063

Koyama, E., Shibukawa, Y., Nagayama, M., Sugito, H., Young, B., Yuasa, T., … Pacifici, M. (2008). A distinct cohort of progenitor cells participates in synovial joint and articular cartilage formation during mouse limb skeletogenesis. *Developmental Biology*, *316*(1), 62–73. https://doi.org/10.1016/j.ydbio.2008.01.012

Kozhemyakina, E., Zhang, M., Ionescu, A., Ayturk, U. M., Ono, N., Kobayashi, A., … Lassar, A. B. (2015). Identification of a *Prg4* -

Expressing Articular Cartilage Progenitor Cell Population in Mice. *Arthritis & Rheumatology*, *67*(5), 1261–1273. https://doi.org/10.1002/art.39030

Kronenberg, H. M. (2003, May 15). Developmental regulation of the growth plate. *Nature*, Vol. 423, pp. 332–336. https://doi.org/10.1038/nature01657

Kudo, S., Mizuta, H., Takagi, K., & Hiraki, Y. (2011). Cartilaginous repair of full-thickness articular cartilage defects is induced by the intermittent activation of PTH/PTHrP signaling. *Osteoarthritis and Cartilage*, *19*(7), 886–894. https://doi.org/10.1016/j.joca.2011.04.007

Kuo, A. C., Rodrigo, J. J., Reddi, A. H., Curtiss, S., Grotkopp, E., & Chiu, M. (2006). Microfracture and bone morphogenetic protein 7 (BMP-7) synergistically stimulate articular cartilage repair. *Osteoarthritis and Cartilage*, *14*(11), 1126–1135. https://doi.org/10.1016/j.joca.2006.04.004

Lanske, B., Karaplis, A. C., Lee, K., Luz, A., Vortkamp, A., Pirro, A., … Kronenberg, H. M. (1996, August 2). PTH/PTHrP receptor in early development and Indian hedgehog-regulated bone growth. *Science*, Vol. 273, pp. 663–666. https://doi.org/10.1126/science.273.5275.663

Lee, G. M., Paul, T. A., Slabaugh, M., & Kelley, S. S. (2000). The incidence of enlarged chondrons in normal and osteoarthritic human cartilage and their relative matrix density. *Osteoarthritis and Cartilage / OARS, Osteoarthritis Research Society*, *8*(1), 44–52. https://doi.org/10.1053/joca.1999.0269

Li, C.-W., Lee, Y.-L., & Chen, B.-S. (2016). Genetic-and-Epigenetic Interspecies Networks for Cross-Talk Mechanisms in Human

Macrophages and Dendritic Cells during MTB Infection. *Frontiers in Cellular and Infection Microbiology*. https://doi.org/10.3389/fcimb.2016.00124

Li, L., Newton, P. T., Bouderlique, T., Sejnohova, M., Zikmund, T., Kozhemyakina, E., … Chagin, A. S. (2017). Superficial cells are self-renewing chondrocyte progenitors, which form the articular cartilage in juvenile mice. *FASEB Journal : Official Publication of the Federation of American Societies for Experimental Biology*, *31*(3), 1067–1084. https://doi.org/10.1096/fj.201600918R

Li, W., Cai, L., Zhang, Y., Cui, L., & Shen, G. (2015). Intra-articular resveratrol injection prevents osteoarthritis progression in a mouse model by activating SIRT1 and thereby silencing HIF-2α. *Journal of Orthopaedic Research : Official Publication of the Orthopaedic Research Society*, *33*(7), 1061–1070. https://doi.org/10.1002/jor.22859

Li, X., Stevens, P. D., Yang, H., Gulhati, P., Wang, W., Evers, B. M., & Gao, T. (2013). The deubiquitination enzyme USP46 functions as a tumor suppressor by controlling PHLPP-dependent attenuation of Akt signaling in colon cancer. *Oncogene*, *32*(4), 471–478. https://doi.org/10.1038/onc.2012.66

Li, Xiaofeng, Zhang, Y., Kang, H., Liu, W., Liu, P., Zhang, J., … Wu, D. (2005). Sclerostin binds to LRP5/6 and antagonizes canonical Wnt signaling. *The Journal of Biological Chemistry*, *280*(20), 19883–19887. https://doi.org/10.1074/jbc.M413274200

Li, Xin, Ellman, M. B., Kroin, J. S., Chen, D., Yan, D., Mikecz, K., … Im, H.-J. (2012). Species-specific biological effects of FGF-2 in articular

cartilage: implication for distinct roles within the FGF receptor family. *Journal of Cellular Biochemistry*, *113*(7), 2532–2542. https://doi.org/10.1002/jcb.24129

Li, Y.-H, Tavallaee, G., Tokar, T., Nakamura, A., Sundararajan, K., Weston, A., … Kapoor, M. (2016). *Identification of synovial fluid microRNA signature in knee osteoarthritis: differentiating early- and late-stage knee osteoarthritis*. https://doi.org/10.1016/j.joca.2016.04.019

Li, Yu-Hui, Zhong, M., Zang, H.-L., & Tian, X.-F. (2018). The E3 ligase for metastasis associated 1 protein, TRIM25, is targeted by microRNA-873 in hepatocellular carcinoma. *Experimental Cell Research*, *368*(1), 37–41. https://doi.org/10.1016/j.yexcr.2018.04.010

Liang, Y., Zhang, P., Li, S., Li, H., Song, S., & Lu, B. (2018). MicroRNA-873 acts as a tumor suppressor in esophageal cancer by inhibiting differentiated embryonic chondrocyte expressed gene 2. *Biomedicine and Pharmacotherapy*. https://doi.org/10.1016/j.biopha.2018.05.152

Lin, E. A., Kong, L., Bai, X.-H., Luan, Y., & Liu, C. (2009). miR-199a * , a Bone Morphogenic Protein 2-responsive MicroRNA, Regulates Chondrogenesis via Direct Targeting to Smad1. *Journal of Biological Chemistry*, *284*(17), 11326–11335. https://doi.org/10.1074/jbc.M807709200

Lin, Z., McClure, M. J., Zhao, J., Ramey, A. N., Asmussen, N., Hyzy, S. L., … Boyan, B. D. (2018). MicroRNA Contents in Matrix Vesicles Produced by Growth Plate Chondrocytes are Cell Maturation Dependent. *Scientific Reports*. https://doi.org/10.1038/s41598-018-21517-4

Liu, T., Zhang, Q., Zhang, J., Li, C., Miao, Y.-R., Lei, Q., … Guo, A.-Y. (2019). EVmiRNA: a database of miRNA profiling in extracellular vesicles. *Nucleic Acids Research*, *47*(D1), D89–D93. https://doi.org/10.1093/nar/gky985

Liu, X., Duan, B., Cheng, Z., Jia, X., Mao, L., Fu, H., … Kong, D. (2011). SDF-1/CXCR4 axis modulates bone marrow mesenchymal stem cell apoptosis, migration and cytokine secretion. *Protein and Cell*, *2*(10), 845–854. https://doi.org/10.1007/s13238-011-1097-z

Liu, Y., Liu, D.-L., Dong, L.-L., Wen, D., Shi, D.-M., Zhou, J., … Wu, W.-Z. (2016). miR-612 suppresses stem cell-like property of hepatocellular carcinoma cells by modulating Sp1/Nanog signaling. *Cell Death & Disease*, *7*(9), e2377. https://doi.org/10.1038/cddis.2016.282

Loeser, R. F., Chubinskaya, S., Pacione, C., & Im, H.-J. (2005). Basic fibroblast growth factor inhibits the anabolic activity of insulin-like growth factor 1 and osteogenic protein 1 in adult human articular chondrocytes. *Arthritis and Rheumatism*, *52*(12), 3910–3917. https://doi.org/10.1002/art.21472

Loeser, R. F., & Shanker, G. (2000). Autocrine stimulation by insulin-like growth factor 1 and insulin-like growth factor 2 mediates chondrocyte survival in vitro. *Arthritis and Rheumatism*, *43*(7), 1552–1559. https://doi.org/10.1002/1529-0131(200007)43:7<1552::AID-ANR20>3.0.CO;2-W

Lolli, A., Narcisi, R., Lambertini, E., Penolazzi, L., Angelozzi, M., Kops, N., … Piva, R. (2016). Silencing of Antichondrogenic MicroRNA-221 in Human Mesenchymal Stem Cells Promotes Cartilage Repair In Vivo. *Stem Cells (Dayton, Ohio)*, *34*(7), 1801–1811.

https://doi.org/10.1002/stem.2350

Longobardi, L, Jordan, J. M., Shi, X. A., Renner, J. B., Schwartz, T. A., Nelson, A. E., … Spagnoli, A. (2018). Associations between the chemokine biomarker CCL2 and knee osteoarthritis outcomes: the Johnston County Osteoarthritis Project. *Osteoarthritis and Cartilage*, *26*(9), 1257–1261. https://doi.org/10.1016/j.joca.2018.04.012

Longobardi, Lara, O'Rear, L., Aakula, S., Johnstone, B., Shimer, K., Chytil, A., … Spagnoli, A. (2006). Effect of IGF-I in the chondrogenesis of bone marrow mesenchymal stem cells in the presence or absence of TGF-β signaling. *Journal of Bone and Mineral Research*, *21*(4), 626–636. https://doi.org/10.1359/jbmr.051213

Lotz, M. K., Otsuki, S., Grogan, S. P., Sah, R., Terkeltaub, R., & D'Lima, D. (2010). Cartilage cell clusters. *Arthritis and Rheumatism*, *62*(8), 2206–2218. https://doi.org/10.1002/art.27528

Loughlin, J., Dowling, B., Chapman, K., Marcelline, L., Mustafa, Z., Southam, L., … Corr, M. (2004). Functional variants within the secreted frizzled-related protein 3 gene are associated with hip osteoarthritis in females. *Proceedings of the National Academy of Sciences*, *101*(26), 9757–9762. https://doi.org/10.1073/pnas.0403456101

Lu, W., Shi, J., Zhang, J., Lv, Z., Guo, F., Huang, H., … Chen, A. (2016). CXCL12/CXCR4 Axis Regulates Aggrecanase Activation and Cartilage Degradation in a Post-Traumatic Osteoarthritis Rat Model. *International Journal of Molecular Sciences*, *17*(10). https://doi.org/10.3390/ijms17101522

Lv, L.-L., Wu, W.-J., Feng, Y., Li, Z.-L., Tang, T.-T., & Liu, B.-C. (2017).

Therapeutic application of extracellular vesicles in kidney disease: promises and challenges. *Journal of Cellular and Molecular Medicine*, *22*(2), 728–737. https://doi.org/10.1111/jcmm.13407

Madry, H., Rey-Rico, A., Venkatesan, J. K., Johnstone, B., & Cucchiarini, M. (2014). Transforming growth factor beta-releasing scaffolds for cartilage tissue engineering. *Tissue Engineering - Part B: Reviews*, *20*(2), 106–125. https://doi.org/10.1089/ten.teb.2013.0271

Makki, M. S., & Haqqi, T. M. (2015). miR-139 modulates MCPIP1/IL-6 expression and induces apoptosis in human OA chondrocytes. *Experimental and Molecular Medicine*, *47*(10), e189–e189. https://doi.org/10.1038/emm.2015.66

Martin, J. A., & Buckwalter, J. A. (2000). The role of chondrocyte-matrix interactions in maintaining and repairing articular cartilage. *Biorheology*, *37*(1–2), 129–140. Retrieved from http://www.ncbi.nlm.nih.gov/pubmed/10912185

Martin, P. (1990). Tissue patterning In the. *Signs*, *1*(3), 323–336. Retrieved from http://www.ijdb.ehu.es/web/pdfdownload.php?doi=1702679

Martinez-Sanchez, A., & Murphy, C. L. (2013). *miR-1247 targets cartilage master regulator SOX9 MiR-1247 functions by targeting cartilage transcription factor SOX9**. https://doi.org/10.1074/jbc.M113.496729

Mastrogiacomo, M., Cancedda, R., & Quarto, R. (2001). Effect of different growth factors on the chondrogenic potential of human bone marrow stromal cells. *Osteoarthritis and Cartilage*, *9 Suppl A*, S36-40. Retrieved from http://www.ncbi.nlm.nih.gov/pubmed/11680686

Matsukawa, T., Sakai, T., Yonezawa, T., Hiraiwa, H., Hamada, T., Nakashima, M., … Ishiguro, N. (2013). MicroRNA-125b regulates the expression of aggrecanase-1 (ADAMTS-4) in human osteoarthritic chondrocytes. *Arthritis Research and Therapy*. https://doi.org/10.1186/ar4164

Matsuzaki, T., Matsushita, T., Takayama, K., Matsumoto, T., Nishida, K., Kuroda, R., & Kurosaka, M. (2014). Disruption of Sirt1 in chondrocytes causes accelerated progression of osteoarthritis under mechanical stress and during ageing in mice. *Annals of the Rheumatic Diseases*, *73*(7), 1397–1404. https://doi.org/10.1136/annrheumdis-2012-202620

Meng, F., Zhang, Z., Chen, W., Huang, G., He, A., Hou, C., … Liao, W. (2016). MicroRNA-320 regulates matrix metalloproteinase-13 expression in chondrogenesis and interleukin-1β-induced chondrocyte responses. *Osteoarthritis and Cartilage*. https://doi.org/10.1016/j.joca.2015.12.012

Mitrovic, D. (1978). Development of the diarthrodial joints in the rat embryo. *American Journal of Anatomy*, *151*(4), 475–485. https://doi.org/10.1002/aja.1001510403

Miyaki, K., Murakami, K., Segami, N., & Iizuka, T. (1994). Histological and immunohistochemical studies on the articular cartilage after experimental discectomy of the temporomandibular joint in rabbits. *Journal of Oral Rehabilitation*, *21*(3), 299–310. https://doi.org/10.1111/j.1365-2842.1994.tb01145.x

Moore, E. E., Bendele, A. M., Thompson, D. L., Littau, A., Waggie, K. S., Reardon, B., & Ellsworth, J. L. (2005). Fibroblast growth factor-18 stimulates chondrogenesis and cartilage repair in a rat model of injury-

induced osteoarthritis. *Osteoarthritis and Cartilage*, *13*(7), 623–631. https://doi.org/10.1016/j.joca.2005.03.003

Mori, Y., Chung, U.-I., Tanaka, S., & Saito, T. (2014). Determination of differential gene expression profiles in superficial and deeper zones of mature rat articular cartilage using RNA sequencing of laser microdissected tissue specimens. *Biomedical Research (Tokyo, Japan)*, *35*(4), 263–270. Retrieved from http://www.ncbi.nlm.nih.gov/pubmed/25152035

Muddasani, P., Norman, J. C., Ellman, M., van Wijnen, A. J., & Im, H.-J. (2007). Basic fibroblast growth factor activates the MAPK and NFkappaB pathways that converge on Elk-1 to control production of matrix metalloproteinase-13 by human adult articular chondrocytes. *The Journal of Biological Chemistry*, *282*(43), 31409–31421. https://doi.org/10.1074/jbc.M706508200

Naka, T., Nishimoto, N., & Kishimoto, T. (2002). The paradigm of IL-6: from basic science to medicine. *Arthritis Research*, *4*(Suppl 3), S233. https://doi.org/10.1186/ar565

Nakamura, A., Rampersaud, Y. R., Sharma, A., Lewis, S. J., Wu, B., Datta, P., … Kapoor, M. (2016). Identification of microRNA-181a-5p and microRNA-4454 as mediators of facet cartilage degeneration. *JCI Insight*, *1*(12), e86820. https://doi.org/10.1172/jci.insight.86820

Nakamura, Y., Miyaki, S., Ishitobi, H., Matsuyama, S., Nakasa, T., Kamei, N., … Ochi, M. (2015). Mesenchymal-stem-cell-derived exosomes accelerate skeletal muscle regeneration. *FEBS Letters*, *589*(11), 1257–1265. https://doi.org/10.1016/J.FEBSLET.2015.03.031

Nakashima, A., Katagiri, T., & Tamura, M. (2005). Cross-talk between Wnt

and bone morphogenetic protein 2 (BMP-2) signaling in differentiation pathway of C2C12 myoblasts. *Journal of Biological Chemistry*, *280*(45), 37660–37668. https://doi.org/10.1074/jbc.M504612200

Narcisi, R., Cleary, M. A., Brama, P. A. J., Hoogduijn, M. J., Tüysüz, N., ten Berge, D., & van Osch, G. J. V. M. (2015). Long-term expansion, enhanced chondrogenic potential, and suppression of endochondral ossification of adult human MSCs via WNT signaling modulation. *Stem Cell Reports*, *4*(3), 459–472. https://doi.org/10.1016/j.stemcr.2015.01.017

Narimatsu, M., Bose, R., Pye, M., Zhang, L., Miller, B., Ching, P., … Wrana, J. L. (2009). Regulation of planar cell polarity by Smurf ubiquitin ligases. *Cell*, *137*(2), 295–307. https://doi.org/10.1016/j.cell.2009.02.025

Neul, J. L., & Ferguson, E. L. (1998). Spatially restricted activation of the SAX receptor by SCW modulates DPP/TKV signaling in Drosophila dorsal-ventral patterning. *Cell*, *95*(4), 483–494. https://doi.org/10.1016/s0092-8674(00)81616-5

Nolte-’t Hoen, E. N. M., Buermans, H. P. J., Waasdorp, M., Stoorvogel, W., Wauben, M. H. M., & ’t Hoen, P. A. C. (2012). Deep sequencing of RNA from immune cell-derived vesicles uncovers the selective incorporation of small non-coding RNA biotypes with potential regulatory functions. *Nucleic Acids Research*, *40*(18), 9272–9285. https://doi.org/10.1093/nar/gks658

Nooshabadi, V. T., Mardpour, S., Yousefi-Ahmadipour, A., Allahverdi, A., Izadpanah, M., Daneshimehr, F., … Ebrahimi-Barough, S. (2018). The extracellular vesicles-derived from mesenchymal stromal cells: A new

therapeutic option in regenerative medicine. *Journal of Cellular Biochemistry*, *119*(10), 8048–8073. https://doi.org/10.1002/jcb.26726

Nuglozeh, E. (2017). Connective tissue growth factor transgenic mouse develops cardiac hypertrophy, lean body mass and alopecia. *Journal of Clinical and Diagnostic Research*, *11*(7), GC01–GC05. https://doi.org/10.7860/JCDR/2017/28158.10284

Ogawa, H., Kozhemyakina, E., Hung, H. H., Grodzinsky, A. J., & Lassar, A. B. (2014). Mechanical motion promotes expression of Prg4 in articular cartilage via multiple CREB-dependent, fluid flow shear stress-induced signaling pathways. *Genes and Development*. https://doi.org/10.1101/gad.231969.113

Ohbayashi, N., Shibayama, M., Kurotaki, Y., Imanishi, M., Fujimori, T., Itoh, N., & Takada, S. (2002). FGF18 is required for normal cell proliferation and differentiation during osteogenesis and chondrogenesis. *Genes & Development*, *16*(7), 870–879. https://doi.org/10.1101/gad.965702

Olney, R. C., Tsuchiya, K., Wilson, D. M., Mohtai, M., Maloney, W. J., Schurman, D. J., & Smith, R. L. (1996). Chondrocytes from osteoarthritic cartilage have increased expression of insulin-like growth factor I (IGF-I) and IGF-binding protein-3 (IGFBP-3) and -5, but not IGF-II or IGFBP-4. *The Journal of Clinical Endocrinology and Metabolism*, *81*(3), 1096–1103. https://doi.org/10.1210/jcem.81.3.8772582

Overview | Autologous chondrocyte implantation for treating symptomatic articular cartilage defects of the knee | Guidance | NICE. (n.d.).

Palazzo, C., Ravaud, J.-F., Papelard, A., Ravaud, P., & Poiraudeau, S.

(2014). The Burden of Musculoskeletal Conditions. *PLoS ONE*, *9*(3), e90633. https://doi.org/10.1371/journal.pone.0090633

Pfander, D., Cramer, T., Weseloh, G., Pullig, O., Schuppan, D., Bauer, M., & Swoboda, B. (1999). Hepatocyte growth factor in human osteoarthritic cartilage. *Osteoarthritis and Cartilage*, *7*(6), 548–559. https://doi.org/10.1053/joca.1999.0259

Pfander, D., Swoboda, B., & Kirsch, T. (2001). Expression of early and late differentiation markers (proliferating cell nuclear antigen, syndecan-3, annexin VI, and alkaline phosphatase) by human osteoarthritic chondrocytes. *The American Journal of Pathology*, *159*(5), 1777–1783. https://doi.org/10.1016/S0002-9440(10)63024-6

Pitsillides, A., & Ashhurst, D. E. (2008, September). A critical evaluation of specific aspects of joint development. *Developmental Dynamics*, Vol. 237, pp. 2284–2294. https://doi.org/10.1002/dvdy.21654

Prasadam, I., & Xiao, Y. (2018). A microRNA screen reveals the critical role of microRNA-23a-3p in maintaining cartilage homeostasis. *Osteoarthritis and Cartilage*. https://doi.org/10.1016/j.joca.2018.02.347

Praxenthaler, H., Krämer, E., Weisser, M., Hecht, N., Fischer, J., Grossner, T., & Richter, W. (2018). Extracellular matrix content and WNT/β-catenin levels of cartilage determine the chondrocyte response to compressive load. *Biochimica et Biophysica Acta. Molecular Basis of Disease*, *1864*(3), 851–859. https://doi.org/10.1016/j.bbadis.2017.12.024

Prokopec, S. D., Watson, J. D., Waggott, D. M., Smith, A. B., Wu, A. H., Okey, A. B., … Boutros, P. C. (2013). Systematic evaluation of

medium-throughput mRNA abundance platforms. *RNA*, *19*(1), 51–62. https://doi.org/10.1261/rna.034710.112

Qiu, W., Chen, L., & Kassem, M. (2011). Activation of non-canonical Wnt/JNK pathway by Wnt3a is associated with differentiation fate determination of human bone marrow stromal (mesenchymal) stem cells. *Biochemical and Biophysical Research Communications*, *413*(1), 98–104. https://doi.org/10.1016/j.bbrc.2011.08.061

Quinn, T. M., Häuselmann, H.-J., Shintani, N., & Hunziker, E. B. (2013). Cell and matrix morphology in articular cartilage from adult human knee and ankle joints suggests depth-associated adaptations to biomechanical and anatomical roles. *Osteoarthritis and Cartilage*, *21*(12), 1904–1912. https://doi.org/10.1016/J.JOCA.2013.09.011

Ragni, E., Viganò, M., Rebulla, P., Giordano, R., & Lazzari, L. (2013). What is beyond a qRT-PCR study on mesenchymal stem cell differentiation properties: how to choose the most reliable housekeeping genes. *Journal of Cellular and Molecular Medicine*, *17*(1), 168–180. https://doi.org/10.1111/j.1582-4934.2012.01660.x

Rasheed, Z., Rasheed, N., Abdulmonem, W. Al, & Khan, M. I. (2019). MicroRNA-125b-5p regulates IL-1β induced inflammatory genes via targeting TRAF6-mediated MAPKs and NF-κB signaling in human osteoarthritic chondrocytes. *Scientific Reports*. https://doi.org/10.1038/s41598-019-42601-3

Ray, A., Singh, P. N. P., Sohaskey, M. L., Harland, R. M., & Bandyopadhyay, A. (2015). Precise spatial restriction of BMP signaling is essential for articular cartilage differentiation. *Development (Cambridge)*, *142*(6), 1169–1179.

https://doi.org/10.1242/dev.110940

Reiter, J., Drummond, S., Sammour, I., Huang, J., Florea, V., Dornas, P., … Young, K. C. (2017). Stromal derived factor-1 mediates the lung regenerative effects of mesenchymal stem cells in a rodent model of bronchopulmonary dysplasia. *Respiratory Research*, *18*(1), 137. https://doi.org/10.1186/s12931-017-0620-z

Roelofs, A. J., Zupan, J., Riemen, A. H. K., Kania, K., Ansboro, S., White, N., … De Bari, C. (2017). Joint morphogenetic cells in the adult mammalian synovium. *Nature Communications*, *8*, 15040. https://doi.org/10.1038/ncomms15040

Rötzer, A., & Mohr, W. [3H-thymidine incorporation into chondrocytes of arthritic cartilage]. *Zeitschrift Für Rheumatologie*, *51*(4), 172–176.

Ruan, M. Z. C., Erez, A., Guse, K., Dawson, B., Bertin, T., Chen, Y., … Lee, B. H. L. (2013). Proteoglycan 4 expression protects against the development of osteoarthritis. *Science Translational Medicine*. https://doi.org/10.1126/scitranslmed.3005409

Ruedel, A., Dietrich, P., Schubert, T., Hofmeister, S., Hellerbrand, C., & Bosserhoff, A. K. (2015). Expression and function of microRNA-188-5p in activated rheumatoid arthritis synovial fibroblasts. *International Journal of Clinical and Experimental Pathology*, *8*(6), 6607–6616. Retrieved from http://www.ncbi.nlm.nih.gov/pubmed/26261542

Salvador, J. M., Brown-Clay, J. D., & Fornace, A. J. (2013). Gadd45 in stress signaling, cell cycle control, and apoptosis. *Advances in Experimental Medicine and Biology*, *793*, 1–19. https://doi.org/10.1007/978-1-4614-8289-5_1

Schubert, F. R., Sobreira, D. R., Janousek, R. G., Alvares, L. E., & Dietrich, S. (2014). Dact genes are chordate specific regulators at the intersection of Wnt and Tgf-β signaling pathways. *BMC Evolutionary Biology*, *14*, 157. https://doi.org/10.1186/1471-2148-14-157

Sensiate, L. A., Sobreira, D. R., Da Veiga, F. C., Peterlini, D. J., Pedrosa, A. V., Rirsch, T., … Alvares, L. E. (2014). Dact gene expression profiles suggest a role for this gene family in integrating Wnt and TGF-β signaling pathways during chicken limb development. *Developmental Dynamics*, *243*(3), 428–439. https://doi.org/10.1002/dvdy.23948

Shi, J., Liu, Y., Xu, X., Zhang, W., Yu, T., Jia, J., & Liu, C. (2015). Deubiquitinase USP47/UBP64E Regulates β-Catenin Ubiquitination and Degradation and Plays a Positive Role in Wnt Signaling. *Molecular and Cellular Biology*, *35*(19), 3301–3311. https://doi.org/10.1128/mcb.00373-15

Shwartz, Y., Viukov, S., Krief, S., & Zelzer, E. (2016). Joint Development Involves a Continuous Influx of Gdf5-Positive Cells. *Cell Reports*. https://doi.org/10.1016/j.celrep.2016.05.055

Singh, P. N. P., Shea, C. A., Sonker, S. K., Rolfe, R. A., Ray, A., Kumar, S., … Bandyopadhyay, A. (2018). Precise spatial restriction of BMP signaling in developing joints is perturbed upon loss of embryo movement. *Development*, *145*(5), dev153460. https://doi.org/10.1242/dev.153460

Smolen, J. S., Schoels, M. M., Nishimoto, N., Breedveld, F. C., Burmester, G. R., Dougados, M., … van der Heijde, D. (2013). Consensus statement on blocking the effects of interleukin-6 and in particular by

interleukin-6 receptor inhibition in rheumatoid arthritis and other inflammatory conditions. *Annals of the Rheumatic Diseases*, *72*(4), 482–492. https://doi.org/10.1136/annrheumdis-2012-202469

Su, X., Wu, Z., Chen, J., Wu, N., Ma, P., Xia, Z., … Qiu, G. (2015). CD146 as a new marker for an increased chondroprogenitor cell sub-population in the later stages of osteoarthritis. *Journal of Orthopaedic Research*, *33*(1), 84–91. https://doi.org/10.1002/jor.22731

Su, Y., Zhang, L., Gao, X., Meng, F., Wen, J., Zhou, H., … Chen, Y.-G. (2007). The evolutionally conserved activity of Dapper2 in antagonizing TGF-beta signaling. *FASEB Journal : Official Publication of the Federation of American Societies for Experimental Biology*, *21*(3), 682–690. https://doi.org/10.1096/fj.06-6246com

Sundararaman, S., Miller, T. J., Pastore, J. M., Kiedrowski, M., Aras, R., & Penn, M. S. (2011). Plasmid-based transient human stromal cell-derived factor-1 gene transfer improves cardiac function in chronic heart failure. *Gene Therapy*, *18*(9), 867–873. https://doi.org/10.1038/gt.2011.18

Suriben, R., Kivimäe, S., Fisher, D. A. C., Moon, R. T., & Cheyette, B. N. R. (2009). Posterior malformations in Dact1 mutant mice arise through misregulated Vangl2 at the primitive streak. *Nature Genetics*, *41*(9), 977–985. https://doi.org/10.1038/ng.435

Symoens, S., Barnes, A. M., Gistelinck, C., Malfait, F., Guillemyn, B., Steyaert, W., … Coucke, P. J. (2015). Genetic Defects in TAPT1 Disrupt Ciliogenesis and Cause a Complex Lethal Osteochondrodysplasia. *American Journal of Human Genetics*, *97*(4), 521–534. https://doi.org/10.1016/j.ajhg.2015.08.009

Tachmazidou, I., Hatzikotoulas, K., Southam, L., Esparza-Gordillo, J., Haberland, V., Zheng, J., … Zeggini, E. (2019, February 1). Identification of new therapeutic targets for osteoarthritis through genome-wide analyses of UK Biobank data. *Nature Genetics*, Vol. 51, pp. 230–236. https://doi.org/10.1038/s41588-018-0327-1

Tang, J., Tao, Z.-H., Wen, D., Wan, J.-L., Liu, D.-L., Zhang, S., … Wu, W.-Z. (2014). miR-612 suppresses the stemness of liver cancer via Wnt/β-catenin signaling. *Biochemical and Biophysical Research Communications*, *447*(1), 210–215. https://doi.org/10.1016/J.BBRC.2014.03.135

Tang, L., Ding, J., Zhou, G., & Liu, Z. (2018). LncRNA-p21 promotes chondrocyte apoptosis in osteoarthritis by acting as a sponge for miR-451. *Molecular Medicine Reports*, *18*(6), 5295–5301. https://doi.org/10.3892/mmr.2018.9506

Tang, X., Muhammad, H., McLean, C., Miotla-Zarebska, J., Fleming, J., Didangelos, A., … Vincent, T. L. (2018). Connective tissue growth factor contributes to joint homeostasis and osteoarthritis severity by controlling the matrix sequestration and activation of latent TGFβ. *Annals of the Rheumatic Diseases*, *77*(9), 1372–1380. https://doi.org/10.1136/annrheumdis-2018-212964

Teran, E., Branscomb, A. D., & Seeling, J. M. (2009). Dpr Acts as a molecular switch, inhibiting Wnt signaling when unphosphorylated, but promoting Wnt signaling when phosphorylated by casein kinase Idelta/epsilon. *PloS One*, *4*(5), e5522. https://doi.org/10.1371/journal.pone.0005522

The jackson laboratory. (n.d.). Mouse Genome Informatics database.

Retrieved from http://www.informatics.jax.org/expression.shtml

Thompson, E. M., Matsiko, A., Farrell, E., Kelly, D. J., & O'Brien, F. J. (2015). Recapitulating endochondral ossification: a promising route to *in vivo* bone regeneration. *Journal of Tissue Engineering and Regenerative Medicine*, *9*(8), 889–902. https://doi.org/10.1002/term.1918

Tian, Y., Zhang, Y.-Z., & Chen, W. (2014). MicroRNA-199a-3p and microRNA-34a regulate apoptosis in human osteosarcoma cells. *Bioscience Reports*, *34*(4). https://doi.org/10.1042/BSR20140084

Tsutsumi, S., Shimazu, A., Miyazaki, K., Pan, H., Koike, C., Yoshida, E., … Kato, Y. (2001). Retention of multilineage differentiation potential of mesenchymal cells during proliferation in response to FGF. *Biochemical and Biophysical Research Communications*, *288*(2), 413–419. https://doi.org/10.1006/bbrc.2001.5777

Uchii, M., Tamura, T., Suda, T., Kakuni, M., Tanaka, A., & Miki, I. (2008). Role of fibroblast growth factor 8 (FGF8) in animal models of osteoarthritis. *Arthritis Research & Therapy*, *10*(4), R90. https://doi.org/10.1186/ar2474

Uhlén, M., Fagerberg, L., Hallström, B. M., Lindskog, C., Oksvold, P., Mardinoglu, A., … Pontén, F. (2015). Tissue-based map of the human proteome. *Science*, *347*(6220). https://doi.org/10.1126/science.1260419

UK government. (2019a). Musculoskeletal Health: applying All Our Health. Retrieved from https://www.gov.uk/government/publications/musculoskeletal-health-applying-all-our-health/musculoskeletal-health-applying-all-our-health

UK government. (2019b). The grand challanges. Retrieved from The grand challanges website: https://www.gov.uk/government/publications/industrial-strategy-the-grand-challenges/industrial-strategy-the-grand-challenges

Vayas, R., Reyes, R., Arnau, M. R., Évora, C., & Delgado, A. (2019). Injectable Scaffold for Bone Marrow Stem Cells and Bone Morphogenetic Protein-2 to Repair Cartilage. *Cartilage*, 1947603519841682. https://doi.org/10.1177/1947603519841682

Vincent, T., Hermansson, M., Bolton, M., Wait, R., & Saklatvala, J. (2002). Basic FGF mediates an immediate response of articular cartilage to mechanical injury. *Proceedings of the National Academy of Sciences of the United States of America*, *99*(12), 8259–8264. https://doi.org/10.1073/pnas.122033199

Wang, J. lian, Zhou, X., Zhang, L. fu, Li, F., Wang, B. yan, Wang, W. dong, & Fu, W. (2018). TGF-β signaling regulates DACT1 expression in intestinal epithelial cells. *Biomedicine and Pharmacotherapy*, *97*, 864–869. https://doi.org/10.1016/j.biopha.2017.11.017

Wang, S., Dong, Y., Zhang, Y., Wang, X., Xu, L., Yang, S., … Yu, J. (2015). DACT2 is a functional tumor suppressor through inhibiting Wnt/β-catenin pathway and associated with poor survival in colon cancer. *Oncogene*, *34*(20). Retrieved from https://www.ncbi.nlm.nih.gov/pmc/articles/PMC4761644/

Wang, Z., Guo, H., Xiao, L., Qing, Z., & Ma, J. (2017). (No Title). In *Int J Clin Exp Pathol* (Vol. 10). Retrieved from www.ijcep.com/

Waxman, J. S., Hocking, A. M., Stoick, C. L., & Moon, R. T. (2004). Zebrafish Dapper1 and Dapper2 play distinct roles in Wnt-mediated

developmental processes. *Development*, *131*(23), 5909–5921. https://doi.org/10.1242/dev.01520

Wei, F., Moore, D. C., Li, Y., Zhang, G., Wei, X., Lee, J. K., & Wei, L. (2012). Attenuation of osteoarthritis via blockade of the SDF-1/CXCR4 signaling pathway. *Arthritis Research and Therapy*, *14*(4), R177. https://doi.org/10.1186/ar3930

Wen, J., Chiang, Y. J., Gao, C., Xue, H., Xu, J., Ning, Y., … Chen, Y.-G. (2010). Loss of Dact1 disrupts planar cell polarity signaling by altering dishevelled activity and leads to posterior malformation in mice. *The Journal of Biological Chemistry*, *285*(14), 11023–11030. https://doi.org/10.1074/jbc.M109.085381

White, E. J. F., Brewer, G., & Wilson, G. M. (2013, June). Post-transcriptional control of gene expression by AUF1: Mechanisms, physiological targets, and regulation. *Biochimica et Biophysica Acta - Gene Regulatory Mechanisms*, Vol. 1829, pp. 680–688. https://doi.org/10.1016/j.bbagrm.2012.12.002

Winkler, D. G., Sutherland, M. S. K., Ojala, E., Turcott, E., Geoghegan, J. C., Shpektor, D., … Latham, J. A. (2005). Sclerostin inhibition of Wnt-3a-induced C3H10T1/2 cell differentiation is indirect and mediated by bone morphogenetic proteins. *The Journal of Biological Chemistry*, *280*(4), 2498–2502. https://doi.org/10.1074/jbc.M400524200

Wu, Q., Huang, J. H., Sampson, E. R., Kim, K. O., Zuscik, M. J., O'Keefe, R. J., … Rosier, R. N. (2009). Smurf2 induces degradation of GSK-3β and upregulates β-catenin in chondrocytes: A potential mechanism for Smurf2-induced degeneration of articular cartilage. *Experimental Cell Research*, *315*(14), 2386–2398.

https://doi.org/10.1016/j.yexcr.2009.05.019

Xue, H., Xiao, Z., Zhang, J., Wen, J., Wang, Y., Chang, Z., … Chen, Y.-G. (2013). Disruption of the *Dapper3* Gene Aggravates Ureteral Obstruction-mediated Renal Fibrosis by Amplifying Wnt/β-catenin Signaling. *Journal of Biological Chemistry*, *288*(21), 15006–15014. https://doi.org/10.1074/jbc.M113.458448

Yacoub, R., Lee, K., & He, J. C. (2014). The role of SIRT1 in diabetic kidney disease. *Frontiers in Endocrinology*, Vol. 5. https://doi.org/10.3389/fendo.2014.00166

Yamashita, M., Ying, S.-X., Zhang, G.-M., Li, C., Cheng, S. Y., Deng, C.-X., & Zhang, Y. E. (2005). Ubiquitin ligase Smurf1 controls osteoblast activity and bone homeostasis by targeting MEKK2 for degradation. *Cell*, *121*(1), 101–113. https://doi.org/10.1016/j.cell.2005.01.035

Yao, X., Zhang, J., Jing, X., Ye, Y., Guo, J., Sun, K., & Guo, F. (2019). Fibroblast growth factor 18 exerts anti-osteoarthritic effects through PI3K-AKT signaling and mitochondrial fusion and fission. *Pharmacological Research*, *139*, 314–324. https://doi.org/10.1016/j.phrs.2018.09.026

Yau, T.-O., Chan, C.-Y., Chan, K.-L., Lee, M.-F., Wong, C.-M., Fan, S.-T., & Ng, I. O.-L. (2005). HDPR1, a novel inhibitor of the WNT/beta-catenin signaling, is frequently downregulated in hepatocellular carcinoma: involvement of methylation-mediated gene silencing. *Oncogene*, *24*(9), 1607–1614. https://doi.org/10.1038/sj.onc.1208340

Yin, X., Xiang, T., Li, L. L., Su, X., Shu, X., Luo, X., … Tao, Q. (2013). DACT1, an antagonist to Wnt/β-catenin signaling, suppresses tumor cell growth and is frequently silenced in breast cancer. *Breast Cancer*

Research, *15*(2). https://doi.org/10.1186/bcr3399

Yu, C.-Y., Yang, C.-Y., & Rui, Z.-L. (2019). MicroRNA-125b-5p improves pancreatic β-cell function through inhibiting JNK signaling pathway by targeting DACT1 in mice with type 2 diabetes mellitus. *Life Sciences*, *224*, 67–75. https://doi.org/10.1016/j.lfs.2019.01.031

Yuan, G., Wang, C., Ma, C., Chen, N., Tian, Q., Zhang, T., & Fu, W. (2012). Oncogenic function of DACT1 in colon cancer through the regulation of β-catenin. *PLoS ONE*, *7*(3). https://doi.org/10.1371/journal.pone.0034004

Zhang, L., Zhou, H., Su, Y., Sun, Z., Zhang, H., Zhang, L., … Meng, A. (2004). Zebrafish Dpr2 Inhibits Mesoderm Induction by Promoting Degradation of Nodal Receptors. *Science*, *306*(5693), 114–117. https://doi.org/10.1126/science.1100569

Zhang, M., Xie, R., Hou, W., Wang, B., Shen, R., Wang, X., … Chen, D. (2009). PTHrP prevents chondrocyte premature hypertrophy by inducing cyclin-D1-dependent Runx2 and Runx3 phosphorylation, ubiquitylation and proteasomal degradation. *Journal of Cell Science*, *122*(9), 1382–1389. https://doi.org/10.1242/jcs.040709

Zhang, Minjie, Mani, S. B., He, Y., Hall, A. M., Xu, L., Li, Y., … Warman, M. L. (2016). Induced superficial chondrocyte death reduces catabolic cartilage damage in murine posttraumatic osteoarthritis. *Journal of Clinical Investigation*, *126*(8), 2893–2902. https://doi.org/10.1172/JCI83676

Zhang, W., Chen, J., Tao, J., Jiang, Y., Hu, C., Huang, L., … Ouyang, H. W. (2013). The use of type 1 collagen scaffold containing stromal cell-derived factor-1 to create a matrix environment conducive to partial-

thickness cartilage defects repair. *Biomaterials*, *34*(3), 713–723. https://doi.org/10.1016/j.biomaterials.2012.10.027

Zhang, Z., Li, L., Yang, W., Cao, Y., Shi, Y., Li, X., & Zhang, Q. (2017). The effects of different doses of IGF-1 on cartilage and subchondral bone during the repair of full-thickness articular cartilage defects in rabbits. *Osteoarthritis and Cartilage*, *25*(2), 309–320. https://doi.org/10.1016/j.joca.2016.09.010

Zhao, H., Yang, L., Han, Y., Li, H., Ling, Z., Wang, Y., … Wu, G. (2017). Dact3 inhibits the malignant phenotype of non-small cell lung cancer through downregulation of c-Myb. In *Int J Clin Exp Pathol* (Vol. 10). Retrieved from www.ijcep.com/

Zhao, X., He, L., Li, T., Lu, Y., Miao, Y., Liang, S., … Fan, D. (2014). SRF expedites metastasis and modulates the epithelial to mesenchymal transition by regulating miR-199a-5p expression in human gastric cancer. *Cell Death & Differentiation*, *21*(12), 1900–1913. https://doi.org/10.1038/cdd.2014.109

Zhong, L., Liao, G., Wang, X., Li, L., Zhang, J., Chen, Y., … Lu, Y. (2018). Mesenchymal stem cells–microvesicle-miR-451a ameliorate early diabetic kidney injury by negative regulation of P15 and P19. *Experimental Biology and Medicine*, *243*(15–16), 1233–1242. https://doi.org/10.1177/1535370218819726

Zhou, Shixia, Zhang, Z., Zheng, P., Zhao, W., & Han, N. (2017). MicroRNA-1285-5p influences the proliferation and metastasis of non-small-cell lung carcinoma cells via downregulating CDH1 and Smad4. *Tumor Biology*. https://doi.org/10.1177/1010428317705513

Zhou, Shuanhu, Eid, K., & Glowacki, J. (2004). Cooperation between TGF-

beta and Wnt pathways during chondrocyte and adipocyte differentiation of human marrow stromal cells. *Journal of Bone and Mineral Research : The Official Journal of the American Society for Bone and Mineral Research*, *19*(3), 463–470. https://doi.org/10.1359/JBMR.0301239

Zhou, Y., Song, T., Peng, J., Zhou, Z., Wei, H., Zhou, R., … Peng, J. (2016). SIRT1 suppresses adipogenesis by activating Wnt/β-catenin signaling in vivo and in vitro. *Oncotarget*, *7*(47), 77707–77720. https://doi.org/10.18632/oncotarget.12774

Zhu, H., Kavsak, P., Abdollah, S., Wrana, J. L., & Thomsen, G. H. (1999). A SMAD ubiquitin ligase targets the BMP pathway and affects embryonic pattern formation. *Nature*, *400*(6745), 687–693. https://doi.org/10.1038/23293

Zhu, K., Jiang, B., Yang, Y., Hu, R., & Liu, Z. (2017). DACT1 overexpression inhibits proliferation, enhances apoptosis, and increases daunorubicin chemosensitivity in KG-1α cells. *Tumor Biology*, *39*(10), 1–8. https://doi.org/10.1177/1010428317711089

Zhu, M., Tang, D., Wu, Q., Hao, S., Chen, M., Xie, C., … Chen, D. (2009). Activation of beta-catenin signaling in articular chondrocytes leads to osteoarthritis-like phenotype in adult beta-catenin conditional activation mice. *Journal of Bone and Mineral Research : The Official Journal of the American Society for Bone and Mineral Research*, *24*(1), 12–21. https://doi.org/10.1359/jbmr.080901

Appendix

Table 6 EVs miRNAs cargo

miRNA
Let-7a-5p
Let-7b-5p
Let-7g-5p
Let-7l-5p
miR-100-5p
miR-125b-5p
miR-127-3p
miR-1285-5p
miR-1290
miR-130a-3p
miR-145-5p
miR-15a-5p
miR-16-5p
miR-181a-5p
miR-188-5p
miR-191-5p
miR-196a-5p
miR-199a-3p
miR-199a-5p
miR-21-5p
miR-22-3p
miR-221-3p
miR-222-3p
miR23a-3p
miR-29a-3p
miR-320e
miR-34a-5p
miR-363-3p
miR-374a-5p

miR-376a-3p
miR-4286
miR-4454+miR7975
miR-451a
miR-612
miR-630
miR-6721-5p
miR-873-3p

Table 7 Top300 up- and down-regulated genes siDACT1 vs siCTRL

Top 150 up-regulated genes		Top 150 down-regulated genes	
Gene ID	Fold Change	Gene ID	Fold Change
MET	0.9196	DACT1	-2.078
LINC00894	0.8375	NEIL2	-1.276
TAPT1	0.8302	RP11-175O19.4	-1.253
SLC26A10	0.7952	LONRF1	-1.226
PTPMT1	0.7809	RASSF3	-1.175
ANKRD20A5P	0.7604	SFT2D2	-1.114
RP11-449J21.3	0.7461	USP46	-1.024
RP11-159D12.6	0.7342	CDK6	-1.023
CA2	0.7327	VAMP3	-0.977
RP11-96D1.8	0.7268	SMURF2	-0.956
SLC36A1	0.7095	RNF130	-0.920
RP11-340I6.6	0.6940	KAZN	-0.905
AC011893.3	0.6849	SLC25A22	-0.893
RP11-84A19.3	0.6805	AMMECR1	-0.891
FAM49B	0.6719	TBPL1	-0.879
EIF4A1	0.6677	LYRM7	-0.866
RPS26	0.6648	TNFRSF10B	-0.866
SNORD104	0.6641	DIXDC1	-0.862
GPT	0.6497	MAML1	-0.861

IL11	0.6475	DICER1	-0.861
CTD-2574D22.3	0.6414	FAM160B1	-0.848
GNB3	0.6370	MTO1	-0.842
MIR222HG	0.6369	C1orf198	-0.826
HERC2P3	0.6356	AP4E1	-0.820
C10orf90	0.6346	SLC2A10	-0.813
AC027601.1	0.6332	PDE8B	-0.810
AGER	0.6323	EIF2S3L	-0.801
SNHG3	0.6317	TBC1D16	-0.788
NNAT	0.6315	CAPN5	-0.787
DDX10	0.6267	RP11-38O23.4	-0.777
H3F3A	0.6201	C7orf60	-0.767
AC010761.8	0.6201	ATXN1	-0.765
OGFOD2	0.6145	AVL9	-0.755
MT-TE	0.6098	AF196972.4	-0.744
RP11-644F5.10	0.6093	TMEM109	-0.744
STARD4-AS1	0.6087	ZFHX3	-0.742
CTD-3035K23.3	0.6083	DCP2	-0.737
RP11-696N14.1	0.6073	RP11-767N6.7	-0.735
RP11-708J19.1	0.6068	RFESD	-0.734
INE1	0.6065	EIF2S3	-0.734
ESR1	0.6050	CBX5	-0.729
SMAP1	0.6046	LINC00619	-0.727
BOD1	0.6031	TBC1D2B	-0.723
LINC01125	0.6030	SYPL1	-0.722
TMEM256-PLSCR3	0.5946	TUG1	-0.719
GOPC	0.5939	DPY30	-0.713
MTATP6P1	0.5934	DDI2	-0.709
EGFL8	0.5913	EFCAB14P1	-0.705
LINC00106	0.5910	DENND5B	-0.699
RP11-540B6.6	0.5883	EFCAB14	-0.693
WSB1	0.5879	NUCKS1	-0.686

AC018766.4	0.5875	ZNF442	-0.685
RP11-1391J7.1	0.5873	AC240274.1	-0.684
KRTCAP2	0.5867	PANK1	-0.680
RP1-152L7.8	0.5862	TDGP1	-0.680
PTPN1	0.5858	RP3-452M16.1	-0.679
PRSS53	0.5852	UBE4A	-0.678
CCDC39	0.5833	TTC1	-0.677
ZNF692	0.5831	MAGI1	-0.674
RP11-573D15.9	0.5805	PLK2	-0.672
AC007191.4	0.5800	MED20	-0.672
CTD-2545G14.4	0.5798	SLC43A2	-0.671
RP11-755F10.3	0.5756	STX17	-0.668
AARSD1	0.5747	PLEKHA1	-0.667
SLC25A25-AS1	0.5709	CDKL5	-0.664
ZCCHC3	0.5695	HLTF	-0.663
KCNAB3	0.5693	CTD-2554C21.1	-0.662
PIF1	0.5661	WDR41	-0.662
RP5-1159O4.1	0.5648	ARPP19	-0.661
RP11-235E17.6	0.5635	SFXN2	-0.657
ERCC5	0.5634	OTUD4	-0.653
DDX39B	0.5595	SCD	-0.652
LPAR2	0.5588	ASAP1	-0.651
AC005253.2	0.5580	NEK6	-0.651
RP11-395G23.3	0.5563	FAM63B	-0.640
PDXDC2P	0.5558	ZDHHC7	-0.640
SNHG25	0.5554	ARHGAP5	-0.638
PDCD6	0.5551	TTPAL	-0.638
RP11-158L12.4	0.5550	FAM46B	-0.635
SNHG4	0.5535	ELAC1	-0.634
ASGR1	0.5534	AHNAK	-0.633
RP11-1348G14.8	0.5526	ANKRD33B	-0.632
CTD-2574D22.4	0.5518	KIAA2013	-0.629

RP1-181J22.1	0.5509	RP11-566E18.1	-0.627
VGLL4	0.5494	HSDL1	-0.626
RP11-264B17.2	0.5493	FAT4	-0.626
AGAP6	0.5485	NCOA2	-0.626
DDX10P2	0.5484	TDG	-0.624
MSRB3	0.5475	RP11-680G24.4	-0.624
RP11-1334A24.5	0.5449	BVES	-0.623
TOMM20	0.5418	PAQR8	-0.621
ID4	0.5406	IST1	-0.619
E2F5	0.5357	DENND1B	-0.619
MTND2P28	0.5353	DCUN1D3	-0.619
NAP1L5	0.5345	B4GALT4	-0.618
RP11-395N3.1	0.5338	LDB2	-0.616
MT-CO2	0.5337	GADD45B	-0.615
AC009506.1	0.5336	KATNAL1	-0.615
EME2	0.5310	SLC9A6	-0.614
MT-ATP8	0.5310	CYR61	-0.613
SAMD15	0.5263	RP1-172N19.4	-0.612
LL0XNC01-7P3.1	0.5261	ATXN1L	-0.609
AC016722.4	0.5261	LAMC1	-0.606
PRICKLE4	0.5258	C2CD5	-0.605
RFXAP	0.5254	NARF	-0.604
RFK	0.5240	MRAS	-0.604
RP13-516M14.10	0.5240	CTDSPL	-0.602
ELMO3	0.5228	TP53INP2	-0.600
PI4KAP1	0.5225	FNIP2	-0.600
CTA-29F11.1	0.5216	ARHGAP19	-0.594
CSPG4P10	0.5191	ENO2	-0.593
MEG3	0.5182	PAG1	-0.591
MIR221	0.5164	SYNGR3	-0.591

RP5-1142A6.9	0.5159	GLMP	-0.590
RP11-802E16.3	0.5136	PRKAA2	-0.589
DNM3OS	0.5125	NT5DC3	-0.589
HOXC-AS3	0.5123	KLHL12	-0.588
BRICD5	0.5116	TSPAN17	-0.588
RP11-264I13.2	0.5115	ISCA2	-0.587
LZTFL1	0.5090	CAPZA1	-0.585
MAPK8IP3	0.5089	IL15RA	-0.584
CCND3	0.5087	ABHD8	-0.583
GABPA	0.5078	ARID1A	-0.581
ATG4A	0.5069	PKI55	-0.579
TSSK4	0.5053	CHST15	-0.579
MPP3	0.5050	LRRC32	-0.579
TBX2-AS1	0.5035	TMEM230	-0.578
KIAA0895L	0.5033	TUFT1	-0.578
LUC7L3	0.5032	TMEM2	-0.576
RP11-320M2.1	0.5030	DENND6A	-0.574
MAT2A	0.5026	HEG1	-0.568
PNISR	0.5026	TANC1	-0.567
RAD54L2	0.5012	CCL2	-0.567
AHSA2	0.5011	ENSAP2	-0.566
AC007383.3	0.5007	LMOD1	-0.566
MT-ND4	0.5001	MTMR9	-0.565
CTD-2270P14.1	0.4996	KBTBD7	-0.565
MT-ND6	0.4996	SLC35B4	-0.565
MT-RNR1	0.4992	NUAK2	-0.561
TTC14	0.4991	ARL6IP1P3	-0.561
SLC25A5-AS1	0.4987	FYCO1	-0.560
ATXN7L2	0.4970	LBH	-0.557
GPC2	0.4969	LRIG3	-0.556
CREM	0.4968	ALX4	-0.555
DNMT3B	0.4960	RPTN	-0.553
HOXB-AS1	0.4944	RUNX1T1	-0.553

PILRB	0.4943	RNPEPL1	-0.552
ATP6V1B1	0.4933	RASSF5	-0.551
CTC-479C5.12	0.4922	FADS2	-0.551
SPRY4	0.4909	TENM4	-0.550